GLYCINE RECEPTOR ANTIBODIES: PATHOGENIC MECHANISMS AND CLINICAL CORRELATES

Alexander Carvajal-González

St Hugh's College

A Thesis submitted for the degree of

DOCTOR OF PHILOSOPHY IN CLINICAL NEUROLOGY

Nuffield Department of Clinical Neurosciences

Medical Sciences Division

UNIVERSITY OF OXFORD

Trinity Term, 2014

Glycine receptor antibodies: pathogenic mechanisms and clinical correlates

Alexander Carvajal-González MD, MSc
St Hugh´s College, University of Oxford

A Thesis submitted for the degree of

DOCTOR OF PHILOSOPHY IN CLINICAL NEUROLOGY

Trinity term, 2014

ABSTRACT

Glycine receptor antibodies have been identified in a few patients with progressive encephalomyelitis with rigidity and myoclonus (PERM), a highly disabling disorder characterised by rigidity, spasm and brainstem symptomatology. The clinical characteristics of patients with glycine receptor antibodies have not yet been fully described and it is not clear whether GlyR-Abs are pathogenic or just an epiphenomenon.

This study examined the clinical features and immunotherapy responses of 45 patients; characterised the GlyR-Ab pathogenicity, subunit specificity and binding to different brain region *in vitro*, and examined mice injected with GlyR-Abs to model the disease *in vivo.*

Most of the patients were classified as PERM but some patients had symptomatology beyond the classical motor manifestations and there were four patients with tumours (thymomas and lymphomas). GlyR-Ab titres were varied in serum and CSF, but there was intrathecal synthesis in the six patients with suitable samples. Most patients were very disabled but almost all showed excellent responses to immunotherapies. The antibodies were mainly IgG1 and IgG3 subclasses, activated complement on glycine receptor-transfected HEK cells at room temperature, and caused internalisation and lysosomal degradation of the glycine receptors at 37°C. GlyR-Abs bound to rodent spinal cord and brainstem co-localising with monoclonal antibodies to GlyRα1 on the surface of neurons.

GlyR-IgG injected intra-peritoneally led to impairment in forced walking ability, sensorimotor function and coordination. Analysis of the brain showed that animals injected with patients' IgG, but not control IgG, had antibodies bound to the brainstem, spinal cord, cerebellum and caudate, co-localising with GlyRα1 monoclonal antibody. Intra-cerebroventricular injection of GlyR-IgG caused an anxiety-like behaviour in mice but no evident motor disturbances.

These results provide the first evidence of *in vitro* and *in vivo* pathogenicity of the GlyR-Abs, supporting the use of long term immunosuppression in these patients to provide them with a good prognosis.

Acknowledgments

First and foremost I would like to thank to Professor Angela Vincent for hosting me in her laboratory and for her wisdom and guidance; it was a real honour to work with one of the world leaders in the field of neuroimmunology and see her ongoing drive and interest.

This work could not have been done without the strengths of the Oxford Neuroimmunology Group in clinical care and diagnostic cell-based assays. Dr Patrick Waters did all the cloning and plasmid constructions, Dr Mark Woodhall tested all the sera and Dr Maria Isabel Leite began the project collecting the clinical data. I would also like to thank her for her support during my clinical internship, which allowed me to see how one can combine neuroscience and clinical neurology.

Special thanks go to Ms Linda Clover; I really enjoyed all the long hours we spent at the microscope, and the sharing of her knowledge and expertise in many laboratory techniques. Thanks to Dr Leslie Jacobson for all the help running the animal experiments and to Dr Bethan Lang for allowing me to perform these under her project license. I would also like to thank Mrs Dominica Luscombe for proof-reading the Thesis and giving me advice on how to write better in this intricate language.

It was a real pleasure to meet Drs Saif Huda and Ester Couthino and to build a friendship which I hope will last. I must thank all members of the lab for all the patience they have had with me throughout the DPhil.

I am grateful to COLFUTURO and COLCIENCIAS for scholarship support.

Last but not least, I would like to thank my parents and my sisters. Without their unconditional and invaluable love, encouragement, understanding and guidance I would not have finished this Thesis. Also, I want to thank Rocio who heard all the ups and downs that I had during this time; she was a real support.

TABLE OF CONTENTS

LIST OF FIGURES

Chapter 5

Chapter 6

LIST OF TABLES

Chapter 1

Chapter 2

Chapter 3

Chapter 4

Chapter 5

LIST OF ABBREVIATIONS

Ab	Antibody
AChR	Acetylcholine receptor
AQP4	Aquaporin 4
ASR	Acoustic startle response
BBB	Blood brain barrier
BSA	Bovine serum albumin
CA	Cornu ammonis
CBA	Cell based assay
CHX	Cycloheximide
CMUA	Continuous motor unit activity
CNS	Central nervous system
CSF	Cerebrospinal fluid
CT	Computed tomography
DAB	3, 3′-Diaminodenzidine tetrahydrochloride
DAPI	4′, 6-diamidino-2-phenylindole
DG	Dentate gyrus
DH	Dorsal horn of the spinal cord
DM	Diabetes mellitus
DMEM	Dulbecco's minimum essential medium
ECG	Electrocardiogram
EEG	Electroencephalogram
EGFP	Enhanced green fluorescent protein
EMG	Electromyogram
Fab	Fragment antigen binding region
Fc	Fragment crystallisable
FCS	Foetal calf serum
GABA	γ-amino butyric acid
GABARAP	$GABA_A$ receptor-associated protein
GAD	Glutamic Acid Decarboxylase
GAD-Abs	GAD antibodies
GlyR	Glycine receptor
GlyR-Ab	Glycine receptor antibodies
GFAP	Glial fibrillary acidic protein
HLA	Human leucocyte antigen
HEK	Human Embryonic Kidney Cells
HRP	Horseradish peroxidase
IgG	Immunoglobulin G
ICV	Intracerebroventricular
IVIG	Intravenous immunoglobulins
LE	Limbic encephalitis
LEMS	Lambert-Eaton myasthenic syndrome
LPS	Lipopolysaccharide
MAP-2	Microtubule-associated protein 2
MG	Myasthenia gravis
mRS	Modified Rankin score scale
NGS	Normal goat serum
NMDAR	N-Methyl-D-Aspartate Receptor
PBS	Phosphate-buffered saline

PBS-T	Phosphate-buffered saline with Triton X-100
PEI	Polyethylimine
PERM	Progressive Encephalomyelitis with Rigidity and Myoclonus
PLL	Poly-l-lysine
PnC	Pontine reticular nucleus
PSA	Penicillin/streptomycin/amphotericin
RIA	Radioimmunoassay
SD	Standard deviation
SEM	Standard error of the mean
SPS	Stiff Person Syndrome
VH	Ventral horn of the spinal cord

CHAPTER 1. Introduction

1.1. Autoimmunity

Autoimmunity was first described by Paul Ehrlich at the start of the twentieth century. He concluded that although the normal focus of the immune system was to respond to foreign antigens, in an autoimmune disease the immune system can initiate an attack on self-tissues. He thought this was due to deterioration of an inbuilt tendency to tolerate self-antigens, and labelled this process as 'horror autotoxicus' (Bell and Bird 2005). On many occasions, since autoantigens cannot be eliminated, the triggered autoimmune response can be sustained over time leading to a chronic autoimmune disease (Janeway et al, 2001).

1.1.1 **Mechanisms of autoimmunity**

Dysregulation of the immune system is the result of changes in the mechanisms influencing the immune response. These can include regulatory T cells, cytokines, chemokines, intracellular signalling and natural autoantibodies. For many years, it was believed that autoreactive cells in the immune system were eliminated, leaving only the T and B cells that recognise specific foreign antigens. However, it has been demonstrated that a low level of autoreactivity is physiological and important for normal immune function. Autoantigen expression helps in the maturation of lymphocytes and in the survival of naive T cells (Goldrath et al, 1999) and B cells (Gu et al, 1991). For example, natural autoantibodies to several self-antigens are found in the serum of normal individuals of all ages (Coutinho et al, 1995); they are polyreactive, have low titre and affinity, and usually belong to the IgM subclass. For

these reasons they are not thought to be harmful to the host (Lacroix-Desmazes et al, 1998).

Since autoreactivity is a physiological process, it is not very clear how it becomes pathological, but several studies suggest a strong association with multiple factors such as genetic predisposition, environment, and immune dysregulation (Davidson, 2001). For instance, inheritance of some MHC and non-MHC genes increases the susceptibility to autoimmune diseases and females are at greater risk than males (Janeway et al, 2001; Antel et al, 2005).

Environmental factors such as infections, exposure to chemical substances and physical insults serve as initiators in predisposed individuals; there is less than 50% of concordance for autoimmune diseases in identical twins (Janeway et al, 2001; Antel et al, 2005). Pathogens may induce autoimmune responses through several mechanisms such as molecular mimicry, in which T or B cells respond to foreign antigens that cross react with self-antigens, or non-specific polyclonal activation (Marrack et al, 2001). Since the focus of this Thesis will be on neurological diseases, the immune system will not be discussed in more detail.

1.1.2 Autoimmune diseases

Autoimmune diseases are defined as clinical syndromes associated with the inappropriate activation of T cells and B cells, or both, usually without any discernible cause. Overall, autoimmune diseases are not rare affecting approximately 5% of the population in western countries (Marrack et al, 2001). Autoimmune diseases are clinically classified as systemic or organ-specific. In systemic autoimmune diseases, such as systemic lupus erythematosus (SLE), the immune response is directed towards

cellular autoantigens broadly expressed, and therefore, the tissue damage occurs in several organ systems. In organ-specific autoimmune diseases, such as Hashimoto's thyroiditis, the immune response is directed to an autoantigen expressed in a specific organ, the thyroid, and the tissue damage is restricted to that organ (Davidson, 2001).In order to define the autoimmune aetiology of a human disease, in 1957 Witebsky established a set of criteria (Witebsky et al, 1957) that was later revisited by (Rose et al, 1993). These are summarized in tables 1.1 and 1.2

Table 1.1. Modified Koch's postulates for autoimmune disease in general

Presence of autoantibodies or self-reactive T cells
Identification of antibody or T cells in the target organ
Transfer of disease by injection of immunoglobulins into mice
Transfer of disease by T cells into sever combined immunodeficient mice
Induction of disease by immunisation against the antigen and transfer of this disease by T
cells or antibody to naïve animals

Table 1.2. Modified postulates for antibody-mediated disease

Autoantibodies to functionally important protein
Plasmapheresis produces marked clinical improvement
Transfer of disease by placental transfer of antibodies to the baby
Transfer of disease by injection of patient serum immunoglobulins into mice
Demosntration of functional effects of antibodies using appropriate cell lines in vitro

1.1.2.1 Autoimmune neurological disorders

Autoimmune disorders, including the autoimmune neurological disorders, can be classified based on the cellular component that is affected (Davidson, 2001). For example, multiple sclerosis (MS) is a chronic inflammatory disease of the central nervous system (CNS) characterized by infiltrates of mononuclear cells; demyelination and axonal loss and believed to be mediated mainly by activated autoreactive T cells generating a cytotoxic response (Antel et al, 2005; Racke et al, 2009). Myasthenia gravis (MG) is a chronic autoimmune disease of the peripheral nervous system (PNS) characterized by painless muscular weakness and mediated mainly by autoreactive B cells generating antibodies (Vincent, 2002). However, it is not always easy to make a clear distinction between T cell and B cell mediated diseases, due to the high interdependence between the cellular and humoral responses. For example, Guillain-Barre syndrome, an immune-mediated neuropathy, is believed to be mediated by activated autoreactive T cells and B cells with antibodies to gangliosides or other peripheral nerve antigens playing an important but not exclusive role (Antel et al, 2005; (Lehmann et al, 2009).

The presence of autoantibodies against proteins of the neural tissue does not necessarily imply pathogenicity. Autoantibodies can target intracellular or extracellular proteins and these are likely to be of different clinical relevance. Autoantibodies against intracellular proteins are present in paraneoplastic neurological disorders; these disorders are associated with tumours, but the symptoms are not related to the local effects of the tumour or metastases, but result from a cellular immune response against intracellular neuronal antigens expressed by the tumour. The activated T cells cross-react with neurons expressing the antigen leading to a cytotoxic attack with subsequent

neural inflammation. In these disorders the intracellular antibodies to antigens (onco-neural antibodies listed in Table 1.3) have not been shown to be pathogenic, but are markers of the T cell responses targeting the tumour and the neurons, that are thought to cause the CNS disease. This is supported by the fact that these disorders tend to have poor responses to immunotherapies probably due to irreversible neuronal loss (Lancaster et al, 2012). On the other hand, autoantibodies against extracellular proteins, mainly directed towards membrane receptors or ion channel-related proteins, can occur in both paraneoplastic and non-paraneoplastic disorders, and have been shown to be pathogenic in some instances. For example, in MG patients autoantibodies against the acetylcholine receptor (AChR) cause a loss of the AChRs at the neuromuscular junction by different mechanisms: crosslinking and internalisation of the receptors, morphological damage to the synapse due to complement activation with subsequent lysis of the postsynaptic membrane, and direct blockade of the AChR function (Vincent, 2002; Drachman et al, 1978). Importantly, the disorders with extracellular autoantibodies tend to have good responses to immunotherapies (Vincent, 2010).

Autoimmune diseases targeting the PNS and CNS can include neuromuscular, autonomic and neuropsychiatric disorders. Antibody-mediated disorders can cause muscle weakness due to reduced neuromuscular junction activity, hyperexcitability of peripheral nerves leading to spontaneous muscle activity and pain, or weakness and sensory loss as a result of peripheral neuropathy. Only recently has it become clear that central nervous system disorders associated with seizures, psychosis, dementia, movement disorders, sensory symptoms and catatonia (Melzer et al, 2013), can be associated with, and likely caused by, autoantibodies to neuronal proteins (Table 1.4).

Table 1.3. Onconeural antibodies, associated clinical syndromes and tumours

Antigen	Cellular localisation	Clinical Syndromes	Associated tumour
Hu proteins	Intracellular	Neuropathy, limbic encephalitis, cerebellar degeneration, autonomic dysfunction	Small-cell lung cancer
Ma (1,2) proteins	Intracellular	Limbic encephalitis, cerebellar ataxia, polyneuropathy	Diverse epidermal tumours (lung, skin, gastrointestinal and renal) and germ cell tumours (Ma2)
Yo proteins	Intracellular	Cerebellar degeneration	Gynaecological cancer (breast, ovarian, endometrial).
Ri proteins	Intracellular	Cerebellar degeneration, encephalitis, myelitis, opsoclonus myoclonus	Breast cancer
Tr	Intracellular	Cerebellar degeneration	Hodgkin lymphoma
Collapsin response mediator protein 5 (CMRP5, CV2)	Intracellular	Corea, optic neuritis, neuropathy, limbic encephalitis	Small-cell lung cancer, thymoma

Table 1.4. Antineuronal antibodies and associated clinical syndromes

Antigen	Cellular localisation	Clinical Syndromes	Pathogenic Mechanism
Glutamic acid decarboxylase (GAD)	Intracellular	Stiff Person Syndrome (SPS) Cerebellar ataxia Epilepsy	Unknown, evidence for both cellular and humoral mediated mechanisms. Antibodies are possibly pathogenic
Amphiphysin	Intracellular	Stiff Person Syndrome (SPS)	Unknown, antibodies are possibly pathogenic
N-methyl-D-Aspartate receptor (NMDAR)	Extracellular	Epilepsy Encephalitis Movement disorders	Pathogenic antibodies cause cross-linking and internalization of receptors
Leucine-rich glioma-inactivated protein 1 (LGI1). VGKC complex	Extracellular	Cognitive impairment Encephalitis Epilepsy Movement disorders	Pathogenic antibodies cause cross-linking and internalization of receptors
Contactin-associated protein-like 2 (CAPR2). VGKC complex	Extracellular	Cognitive impairment Encephalitis Epilepsy Morvan´s syndrome Movement disorders	Unknown
GABAA receptor	Extracellular	Encephalitis	Unknown
GABAB receptor	Extracellular	Encephalitis	Unknown

		Cognitive impairment	
Dopamine 2 receptor	Extracellular	Encephalitis Movement disorders	Unknown
Aquaporin 4 (AQP4)	Extracellular	Optic neuritis	Pathogenic antibodies cause cross-linking and internalization of receptors
P/Q-type voltage-gated calcium channels (VGCC)	Extracellular	Lambert-Eaton myasthenic syndrome	Pathogenic antibodies block channels at presynaptic terminal of neuromuscular junction.
AMPA receptor	Extracellular	Limbic encephalitis	Pathogenic antibodies cause cross-linking and internalization of receptors
Myelin Oligodendrocyte Glycoprotein (MOG)	Extracellular	Optic neuritis Longitudinally extensive transverse myelitis (LETM)	Unknown
Nicotinic acetylcholine receptors (NAChR)	Extracellular	Myasthenia gravis	Pathogenic antibodies block channels at postsynaptic terminal of neuromuscular junction, cause cross-linking and internalization of receptors and cellular lysis by complement activation.

Glycine receptor (GlyR)	Extracellular	Stiff person Syndrome (SPS) Progressive Encephalomyelitis with Rigidity and Myoclonus (PERM) Epilepsy	Unknown
Ganglioside GM1	Extracellular	Guillain-Barré syndrome	Unknown

AMPAR: α-amino-3-hydroxy-5-methyl-4-isoxazolepropionic acid receptor; GABA: γ-aminobutyric acid; VGKC: Voltage gated potassium channels.

These disorders have gained increasing recognition over the last 10 years despite the traditional assumption that the PNS and CNS are separated from the circulation by the blood-nerve barrier (BNB) and the blood-brain barrier (BBB) respectively, and therefore 'immune-privileged'. The blood-brain barrier (BBB) is the interface between the central nervous system (CNS) and the immune system, employing mechanisms that both separate and connect the two systems. The BBB blocks the exchange of unregulated substances between the CNS and the circulation, allowing only the passage of regulated substances including immunomodulatory molecules such as chemokines, cytokines, and immune cells in response to signals secreted from both the CNS and the immune system (Banks and Erickson, 2010; Erickson et al, 2012). Immunoglobulins, for instance, are normally present at low levels in the cerebral spinal fluid (CSF). However, this does not mean that the CNS is isolated and without reach from the immune system; on the contrary, there are complex and interdependent mechanisms through which the immune system monitors the movement of cells and substances to and from the CNS (Hickey et al, 2001).

The criteria for defining autoimmune mediated disease (Table 1.2) have been achieved in some autoimmune neurological disorders of the PNS, such as MG, the Lambert–Eaton myasthenic syndrome (LEMS) and acquired neuromyotonia (NMT), which have pathogenic autoantibodies to acetylcholine receptor, voltage-gated calcium and potassium ion channel related proteins respectively (Lang et al, 1981; Lang et al, 2003). However, these criteria have not been fully met in many autoimmune neurological disorders of the CNS, with the exception of the N-methyl-D-Aspartate receptor (NMDAR) encephalitis (Lancaster et al, 2012) in which the data are still not complete. One of the difficulties is that the relative impermeability of the BBB to the antibodies in animal model makes it more difficult to demonstrate direct causality between the circulating antibodies and clinical features.

One particular disorder of the CNS with known autoantibodies, that has not fulfilled the criteria for autoimmune mediated diseases, and therefore need further investigation, is the stiff person syndrome (SPS) and its variants, with GAD or glycine receptor antibodies.

1.2. Stiff person syndrome (SPS) and related diseases – historical overview

Stiff person syndrome (SPS) is a very rare and progressive disease of the CNS that was first described by Moersch and Waltman in 1956. SPS has a prevalence of 1 per million in the European population, a female to male ratio of 2:1 (Duddy and Barker, 2009), and is characterized by axial and appendicular stiffness with superimposed episodic stimulus-sensitive spasms without other neurological signs (Meinck and Thompson,

2002). Since the original report of SPS, which was called stiff man syndrome (SMS), several variants presenting with other neurological signs have been reported making the clinical picture more complex (Dalakas, 2000). In order to help to establish the phenotypes, some authors have proposed criteria for diagnosis (Barker, 1998) (Brown and Marsden, 1999).

1.2.1 **Classical SPS**

1.2.1.1 Clinical presentation

The age of onset is usually 30–50 years of age. The onset is generally insidious with rigidity in the axial muscles, which becomes constant in weeks to months, spreading into the proximal limbs. Muscle stiffness affects principally the lumbar paraspinals giving rise to the characteristic hyperlordosis, and is usually symmetrical in the proximal limbs where continuous co-contraction of agonist and antagonist muscles makes motion in the joints very difficult. This gives rise to a wooden posture on voluntary movement, particularly when walking. SPS has three different stages: early, late and end stage. In the initial stages the rigidity fluctuates but as the disease progresses rigidity becomes fixed. In some cases the rigidity can affect the respiratory muscles producing ventilatory restriction and dyspnoea (Dalakas, 2000).

Muscle spasms often induced by sudden stimuli are superimposed. Stimuli such as sudden noise, touch, active motion and emotional responses (anger, fear) precipitate the spasms and increase the rigidity. Spasms may appear as myoclonic jerks, are usually bilateral involving the limbs and trunk, and are followed by tonic activity that slowly subsides over time. Spasms can be accompanied by intense pain and eventually cause skeletal fractures and joint subluxations (Meinck and Thompson, 2002). SPS patients

also often present with anxiety and task-specific phobias which, coupled with emotionally triggered spasms, contribute to the initial misdiagnosis as a psychogenic disorder (Dalakas et al, 2009).

SPS patients usually have a slow progression with eventual stabilisation of the disease, but are left with severe disability that affects quality of life and life expectancy (Barker, 1998).

1.2.1.2 Aetiology

The aetiology of SPS is unknown but it is believed to be an autoimmune-mediated disease since individuals with SPS have a high association with other autoimmune diseases, and autoantibodies. Approximately 40% of SPS patients have diabetes mellitus type I and/or have other organ specific autoimmune disorders, including Hashimoto's thyroiditis, pernicious anaemia, myasthenia gravis or vitiligo. They frequently also have serum autoantibodies: anti-nuclear, anti-thyroglobulin, anti-parietal cells, anti-intrinsic factor, anti-RNP, anti-Jo1 and anti-gliadin (Dalakas, 2000).

More relevant, approximately 60 to 80% of SPS patients have antibodies to synaptic proteins such as glutamic acid decarboxylase (GAD) or amphyphysin; much less common are antibodies to gephyrin and GABAA receptor associated protein (GABARAP) (Dalakas et al, 2009). A recent study found GAD antibodies in 100% of patients with the full spectrum of non-paraneoplastic SPS (Chang et al 2013). GAD is the rate-limiting enzyme in the synthesis of GABA, a major inhibitory neurotransmitter in the CNS, and a disruption of the inhibitory GABAergic pathways, that regulate motor behaviour, would be consistent with the symptomatology of SPS. However, the presence of GAD antibodies in other neurological syndromes such as cerebellar ataxia

and basal ganglia disease (Meinck et al, 2001) and also in type 1 insulin-dependent diabetes mellitus and other autoimmune endocrinopathies, questions their relevance, although the antibody titres are lower in diabetes than in SPS patients (Chang et al. 2013). However, this raises the possibility that the presence of GAD antibodies is only an epiphenomenon rather than a primary pathological process directed against the GABAergic neurons that contain the enzyme. On the other hand, it has been shown that SPS patients have a raised GAD antibody index (ASI, antibody specific index) suggesting that GAD antibodies are being produced in the CNS (Saiz et al, Brain 2008). It is widely considered that the intrathecal synthesis of GAD autoantibodies would be consistent with an immune-mediated chronic encephalomyelitis, which correlates with the pathological findings (Koerner et al, 1999: Dalakas et al, 2001).

1.2.1.3 Treatment

The aims of the treatment in SPS patients are:

a) Symptomatic relief by increasing cortical and spinal inhibition: agents that enhance GABAergic neurotransmission such as benzodiazepines and baclofen, and anti-convulsants such as valproate, vigabatrin, tiagabine, and leviteracetam, that have been used with variable rates of success. High doses have to be used due to habituation or disease progression, leading to undesired and potentially fatal side effects, and since there is no effective monotherapy, a combination of benzodiazepines, muscle relaxants, and anticonvulsants is often required..
b) To reduce the levels of the antibodies by immunologic interventions: plasmapheresis, intravenous immunoglobulin (IvIgG), corticosteroids, and other immunomodulatory agents including rituximab, azathioprine, methotrexate, cyclophosphamide and mycophenolate mofetil have been used in SPS patients

but also to different extents of success. IvIg was shown to be beneficial in a placebo-controlled, cross-over trial (Dalakas et al, 2001), while plasmapheresis and corticosteroids were effective in some reported cases, but no controlled trials have has been conducted(Meinck and Thompson, 2002), In addition, the use of corticosteroids in SPS has to be weighed against the possibility of diabetes exacerbation or initiation. A controlled trial is being conducted for rituximab (Dalakas et al, 2009).

1.2.2 **Variants of SPS**

1.2.2.1 Stiff limb syndrome (SLS)

Approximately 30% of the SPS patients present with asymmetrical or unilateral rigidity and painful spams affecting the limbs distally. SLS patients do not show lumbar hyperlordosis, but present with fixed posturing of the distal limbs. About 40 to 50% of SLS patients have mild sphincter and brainstem disturbance but this is usually transient and, unlike the progressive course of SPS, SLS has a relapsing remitting course. SLS has a poorer prognosis in terms of disability as half of the patients become wheel-chair or bed bound after a few years. They do not respond very well to symptomatic treatments; diazepam and baclofen provide relief to spasms but they are not very effective in relieving stiffness. The response to immunotherapy has not been established in these patients (Duddy and Barker, 2009).

SLS is not usually associated with T1DM, and GAD-Abs were found in only 15% of the patients (Barker, 1998). Meinck, Thompson and Dalakas, in the description of their series, found a high clinical overlap between SPS and SLS and about 75% progress from SLS to SPS.

1.2.2.2 Jerking SPS

Patients with jerking SPS initially present with the characteristic progressive axial and appendicular rigidity of SPS, before the onset of reticular reflex myoclonus. However, some series have reported seizures, nystagmus, and ataxia, indicating a more widespread syndrome affecting the cerebellum, brainstem and cerebral cortex. Post-mortem studies in some of these patients showed an encephalopathic process with cerebellar degeneration, brainstem and spinal cord lesions (Duddy and Barker, 2009). Other authors called this syndrome SPS plus (Dalakas et al, 2009).

1.2.2.3 Paraneoplastic SPS

Segmental or generalised muscle rigidity, spasms, and myoclonus confined to the upper limbs without lumbar hyperlordosis, or sensory manifestations, and often with a rapid progression over months are characteristics of SPS associated with malignancies. Breast and small lung cancers are the most common tumours found in these patients and the neurological symptomatology may precede the discovery of cancer by several years. Paraneoplastic SPS patients account for only 5% of all cases and may have antibodies to amphyphysin I, a synaptic vesicle protein; in rare patients GAD-Abs may be present and one case had antibodies to gephyrin, a postsynaptic anchoring molecule present in inhibitory synapses (Rosin et al, 1998). This patient had gait disturbance, jerking, dysarthria, and dysphagia due to stiffness in the tongue, as well as stiffness in the neck, trunk, shoulders, and legs associated with an undifferentiated carcinoma of the mediastinum. Most cases of paraneoplastic SPS have a poor response to diazepam, but improve with steroids (Murinson, 2004), and treatment of the underlying tumour.

1.2.2.4 Progressive encephalomyelitis with rigidity and myoclonus (PERM): historical perspective

PERM is classically considered an SPS variant. It is a more generalised disorder than SPS, and includes prominent brain stem findings, long-tract signs, sensory symptoms, autonomic dysfunction, and rapid progression. PERM was first describe by Whiteley et al (1976), but possibly the first case report was published by Campbell and Garland in 1956 when they called it 'subacute myoclonic spinal neuronitis' (Whiteley et al, 1976; Duddy and Barker, 2009). PERM patients present with axial muscle stiffness, rigidity, and painful spasms, similar to SPS; but myoclonic jerks involving all limbs, other diffuse brainstem signs such as dysarthria, dysphagia ophthalmoplegia, nystagmus, the presence of long tract signs (upper motor neuron signs and sensory symptoms), and cranial nerve involvement, distinguish PERM from SPS. About 60% of PERM patients have autonomic disturbance that may be potentially fatal, and up to 10% present with a more diffuse cortical disturbance (seizures or cognitive impairment). Less common symptoms and signs include sphincter disturbance, lower motor neuron signs, and retinopathy (Duddy and Barker, 2009; Murinson, 2004).

The onset of the disease is often subacute over weeks, and there can be rapid progression, unlike SPS, with exacerbations and remissions. Traditionally, PERM has a poor prognosis; 25% of the patients require prolonged intensive care treatment and the mortality rate can be as high as 40% (Duddy and Barker, 2009). There is little information about treatment responses and outcomes in PERM patients, but a number of recent cases report a good response to a combination of diazepam, baclofen, with corticosteroids, IvIg or plasma exchange, as will be described in more detail below.

1.2.3 **Clinical classification of SPS and its variants**

Classical SPS and its variants demonstrate distinct clinical characteristics, albeit the overlap in rigidity, spasms, immunological and pathological features suggest that they are closely related. For example after many years, SPS may evolve into a clinical picture similar to PERM. The similarity in some of the clinical findings and the variability in the course of the disease can make it difficult to reach a definite diagnosis, and patients need regular diagnostic evaluation to define the right clinical spectrum. In order to establish distinctions between these syndromes, a classification based on the presence of encephalomyelitis was proposed. Two main syndromes were defined a) SPS without encephalomyelitis which includes classical SPS, b) SPS with encephalomyelitis, or SPS plus, which includes SLS, jerking SPS and PERM. This classification seems to correlate fairly well with the presence of GAD-Abs, the response to treatment and prognosis; SPS patients with GAD antibodies tend to have better responses and outcomes compared with the SPS plus patients, some of whom may have a paraneoplastic origin (Brown and Marsden, 1999).

The discriminating features are summarized in table 1.5, but, there are some patients whose semiology do not fit completely and should be classified as ‘atypical SPS’ until a better understanding of the disease allows a proper classification of those patients. Moreover, during the last few years it has become clear that PERM is often a distinct antibody-mediated disease, and the focus will now be on that condition.

Table 1.5. Discriminating features of classical SPS and its variants

	Classical SPS	SLS	Jerking SPS	PERM	Paraneoplastic SPS
Distribution of rigidity	Axial	Distal limb	Axial	Axial and limb	Axial
Brainstem signs	-	-	+	++	-
Long tracts involvement	-	-	±	++	-
Clinical course	Slow progression	Relapsing and remitting	Slow progression	Rapid progression	Slow progression
GADAbs	70-98%	15-83%	?	0-76%	
Other antibodies	-	-	-	GlyRabs	Amphyphysin Gephyrin GABARP
CMUA	Axial muscles	Limb muscles	Axial muscles	Axial and limb muscles	Axial muscles

Modified from Chang T. 2007.

1.3. Progressive encephalomyelitis with rigidity and myoclonus (PERM)

As briefly discussed above, PERM is a rare disease of unknown aetiology formally described as an SPS variant, and possibly caused by inflammation of the brainstem and the spinal cord.

1.3.1 Physiopathology of SPS and related syndromes

The exact physiopathological mechanism underlying the clinical picture of PERM and related conditions is unclear. The evidence suggest an impairment in cortical and spinal inhibitory circuits as the most likely mechanism, but it is unknown if the deficit is due to a functional block of synaptic transmission at the presynaptic and postsynaptic level, or is a reflection of primary neuronal loss.

1.3.1.1 Neurophysiology of SPS and related syndromes

The motor units of normal individuals do not fire when muscles are at rest; they fire only during voluntary contraction. In SPS and related conditions patients have involuntary continuous motor unit activity (CMUA) in agonist and antagonist muscles which gives rise to rigidity despite attempted relaxation. The presence of CMUA at rest is the physiological hallmark of these patients, although it can be present in other neurological diseases such as tetanus and focal lesions of the spinal cord (Levy et al, 1999). Most of the electrophysiological results have been obtained in SPS patients.

CMUA is found in axial and appendicular muscles; the motor unit potentials have normal morphology and there are no signs of denervation. Rigidity and CMUA lessen or disappear during sleep, anaesthesia or after diazepam administration, pointing to a

central origin. The origins of CMUA and the contribution from different levels of the motor system have been investigated using the H reflex, the electrophysiological equivalent of the stretch reflex. Studies have shown that the CMUA is not a primary abnormality of the motor neuron or of the monosynaptic stretch reflex arc, in contrast to the CMUA observed in tetanus, suggesting that CMUA is driven by inputs to spinal motor neurons either at a spinal or cortical level (Meinck and Thompson, 2002; Rakocevic and Floeter, 2012).

CMUA in SPS and related conditions not only occurs at rest but also during voluntary contraction. In normal conditions the contraction of the agonist muscle will induce a reflex relaxation in the antagonist muscle, called reciprocal inhibition. This is mediated by the la spinal interneurons. SPS patients have a disrupted reciprocal inhibition leading to simultaneous co-contraction of agonist and antagonist muscles that impedes the normal movement and results in rigidity (Fig. 1.1) (Floeter et al, 1998).

One characteristic observed in SPS patients, but not in patients with other causes of hypertonia, is that exteroceptive or cutaneomuscular reflexes are enhanced and poorly habituated, accounting for the stimulus-induced spasms and jerks observed in these patients. Cutaneomuscular reflexes are polysynaptic reflexes mediated by sensory stimulation and modulated, by descending afferents, via presynaptic inhibition; in SPS patients the exaggerated exteroceptive reflexes can spread unilaterally or bilaterally to muscles distant from the site of stimulation that are not involved in the reflex. After eliciting the normal reflex, the exaggerated response is characterized by an initial myoclonic burst followed by a period of tonic activity (Meinck and Thompson, 2002). Further consideration of the neurophysiology of these phenomena will be discussed below.

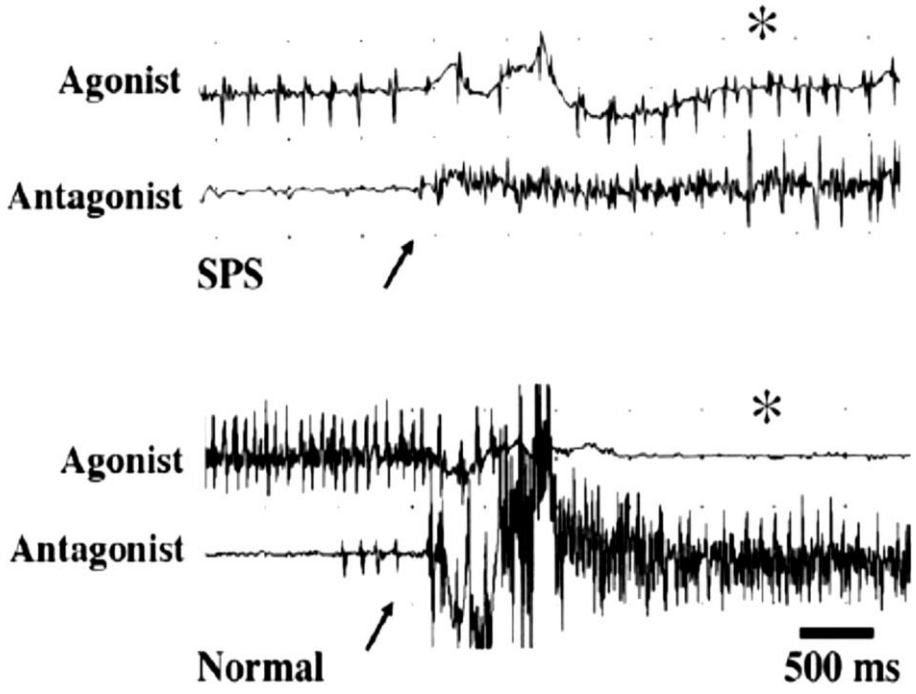

Fig. 1.1. Needle electromyographic recordings in a patient with SPS (upper trace) shows involuntary continuous motor unit activity (CMUA) in both the agonist and antagonist muscles (asterisk) at rest and after voluntary contraction (arrows). By contrast the same recordings in a normal patient (lower trace), the continuous motor unit activity is silenced after voluntary contraction (asterisk), showing reciprocal inhibition between antagonist muscles. (Figure obtained from Racocevic and Floeter, 2012).

1.3.1.2 Neuropathology of SPS and related syndromes

Abnormalities in the CSF include pleocytosis, elevated protein levels, oligoclonal bands and autoantibodies in the CSF (Duddy and Barker, 2009; Meinck and Thompson, 2002) but the pathological findings have been inconsistent. Initial post-mortem reports were normal, but more recent reports showed GABAergic neuronal loss predominantly in the spinal cord and the cerebellum and loss of spinal motor neurons (Meinck and Thompson, 2002; Duddy and Barker, 2009).

By contrast, the pathological findings in PERM patients have been more consistent, showing a generalised inflammatory picture with perivascular infiltration of neural parenchyma by lymphocytes, monocytes, and plasma cells, accompanied by gliosis, demyelination and neuronal loss. These changes are most intense in the brainstem and spinal cord, but have been observed sparsely in other brain regions including the basal ganglia, cerebral and cerebellar cortices (Marsden et al, 2012). The neuronal loss within the spinal cord appeared restricted to the central grey zones affecting the spinal interneurons (spinal interneuronitis), leaving lower motor neurons and corticospinal tracts relatively unimpaired (Whiteley et al, 1976; Howell et al, 1979; Watanabe et al, 1984). In addition, there have been some reports of PNS involvement, mainly ganglionitis, affecting both the sympathetic and dorsal root ganglia (Barker et al, 1998), and moderate neurogenic atrophy in muscles, without histopathological evidence of damage in the peripheral nerves (Howell et al, 1979). To date ten PERM cases have been reviewed showing a consistent meningo-polyencephalomyelitis, affecting principally the spinal cord and brainstem with some sparse involvement in other brain areas (Table. 1.6).

Table 1.6. Summary of the pathological findings in patients diagnosed with progressive encephalomyelitis with rigidity and myoclonus (PERM)

Case	Diagnosis	Pathological findings
Campbell & Garland (1956) Case 1	Subacute myoclonic spinal neuronitis	Widespread perivascular lymphocytic cuffing
Campbell & Garland (1956) Case 3	Subacute myoclonic spinal neuronitis	Subacute encephalomyelitis
Kasperek & Zebrowski (1971)	SMS encephalomyelitis	Perivascular lymphocyte cuffing, brainstem cord gliosis, demyelination
Lhermitte et al. (1973)	Brainstem encephalomyelitis	Brainstem, cord perivascular lymphocyte cuffing gliosis, neuronal loss
Whiteley et al. (1976) Case 1	PERM	Brainstem, cord perivascular lymphocyte cuffing gliosis, neuronal loss, demyelination
Whiteley et al. (1976) Case 2	PERM	Brainstem, cord perivascular lymphocyte cuffing gliosis, neuronal loss
Howell et al. (1978)	PERM	Brainstem, cord perivascular lymphocyte cuffing gliosis, demyelination selective loss spinal interneurons
Bateman et al. (1990)	Paraneoplastic encephalomyelitis	Perivascular lymphocytic infiltrate
Back et al. (1997)	PERM and Cerebellar ataxia	Perivascular lymphocytic cutting, neuronal cell loss, and micro/astrogliosis
Turner et al. (2011)	PERM	Oedema, inflammation in the hypocampus and cerebellum, perivascular lymphocyte infiltrate

1.3.2 Aetiology of SPS and related syndromes

It is believed that SPS has an autoimmune aetiology. SPS patients have autoantibodies to GAD, show association with other autoimmune diseases such as autoimmune thyroiditis and pernicious anaemia and with certain human leucocyte antigens (HLA) such as HLA-DQB1*0201 (Pugliese et al, 1993) and HLA-DRB1*0301 (Dalakas et al, 2000). The classification of PERM as an SPS variant based on the clinical overlap between PERM and SPS, have led some authors to raise questions about the distinction between these two syndromes, based only on the type of onset and the progression of the illness (Espay and Chen, 2006); therefore, it has been believed that PERM has the same autoimmune aetiology as SPS.

1.3.2.1 Autoimmunity in SPS and variants

The mechanisms that trigger the loss of immune tolerance are not well understood in many autoimmune diseases including SPS, but there is one case report that shows a temporal association between a preceding viral infection (West Nile virus) and the occurrence of SPS, suggesting a possible autoimmune activation with cross-reacting antigens. In addition, molecular mimicry between GAD65 and other viruses such as coxsackie virus and cytomegalovirus have been reported (Atkinson et al, 1994; Hiemstra et al, 2001). This evidence, plus the presence of GAD65 reactive T-cells required for the production of high affinity switched-class antibodies, in conjunction with the presence of antibodies against proteins relevant for the function of GABAergic synapses, argues in favour of an autoimmune aetiology in SPS (Dalakas et al, 2009; Rakocevic and Floeter, 2012).

However, whether these autoantibodies are the pathogenic cause of the disease remains controversial. Mainly, because a) Intrathecal GAD antibody titres do not correlate with disease severity or duration; b) GAD65 antibodies do not transfer the disease from mothers to infants (Burns, 2005); c) all SPS antigens, GAD, amphyphysin and gephyrin, are intracellular and thus protected from antibodies by the cellular membrane.

Nevertheless, evidence in favour of a pathogenic role of GAD-Abs in SPS comes from in vitro studies that show effects on GABA synthesis and presynaptic release. Rat cerebellar extracts showed reduced production of GABA after being exposed to purified IgG from GAD-Ab positive patients (SPS and T1DM); although in two patients the effect was observed with serum but not with purified IgG (Dinkel et al, 1998). Another study also showed reduced synthesis of GABA from radiolabelled glutamate sera from 6 of 12 GADAb-positive patients which blocked the enzymatic production of recombinant GAD65, but control sera were not tested (Raju, 2005). Two additional studies, using patch-clamp recordings from intact neurons in slices of rat cerebellum or hippocampus, showed decreased amplitude of inhibitory postsynaptic currents when slices were perfused with GAD-Ab positive CSF from patients with various CNS syndromes (Ishida et al, 1999; Vianello et al, 2008), and the effects were not observed when slices were exposed to normal control CSF. A later study suggested that the GAD IgG acted presynaptically impairing the release of GABA, since there was an increased paired pulse ratio (Mitoma et al, 2000).

In vitro effects of amphyphysin antibodies have also been demonstrated. One study using calcium imaging to measure postsynaptic potentials, showed that amphiphysin IgG from a patient with paraneoplastic SPS caused a reduction in GABA-induced calcium influx into cultured embryonic motor neurons (Geis et al, 2009), and patch-

clamp recordings in hippocampal granule cells, found an activity-dependent decrease of the amplitude of evoked inhibitory postsynaptic currents in brain slices treated with amphiphysin antibodies. The same group showed internalisation of the IgG in cultured hippocampal neurons, which was not observed when cells were treated with control IgG (Geis et al, 2010).

More recent evidence comes from passive transfer models into rats. In one study, rats were injected intraperitoneally with IgG from an SPS patient, with antibodies to amphyphysin, 4-5 days after adoptive transfer EAE. The rats developed transient axial spasms with increased EMG activity, dragging gait and increased lordosis; these effects were not observed when rats were injected with control IgG (Sommer et al, 2005). In another study, intrathecal passive transfer of anti-amphyphysin antibodies from two SPS patients caused axial and appendicular rigidity accompanied by spasms and gait disturbance, and diminished post-activation depression of the Hoffmann reflex, not seen with control IgG (Geis et al, 2010), and a further study demonstrated anxiety-like behaviour in rats injected with amphyphysin IgG into the brain associated with immunostaining in specific brain structures such as the amygdala (Geis et al, 2012).

Finally, the same group have found that intracerebroventricular (icv) but not intrathecal injections of purified IgG form a GAD65-Ab positive patients caused motor dysfunction, characterized by impaired walking ability and reduced grip strength of the upper limbs, as well as postural and sensorimotor dysfunction. These rats showed IgG deposits in brain structures involved in motor control including the globus pallidus, internal capsule, striatum and anterior thalamus. No anxiety-like behaviour was observed in test or control groups of rats (Hansen et al, 2013).

However, in these studies the effects cannot be entirely attributed to GAD-Abs, as there could be other antibodies present in the sera, CSF or IgG fractions of the patients. Additionally, the electrophysiological effects occurred very fast after IgG administration and it is difficult to envisage how the antibodies can be taken up by the neurons so quickly to exert a rapid effect; and finally why amphyphysin antibodies preferentially affect the function of GABAergic synapses if amphyphysin is also present in glutamatergic synapses (Vincent, 2010). Indeed some of the motor effects observed in these studies may be non-specific; transient spasmodic reflexes and gait alterations are commonly observed in rodents that are injected with large volumes of fluid intraperitoneally. Furthermore, neither intrathecal or intracerebroventricular injection of GAD antibodies produced spasms or pronounced stiffness, nor deficits of H-reflex modulation in the injected rats, and these are the most relevant clinical and electrophysiological findings in SPS patients (Geis et al, 2012).

Perhaps, the most important question is how do the antibodies get internalised into the nerve terminals? These autoantibodies may be able to penetrate the cell possibly via ganglioside binding or Fc-receptor mediated binding (Wenthold et al, 1984), as suggested for autoantinuclear antibodies in systemic lupus erythematosus (Deng et al, 2000). This mechanism requires that certain peptide fragments could be expressed at the cell surface during GABA exocytosis, when synaptic vesicles transiently fuse with the neuronal membrane, allowing antibody recognition and antigen presentation to T cells. However, there is no experimental evidence that amphiphysin epitopes are exposed during this process.

Another possibility is cytotoxic mediated cell damage as observed in T1DM where a Th1 response against the GAD of the pancreatic B-cells is found. However, there is

very little evidence in favour of this mechanism. In fact, T cell responses were reported in only a small number of patient samples, and they do not show high production of interferon gamma required for an adequate T cell response (Costa et al, 2002). Another study showed a SPS-like encephalomyelitis disrupting GABAergic neurons in rats injected with activated T GAD65 CD4 cells (Burton et al, 2010), but in post-mortem studies of SPS patients there is no evidence of significant T-cell infiltration in the brain or the spinal cord (Holmoy et al, 2009). In addition, SPS patients have very high GAD titres which may be more consistent with a Th2 response that suppresses T-cell–mediated cytotoxicity (Lohmann et al, 2003). Overall, there are too few studies reporting T cell responses to draw any valid conclusion, and any T cell response may only be important in the early stages of SPS, driving humoral autoimmune processes (Skorstad et al, 2009).

Taken together these observations cast doubt on the pathogenic role of GAD and amphiphysin antibodies, addressing the necessity to search for other responsible autoantigens. In fact, a recent paper showed the existence of antibodies against undefined extracellular antigens on GABAergic neurons in the plasma of SPS patients (Chang et al, 2013)

1.4. A glycine receptor antibody-mediated disease?

As summarised above, PERM is a progressive debilitating disorder with increased mortality, and a highly variable course; the findings are similar to those of SPS with the addition of more widespread neurologic deficits. Despite its similarities with SPS, PERM is best described as a poly-encephalomyelitic process principally affecting the brainstem and the spinal cord (Duddy and Barker, 2009).

Whether, GAD autoimmunity plays a role in PERM patients is controversial. There are differences in the percentage of PERM patients in the reported series of cases. For example, Meinck and Thompson in 2002, described the presence of GAD antibodies in 76% of PERM patients, but other series of patients report a lower number of GAD-Ab positive patients ranging from 0% to 33% (McKeon et al, 2012; Barker et al, 1998); these differences may be due to different clinical diagnostic criteria used by the authors, and in general there seems to be an agreement that PERM patients have a weaker association with GAD antibodies and therefore belong to the group of GAD sero-negative SPS like syndromes (Murinson, 2004; McKeon et al, 2012).

The absence of GAD antibodies in PERM patients does not exclude an autoimmune aetiology. A patient who presented with hyperekplexia, rigidity, brainstem signs, and CSF lymphocytosis consistent with PERM, and was GAD-Ab negative but improved with immunosuppressive therapy, was the first to be described as having antibodies to the glycine receptor alpha1 subunit (GlyR α1) (Hutchinson et al, 2008). Since glycine receptors are expressed on the cell surface, they could be recognised as targets by the pathogenic antibodies which could then disrupt glycinergic inhibition and cause the loss of inhibition in these patients. This case report was the first to demonstrate an autoimmune aetiology which correlates with the clinical course of the patient.

During the course of the work for this Thesis, 16 cases of PERM GlyRα1-Ab positive patients were reported; 15 were GAD-Ab negative and responded well to immunosuppressive therapy (Iizuka et al, 2012; Peeters et al, 2012; Stern et al, 2013: Mas et al, 2011; Damasio et al, 2013; McKeon et al, 2013). Only one case appeared to be paraneoplastic since a thymoma was found and the patient recovered after thymectomy and immunotherapy (Clerinx et al, 2011). GlyR-Abs may be present with

other antibodies and may correlate with the symptomatology and the histological findings in these patients. For example, a case of PERM reported the coexistence of GlyR-Abs and NMDAR antibodies, and in this patient the neuropathological findings consisted in disseminated encephalomyelitis with IgG deposition on neurons and glial cells, accompanied with the presence of plasma cells and the presence CD8+ cytotoxic T cells in the hippocampus and cerebellum, suggesting a final pathway of T-cell mediated neuronal damage (Turner et al, 2011). Also, a more recent study showed the coexistence of GlyR-Abs and GAD antibodies in patients with an SPS phenotype, but some GAD-Ab negative patients had GlyR-Abs suggesting that GlyR-Abs may be present in a range of SPS phenotypes (McKeon et al, 2013).

In summary, GlyR-Abs are present in patients with brainstem and spinal cord hyperexcitability, but these patients may present additional clinical features and additional antibodies. GlyR-Abs may be pathogenic, since they bind to extracellular neuronal receptors, and patients with these antibodies respond to immunosuppressive therapy. Although the immune factors contributing to PERM may be diverse, including T cells, antibodies and cytokines, the recent evidence for GlyR-Abs strongly implies an antibody-mediated mechanism. The rest of the Introduction will concentrate on the role of GlyRs in spinal activity and how these may be disrupted in different disease states.

1.5. Glycinergic inhibition

1.5.1 Glycine receptor

Glycine is an amino acid with several functions in the body. It serves as a protein precursor, as a biosynthetic intermediate in metabolism, and in the central nervous system as an inhibitory neurotransmitter and co-agonist in excitatory synapses. The

action of glycine in the CNS is mediated through its interaction with the glycine receptor (GlyR). GlyR belongs to the superfamily of ligand gated ion channels, specifically the cysteine-loop (cys-loop) family, proteins that have a highly conserved 15-amino acid-spaced disulphide loops in their extracellular ligand-binding domain (Cascio et al, 2004); other ion channels that also belong to this family are the excitatory cation-permeable nicotinic and muscle acetylcholine receptors, the inhibitory anion-permeable γ-aminobutyric acid, type A and type C receptors ($GABA_A$Rs), and the cation-permeable serotonin type 3 receptor (5-HT3R) (Lynch, 2004; Webb, 2007).

GlyR opens in response to agonist binding leading to an influx of Cl- into the neurons, hyperpolarizing the membrane potential; thus glycine is considered an inhibitory neurotransmitter. GlyR and $GABA_A$R are responsible for mediating fast inhibitory neurotransmission in the mature central nervous system. The chloride-permeant glycine receptors are highly inhibited by the competitive binding of strychnine, distinguishing them from the glycine binding site on the N-methyl-D-aspartate family of glutamate receptors (Grenningloh et al, 1987). At the NMDA receptor, glycine is a required co-agonist along with glutamate regulating its activity; thus glycine has a role in excitation role as well.

GlyR are pentameric proteins comprised of five homologous membrane-spanning subunits arranged symmetrically around a central pore. Each subunit is composed of a large globular extracellular ligand-binding domain, four transmembrane α-helices (TM1-TM4) and a large intracellular loop between the third and fourth TM domain (Fig.1.3) (Lynch, 2004; Betz and Laube, 2006). GlyR have molecular heterogeneity; to date, 4 different alpha (α) subunits (α1, α2, α3, α4) and one beta (β) subunit have been identified. Sequence homology studies showed that α subunits have an amino acid

sequence similarity >90% with each other, and a 47% amino acid sequence homology with the β subunit (Lynch, 2004; Lynch, 2009) (Fig. 1.2). The α subunits have the glycine binding site and all α subunits can form functional homomeric pentamers; by contrast, the β subunit, which is responsible for the assembly and properties of the channel, can only be functionally expressed as a heteromeric pentamer with the α subunit, in a stoichiometric ratio of 3α:2β or 2α:3β (Betz and Laube, 2006) (Fig. 1.3).

Several GlyR subtypes are expressed in different CNS regions and are developmentally regulated. For example, in embryonic rats homomeric α2 receptor subtypes have been found to be predominant, with a decline in the first three weeks after birth, accompanied by an increase in expression of α1 and β subunits. In adult rats, glycinergic neurotransmission is mediated by α1β receptor subtype, but α2β, α3β, α4β heteromers are also found to a lesser extent in certain areas of the CNS; for example, α2β heteromers are found in the retina, hippocampus and cerebellum (Danglot et al, 2004; Garcia-Alcocer, 2008; Haverkamp et al, 2004). However, α2 neurotransmission is not indispensable for normal CNS function, since α2 knockout mice lack obvious neurological and visual deficits (Lynch, 2009). α3β heteromers are found in the retina, hippocampus, cerebellum and spinal cord (Haverkamp et al, 2003; Garcia-Alcocer et al, 2008; Eichler et al, 2009; Harvey, 2004) but α3 neurotransmission maybe be relevant to central pain sensitisation, since α3 knockout mice showed absence of pain sensitisation in chronic peripheral inflammation compared to normal mice, but no other neurological or visual deficits (Lynch, 2009). α4β heteromers are also found in the retina (Heinze et al, 2007). Extra-synaptic homomeric α1 and α3 GlyRs have been found widely distributed throughout the adult CNS, specifically present on presynaptic nerve

Fig. 1.2. Sequence alignment and homology of GlyRα subunits. CLUSTAL 2.1 software.

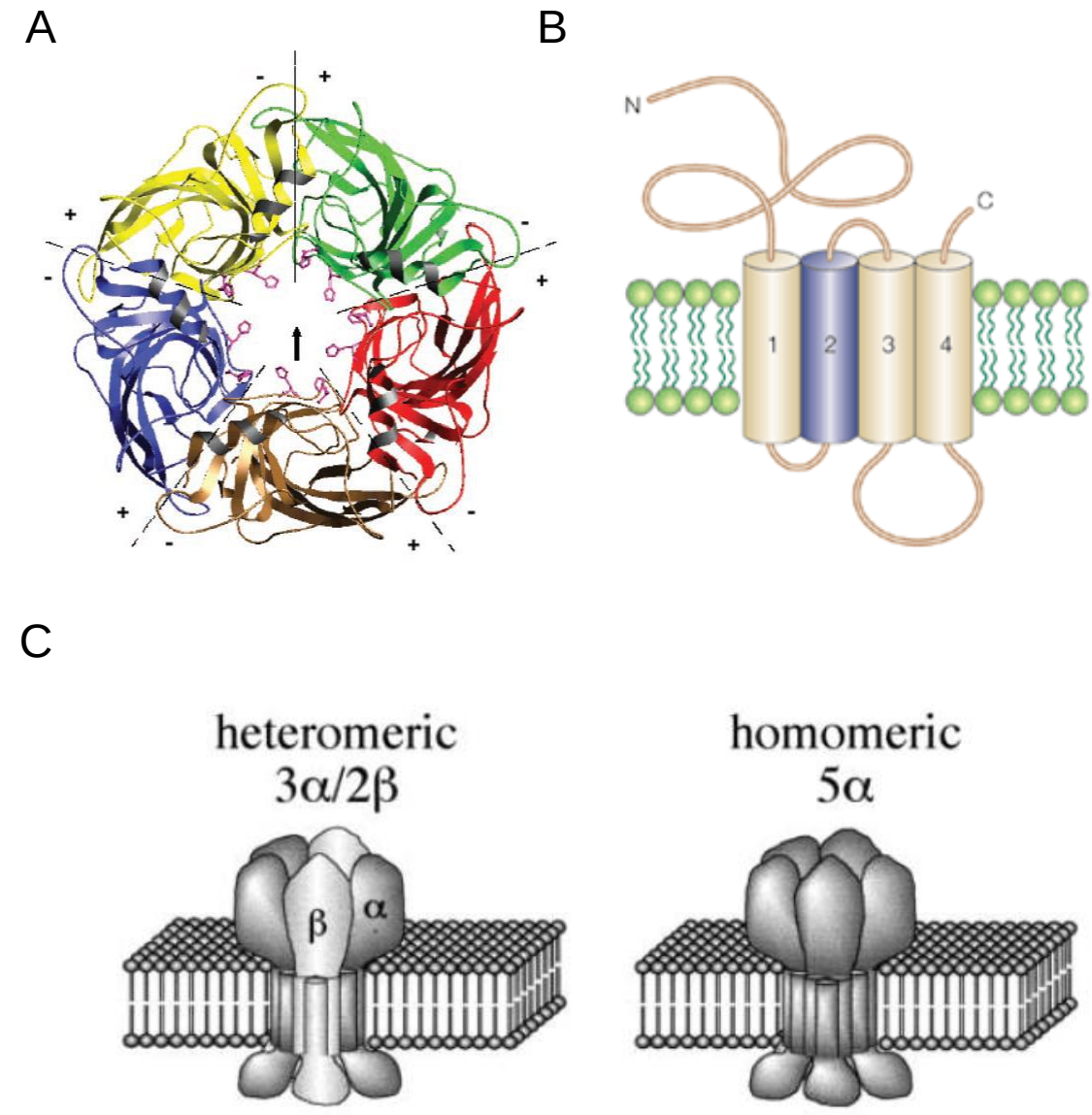

Fig. 1.3. Glycine receptor structure. A. Ribbon representation of the receptor viewed from the synapse showing the central pore, ***B.*** Membrane topology of the glycine receptor alpha1 subunit showing the transmembrane domains. The pore is located in the transmembrane domain 2. ***C.*** Arrangement of the glycine receptor in its heteromeric and homomeric conformations. Modified figures obtained from Lynch, 2004 and Legendre, 2001)

terminals regulating the release of glutamate, glycine or GABA neurotransmitters (Lynch, 2009).

1.5.2 Glycinergic synapse

Hetero-pentameric GlyRs are highly enriched and clustered on the postsynaptic neuronal membrane. Like GABARs, the clustering of GlyRs is mediated by the anchoring protein gephyrin, since GlyR clustering is abolished in gephyrin knock-out mice (Kirsch et al, 2006). These postsynaptic GlyR clusters are symmetrically opposed to presynaptic densities on glycinergic nerve endings. In the presynaptic boutons, glycine arises from the catalysis of serine by the isoenzime serine-hydroxymethyltransferase (SHMT), and reuptake by the glycine transporter 2 (GlyT2), a sodium/chloride transporter. Glycine accumulates in synaptic vesicles but no specific reticular glycine transporter has been described; it is thought that glycine uses the vesicular inhibitory amino acid transporter (VIAAT) which also transports GABA. This is supported by evidence showing that some presynaptic terminals can contain both GABA and glycine (Jonas et al, 1998). Glycine is degraded in the astrocytes by a mitochondrial and cytosolic enzyme cleavage system (GCS) (Daly et al, 1976) (Fig.1.4).

Released glycine can be controlled by another transporter of the Na+/Cl- family, the glycine transporter 1 (GlyT1), which is expressed in glial cells. GlyT1 is expressed mainly in the spinal cord, brainstem, diencephalon, retina, olfactory bulb and brain hemispheres, while GlyT2 is restricted to spinal cord, brainstem and cerebellum (Legendre, 2001) (Table 1.7).

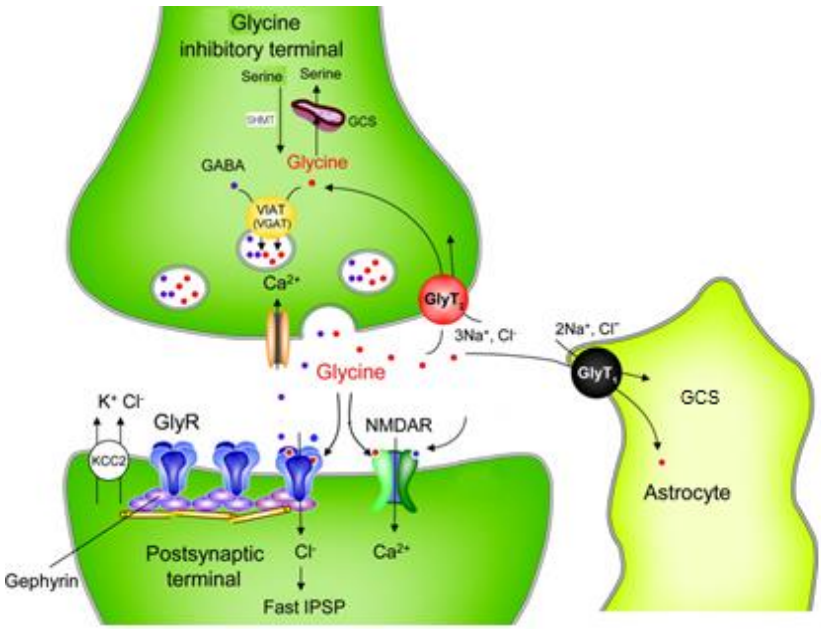

Fig 1.4. Diagram showing the glycinergic synapse with its presynaptic and postsynaptic components. (SHMT: serine-hydroxymethyltransferase, GCS: Glycine cleavage system). Note that glycine exerts a modulatory effect on NMDAR. Modified figure obtained from Benarroch, 2011.

Table 1.7. Distribution of GlyR subunits in different regions of the adult rat central nervous system

Area	α1	α2	α3	α4	β
Cerebral cortex	-	+	+	-	+
Hippocampus	-	+	+	-	+
Thalamus	+	+	-	-	+
Hypothalamus	+	-	+	-	+
Basal ganglia	-	-	-	-	+
Cerebellum	+	-	+	-	+
Brainstem	++	-	-	-	++
Spinal cord	++	+	+	+	++
Retina	+	+	+	+	+
Autonomic ganglia	+	-	-	+	+

Glycine, taurine, β-alanine and L-serine are all agonists, while strychnine, α-colubrine, cacotheline, nipecotic acid and isobutyric acid among other substances, are antagonists. Compounds that modulate the activity of glycinergic synapses include zinc, alcohol, picrotoxin, cocaine, cannabinoids and some anaesthetics and anticonvulsants (Legendre, 2001; Kirsch et al, 2006; Webb et al, 2007; Betz and Laube, 2006).

Glycinergic synapses were initially thought to be localised only in the spinal cord and brainstem where they regulate motor behaviour, but more recently glycinergic neurotransmission has also been demonstrated more widely in the CNS. For example, GlyRs have been identified in the spinal cord pain sensory pathways (Ahmadi et al, 2003), various brainstem nuclei including the brainstem reticular formation (Fort et al, 1993), and nuclei involve in central auditory pathways such as the medullary cochlear nucleus, the trapezoid body and the superior olivary complex of the pons (Ferragamo et

al, 1998; Kotak et al, 1998; Smith et al, 2000). Also, glycinergic synapses have been found in several cranial nerve nuclei, such as the medullary trigeminal (Yang et al, 1997), abducens (Russier et al, 2002) and hypoglossal motor nuclei (O'Brien et al, 1999).

Other regions where GlyRs have been found include the retina (Grunert et al, 1993) Greferath et al, 1994) and the cerebellum. In the cerebellum, glycinergic synapses mediate inhibitory neurotransmission between Lugaro cells and Golgi cells in the cerebellar cortex (Dieudonne et al, 1995), and between interneurons and principal cells in the deep cerebellar nuclei (Kawa et al, 2003).In the thalamus, GlyRs have been found in cell bodies and fibres but in the hypothalamus, GlyRs were found only in fibres, suggesting that the glycinergic projections originate from distant neurons (Rampon et al, 1996). More recently, glycinergic synapses have been found in the forebrain specifically in the human basal ganglia, substantia nigra (Baer et al, 2009) and also in structures of the limbic system, such as the amygdala (McCool et al, 2007). However, a detailed morphological and physiological characterisation of which GlyR subunits are expressed in different synapses is scant and there is no evidence of the presence of GlyRs in the cerebellum, hippocampus and cortex by immunohistochemical studies in the human brain.

Nevertheless, electrophysiological studies suggest a wider distribution. GlyR have been found extrasynaptically in several regions including the granular layer in the cerebellum (Kaneda et al, 1995), dopaminergic neurons of the juvenile immature substantia nigra pars compacta (Hausser et al, 1992), developing cortical neurons (Flint et al, 1998), and in the hippocampus (Danglot et al, 2004). The function of these extrasynaptic GlyRs is unclear but they may be involved in CNS development in the cortex (Flint et al, 1998),

and may play a regulatory role in the firing activity of the neurons in the hippocampus (Song et al, 2006). NMDA receptors are also located in the hippocampus and glycine exerts a regulatory activity by binding inside the NMDA receptor, which is possibly more important than its inhibitory role (Kemp et al, 199; Ahmadi et al, 2003).

In summary, a well-established role of glycinergic neurotransmission has been demonstrated for motor and sensory processing for movement control, inflammatory pain sensitization, vision and audition; a functional role remains to be demonstrated in many brain areas where glycine fibres and/or GlyR-subunit mRNA transcripts have been detected (Kirsch, 2006; Legendre, 2001; Betz and Laube, 2006).

1.5.3 Glycine and motor control

1.5.3.1 Spasticity and rigidity

Spasticity is observed in several neurological disorders, manifested as a sustained increase in muscle tone perceived during passive lengthening. Spasticity is due to an increase in the tonic and phasic stretch reflexes and in many cases is accompanied by exaggerated tendon jerks and pain (Mukherjee et al, 2010).

The physiopathology of spasticity includes alteration in spinal and supraspinal mechanisms. See Fig. 1.5 and Table 1.8

a) Spinal mechanisms: During voluntary movement the CNS uses sensory information to control the movement. In order to achieve this, activated sensory receptors elicit muscles reflexes, which adapt to different motor tasks and produce coordinated patterns of muscle contraction; the circuitry of these reflexes is located in the spinal cord.

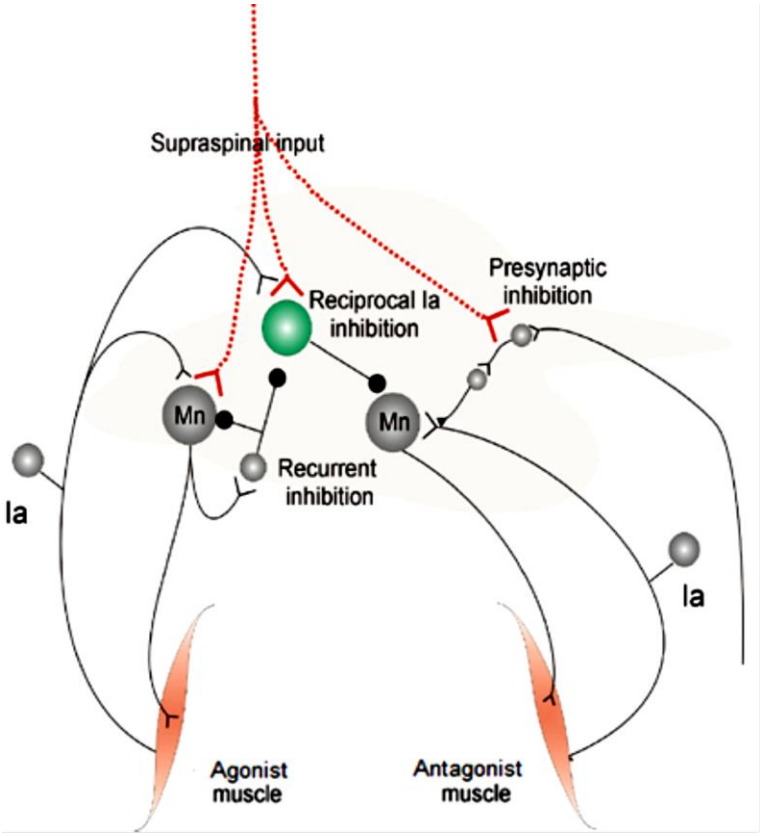

Fig. 1.5. Scheme of the spinal cord circuits. Supraspinal inputs are GABAergic while spinal circuits are glycinergic and GABAergic. Mn: Motoneuron. Modified figure obtained from F Biering-S et al, 2006.

Spinal reflexes can be monosynaptic (the stretch reflex) or polysynaptic. Some that are stretched excite the muscle spindles which in turn will cause a reflex contraction of the muscle; this reflex is important for the generation of muscle tone. Polysynaptic reflexes require the action of interneurons to integrate the information. Several spinal interneurons required for their reflexes have been described (Kandel and Schwartz, 2012):

Ia inhibitory interneurons are involved in reciprocal inhibition; they are stimulated by Ia sensory afferents from the muscle spindle and will inhibit alpha motor neurons innervating homonymous or heteronymous antagonist muscles. When reciprocal examination is evaluated through the H-reflex, it has two components: the early component is mediated by the release of glycine, and the late component is mediated by the release of GABA (Knikou et al, 2008).

Renshaw cells are involved in recurrent inhibition; they are situated in lamina VII of the ventral horn and stimulated by collaterals of the axons of motor neurons that inhibit the alpha motor neurons that innervate the agonist muscles. They also inhibit la inhibitory interneurons and gamma motor neurons. Renshaw cells release glycine and GABA neurotransmitters (Knikou et al, 2008).

Ib inhibitory interneurons are involved in non-reciprocal inhibition. They are stimulated by Ib afferent fibres from Golgi tendon organs and inhibit alpha motoneurons, innervating both homonymous and heteronymous agonist muscles. This disynaptic reflex was thought to be merely protective (autogenic inhibition) providing a safety mechanism to prevent muscle damage, but it is also involved in regulating muscle tension to control posture and movement. Ib inhibition was initially thought to be mediated by glycine but some effects are

likely to involve a presynaptic component and therefore mediated by GABA (Knikou et al, 2008).

Segmental interneurons are involved in presynaptic inhibition. They are activated by group I afferents, inhibited by flexor reflex afferents, and controlled by descending tracts (Jankowska et al, 1992). These interneurons are important for controlling sensory afferent feedback input from skin (skin-muscle reflexes), tendons, joints, viscera and muscles to the α-motor neurons through axo-axonic synapses. Presynaptic inhibition is mediated by GABA (Knikou et al, 2008).

Intermediate zone interneurons are involved in inhibition from group II afferents. They are stimulated by secondary sensory afferents from the nuclear chain fibres of the muscle spindle and excite gamma motor neurons innervating the intrafusal fibres. This regulates the sensitivity of the muscle spindle. Inhibition by group II afferents is mediated by interneurons that release GABA and glycine (Kandel and Scwarthz, 2012; Mukherjee et al, 2010).

b) Supraspinal mechanisms: Synaptic transmission in spinal reflexes can be modulated by descending pathways; it appears that voluntary processes can regulate the strength of the spinal reflexes at three sites: a) alpha motor neurons, b) interneurons, and c) presynaptic terminals of the afferent fibres. Supraspinal inputs come from five descending tracts, one originating in the cerebral cortex, (the corticospinal tract) and the other four originating from the brainstem, (the reticulospinal, the vestibulospinal, the rubrospinal, and the tectospinal tracts) (Kandel and Schwartz, 2012).

In humans, spasticity has been related to lesions in the corticospinal, reticulospinal, and vestibulospinal tracts, which in turn regulate Ia inhibitory presynaptic GABAergic interneurons. Disruption in the level of tonic

descending inhibition will lead to an increased response of alpha motor neurons to Ia input evidenced by an increase in tonic and phasic responses of the stretch reflex (Mukherjee et al, 2010).

Table 1.8. Summary of the inhibitory mechanisms involved in movement control and the neurotransmitter involved

Mechanism	Interneuron	Neurotransmitter	Localization
Reciprocal inhibition	Ia inhibitory	Glycine, GABA	Spinal cord
Non-reciprocal inhibition	Ib inhibitory	Glycine, GABA	Spinal cord
Recurrent inhibition	Renshaw cell	Glycine	Spinal cord
Presynaptic inhibition	Segmental	GABA	Spinal cord
Inhibition from group II afferents	Intermediate zone	GABA, Glycine	Spinal cord
Supraespinal descending input	Descending pathway	GABA	Brainstem, cortex

Electrophysiological studies in individuals with hereditary hyperekplexia, a condition caused by mutations in the GlyRα1 subunit, have alterations in the first period of reciprocal inhibition with no alterations in the GABAergic mediated presynaptic inhibition. Interestingly, recurrent inhibition and non-reciprocal inhibition, initially thought to be glycinergic-mediated were normal in these patients, which correlate with recent findings suggesting that these spinal pathways have a mixed GABAergic and glycinergic component. Indeed vesicles containing GABA and glycine have been found in spinal interneurons (Todd et al, 1996) and thus the GABAergic component may compensate for the glycinergic dysfunction (Floeter et al, 1996). This is consistent with

the whole cell patch-clamp recordings of spinal cord slices of the GlyRα1 mutant mouse, *spastic,* which showed decreased GlyR and GABAR mediated IPSCs compared to wild type mice, implying a possible presynaptic cross-modulation of GlyRs and GABAARs (von Wegerer et al, 2003).

When electrophysiological studies were performed in individuals with SPS, the results showed alterations in presynaptic inhibition, but not in the second period of reciprocal inhibition, although both are considered to be GABAergic-mediated. The authors suggested a differential effect of antibodies on different subsets of GABAergic neurons. No consistent abnormalities were found in the glycinergic-mediated recurrent inhibition, non-reciprocal inhibition Ib, or the first period of reciprocal inhibition, but in a few patients non-reciprocal inhibition was found to be diminished, which suggests mixed GABAergic and glycinergic components in recurrent and non-reciprocal inhibition (Floeter et al, 1998).

In summary, the modulatory pathways regulating spinal reflexes are more complex than initially thought and may include compensatory mechanisms between the different inhibitory pathways, and a differential susceptibility of interneuron populations or descending pathways. The heterogeneous clinical findings observed in patients with spasticity due to disruptions of glycinergic or GABAergic pathways are correspondingly complex.

1.5.3.2 Startle response

Startle is a fast stereotypical response to sudden and unexpected intense stimuli, which may be acoustic, tactile, visual or vestibular. The startle response is found throughout all mammals, and it is likely to have protective functions, preparing the animal for a

flight/fight response. It is composed of motor, autonomic, and emotional components. Startle is a prototype of reticular reflex myoclonus, since it cannot be supressed voluntarily.

The acoustic startle response (ASR) is mediated by a relatively simple neuronal circuit located in the brainstem that links the cochlear nuclei with the muscles of the face, neck, trunk, and limbs (Fig. 1.6). Neurons of a relay nucleus, the caudal pontine reticular nucleus (PnC), are important in the primary ASR pathway; the PnC is the origin of the reticulo-spinal tracts that monosynaptically innervate motor neurons in the brainstem and spinal cord. The PnC receives dense somatosensory inputs (trigeminal pathways), and also modulatory inputs from brain regions involved in emotional and learning processes, such as the limbic system; and in sensory gating, motivational and arousal states such as the colliculus, nucleus accumbens, prefrontal cortex and raphe nucleus via the pedunculopontine tegmental nucleus. Therefore, the ASR magnitude in humans and animals can be increased or decreased by a variety of physiological and pathological conditions and by drugs (Koch, 1999) (Fig. 1.7).

Glycinergic inhibition plays a role in controlling and modulating the startle response, as shown by exaggerated startle responses observed in strychnine intoxication, human hyperekplexia, mouse mutants lacking functional glycine receptors, and also mice with a mutation at the Zn+ binding site of the GlyRα1 subunit (Glra1(D80A)) that impairs potentiation of glycinergic currents by zinc (Hirzel et al, 2006). However, it is not clear whether the impairment in glycinergic inhibition occurs in the spinal cord or also includes additional impaired central glycinergic inhibition of the startle pathway in the brainstem.

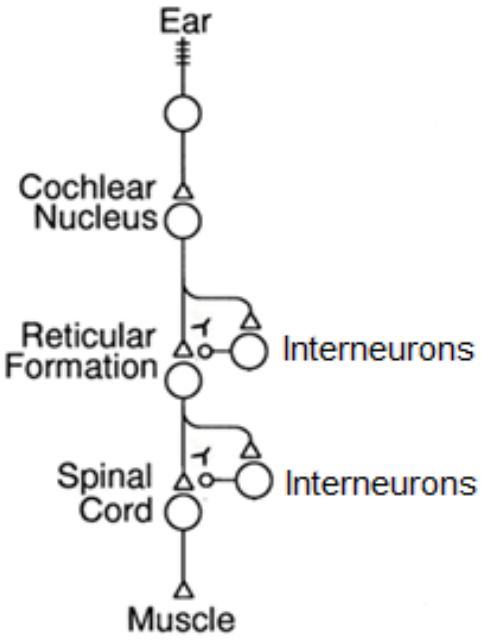

Fig. 1.6. Scheme of the acoustic startle response (ASR) neuronal circuit.

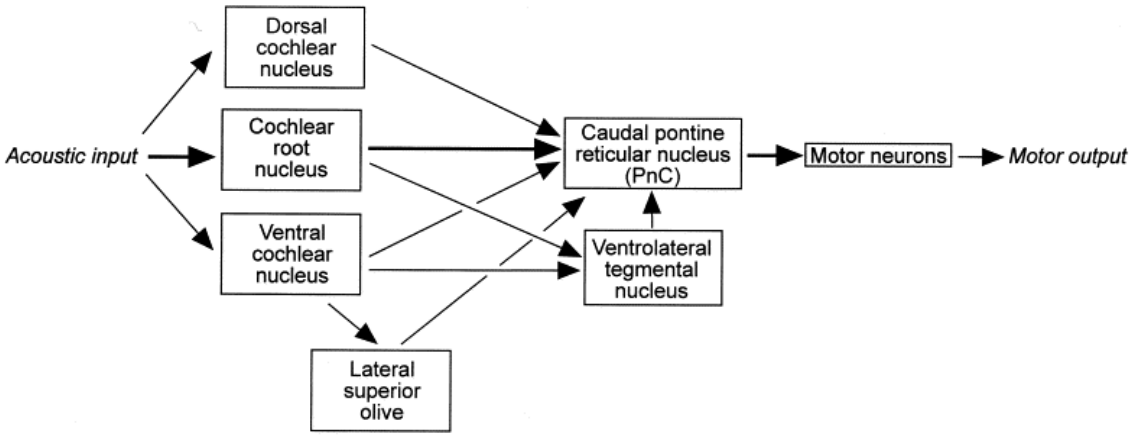

Fig. 1.7. Hypothetical acoustic startle response pathway (Figure obtained from Koch, 1999).

Evidence for additional glycinergic inhibition in the brainstem is contradictory; immunohistochemistry and situ hybridization studies have shown abundant GlyRs in the brainstem (Rampon et al, 1996; Koch et al, 1995), including cell bodies of giant neurons and fibres in the PnC (Waldvogel et al, 2010), and activation of GlyR might play a role in intrinsic or extrinsic modulation of the startle response. In fact, all the GLRA1 mutant mice show a decreased startle threshold, a sensory feature believed to arise upstream of the spinal cord, in the brainstem (Plappert et al, 2001). Additionally, rats injected with strychnine into the cisterna magna showed facilitation of startle response to acoustic stimulation (Kehne et al, 1981). These findings correlate broadly with the electrophysiological and clinical findings in hyperekplexia patients (Brown et al, 1991).

However, functional studies in rats show contradictory findings. On one hand, studies using selective lesions of the PnC (Koch, 1999; Davis et al, 1982) and electrophysiological studies in vivo (Lingenhohl et al, 1994), found that PnC giants neurons are involved in modulation of the ASR, particularly in PPI-like and habituation-like phenomena. On the other hand, combined pharmacological and electrophysiological studies in anesthetized rats (Koch, 1995) failed to show any significant effect of strychnine or β-alanine injections into the PnC on startle inhibition in vivo. When brain slices were studied, glycine injections caused a profound inhibition of PnC neurons, an effect that was abolished by strychnine, but failed to find a role for glycine in feed-forward inhibition, or in controlling short-term habituation of startle (Geis et al, 2011). Overall, these contradictory results point towards a role of glycine in modulating the startle response, possibly not necessarily intrinsically within the ASR pathway but perhaps extrinsically through excitatory and inhibitory projections from the

midbrain and higher brain structures into the PnC (Bosch et al, 2008; Koch, 1999; Yeomans et al, 2006). Indeed, GlyR alpha1 subunit mutant mice show significantly reduced prepulse inhibition of the startle response (Yeomans et al., 2006b).

Electrophysiological studies in individuals with hereditary hyperekplexia and SPS showed exaggerated acoustic startle responses (Tijssen et al, 1997; Matsumoto et al, 1994), but decreased ASR habituation, and prolonged spasms after ASR in SPS patients (Matsumoto, 1994). Additionally, disinhibition (exaggerated reflex excitation and attenuated inhibition) of other brainstem reflexes such as the monosynaptic masseter reflex, the masseter inhibitory reflex, the glabella reflex, and the blink reflex, was also found in patients with familial hyperekplexia and SPS (Khasani et al, 2004). In conjunction, these findings suggest a physiological relationship between hyperekplexia and SPS, with a biased reflex transmission in the brainstem towards excitation secondary to a disruption in glycinergic and GABAergic interneurons. GABA and glycine receptors both mediate PPI of startle (Yeomans et al, 2010; Yeomans et al., 2006b, 2010).

In summary, the startle response may have a relatively simple neuronal circuitry but its regulation by modulatory pathways is more complex than initially thought, which may explain the differences in habituation and in the spreading of the response between familial hyperekplexia and SPS, perhaps related to a differential disruption of the glycinergic and GABAergic pathways mediating the startle response.

1.5.4 Genetic alterations of GlyR

Hereditary defects of the glycine receptor have also been observed in several mammalian species including mice, cattle, horses, dogs and humans (Harvey and Rigo

2010). The principal manifestation in these defects is a motor disturbance characterised by hypertonia, generalised stiffness, hyperexcitability and exaggerated startle response.

1.5.4.1 Murine models

Three autosomal recessive mutations in α or β GlyR subunit genes have been identified with complex motor disease phenotypes characterized by hypertonia and hyperexcitability. The mice are asymptomatic at birth but the phenotype becomes apparent two weeks later. These three strains of mutant mice are called spastic (spa), spasmodic (spd), and oscillator (spodt) (Becker, 1995) Table 1.9.

Table 1.9. Mice genetic defects in glycinergic transmission

Mice	Gene	Mutation and Location	Functional effect	Mode of inheritance	Phenotype
Spastic (spa)	GLRB	LINE-1 insertion in premRNA Chromosome 3	Truncated Glrb mRNA: loss of >90% of expressed functional β subunits	AR	Muscle rigidity, tremor, myoclonic jerks and exaggerated startle reactions
Spasmodic (spd)	GLR A1	Ala52Ser N-terminal domain Chromosome 11	Increases EC50 Decreased ligand sensitivity	AR	Muscle rigidity, tremor, myoclonic jerks and exaggerated startle reactions
Oscillator (spodt)	GLR A1	7-bp deletion exon 8 (TM3 domain) Chromosome 11	Total reduction of adult isoform	AR	Massive tremor, hypertonia and death at 3 weeks of age

Knockout / Knockdown	GLRA2	Chromosome X	Reduced receptor expression	Gene targeting in embryonic stem cells	Normal behavioural phenotype. Decreased number of photoreceptors and spinal interneurons
Knockout	GLRA3	Chromosome 8	Reduced receptor expression	Gene targeting in embryonic stem cells	Normal behavioural phenotype. Reduction in chronic pain sensitisation

1.5.4.2 Hereditary hyperekplexia

Hypereplekxia was first described in 1958 by Kirstein and Silfverskiold in four members of a Swedish family with exaggerated startle reflexes and violent falls due to generalised stiffness, but later in 1966 the term 'hyperekplexia' was introduced by Suhren and colleagues who described a large Dutch family with similar symptoms. This is an autosomal dominant disorder, and has two clinical forms: a) Major form; b) Minor form (Bakker, van Dijk et al. 2006; Dreissen, Bakker et al. 2012).

The major form also called stiff-baby syndrome is characterized by generalised stiffness at birth, excessive startling and temporary generalised stiffness after being startled, which often causes patients to fall as they get older. Newborns can have sudden infant death due to laryngospasm and cardiorespiratory failure, and psychomotor development delay. Other symptoms included exaggerated head-retraction reflex (HRR) which is a brisk and violent dorsiflexion of the head, often associated with retropulsion of the trunk following slight taps to the nose and upper lip (often also to the glabella and chin). No abnormalities are found in standard tests of serum, urine and CSF, nor in

computerized tomography, electroencephalography and magnetic resonance imaging (Meinck 2006).

In about 80% of patients with hereditary hyperekplexia a gene mutation can be identified on chromosome 5q32 with an autosomal dominant, recessive or compound heterozygote trait; the gene encodes the alpha1 subunit of the glycine receptor (GlyRA1). In the other 20% of the patients with no mutations in GLRA1, a different mutation was found, these patients have a mutation in the gene encoding for the presynaptic sodium- and chloride-dependent glycine transporter 2 (GlyT2 (SCL6A5)) with a recessive or compound heterozygosity inheritance (Rees et al, 2006); in one family a dominant mutation was identified (Harvey et al. 2008). Other mutations affecting postsynaptic glycinergic proteins have been found in rare sporadic cases of hyperekplexia including mutations in the GlyR subunit (GLRB), gephyrin (GPHN) and RhoGEF collybistin (ARHGEF9) (Harvey et al, 2008).

In contrast, the minor form is characterized by late onset excessive startling without stiffness or other neurological signs, or acquired idiopathic excessive startling. Initially, it was considered a different expression of the same gene defect but clinical, genetic and neurophysiological studies suggest that the ‘minor’ form is a heterogenic group of excessive startling disorders, without a genetic relation to hyperekplexia in the great majority of cases. Some of these cases are secondary to brainstem or cerebral damage and therefore labelled as symptomatic hyperekplexia (Bakker et al, 2006; Dreissen et al, 2012).

Treatment in hereditary hypereplekxia and symptomatic hyperekplexia is based on case reports and very few double-blind placebo-controlled studies, with clonazepam showing

the most consistent symptomatic relieving effects (Bakker, van Dijk et al. 2006; Meinck 2006).

1.6. Conclusions and aims

PERM is a rare disease of the CNS with unclear aetiology and pathogenicity but with evidence for autoimmunity. The clinical presentation likely arises from impairment of brainstem and spinal inhibitory circuits, mainly glycinergic and perhaps also GABAergic. PERM shares the core symptomatology of stiffness and stimulus-sensitive spasms of SPS but has additional brainstem and other CNS abnormalities, and in general it is accepted that PERM has a more severe, rapidly progressive and often fatal course in contrast with the slowly progressive and long-standing course of SPS.

Recent evidence has shown the presence of autoantibodies against the GlyRα1 subunit. It may be that the wide spectrum of clinical features in PERM patients is a consequence of the effects of antibodies to different types of GlyRs. However, the frequency of these antibodies, their clinical relevance, and their possible mechanisms has not been studied. The aims of this Thesis were:

- To describe the clinical characteristics of patients whose sera and/or CSF have been found to be positive for GlyR alpha1 antibodies.
- To characterize the immunological profile of GlyR-Abs.
- To determine the pathogenic role of GlyR autoantibodies *in vitro*.
- To describe the immunohistochemical localisation of their target antigens in rodent brain.

- To correlate the cellular and histological findings with the clinical manifestations.
- To try to recreate some of the phenotypic clinical features of the disease by an *in vivo* passive transfer of GlyR IgG into mice.

CHAPTER 2. MATERIAL AND METHODS

2.1 Identification of Patients

The Neuroscience Group in Oxford routinely receives national and international samples for antibody screening and this allowed the identification of positive patient samples for glycine receptor antibodies. Ethical approval consent for this study was obtained from the Regional Ethics Committee Ref: 07/Q1604/28. Positive sera for GlyR-Abs were identified by a cell-based assay either by Dr Jacobson or Dr Woodhall. 779 samples referred to the Oxford Neuroimmunology service from Oct 2008 to March 2012 for routine diagnostics for GlyR-Abs were screened; some were serum/CSF pairs. All sera were aliquoted and stored at -20° C until required.

Consent forms and clinical questionnaires were sent to all neurologists (Appendix 1) who referred positive samples and the data was collated and analysed in Oxford. The questionnaires include modified Rankin scores (from Graus et al, 2001) to describe the level of functional disability and ranged from zero to six (0= Asymptomatic patient; 1= No disability, symptoms do not interfere with lifestyle; 2= Slight disability, symptoms lead to some restriction in daily activities but do not prevent independent existence; 3= Moderate disability, symptoms significantly interfere with daily activities and requires some assistance; 4= Moderately severe disability; symptoms prevent independent existence, but patient does not require constant attention; 5= Severe disability; patient totally dependent, requiring constant attention day and night; 6= Dead).

2.2 Expression vectors

Plasmid constructs for GlyR α1, α2, α3 subunit expression in cells were designed by Dr Patrick Waters (Neurosciences Group, Oxford). To develop a fluorescent cell based

assay for the glycine receptor α1 subunit the cDNA for EGFP was inserted into the coding region of the α1 subunit in the plasmid pRK-GlyRα1 (a kind gift of Prof. Cord-Michel Becker). The protein did not express at the cell surface when EGFP was cloned into either the N- or C-termini, so it was cloned into the large cytosolic loop between the third and fourth transmembrane domains. A BamHI restriction site was generated at nucleotides 1152-3 of the GlyRα1 subunit with the primers GGCATCTCAGTCAAGGGATCCAACAACAGTAACACCACC and GGTGGTGTTACTGTTGTTGGATCCCTTGACTGAGATGCC. EGFP was PCR amplified from pEGFP-C3 (Clontech, Palo Alto, USA) with the primers GACTGGATCCATGGTGAGCAAGGGCGAGGAGC and GCATGGATCCCTTGTACAGCTCGTCCATGCCGAG. The vector and PCR product were digested with BamHI (New England Biolabs, Ipswich, USA) and ligated to generate pRK-GlyRα1-EGFP.

2.3 Amplification and purification of DNA plasmids

On Day 1, JM109 Escherichia Coli competent cells were transformed under a roaring Bunsen flame to prevent contamination. 50 µl of cells were mixed with 50 ng of DNA diluted in nuclease-free water (Promega, Southampton, UK) for 20 min on ice. Cells were heat-shocked for 1 min at 42°C, and placed again on ice for 5 min, then 100 µl of LB media was added to the cell solution and incubated at 37°C for 30 min with shaking (200 rpm) and spread onto a LB agar plate, supplemented with 100 µg/ml of ampicillin. Inverted Petri dishes were then incubated overnight at 37°C. Two control plates without antibiotic were used. One plate was spread with transformed E.coli; the other plate was not spread with transformed bacteria.

On Day 2 LB plates were inspected for the presence of numerous colonies, comparing the growth observed among plates. The growth on the LB+ Ampicillin plate was spotted and scarce compared to the thick and abundant growth of the two control plates. A single colony from the LB+ Ampicillin plate was then inoculated in 10 mls of LB media containing ampicillin and incubated at 37° C for 8 hours (shaking 200 rpm). Initial cultures were then poured into conical flask containing 250 ml of LB medium and 100 µg/ml of ampicillin, and then incubated overnight at 37° C, 200 rpm in a upright shaker certomat STR6 (Stuart scientific).

On Day 3 DNA was extracted and purified from transformed cultures using a Pure Yield Plasmid Maxiprep System (Promega, Southampton, UK) following manufacturer's instructions. DNA concentration was determined by spectrophotometry (shimdazu CPS-240A) and by nanodrop ND1000 (Thermo scientific).

2.4 Transfection and human embryonic kidney cell culture

Human embryonic kidney cells (HEK293) were cultured in Dulbecco's modified Eagle's Medium (DMEM), supplemented with 10% foetal calf serum (FCS, TCS Cellworks Ltd, Buckingham, UK) and 1% penicillin-streptomycin-amphotericin (PSA, Invitrogen, CA, USA) in disposable plastic flasks at 37° C, 5% CO2. Every four days cells were split using trypsin (GIBCO, 0.5% diluted in phosphate buffer solution PBS) to dislodge cells prior to centrifugation (1300 RPM, 5 min, at room temperature). Pellets were resuspended in 10 ml of medium and counted in a haemocytometer using trypan Blue (0.08%) to stain dead cells and exclude them from the counting.

For transfection HEK293 cells were plated (400,000 cells/well) on poly-L-Lysine (PLL) coated glass coverslips (or without coverslips for immunoabsorption

experiments) in six well plates at 37° C in 5% CO2. On the second day when cells were grown to approximately 40% of confluence, cells were transfected with 3 µg cDNA 0.8 µg/ml in the presence of 1.25 µl of polyethyleneimine and 1.5 µl of 20% sterile glucose solution per well. After 14 hours, the medium was replaced with fresh medium. At 48 hours post-transfection, the coverslips were transferred to a 24-well plate for the cell based assay.

2.5 *In vitro* experiments

2.5.1 Cell-based assay (CBA)

To confirm the reactivity to GlyR, the sera (1:20), CSF (1:2) or commercial antibodies to GlyR α1 (1:500; Synaptic Systems, Göttingen, Germany) diluted in DMEM medium supplemented with 4-(2-hydroxyethyl)-1-piperazineethanesulfonic acid (HEPES) and 1% bovine serum albumin (BSA) were incubated for 1 hour at room temperature with live human embryonic kidney cells (HEK 293), transfected to express GlyR α1 subunit. Cells were washed and fixed with formaldehyde 4% for 5 min, washed again and incubated with Alexa Fluor goat anti-human IgG (1:750) for 30 minutes at RT to detect bound human IgG. 4', 6-diamidino-2-phenylinole (DAPI) was used as a nuclear counterstain (1:1000).

The binding of the patients' antibodies was scored semi-quantitatively by 2 independent observers who evaluated the intensity of the staining (0 to 0.5, no binding or slight labelling without colocalisation; 1, weak labelling; 2, moderate labelling; 3, strong labelling; and 4, very strong labelling) copied from (Leite et al, 2008). For titres, the end-point dilutions (dilutions giving a score of 1) were obtained with serial dilutions of sera (1:20, 1:40; 1:80, etc.). All sera and CSFs with positive binding were retested and

checked for negativity against a second antigen to confirm specificity; and were also tested for NMDAR and GAD antibodies by routine CBA assays and radioimmunoassay (RIA) performed by Dr Jacobson and Prof Vincent.

To assay for antibodies to different GlyR subunits the HEK cells were transfected with the individual subunits instead of the α1 subunit. The plasmids used were pRK5-GlyRα3L, pRK5-GlyRα3S (Nikolic et al, 1998), pRK7-GlyRβ (Milani et al, 1998) (kind gifts from Prof. Cord-Michel Becker) or pcDNA3-GlyRα2 (Grenningloh et al, 1990) (kind gift from Prof. Robert Harvey). Serum (1:80) dilution was added to the coverslips for 1 hour at RT, and bound antibodies were detected and scored as previously described. GlyRα2, GlyRα3S or GlyRα3L expression was confirmed by unfixed live cells HEK293T cells incubated with polyclonal rabbit antibodies to GlyRα2 (1:250, OriGene Technologies, Rockville, MD, USA), and GlyRα3 (1:500, Millipore, Billerica, USA).

The subclass of the GlyR-Abs was determined by Dr Leite and Dr Coutinho using specific anti-subclass antibodies to IgG1, IgG2, IgG3, IgG4 and IgM (Invitrogen, UK). Their ability to fix complement was also demonstrated on the transfected HEK293 cells. After the addition of the heat inactivated patient serum (1:20) and washing, fresh human complement was added at 37°C for 1 h. Surface-bound C3b was detected with a fluorescent commercial antibody (Dako, Eindhoven, Netherlands) as previously described (Leite et al., 2008; Waters et al., 2008). Mounted coverslips were visualised using a fluorescence microscope (Leica DM 2500, fitted with a Qimaging Rolera XR camera).

2.5.2 Internalisation Assay

To study internalisation following patient IgG binding, the cell-based assays were modified as follows:

1. To show surface binding and loss over time at different temperatures, HEK cells expressing GlyR α1-EGFP cDNA were incubated with sera (scoring 3 at 1:80 - 1:160) for 1 hour at 4º C and washed. Some coverslips were fixed at this point with 3% formaldehyde for 5 mins. The fixed or live cells were then incubated at either 4º C, or 37º C for 5 min to 16 hours. All cells were then fixed/re-fixed with 3% formaldehyde for 5 mins. Surface bound human IgG was detected with AlexaFluor goat anti-human IgG 568 (red; 1:750, Invitrogen, UK). All coverslips were scored in the same manner as the diagnostic assay. The mean ± SEM of 4 experiments were plotted.

2. To see if loss of GlyR-Ab IgG from the cell surface was due to internalisation rather than dissociation of the antibody, surface bound GlyR-Ab was detected with Alexa Fluor 488 (green) goat anti-human IgG after fixation, as above. Some cells were then permeabilised with 0.3% Triton-X-100 and incubated with Alexa Fluor 568 (red) goat anti-human IgG for 30 min at RT. The percentage of cells showing red spots near the nucleus was quantified in five areas (four from each quadrant and one from the centre). The areas were chosen based on the DAPI nuclear staining which confirmed the uniformity of the cell densities before changing filters from the blue channel to the merge red/green channel. Red and green dual colour confocal images were taken and imported into Image J software for image analysis, using the cell counter module.

3. To demonstrate loss of GlyRs from the surface by the action of GlyR-Abs, the same procedure was carried out but cycloheximide (50 µg/ml, Sigma-Aldrich, Dorset, UK) was added to the growth medium for 1 hour before the addition of the sera to prevent new GlyR synthesis. The percentage of cells with GlyR-EGFP protein were counted and analysed as above.

4. To evaluate if GlyR was targeted to the endolysosomal pathway after exposure to patient or healthy control serum, the transfected HEK cells were incubated with patient sera at 37ºC for different periods of time (0-4 hours), washed, fixed, permeabilised and incubated with mouse antibodies to the early endosomal antigen (EE1) (1:250; SantaCruz, CA, USA) and to the late endosomal antigen (1:250; SantaCruz, CA, USA), followed by Alexa Fluor 568 goat anti-mouse IgG (Invitrogen, UK) before analysis as above, looking for colocalisation of the internalised GlyR-enhanced green fluorescent protein with the monoclonal antibodies.

2.6 Immunohistochemistry

2.6.1 Immunohistochemistry on rat tissue

To localise the regions of the CNS that express GlyR, the following monoclonal antibodies were used:

1. GlyR4a monoclonal antibody (pan-GlyR), raised against aa 96-105 of GlyR α1 and recognises different α and β subunits (Synaptic Systems, Göttingen, Germany).

2. GlyR2b monoclonal antibody (alpha1 subunit), raised against aa 1-10 of GlyR α1 and recognises the α1 subunit only (Synaptic Systems, Göttingen, Germany).

3. GLRA2 polyclonal antibody (alpha2 subunit), raised against aa 1-186 of GlyR α2 and recognises this only (OriGene Technologies, Rockville, MD, USA).

4. GLRA3 polyclonal antibody (α3 subunit), raised against aa 355-368 of GlyR α3 and recognises this only (Millipore, Billerica, USA).

Eleven-micron thick cryostat sagittal frozen sections of the whole rat brain were thaw-mounted on SuperFrost Plus glass slides and stored at -20ºC. Sections were fixed with formaldehyde 3% for 5 minutes, 3% H_2O_2 in 70% methanol was added to inhibit endogenous peroxidases, washed again in PBS. The sections were then blocked at room temperature (RT) for 1 hour in 10% normal goat serum, and incubated with primary mouse monoclonal glycine receptor antibodies (mab2b, mab4a) diluted (1:100). Slides were washed with PBS and incubated with biotinylated anti-mouse IgG secondary antibody (diluted 1:200) for 1 hour at room temperature, washed again in PBS and incubated with streptavidin-HRP at RT for 30 min. The sections were reacted in 3-amino-9-ethylcarbazole (AEC) and 0.01% H_2O_2 in 0.1 M phosphate buffer, pH 7.4, for 15 min to produce a brown reaction product. The sections were washed in distilled H_20 and counterstained with hematoxilin-eosin to visualise the nucleus. Finally the slides were covered with mounting medium (Dako) and images were photographed under a light microscope with a digital camera.

Immunofluorescence: To determine the brain regions where other possible antigens involved in glycinergic neurotransmission such as GlyRβ subunit, glycine transporters 1

and 2, or other known antigens previously related with PERM patients like glutamic acid decarboxylase are expressed in the brain, sections were incubated as above with primary mouse monoclonal antibody to GLRB (1:500; Synaptic Systems, Göttingen, Germany) or primary goat polyclonal antibody to GlyT1 (1:250; SantaCruz, CA, USA) or primary rabbit polyclonal antibody to GlyT2 (1:250; SantaCruz, CA, USA) or primary rabbit polyclonal antibody to glutamic acid decarboxylase (GAD) (1:500; Sigma, St Louis, USA), followed by incubation with Alexa Fluor 4888 goat anti-mouse or anti-rabbit IgG (1:1000; Invitrogen, UK).

To determine the different cellular populations that express GlyRs and its cellular localisation double immuno-labelling methods were performed, using different neuronal, interneuronal and glial markers (Table 2.1). Frozen Sections were incubated with primary mouse monoclonal antibody to GlyRα1 and either primary rabbit polyclonal antibody to microtubule-associated protein 2 (MAP-2) (1:500; Sigma, St Louis, USA) for neuronal staining, primary rabbit polyclonal antibody to choline acetyltransferase (ChAT) (1:100; Millipore, Billerica, USA) for motoneuron staining and intracellular staining, primary polyclonal antibodies to parvalbumin (1:2000; SWANT, Switzerland), calbindin (1:500; Sigma, St Louis, USA) and calretinin (1:1000; Millipore, Billerica, USA) for interneuron staining, primary rabbit polyclonal antibody to glial fibrillary acidic protein (1:1000; DAKO, Eindhoven, Netherlands) for glial staining, primary polyclonal antibody to gephyrin (1:1000; AVIVA Systems Biology, San Diego, USA) for postsynaptic staining or primary polyclonal antibodies to GlyT1 and GlyT2 (1:250; SantaCruz, CA, USA) for presynaptic staining; followed by incubation with the appropriate secondary Alexa Fluor secondary antibodies (1:1000; Invitrogen, UK).

Table 2.1. List of intracellular neuronal, interneuronal and glial markers used

Marker	Function
Gephyrin	Anchors GlyR and GABAR in the postsynaptic membrane (Craig et al, 1996)
Microtubule-associated protein 2 (MAP2)	Assembles microtubules in neurons (Gambling et al, 1996)
Glial fibrillary acidic protein (GFAP)	Intermediate filament expressed in astrocytes necessary for tissue architecture and cell communication (Liedtke et al, 1996)
Choline acetyltransferase (ChAT)	The rate limiting enzyme for synthesizing the acetylcholine neurotransmitter in motoneurons (Fulton and Nachmansohn, 1943)
Parvalbumin	Calcium-binding protein expressed in interneurons, involved in cell signalling (Celio and Heizmann, 1981)
Calretinin	Calcium-binding protein expressed in interneurons, involved in cell signalling (Rogers, 1990)
Calbindin	Calcium-binding protein expressed in interneurons, involved in cell signalling (Jandé et al, 1981)

To show that GlyR abs bind to antigenic targets in central nervous system tissue indirect single and double immunofluorescent methods were performed on frozen rat brain and spinal cord sections. Cryostat sections of fresh frozen rat brain were fixed with formaldehyde 3% for 5 minutes, blocked at RT for 1 hour in 10% normal goat serum, and incubated overnight at 4º C with combinations of human sera (diluted 1:800) and primary mouse monoclonal antibodies to glycine receptor (diluted 1:500) to co-localise the staining with that of the commercial anti-GlyR-Ab. Slides were washed with PBS and incubated with Alexa Fluor 488 goat anti-human and Alexa Fluor 568 rabbit anti-mouse secondary antibodies (diluted 1:1000) for 1 hour. Cell nuclei were visualised with DAPI (4, 6-diamidino-2-phenylindole) (Sigma-Aldrich, Dorset, UK).

To demonstrate the specificity of the patient's antibodies, four sera were pre-adsorbed against HEK cells expressing GlyRα1, GlyRα2, Glyα3 or un-transfected HEK cells. 250 µl of sera (1:800) were incubated in a well of a 6 well plate containing 1.600.000 cells/ml (approx.) for 1 hour in a shaker at RT, then the sera was aspirated and transferred to the next well and so on until the sera had passed through all six wells. The sera were also pre-absorbed with recombinant GAD (12.5 µg/ml; RSR Ltd, UK) overnight at 4ºC. The pre-adsorbed serum was then applied to rat brain sections as above.

To demonstrate binding of GlyR-Abs to appropriate motor neurons, the sections were incubated with human sera (1:200 to 1:800), primary mouse monoclonal antibody to glycine receptor (1:500; Synaptic Systems, Göttingen, Germany) and either primary rabbit polyclonal antibody to microtubule-associated protein 2 (MAP-2) (1:1000; Sigma, St Louis, USA) for neuronal staining or primary rabbit polyclonal antibody to choline acetyltransferase (ChAT) (1:100; Millipore, Billerica, USA) for motoneuron staining.

2.6.2 Immunohistochemistry on mouse tissue from passive transfer experiments

To determine human IgG deposition, brain and spinal cord sections were incubated at 4° C overnight with a highly cross-absorbed polyclonal CF633 goat anti-human IgG (1:1000; Biotium, CA, USA). To demonstrate the localisation of the human IgG deposits, sections were incubated with CF633 goat anti-human IgG and with primary mouse monoclonal antibody to Von-Willebrand factor (1:2000; Dako, Eindhoven, Netherlands) as above washed and incubated with Alexa Flour 568 highly cross absorbed anti-mouse IgG (1:1000; Invitrogen, UK) for 1 hour at RT, coupled with DAPI counterstaining.

To demonstrate the binding specificity of the human IgG deposits and characterize the neurons with human IgG deposits, sections were incubated with CF633 goat anti-human IgG and with primary rabbit polyclonal antibody to GlyRα1 (1:500; Synaptic Systems, Göttingen, Germany) as above washed and incubated with Alexa-Fluor 568 donkey anti-rabbit IgG (1:1000, Invitrogen, UK) for 1h at RT, coupled with DAPI counterstaining. Slides were covered with mounting medium (Dako) and images were photographed under a Zeiss fluorescence microscope and the appropriate filter settings with a digital camera.

2.7 Western blotting

2.7.1 Quantification of total IgG and albumin in patients' sera and CSFs

The total levels of IgG in paired GlyRα1 positive serum and CSF samples were measured by western blot. Paired sera (diluted 1:300 in DNase free H2O) and undiluted CSF were mixed with appropriate amounts of NuPAGE sample reducing agent (10X) and LDS sample buffer (4X) (Invitrogen, CA, USA) and the mixed solution was boiled for 5 minutes at 95° C.

10 µl of the mixed sera and 5 µl of SeeBlue Plus2 pre-stained standard molecular weight marker (Invitrogen, CA, USA) were loaded into 3-8% NuPAGE Bis-Tris SDS polyacrylamide gel lanes (Invitrogen, UK) and electrophoresed (150 mV for 1-1.5 hours) on a 4-12% bis-tris gradient gel and transferred using X Cell II BLOT (Invitrogen, UK) (25 mV for 30 min, 50 mV for 30 min) onto nitrocellulose membranes. The nitrocellulose blots were blocked with 3% milk (Marvel) in PBS/1% tween for 1 hour and, to assess the success of the transfer, nitrocellulose membranes were rinsed with distilled water and reversibly stained with Ponceau S (0.1% (w/v)

ponceau in 5% acetic acid) and scanned between two sheets of acetate film. Membrane blots were then incubated with rabbit anti-human IgG HRP (1:2000) for two hours at RT. The blots were washed three times with PBS/1% tween and developed with 3, 3' diaminobenzidine (DAB-HCl, 50 mg/ml in PBS).

To determine the albumin content in the samples, identical blots were incubated overnight at 4º C with goat anti-human albumin (1:1000; Dako, Eindhoven , Netherlands), and then treated as above but were detected with rabbit anti-goat IgG HRP (1:2000; Dako, Eindhoven,Netherlands) for two hours at RT, before developing with DAB-HCl as above. Dried blots were then scanned and the 50 kD IgG heavy chain or albumin bands (67 kD) analysed with ImageJ (NIH, USA). IgG and albumin standards were run in parallel and the IgG or albumin concentrations in the samples were calculated by comparison with standard IgG and albumin curves. Paired serum and CSF samples were used to determine the integrity of the blood–brain barrier, the IgG index and the intrathecal synthesis of specific antiGlyR IgG. As an indicator of blood/CSF integrity the serum albumin–to–CSF albumin ratio was determined (normal >130). The IgG index was calculated according to this formula [CSF IgG (mg/mL)/Serum IgG (mg/mL)] / [CSF albumin (mg/mL)/Serum albumin (mg/mL)] (normal <0.67). For intrathecal synthesis of specific IgG against GlyR, the antibody index formula was used as follows [CSF GlyRα1 endpoint titre/CSF total IgG] / [Serum GlyRα1 endpoint titre/Serum total IgG] (normal <1.4) (Dalakas, 2001).

2.7.2 Quantification of IgG in mice sera from passive transfer experiments

To quantify the concentration of human IgG present in the mice blood, animals were bled by cutting the central vein of the tail at day 7 of treatment and also at day 14

during the perfusion procedure. Serum was obtained after blood centrifugation (13000 RPM, RT for 30 min). Mouse sera and purified human IgG were diluted at 1:100 and run on western blot as above.

2.8 *In vivo* experiments

2.8.1 IgG Purification

IgG fractions were purified from plasmapheresis filtrates of two PERM patients obtained as part of standard clinical care, and from pools of healthy control plasmas, using ammonium sulphate. Ammonium sulphate was added to the samples until it reached a 45% saturation, the mix was left rotating overnight at 4°C, then it was centrifuged (5000 G, 30 min) to remove the supernatant. The pellet was then diluted in Ringer´s lactate solution (Baxter, USA) and dialysed in phosphate-buffered saline PBS (1:10) three times at RT; the last dialysis was performed overnight at 4°C. The following day the IgG fractions were dialysed (1:10) two times in Ringer´s lactate (Baxter, USA), aliquoted, filter sterilized with 0.20 mm membranes and stored at -20°C until use.

2.8.2 Systemic passive transfer of IgG

Twenty-four C57/BL6j male mice were used in the experiments (6–8 weeks old, purchased from BMS (University of Oxford, UK). Animals were kept ad-libitum and after habituation, they were randomized (n=6) to receive GlyRα1-Ab positive IgG (concentration 12.4 mg/ml), Control IgG (concentration 14.6 mg/ml), saline or no treatment. Animals received 0.5 ml i.p. of one of these treatments over twelve consecutive days, on days 3 and 8 in order to disrupt the blood brain barrier all animals

received I.P. injections of lipopolysaccharides (LPS) at a dose of 3 mg/kg and 1.5 mg/kg respectively. Mouse behaviour was evaluated at baseline and two days after each LPS injection (Fig. 2.1). For the second experiment the no treatment group was eliminated.

2.8.2 Acute intracerebroventricular (icv) passive transfer of IgG

Twelve C57/BL6j male mice were used in the experiments (6–8 weeks old, purchased from BMS (University of Oxford, UK). Animals were kept ad-libitum and 24 hrs before the procedure, the mice were habituated and the baseline behaviour was evaluated. Animals were randomised to receive a single injection of either IgG fractions from GlyRα1-Ab positive patients (concentration 12.4 mg/ml) or purified Control IgG (concentration 14.6 mg/ml) as above.

Stereotactic surgery was performed by Dr Louise Upton. The mice were deeply anesthetised by an inhaled mixed of isofluorane and pure oxygen (4% for induction and 1-2% for maintenance). Depth of anaesthesia was checked by testing the paw-pinch reflex and monitoring the breathing rate (1-2 Hz). In addition, systemic analgesics were given to the animals (buprenorphine at 0.1 µg/g and meloxicam at 1 µg/ g) to prevent post-operative pain.

The skull surface was exposed and a single burr-hole made at the appropriate stereotaxic co-ordinates for targeting the third ventricle: 0.94 mm caudal of bregma and 0.75mm lateral. A Hamilton syringe was inserted in to the brain at an angle of 20 degrees, to a depth of 2.25 mm and 8 µl of purified IgG were injected over 20 minutes. 300 nl of fluorescent beads (Lumaflour Inc., US) were injected with the IgG to verify the position of injection post-mortem.

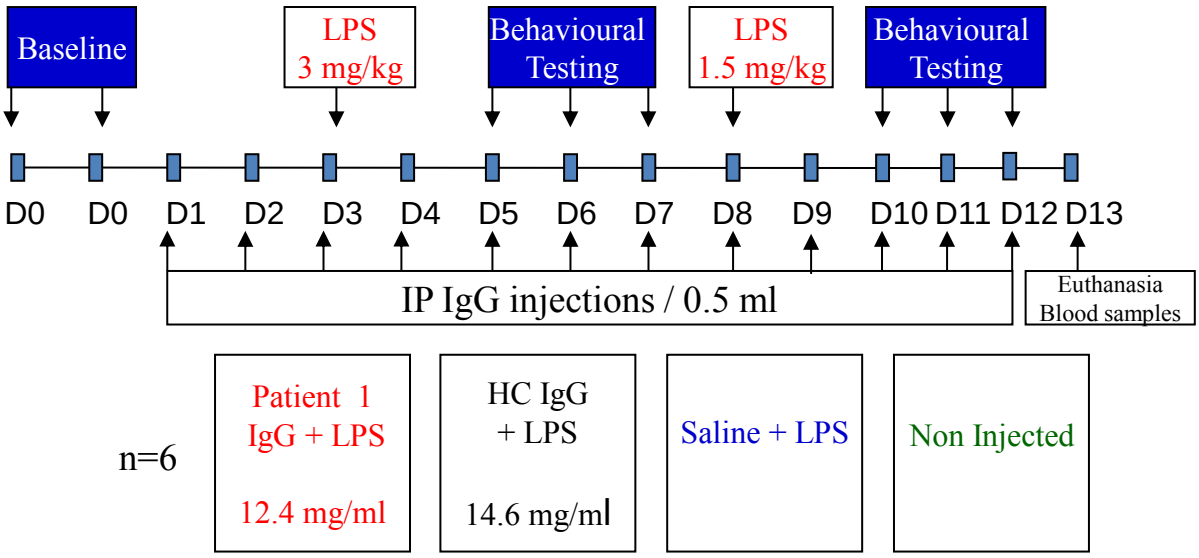

Fig. 2.1. Experimental protocol of systemic passive transfer of GlyR-IgG into mice.
LPS: Lipopolysaccharide; IP: Intraperitoneal; D: Day; IgG: Immunoglobulin.

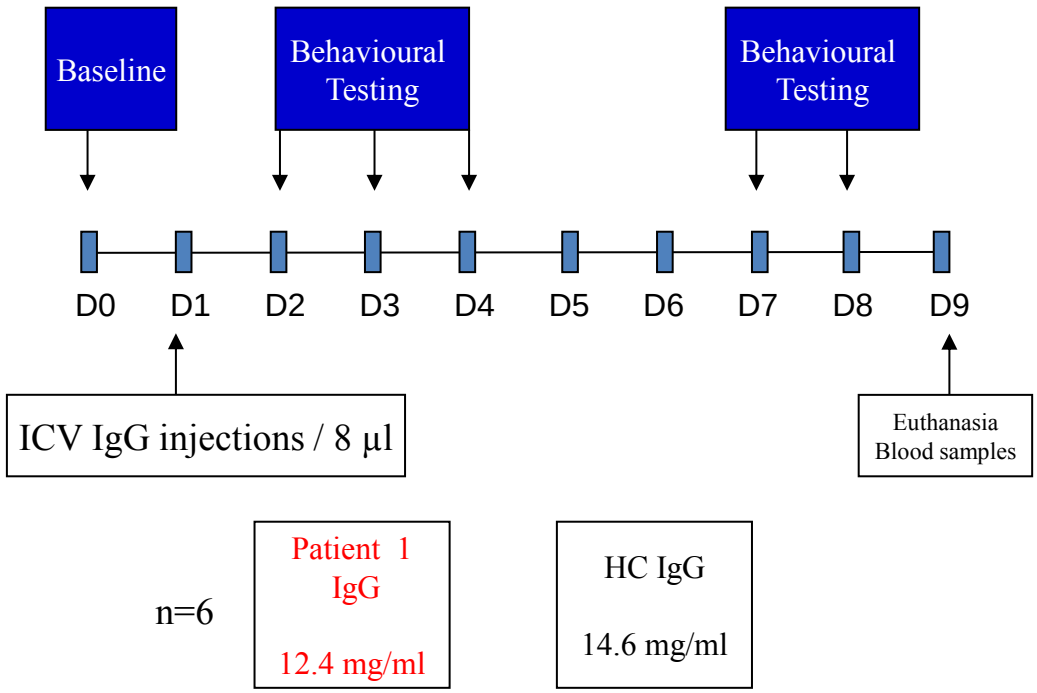

Fig. 2.2. Experimental protocol of intracerebroventricular injection of GlyR-IgG into mice.
LPS: Lipopolysaccharide; IP: Intraperitoneal; D: Day; IgG: Immunoglobulin.

The procedure was well tolerated by the mice and 24 hrs after the procedure, the mice behaviour was evaluated for three consecutive days and after a two day break for another two consecutive days (Fig. 2.2).

2.9 Behavioural tests

Behavioural tests were selected with the aim to identify mouse behaviour that could be related to motor and neuropsychiatry manifestations observed in PERM patients. For motor evaluation, the following tests were used (Deacon, 2013) (Fig. 2.3):

a) Rotarod: The rotarod has been used widely for testing balance and coordination in rodents, several protocols are used but the one used in this Thesis is the continuous acceleration protocol.
b) Grip strength: The inverted screen evaluates the muscular strength in all four limbs in rodents.
c) Beam walking: The beam walking evaluates sensorimotor coordination and balance in rodents.
d) Footprint analysis: Footprints obtained when rodents cross a wide runaway have been used for characterizing overground locomotor gait.

For neuropsychiatry evaluation, tests focusing on anxiety responses, which is one of the main symptoms in PERM patients, were used is such as: a) Light-Dark box, b) Successive alleys (Deacon 2013), and c) open field, although, the open field also evaluates general motor activity (Fig. 2.4).

All behavioural tests were conducted with the investigator blind to the group allocation of the mice. Previous to all the tests the animals were habituated for 5 min to each instrument and also to the room where the test took place in order to diminish the

arousal and anxiety levels. Between mice the walls and floor of the different instruments were cleaned with a moist tissue, followed by a dry tissue.

2.9.1 Light-dark box

The apparatus consisted of an open white compartment 30 x 20 x 20 cm joined by a 3 x 3 cm opening to a dark box 15 x 20 x 20 cm covered by a lid. The white compartment was illuminated by a 60 W anglepoise lamp placed 45 cm above the centre of the floor of the light side of the box. One side of the box was transparent, which permitted the observation of the mouse from the side. The mouse was placed in the centre of the light box facing away from the opening and the mouse behaviour was observed for 5 min. The latency to cross with the four paws to the dark side of the box, time spent in the dark side of the box, time spent in the light side of the box and the number of crosses made through the opening were recorded. The number of faecal boli and the presence/absence of urine were also recorded.

2.9.2 Open field

The open field was a dark enclosed arena of 50 x 50 cm divided into 10 cm squares illuminated with a 60 W anglepoise lamp placed 45 cm above the centre of the floor of the box. The mouse was placed into a corner square facing the corner and observed for 5 min. The latency to move, number of peripheral and central squares entered (whole body) and rears (both paws off the ground, but not as a part of grooming) were counted. The number of faecal boli and the presence/absence of urine were also recorded.

2.9.3 Successive alleys

The apparatus consisted of four successive linearly connected alleys of putatively increasing anxiogenic character. Each alley was 25 cm long. Alley 1 had 25 cm high walls, was 8.5 cm wide and was painted in black. A 0.5 cm step down led to Alley 2 which was 8.5 cm wide, had 1.3 cm high walls and was painted grey. A 1 cm step down led to Alley 3 which was 3.5 cm wide had 0.8 cm high walls and was painted white. A 0.4 cm step down led to Alley 4 which was 1.2 cm wide, had 0.2 cm high walls and was painted white. The apparatus was elevated 50 cm from the floor and 10 cms of Alley 1 and all the others alleys were away from the stand. A mouse was placed at the closed end of alley 1 facing the wall and observed for 5 min. The latency to enter each alley, the time spent in each alley and the entering to each alley (all four paws) were recorded. If a mouse fell off, it was replaced on the alley from which it fell, facing Alley 1.

2.9.4 Accelerating rotarod

The rotarod was set to a start speed 4 rpm and an accelerating rate of 20 rpm/min. Each mouse was placed on the rotating rod, facing opposite to direction of the rotation and then the acceleration was commenced for a maximum of 5 min. The duration spent on the rotarod before the mouse fell was recorded. The average of five trials was taken as a final result.

2.9.5 Kondziela's inverted screen test (Grip strength)

The inverted screen consisted in a 43 cm square of wire mesh consisting of 12 mm squares of 1 mm diameter wire, surrounded by a 4 cm deep wooden beading to prevent the mouse attempts to climb to the other side. Each mouse was placed in the centre of the wire mesh screen, then a timer was started and the screen was rotated to an inverted

position over 2 sec. The inverted screen was held steadily 40-50 cm above a padded surface for a maximum of 5 min. The time the mouse falls off was recorded. The average of five trials was taken as a final result.

2.9.6 Gait analysis

Locomotion was assessed as described by (Kunkel-Bagden et al., 1993). Mice were habituated and trained to traverse two different runways (wide runway and narrow beam) from the initial point to the scape box. The runways were (120 cm length) and were placed 1 m elevated from the floor. The wide runway was a flat board 4 cm wide and the narrow bean was 1 cm wide. Mice were placed in the initial point facing away from the scape box, and allowed to cross the runways. The time, number of steps needed to cross and the numbers of errors (footfalls from the runway) made while crossing were recorded. Two additional parameters were recorded in the narrow beam; the time to turn around on the narrow beam to evaluate coordination and to analyse the sensorimotor function, the walking over the narrow beam was qualitatively analysed using a slightly modified rating scale consisting of four distinct categories: coordinated stepping, tail use, postural control and footfall recovery. Each category was rated on a 3-point scale with a score of zero for absent movement, a score of one for atypical movements, and a score of two for typical movements (Metz and Whishaw, 2009; Shriner et al., 2009). Crosses of the wide beam were used for footprint analysis, the prints were used to measure the base of support and stride length.

2.9.7 Stiffness score

Stiffness was rated semi-quantitatively, similar to the clinical testing performed in humans with SPS (Dalakas et al., 2000). The following abnormal signs were scored on

a scale of 0 to 4: 0. Absent. 1. Slowing when in free motion; 2. Trunk stiffness during walking; 3. Reduced climbing ability and 4. Muscle spasms and dystonic movements Numbers of spasms per rat were counted.

2.10 Statistical analysis

All statistical analyses were performed using SPSS version 13 for windows (SPSS Inc., Chicago, USA) and all figures were created using GraphPad Prism version 5 for windows (GraphPad Software, San Diego, California, USA). The data were presented as mean ± standard error of the mean. Variables were tested for differences using Student´s t-test, One-way ANOVA, Two-way ANOVA or Kruskal–Wallis one-way analysis of variance depending on the number of groups and the data distribution.

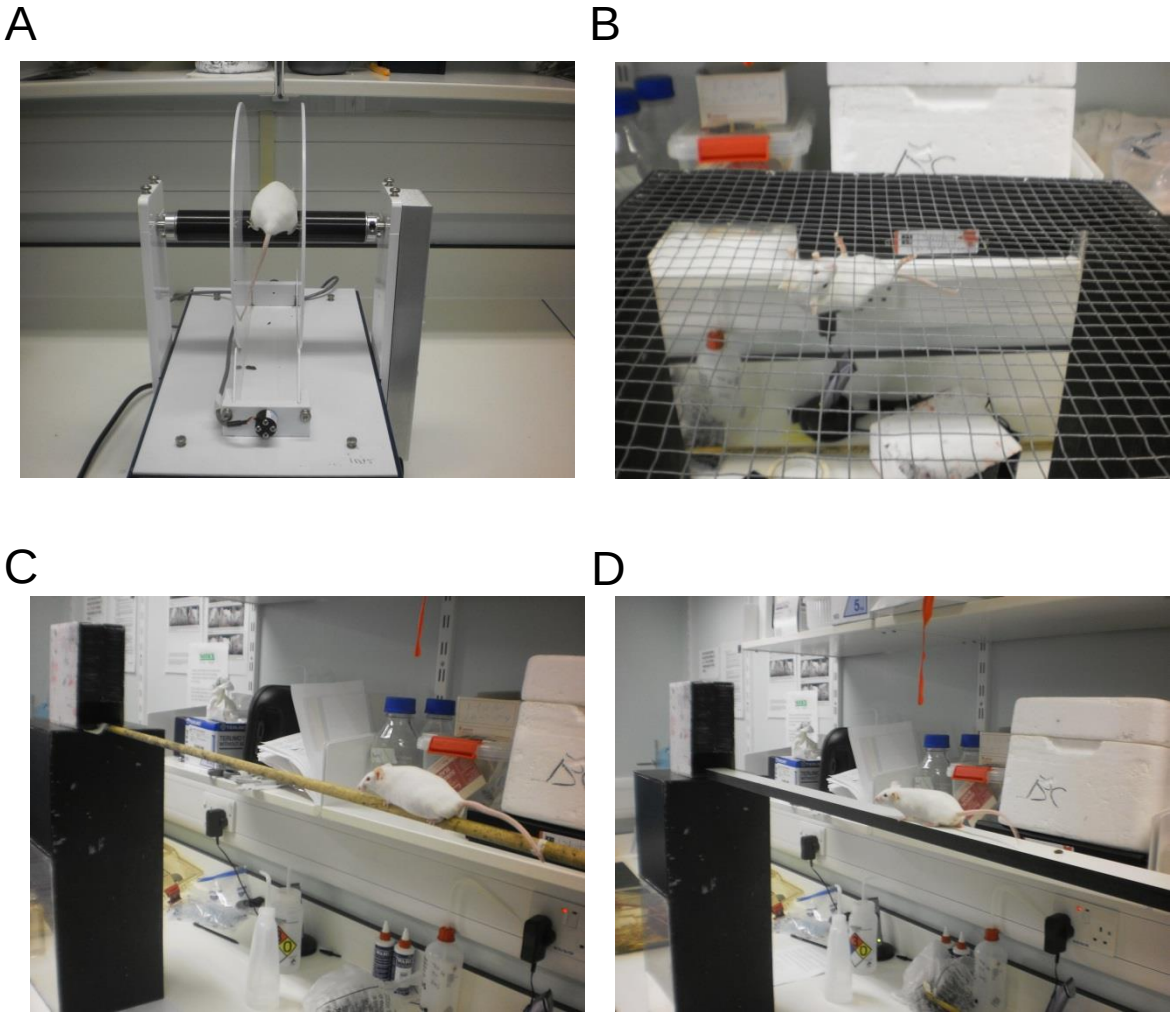

Fig. 2.3. Instruments used for motor testing. A. Rotarod, ***B.*** Inverted mesh grid, ***C.*** Narrow beam, ***D.*** Wide runaway.

A

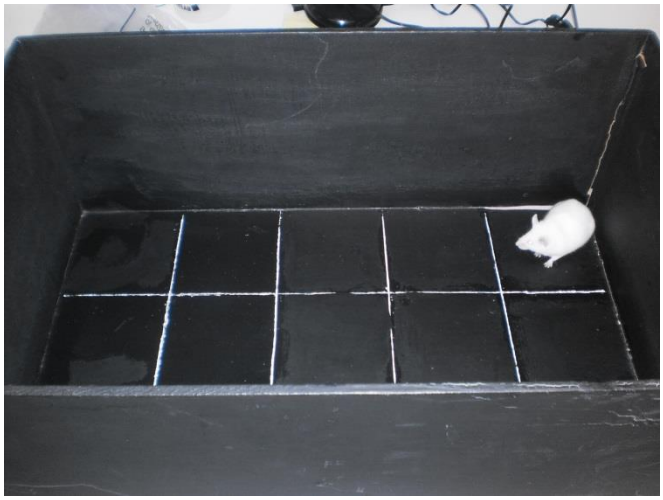

B

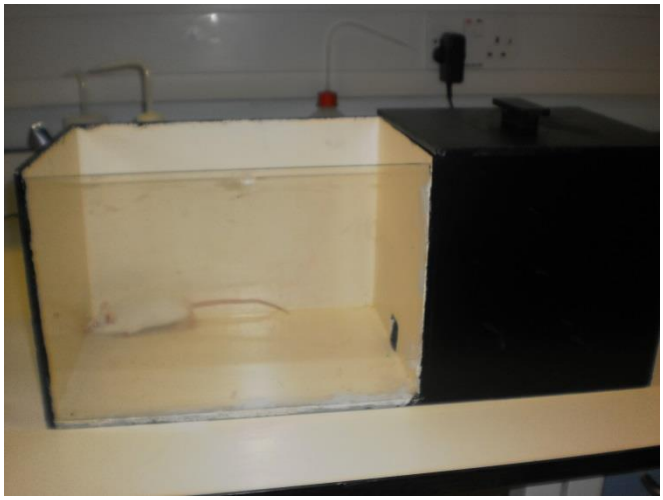

C

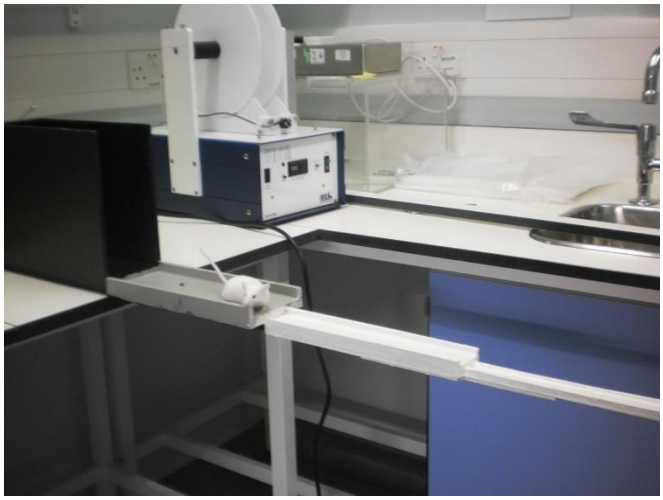

Fig. 2.4. Instruments used for anxiety and exploratory behaviour testing. A. Open field, ***B.*** Dark and Light box, ***C.*** Successive alleys.

CHAPTER 3. Clinical Characteristics of GlyR positive patients

3.1 Introduction

PERM is a rare neurological disease that can be very severe and potentially fatal. It is characterized by muscular rigidity, stimulus-sensitive spasms, myoclonus, hyperekplexia, brainstem dysfunction, autonomic dysfunction and variable sensory symptoms. It is believed that PERM is a subtype of SPS, but more severe and more rapidly progressive in comparison to the slowly progressive and long-standing SPS (Meinck and Thompson 2002; Brown and Marsden 1999). Some PERM patients have GAD antibodies and some respond to immunosuppressive therapy.

Several recent case reports have found antibodies to glycine receptor (GlyR), without GAD antibodies, in PERM patients with a wide array of symptoms (Hutchinson et al 2008, Mas et al 2011; Turner et al 2011; Clerinx et al 2011; Piotrowicz et al 2012; Iizuka et al 2012; Damasio et al 2013; Stern et al 2013; De Blauwe et al, 2013; Wuerfel et al, 2014; Zuliani et al, 2014). Since GlyR are widely expressed in the CNS, it is likely that the wide spectrum of clinical features in PERM patients is a consequence of the effects of GlyR-Abs. This chapter analyses the clinical details of 45 patients found to have serum and/or cerebrospinal fluid (CSF) GlyRα1 antibodies, aiming to phenotype in more detail the clinical spectrum and the immunological profile of the patients, and to determine the overall responses to treatment.

Most of the work described in this chapter comes from the paper (Carvajal-González et al, 2014) and includes contributions from all the co-authors.

3.2 Prospective cohort

3.2.1 Patients identified

In order to identify GlyR-Ab positive patients and measure accurately the antibody titres, patient sera and CSFs were tested for binding to HEK cells expressing EGFP-tagged GlyRα1. Patient sera bound strongly to HEK cells, whereas the control sera were negative (Fig. 3.1A). The patients were prospectively identified prior to the start of the project from samples referred for testing from late 2007 to March 2012 (774 sera, 68 CSFs, including 63 paired samples). Fifty-two patients (41 sera and 11 serum/CSF pairs) were positive; the remaining 727 patients, including 52 with serum/CSF pairs and five unpaired CSF samples, were negative. Thirty-three sera from healthy individuals and samples identified as positive for NMDAR or AQP4 antibodies, and multiple sclerosis CSFs, were used as controls. Only 3 sera out of 398 with AQP4 antibodies were positive (scores above 1) (<1%), and all of those with NMDAR-Abs were negative (Figure 3.1B). None of the control sera or CSFs bound (CSFs>0) detectably to GlyR expressing HEK cells (Figure 3.1C).

3.2.2 Antibody characteristics

On titration the positive serum samples showed titres ranging from 1:20 and 1:60,000, while none of the 33 healthy sera bound at 1:20 (Fig. 3.1D) (unpaired Student´s t-test, $p < 0.0001$). Ten paired serum/CSF samples were end-point titrated and the CSF titres also showed a wide range (1:2.5 to 1:640) (Fig. 3.1E). Strikingly, three patients had CSF levels very similar to serum levels suggesting marked intrathecal synthesis of the specific GlyR-Ab. To assess this systematically, serum and CSF IgG and albumin levels were measured in each of eight patients who had samples still available and in two

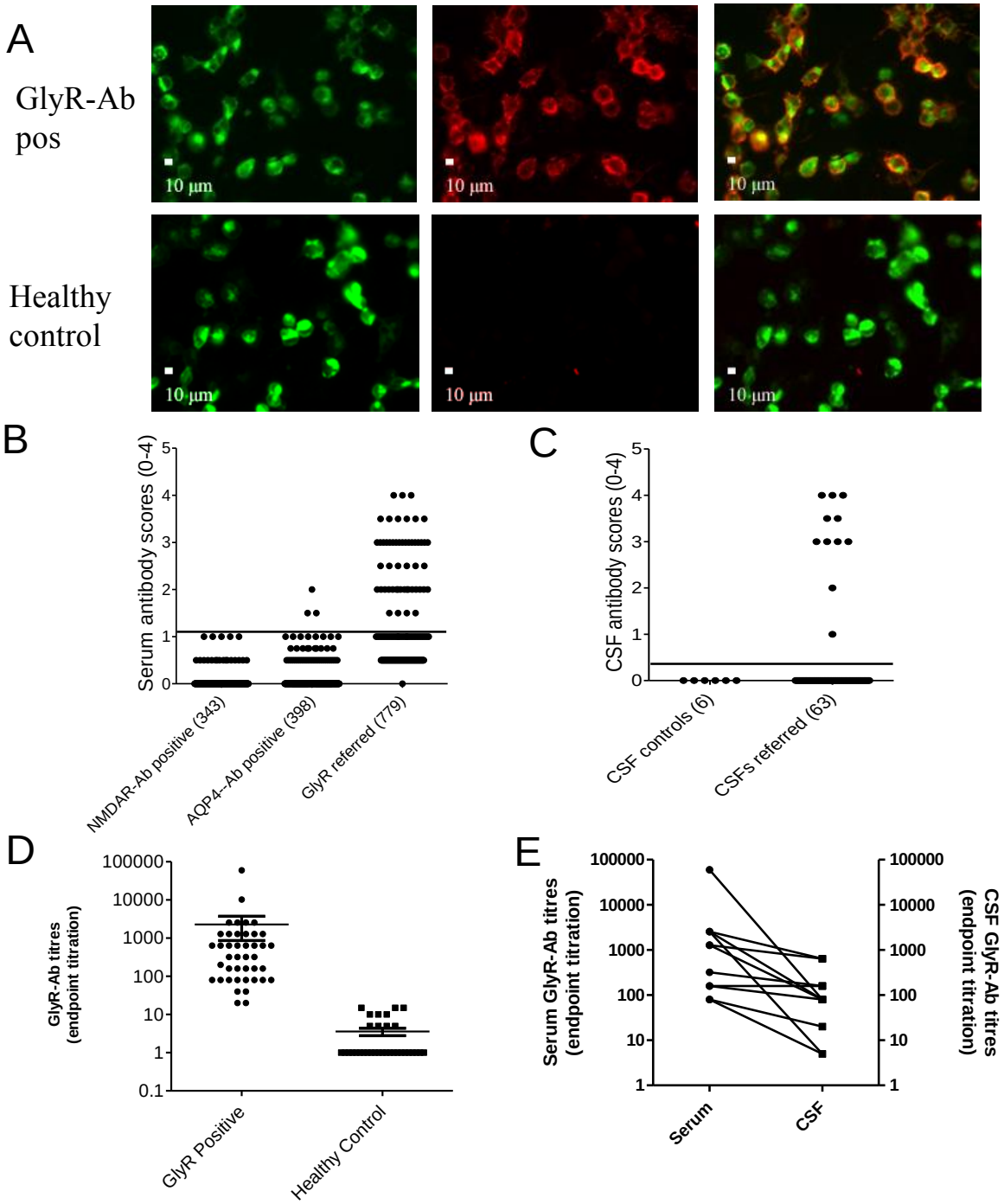

Fig. 3.1. Determination of glycine receptor antibody specificity in PERM and related disorders. ***A.*** Patient sera bind to HEK 293 cells expressing GlyRα1-EGFP (green); the IgG binding is detected with anti-human IgG (red). Control IgG does not bind to the GlyRα1-EGFP expressing cells. ***B.*** Visual scores of sera (diluted 1:20) referred for routine GlyR antibody testing compared with scores in sera positive for NMDAR or aquaporin 4 (AQP4) antibodies studied as neurological controls. ***C.*** Scores of referred CSF samples (diluted 1:1) compared with multiple sclerosis control CSFs. ***D.*** Endpoint titrations for GlyR positive patients and healthy individuals (highest dilution giving a visual score of 1). The endpoint dilutions ranged between 1:20 to 1:64000 whereas none of the 33 healthy control sera scored 1 or greater at 1:20. Mean ± SEM, two sided students t-test ($t=4.339$ $df=49$; $p < 0.0001$). ***E.*** Endpoint titrations for sera and paired CSFs; the CSF titres are generally lower than serum titres but in three patients are equal or only a dilution lower.

healthy controls by western blotting (Fig. 3.2A-D, Table 3.1). The ratios of serum:CSF IgG (136.2 to 592.9) and albumin (187.7 to 403.2) were within normal limits with an albumin quotient (QAlb) ranging from 0.74 to 1.59 (normal 0.7 to 1.3), indicating no general blood brain barrier breakdown. By contrast, the IgG indices (0.69 to 2.62) were above the normal reference value (normal 0.23 to 0.67) indicating intrathecal synthesis of IgG but only >1.1, in four patients (Fig 3.2E). The indices for the GlyR-specific antibodies ([CSF endpoint titre/Total CSF IgG] / [serum end-point titre/Total serum IgG]), ranged from 6.8 to 402.2 (>1.4 considered intrathecal synthesis) (Fig 3.2F). These values represent substantial intrathecal synthesis of the specific GlyR-Abs, particularly in the three patients with values >50; interestingly one patient with very low serum IgG but very high serum GlyR-Abs did not show intrathecal synthesis (antibody index = 0.18).

3.2.2.1 Antibody profiling

In order to see if patient sera bind to other GlyR α subunits, they were tested for binding to HEK cells expressing GlyRα2, GlyRα3S or GlyRα3L homomers. Expression was first demonstrated by incubating HEK cells expressing GlyRα1, α2 and α3 subunits individually with polyclonal rabbit antibodies to GlyRα1, GlyRα2 and GlyRα3, which also allowed checking the specificity of the commercial antibodies. GlyRα1 monoclonal antibody bound to GlyRα1-EGFP expressing HEK cells, but did not bind to HEK cells expressing either GlyRα2 or α3 subunits; GlyRα2 and GlyRα3 polyclonal antibodies bound to HEK cells expressing GlyRα2 and α3 subunits respectively, but did not bind when HEK cells expressed either of the other two GlyRα subunits (Fig. 3.3).

Patient sera bound variably to HEK cells expressing all three subunits colocalising with monoclonal antibodies to GlyRα1, 2 or 3 respectively (Fig. 3.4 A, B). Forty-four sera

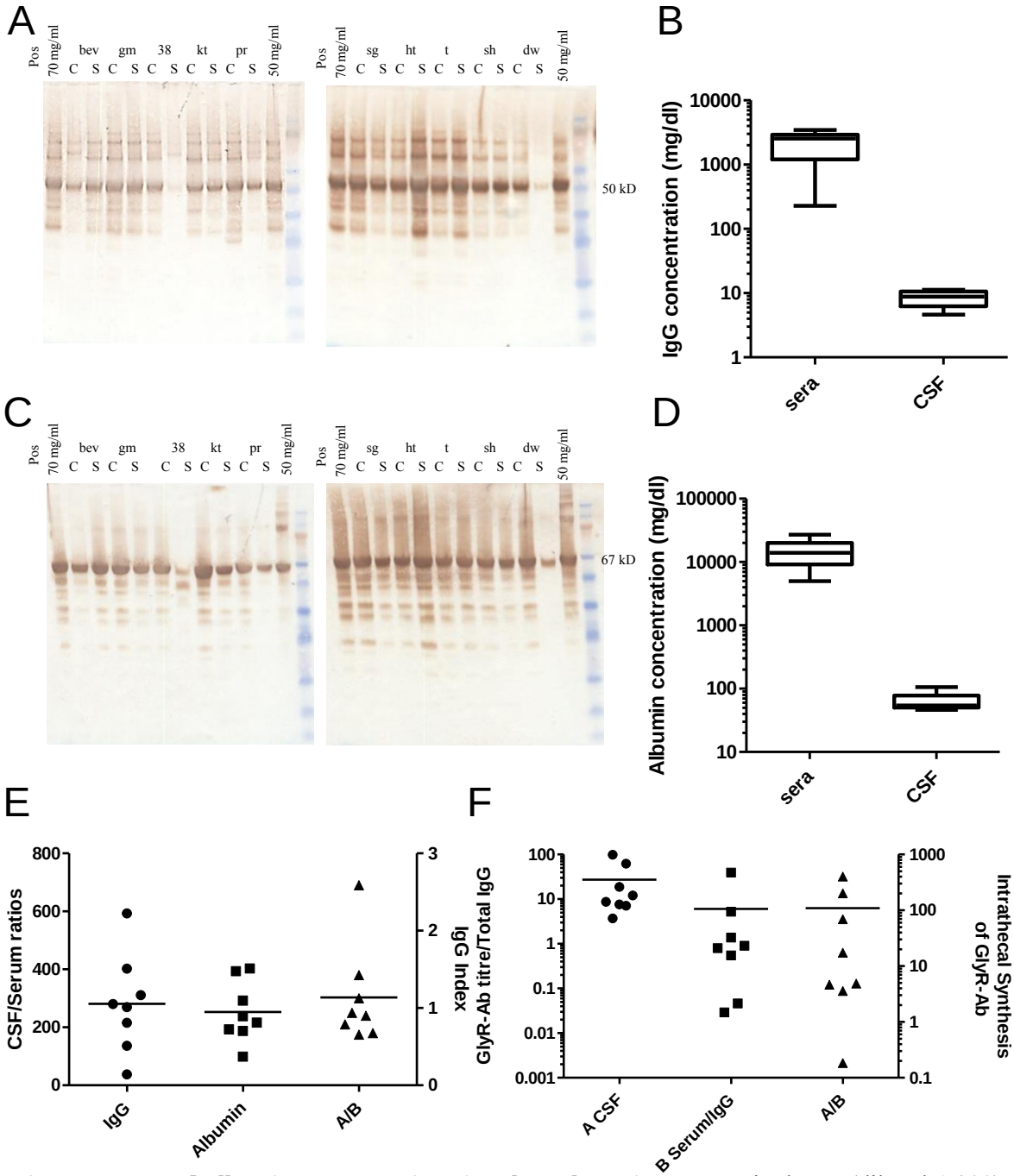

Fig. 3.2. IgG and albumin concentrations in GlyR-Ab patients. A. Paired sera (diluted 1:300) and CSF IgG from GlyR-Ab positive patients and healthy controls were blotted for detection of IgG, IgG heavy chains bands can be observed at 50 kDa. ***B.*** Quantification of the IgG bands showed that on average the serum:CSF IgG ratio was within normal values (252.5). ***C.*** Paired sera (diluted 1:300) and CSF albumin from GlyR-Ab positive patients and healthy controls were detected on western blot , albumin bands can be observed at 67 kDa. ***D.*** Quantification of the albumin bands showed that on average the serum:CSF albumin ratio was within normal values. ***E.*** The IgG index of eight patients on average was slightly raised (1.15; normal < 0.67). ***F.*** Calculation of intrathecal synthesis in eight paired CSFs. GlyR antibody titres (from figure 1d) divided by IgG concentration for sera (serum/IgG) or for CSFs (CSF/IgG). Intrathecal synthesis rates are given as the ratio between these values, as described and are raised in 7/8 patients, particularly in three.

Table 3.1. Analysis and quantification of IgG and Albumin in serum and CSF by western blotting

	IgG			Albumin			Serum	CSF		
Patient	**Sera**	**Sera*300**	**CSF**	**sera**	**Sera*300**	**CSF**	**Ab titre/300**	**titre**	**IgG Index**	**Antibody Index**
1	5.103	1530.857	11.243	32.870	9861.009	52.545	200	80	1.378	0.182
2	6.178	1853.410	6.613	68.402	20520.717	106.319	8.533	80	0.689	8.759
HC1	0.761	228.425	5.566	23.692	7107.735	74.583	N/A	N/A	N/A	N/A
3	9.439	2831.844	10.496	63.821	19146.282	88.585	8.533	80	0.801	8.432
4	9.130	2738.914	4.619	90.156	27046.716	67.073	0.267	40	0.680	296.489
5	0.816	244.826	6.470	16.647	4993.986	50.410	4.267	640	2.618	18.922
HC2	9.133	2739.916	9.073	38.248	11474.502	46.180	N/A	N/A	N/A	N/A
6	10.656	3196.908	10.289	48.327	14497.980	49.603	8.533	640	0.941	77.678
7	11.492	3447.696	8.573	66.339	19901.775	50.579	0.533	160	0.978	402.180
8	7.804	2341.313	10.843	44.493	13347.816	56.019	4.267	40	1.103	6.748

HC = Healthy control; IgG = Immunoglobulin G; CSF = Cord spinal fluid .

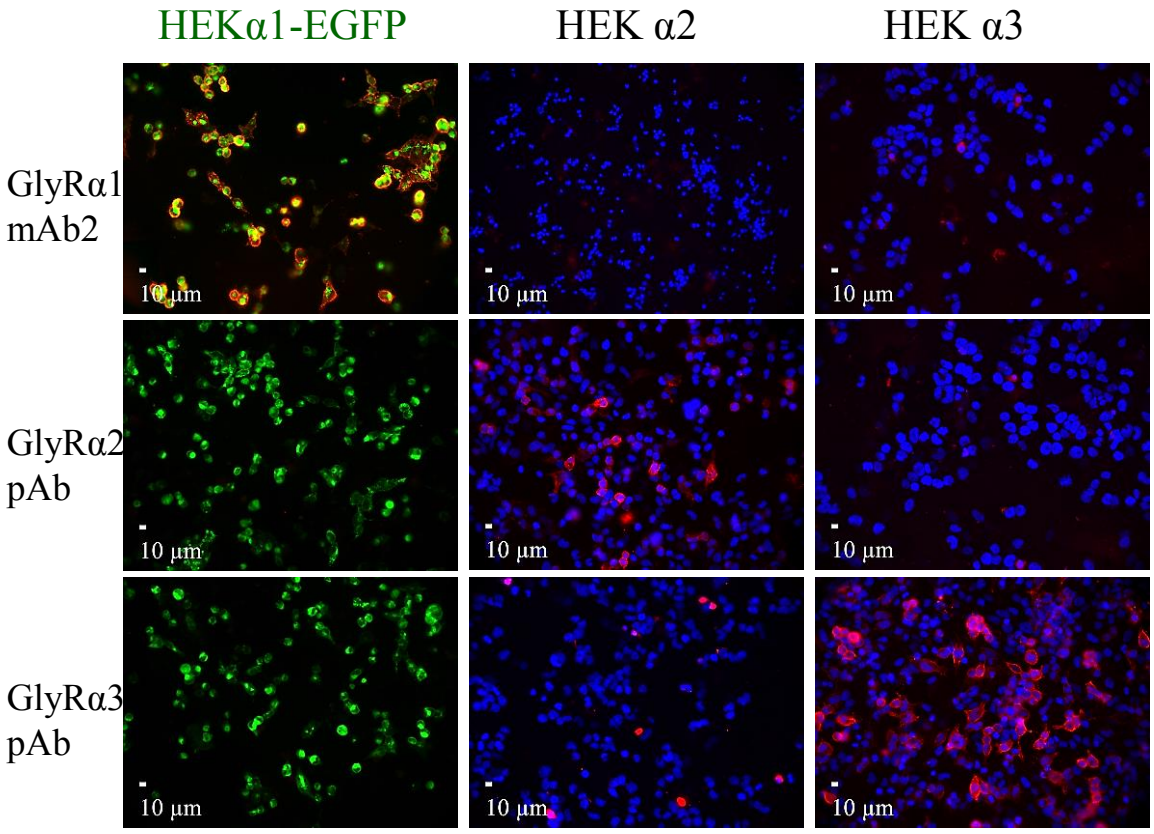

Fig. 3.3. Commercial antibodies specificity for different GlyR subunits. A. Commercial antibodies to GlyRα1, GlyRα2 and GlyRα3 were tested for specificity on HEK cells expressing each GlyRα subunit. Each monoclonal antibody bound to HEK cells (red) expressing their corresponding target and not the others.

were tested for binding at 1:80 dilution. Thirteen patients (29.5%) had antibodies only to the GlyRα1subunits, two (4.6%) had antibodies that bound to both the GlyRα1 and GlyRα2 subunits, ten (22.7%) had antibodies that bound to both the GlyRα1 and GlyRα3 subunits, and the remaining 19 (43.2%) had antibodies that bound to all three GlyR alpha subunits. These different reactivities did not relate to the overall GlyRα1 titres (one-way ANOVA, $p = 0.246$) (Fig. 3.4C). Although the addition of the α2 or α3 subunits slightly increased antibody binding in a few cases, the majority of the patients' sera bound predominantly to the GlyRα1 subunit, as confirmed by immunoadsorption against HEK cells expressing GlyRα1 subunit. But the serum binding was also lost after immunoadsorption against HEK cells expressing GlyRα2 or GlyRα3 subunits suggesting a shared epitope (Fig. 3.5).

3.2.3 Clinical aspects of patients with GlyR-Ab positive referred samples

For the 52 prospectively-referred GlyR-Ab positive patients, questionnaires were sent to the referring neurologists. Seven patients with very low GlyR-Abs (not titrating beyond 1:40) were excluded from the cohort because they had minimal symptoms and were lost to follow-up (n=2), the clinician did not respond (n=1) or the patients received a different diagnosis: one with CJD (Angus-Lepan et al 2013), one with confirmed hereditary myoclonus dystonia (DYT_11), one with a motor polyneuropathy and one with a possible psychogenic movement disorder. Of the remaining 45 patients, 38 (84.4%) were referred from Europe, six (13.3%) from Asia and one (2.22%) from North America.

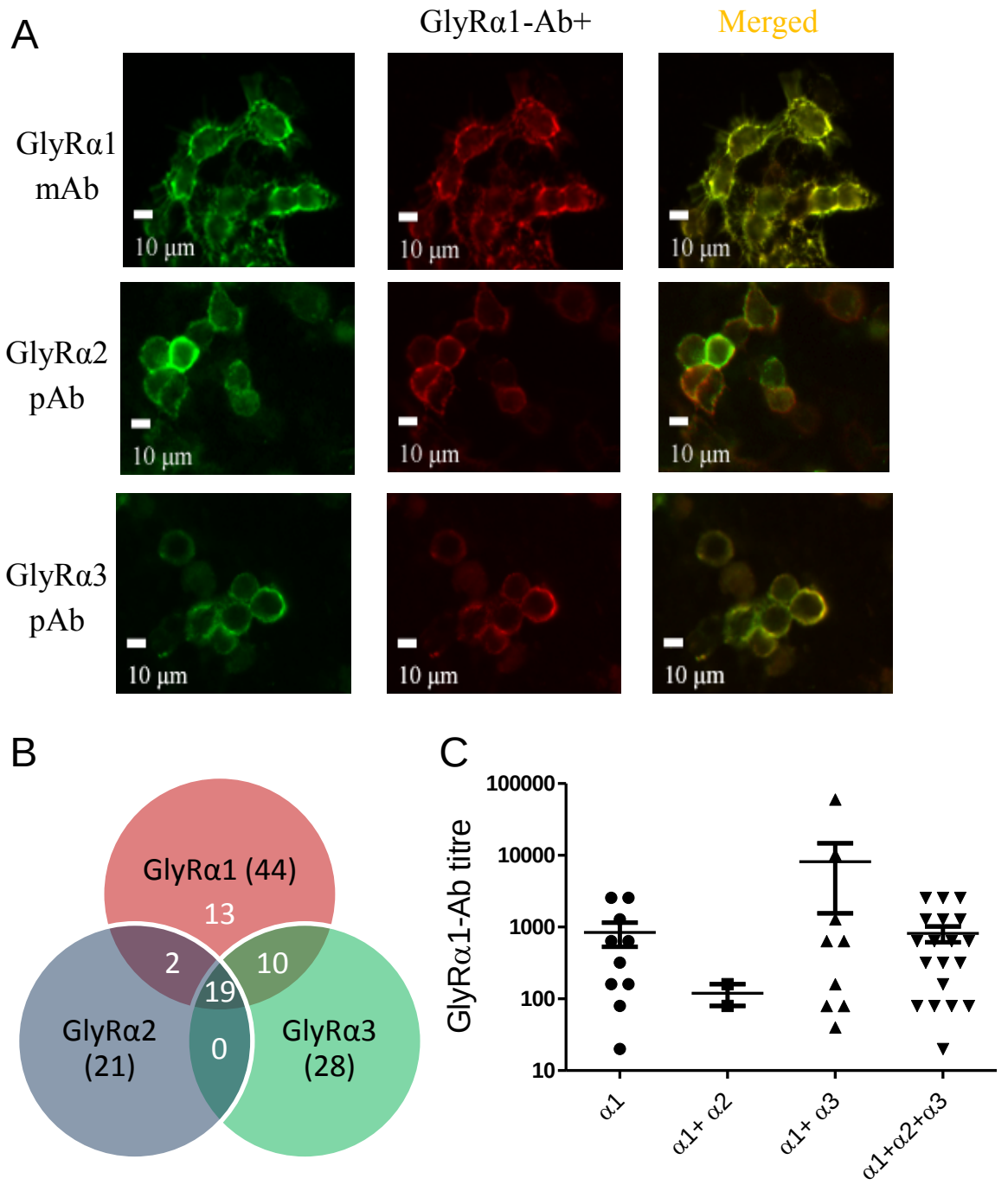

Fig. 3.4. Patient´s sera binds to more than one GlyRα subunits. A. Example of a patient serum (red) binding to HEK cells expressing GlyRα1, α2 or α3 subunits and colocalising with monoclonal antibodies to GlyRα1, 2 or 3 respectively (green). ***B.*** All patients' sera had antibodies to GlyRα1, 13 exclusively; two bound to α1 and α2 subunits, 10 bound to α1 and α3 subunits and the other 19 sera bound all three α subunits tested. ***C.*** GlyRα1-ab titres in 40 patients plotted according to their reactivity with the different subunits. All sera were tested at 1:80; titrations were not performed for reactivity with the α2 or α3 subunits. Two-way ANOVA ($F=1.439$, df:3, $p = 0.246$).

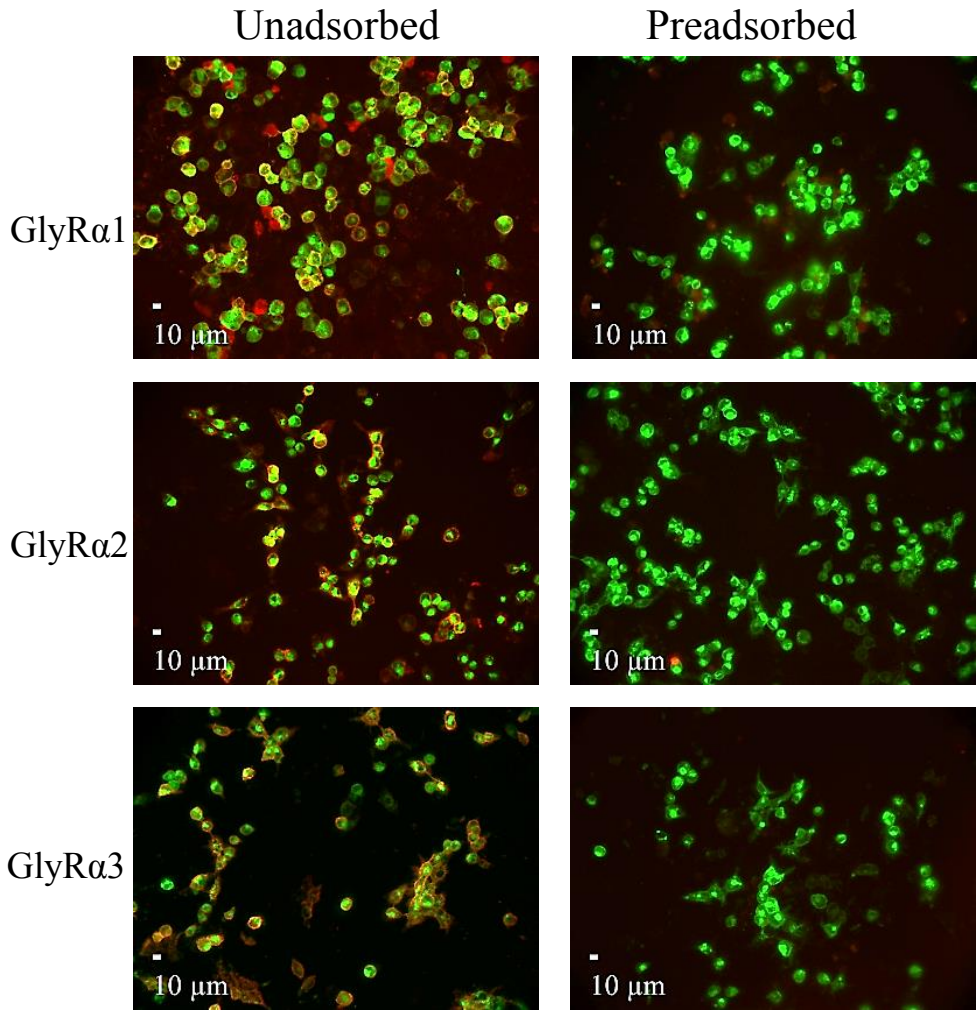

Fig. 3.5. Patient sera binding to HEK cells expressing GlyRα1 is lost after serum preadsorption against each GlyRα subunit. Images were taken at 20x magnification. Patient's serum (red) binding to HEK GlyRα1-EGFP cells is lost after serum preadsorption with HEK cells expressing either GlyRα1, GlyRα2 or GlyRα3.

3.2.3.1 Demographics

General features of the patients are summarised in table 3.2. The age of onset was 1 to 75 years (median 50 years). Adults were predominantly affected (41; 91.1%) but there were four children (4; 8.9%); males were slightly more affected in the adult population (24/41; 53.3%) than females (21/41; 46.7%) but all four children were female.

3.2.3.2 Disease presentation and clinical course

At the time of first GlyR-Ab positive test, the duration of symptoms was highly variable ranging from < 1 to 96 months but half were <2.5 months. For disease presentation acute was defined as a disease developed within 1 week, subacute as a disease developing over a longer period of time (1 to 4 weeks) and chronic as a disease that last more than 4 weeks. The disease presentation was described as acute in 9/45 (20%), subacute in 23/45 (51.1%) or chronic in 13/45 (28.9%). The subsequent clinical course was also variable, four patients (8.9%) died during the initial hospitalisation, with 12 (26.7%) having an apparently monophasic disease, 18 (40%) having recurrent or relapsing disease, and 9 (20%) were reported as chronic and progressive. 2 patients (4.4%) were lost to follow-up, thus the subsequent course is unknown (Table 3.2).

3.2.3.3 Comorbidity

Comorbidity was common in these patients. Thirteen of 45 (29%) patients had autoimmune diseases (six thyroid disease, three diabetes, one rheumatoid arthritis, one mixed connective tissue disease, one sarcoid and one psoriasis). Tumours were also associated in 9/45 (20%) patients: five patients had previous successfully-treated tumours (breast, malignant melanoma, Hodgkins lymphoma, thymoma and lymphoma), and four patients had active tumours during the neurological illness (three thymomas,

Table 3.2. General features of patients with GlyR antibodies referred 2008-2012

Demographics, clinical course and outcome	Total patients	(%)
Total number of patients	45	
Gender F:M	21:24	53.3:47.6
Children F:M	4:0	100:0
Age at onset (years)	1-75	
Disease presentation		
Duration at time of diagnosis, months (median) (no)	0.1-96 (2.5) (only provided in 18 cases)	
Acute	9	20%
Subacute	23	51.1%
Chronic	13	28.9%
Course of disease		
Monophasic	12	26.7%
Recurrent	18	40%
Chronic progressive	9	20%
Undefined (too short follow-up, unknown, died)	6	13.3%
Disability		
Moderate (mRS 2-3)	8	17.8%
Severe (mRS 4-5)	37	82.2%

Preceding events/associated conditions at any time		
Autoimmune/inflammatory diseases (known at onset)	13 (1 psoriasis; 6 thyroid disease; 3 diabetes; 1 rheumatoid arthritis; 1 sarcoid; 1 mixed connective disease)	28.8%
Tumours in past medical history and succesfully treated	5 (1 breast cancer; 1 breast cancer and thymoma; 1 thymoma and lymphoma; 1 Hodgkin lymphoma; 1malignant melanoma	11.1%
Tumours found during current neurological illness	4 (3 thymoma; 1 B cell marginal zone lymphoma associated with monoclonal gammapathy IgM (10%); 1 metastases from previous treated breast cancer	8.8%

mRS = Modified Rankin Scale.

one B cell marginal zone lymphoma with IgM monoclonal gammapathy). In addition, one woman presented with metastases from her previously treated breast cancer (Table 3.2).

3.2.3.4 Clinical features

The clinical manifestations of the 45 patients are summarised in Table 3.3. At presentation, the most common features were motor, including spasms, often painful, stiffness and rigidity of axial and limb muscles, which were associated with walking difficulties and falls (69%). Brainstem symptoms were also frequent such as excessive startle (42%), oculomotor disturbance, dysphagia, and dysarthria (47%). 29% of patients had symptoms of autonomic dysfunction (dry mouth, dizziness, hyper/hypohidrosis, urinary retention, bowel and sexual problems). Non-specific sensory symptoms (pruritus, dysesthesias, hyperaesthesias and pain) and pyramidal signs (limb paresis) were reported in 22% of patients. Unexpectedly, 29% of patients had cognitive disturbance, sleep problems or seizures (13%). Less common symptoms included cerebellar signs (ataxia, nystagmus) in 13% of patients.

The clinical features of 30 patients who had a delayed diagnosis and treatment, and therefore likely a more advanced course of the disease, were also documented at nadir. As expected, the clinical features were more prominent with spasms and stiffness present in 80% of the patients with brainstem signs or hyperekplexia in 55% and 57% of the patients respectively. Autonomic disturbance was present in 43%. In addition, pyramidal signs (60%), sensory symptoms (47%), cognitive deficits and encephalopathy (50%) were also much more evident at nadir (Table 3.3).

Table 3.3. Clinical features of GlyR antibody positive patients referred 2008-2012

Clinical features	Clinical features at onset	Clinical features at peak reported in 30 patients
Total number of patients	45	30
Spasms /Stiffness/Rigidity (neck, trunk or limb muscles)	31 (69%)	24 (80%)
Oculomotor disturbance: nerve or gaze palsy (eyelid ptosis, diplopia, nystagmus, slow/jerky movements)	18 (40%)	16 (53%)
Trigeminal, facial and bulbar disturbance (dysphagia, dysarthria, difficulty chewing, facial numbness, trismus)	21 (47%)	17 (57%)
Excessive startle (spontaneous or triggered by noise or touch)	19 (42%)	17 (57%)
Walking difficulties/falls, mostly related to stiffness/rigidity/spasms)	19 (42%)	24 (80%)
Limb paresis/pyramidal signs	10 (22%)	18 (60%)
Limb or gait cerebellar ataxia	6 (13%)	6 (20%)
Autonomic disturbances (hyper/hypohidrosis, dry mouth, brady/tachycardia, hypo/hypertension, bladder, bowel or sexual dysfunction)	13 (29%)	13 (43%)
Cognitive impairment /encephalopathy / sleep disorders/ seizures	16 (36%)	15 (50%)
Sensory symptoms/pain	10 (22%)	14 (47%)
Respiratory failure (admission in ICU/ventilation)	8 (18%)	8 (27%)

ICU = Intensive care unit.

3.2.3.5 Investigations

Investigations performed were variable and included imaging studies (magnetic resonance imaging (MRI), computed tomography scan (CT), positron emission tomography (PET)), electrophysiology studies (EMG, EEG), chemical and cytological analysis of blood and CSF and autoantibody screening (onconeuronal, cell surface antigens); the results are summarised in Table 3.4.

In general brain and spinal cord MRI were uninformative, with only non-specific findings in less than 25% of the patients (white matter lesions in 3 patients, cortex atrophy in 1 patient, temporal lobe inflammation in 2 patients, other FLAIR lesions in 2 patients, small vessel disease in 2 patients and short and long lesions in the spinal cord in 4 and 1 patients respectively). CT and PET imaging were used to diagnose possible tumours (3 thymomas, 1 abdominal mass and 1 breast metastases). EMG was performed in 29 patients and more than 50% of the patients had specific changes compatible with motoneuron hyperactivity (eight had continuous motor unit activity, six had spontaneous or stimulus-induced activity and one had neuromyotonic discharges); two patients had evidence of sensory neuropathy. In 71.4% of patients (15/21) the EEG showed changes in brain electrical activity (11 had slow activity; three had focal temporal lobe epileptiform activity and one cortical disturbance).

CSF examination in 30 patients showed nonspecific changes in 60% (pleocytosis in 13 patients, raised protein levels in four patients and oligoclonal bands in six patients). The presence of other autoantibodies was reported in 18 patients (5 GAD-Ab, 3 VGKC-complex-Ab, 3 NMDAR-Ab, 6 thyroid and 1 ANA-Ab); no onconeural antibodies were reported.

Table 3.4. Clinical investigations of GlyR antibody patients referred 2008-2012

Total number of patients	45	
Investigations (no performed)	**Results**	**Number of abnormal results/number tested**
Brain MRI (36)	3 with white matter lesions, 1 atrophy, 2 temporal lobe inflammation, 2 other FLAIR lesions, 2 small vessel disease, 26 normal	10/36
Spinal cord MRI (23)	4 short or patchy lesions; 1 longitudinally-extensive lesion; 18 normal	5/23
EMG (29)	8 continuous motor unit activity, 6 spontaneous or stimul-induced activity, 2 sensory neuropathy, 1 neuromyotonic discharges; 12 normal	17/29
EEG(21)	11 slow activity, 3 focal epileptic, 1 cortical disturbance, 6 normal	15/21
CSF(30)	Any abnormality: 18 13 pleocytosis; 4 prot (>1g/L); 6 OCB or >IgG; normal 12	18/30
GAD-Abs (43)	4 >1000 U/ml (approx 25,000 IU/ml); 1 100 U/ml; 38 negative	5/43
Chest CT/whole body PET scan (20)	3 with thymoma; 1 abdominal masses ? lymph nodes; 1 breast metastases; 15 normal	5/20
Onco-neuronal abs	None	0.0
Other autoantibodies	1 high VGKC (2248 pM), 2 low VGKC (<200pM); 3 low NMDAR; 6 thyroid; 1 ANA; 1 Sjogrens Syndrome; 15 normal; no paraneoplastic reported	13/28

ANA = antinuclear antibodies; OCB = oligoclonal bands; GAD= Glutamic acid decarboxylase; VGKC = Voltage gated potassium channels; NMDAR = N-Metil-D-Aspartate receptors.

3.2.3.6 Diagnoses

Clinical diagnoses of the patients were made using the summary of the symptoms and signs the physicians provided in the questionnaires and based on the criteria of Meinck and Thompson (2002) and Brown and Marsden (1999). These define SPS as axial stiffness with or without hyperekplexia and/or autonomic disturbance or seizures, but without other apparent brainstem involvement, and PERM as SPS but with clear brainstem involvement, ataxia or seizures. Patients who had only brainstem features, epilepsy or limbic encephalitis were classified in separate categories even though they might have had an evolving SPS or PERM clinical presentation.

Clinical characteristics of the patients are summarized in Table 3.5. Thirty-three patients (73.4%) were classified as PERM, two (4.4%) as SPS (one with seizures), two (4.4%) with brainstem involvement (one respiratory, one auditory and balance problems), five (11.1%) with limbic or other encephalopathy without brainstem or spinal cord features, and three (6.7%) as other (two with probable demyelinating syndromes, and one with slowly progressive cognitive impairment and dizziness of unclear origin). Of the four children two (50%) had PERM, one (25%) had an epileptic encephalopathy and one (25%) had optic neuritis/ADEM.

3.2.3.7 Treatment

Therapeutic approaches included symptomatic treatment, immunotherapies (steroids, intravenous immunoglobulin, plasma exchange, azathioprine, rituximab, cyclophosphamide, mycophenolate, cyclosporine and surgery or chemotherapy when patients had a neoplastic disease. The variability in treatments possibly reflects the lack of clear guidelines on how to treat these patients.

Table 3.5. Diagnoses, tumours, immunotherapies, GlyR-Ab profiles and immunostaining patterns in 45 patients with GlyR-Abs

Patient	Diagnosis	Serum titre	CSF titre	Tumours	mRS before treatment	CBA score before treatment	Immunotherapies	mRS after treatment	CBA score after treatment	GlyR-Ab profile	Immunostaining pattern
m49	PERM	20		Thymoma	4	1	st pex	2	*	α1	1
m48	PERM	640			4	3	st ivig	2		α1+ α2 + α3	1
m58	PERM	2560	80		4	3.5	st pex AZA Myc	1	1.5	α1+ α2 + α3	1
f37	PERM	1280	640		5	3	st pex, AZA	1	2.5	α1+ α2 + α3	1
m40	PERM	1280			5	3.5	st pex ivig	3	2.5	α1+ α2 + α3	1
m54	PERM	2560	5		5	3.5	st pex ivig, Myc	2	2	α1+ α2 + α3	1
m53	PERM	80			5	2	St	1		α1+ α2 + α3	1
m56	PERM	60000	80		5	4	st ivig	2		α1+ α3	1
m54	PERM	640			5	3.5	st pex, Cyp	6	0.75	α1+ α3	1
m39	PERM	640			3	3.75	pex ivig	1	1.5	α1+ α2 + α3	2
m51	PERM	320		Lymphoma	3	2	st ivig	4		α1+	2

										α2 + α3	
f28	PERM	1280			4	4	None	0	0	α1+ α2 + α3	2
f33	PERM	40			4	2.25	St Ivg	1		α1+ α3	2
m54	PERM	80	40		4	3	st pex cyp	2	0	α1+ α3	2
m28	PERM	640			5	3	None	6	2	α1	2
m29	PERM	160	160		5	2.5	St AZA	1		α1+ α2 + α3	2
m49	PERM	80			5	3	Pex	0	0.5	α1+ α2 + α3	2
m68	PERM	640			5		st pex ivg	6		α1+ α2 + α3	2
f61	PERM	20			5	1.5	Ivg	0		α1+ α2 + α3	2
f1	PERM	320			5	3	st ivig, Myc	1	2	α1+ α2 + α3	2
f61	PERM	320			5	2.5	st ivig	0		α1+ α2 + α3	2
m50	PERM	80			5	1.75	st ivig	2		α1+ α2 + α3	2
m69	PERM	160			5	3	st ivig	1		α1+ α3	2

f61	PERM	2560	640		2	1	st ivig cysp	2		α1+ α2 + α3	3
f14	PERM	640			4	3.5	st pex ivig	1	1	α1+ α2 + α3	3
m34	PERM	160		Thymoma	5	3	unknown	6		α1+ α2	3
f50	PERM	80		Breast cancer, Thymoma	4	2	Pex	1	0	α1+ α3	3
m75	PERM	1280	80	Thymoma	5	2	Pex	1	2.5	α1+ α3	3
f47	PERM	80			5	1.5	Ivig	1		α1+ α2	5
f40	PERM	160			3	2.5	St	1		α1	6
f65	PERM			Breast cancer	5	3.5	st pex	1	1		
m60	PERM	200			5	3	None	5			
m72	PERM	640		Lymphoma	5		st pex	1			
f53	SPS	80	2.5		4	2	St	3	2.5	α1	3
f22	SPS			Thymoma, Lymphoma	4	3	none	5			
m25	Encephalopathy	2560			5	3.5	st ivig	1	2.5	α1	3
f55	Encephalopathy	10240			4		ivig	1	1.5	α1+ α3	2
f48	Encephalopathy	160			3	1.5	none	2		α1	4
f31	Encephalopathy	640			4	4	none	3	1.5	α1	4
f5	Encephalopathy	2560			5	3	st pex ivig	3	2.5	α1	6
m68	Brainstem ence	1280			2	3	St, AZA	1	2	α1	2
f58	Brainstem ence	80		Melanoma	4	2.5	none	0		α1+ α2 +	5

										α3	
f70	Dementia like	100			2	3.5	none	0	2	α1+ α3	2
f8	ADEM optic	320			5	2.5	st ivig	1	2	α1	2
m28	Optic	640			2		st pex cyp	0			

PERM = Progressive encephalomyelitis with rigidity and myoclonus; SPS = Stiff person syndrome; ADEM = acute demyelinating encephalomyelitis; Myc = mycophenolate mofetil; Aza = azathioprine; CyP = cyclophosphamide; CySp = cyclosporine; Rtx = rituximab; mRS = Modified Rankin Scale.

Symptomatic treatment included muscle relaxants such as baclofen, clonazepam or antiepileptics such as valproate, carbamazepine and lamotrigine, which appeared helpful in most patients. Patients with neoplasias at presentation were treated with surgery (two removal of thymoma), or chemotherapy (one B cell lymphoma) in combination with immunotherapies, and all these improved dramatically. One patient who had a thymoma died before surgery as a result of a pulmonary embolism.

Immunotherapies alone or in combination were given in 37 patients (82.2%) (Intravenous steroids in 27 patients, plasma exchange in 15 patients, intravenous immunoglobulins in 18 patients, all three in 5 patients). Seven patients (15.5%) did not receive any immunotherapy and information was unavailable in one patient. Many patients received repeated courses or additional immunosuppressive treatment; four had cyclophosphamide, four received azathioprine, three received mycophenolate, one received cyclosporine, and two rituximab (one as part of his lymphoma treatment) before discharge or as a part of ongoing treatment (Table 3.6).

3.2.3.8 Severity at onset and outcomes

Modified Rankin scores (mRS) at onset and at latest follow-up were provided or based on the information provided by the neurologists on the questionnaires. The results are summarised in Table 3.6. In general, the majority of patients (38, 84.4%) had high levels of disability at onset or nadir. Twelve patients (33.3%) were graded as 4, but 26 patients (57.7%) were graded as 5, which included eight patients (18%) requiring ICU admission. The remaining seven patients (15.5%) had mild moderate (mRS 2-3) disability scores. 70% of the PERM patients had high levels of disability (mRS 5) compared with 25% of those with SPS or other features (Fisher´s exact test, $p < 0.0149$) (Table 3.7; Fig. 3.6A)

Table 3.6. Patient´s treatment and clinical outcome

Immunotherapies		
Intravenous Steroids	27	60%
Plasma Exchange	15	25.6%
Intravenous Immunoglobulines	18	40%
All three	5	11.1%
None (symptomatic treatment BZD, Baclofen)	7	15.6%
Second line immunosuppressive treatment	14 (3 Myc, 4 Aza, 4 CyP, 1 CySp, 2 Rtx)	31.1%
Outcome (disability)		
Mild (mRS 0-1)	26	57.8%
Moderate (mRS 2-3)	12	26.7%
Severe (mRS 4-5)	2	4.4%
Death (mRS 6)	4	8.8%

BZD = Benzodiazepines; Myc = mycophenolate mofetil; Aza = azathioprine; CyP = cyclophosphamide; CySp = cyclosporine; Rtx = rituximab; mRS = Modified Rankin Scale.

Table 3.7. Comparison between the frequencies of high disability with clinical syndrome

mRS scores	PERM N=33	Not PERM (SPS, Brainstem, Encephalopathy, Other) N=12	P
< 5 (Mild to high disability)	10 (30%)	9 (75%)	0.0149
= 5 (Very high disability)	23 (70%)	3 (25%)	

To analyse the clinical outcome, the mRS scores at latest follow-up and the change in mRS scores were stratified according to disease classification or immunotherapies used. The outcomes were generally very good with the mRS scores falling from a median of 5 at maximum severity to 1 (paired students t-test, $p < 0.0001$) (Fig. 3.6B), irrespectively of the clinical syndrome (one way ANOVA, $p < 0.0001$) (Fig. 3.6C). There were no differences in the change of mRS among the patient groups (one way ANOVA, $p = 0.1$) (Fig. 3.6D). However, four patients had died in hospital (mRS = 6), two during the acute illness and two from indirect causes (one pulmonary embolism while recovering from respiratory failure, one following a fall while on warfarin).

The dead patients were excluded for treatment dependent long-term outcomes. Treated patients had a significant improvement of their mRS scores independent of the immunotherapy received (one way ANOVA, $p < 0.0001$) (Fig. 3.7A), even when they had only symptomatic treatment (paired t-test $t=2.607$, $df=5$, $p = 0.0478$). However, there were significant differences in degrees of improvement between treatments (one way ANOVA, $p = 0.0397$) (Fig. 3.7B). Patients who received symptomatic treatment or steroids alone had less improvement in their disability scores compared to patients who received plasmapheresis or IvIg alone ($p < 0.05$). The differences across

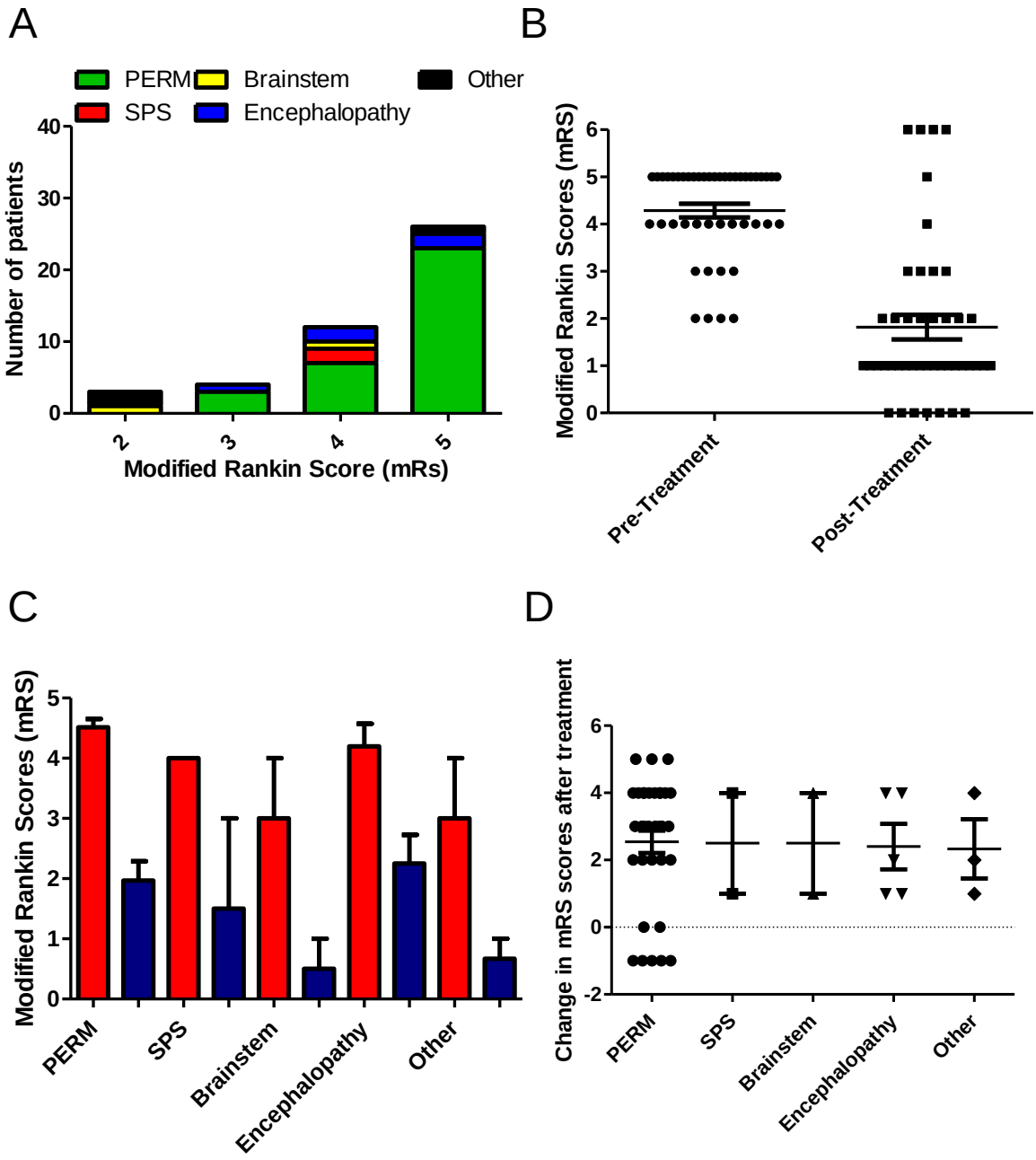

Fig. 3.6. Modified Rankin scale (mRS) scores at maximum severity and at recent follow-up. Two patients were lost to long-term follow-up. ***A.*** The majority of PERM patients had high disability scores while the other syndromes had lesser degree of disability. ***B.*** GlyR-Ab positive patients had high disability but improved significantly after treatment. Paired students t-test ($t=8.010$, $df=43$, $p < 0.0001$). ***C.*** Modified Rankin scale scores according to the clinical syndrome compared between maximum severity and follow-up in all patients including the four who died (modified Rankin score 6). One way ANOVA ($F= 9.176$, $df= 9$, $p < 0.0001$). ***D.*** No significant differences in the change in mRS scores after treatment among clinical groups were observed. One way ANOVA ($F=0.01389$, $df= 4$, $p = 0.1$).

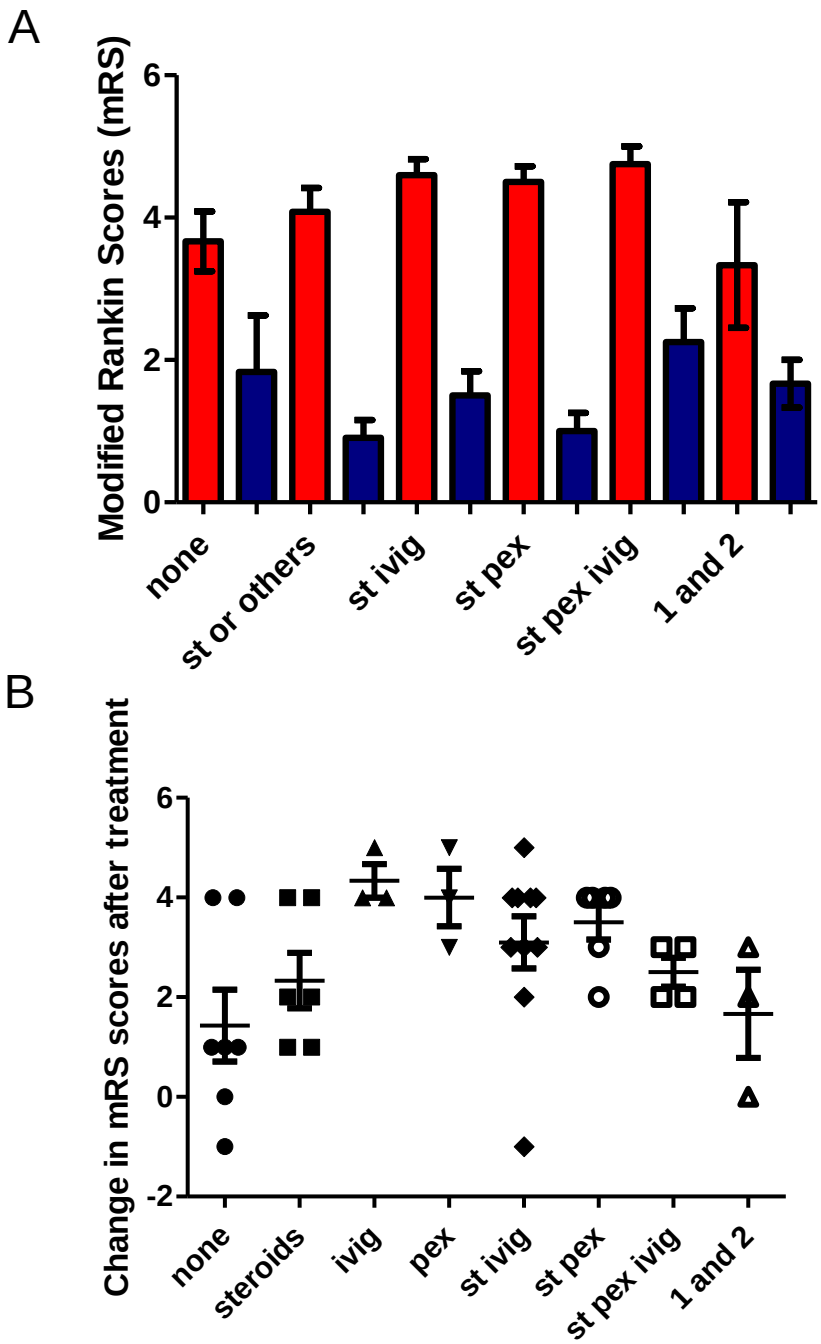

Fig. 3.7. Modified Rankin scale (mRS) scores in patients with PERM or related syndromes after different treatments. Four patients who died were excluded. ***A.*** Modified Rankin scale scores improved with different immunotherapy strategies. One way ANOVA ($F= 15.11$, $df= 11$, $p < 0.0001$). ***B.*** Treatment with combinations of immunotherapy agents produced larger changes in mRS scores compared with mono-therapy or symptomatic treatment only. One way ANOVA ($F= 2.425$, $df= 8$, $p = 0.0397$).

immunotherapies have to be interpreted cautiously, since the interventions used may have reflected the disease severity, which could have influenced outcomes, and the numbers in each group were small.

3.2.3.8 Clinico-serological correlations

In order to determine if the clinical heterogeneity in presentation and the differences in severity and outcomes among patients can be explained by specific differences in the immunological profile of the antibodies, GlyR-Ab positive patients were segregated by clinical syndrome and then we analysed antibody titre in serum or CSF, specificity for GlyR subunits, or serum binding profile to rat tissue (see Chapter 4).

Although, patients with PERM tended to have higher GlyR-Abs titres, there was no clear relationship between GlyR-Ab titre and clinical picture (one way ANOVA, $p = 0.988$) (Fig. 3.8A) and no clear correlation between GlyR-Ab titre in serum and disability mRS scores ($r2 = 0.0042$, $p = 0.684$, $n = 42$) (Fig. 3.8B). CSF samples were available only in patients with PERM but showed no correlation between GlyR-Ab titre and disease severity ($r2 = 0.092$, $p = 0.364$ $n = 11$) (Fig. 3.8C).

GlyR subunit antibodies profiling across clinical syndromes was analysed in 40 patients, PERM patients had antibodies with all GlyR-Ab binding profiles, whereas the other clinical presentations did not have all GlyR binding profiles. (Fig.3.9; Table 3.8). The only clear correlation between GlyR-Ab profile and clinical presentation was that antibodies that bound only to GlyRα1 subunit were present in all the clinical presentations while antibodies that bound to more than one α subunit, especially those binding to all three GlyR α subunits, which were the most common, were only present in patients with PERM or brainstem symptoms (Fisher´s exact test, $p < 0.0021$) (Table

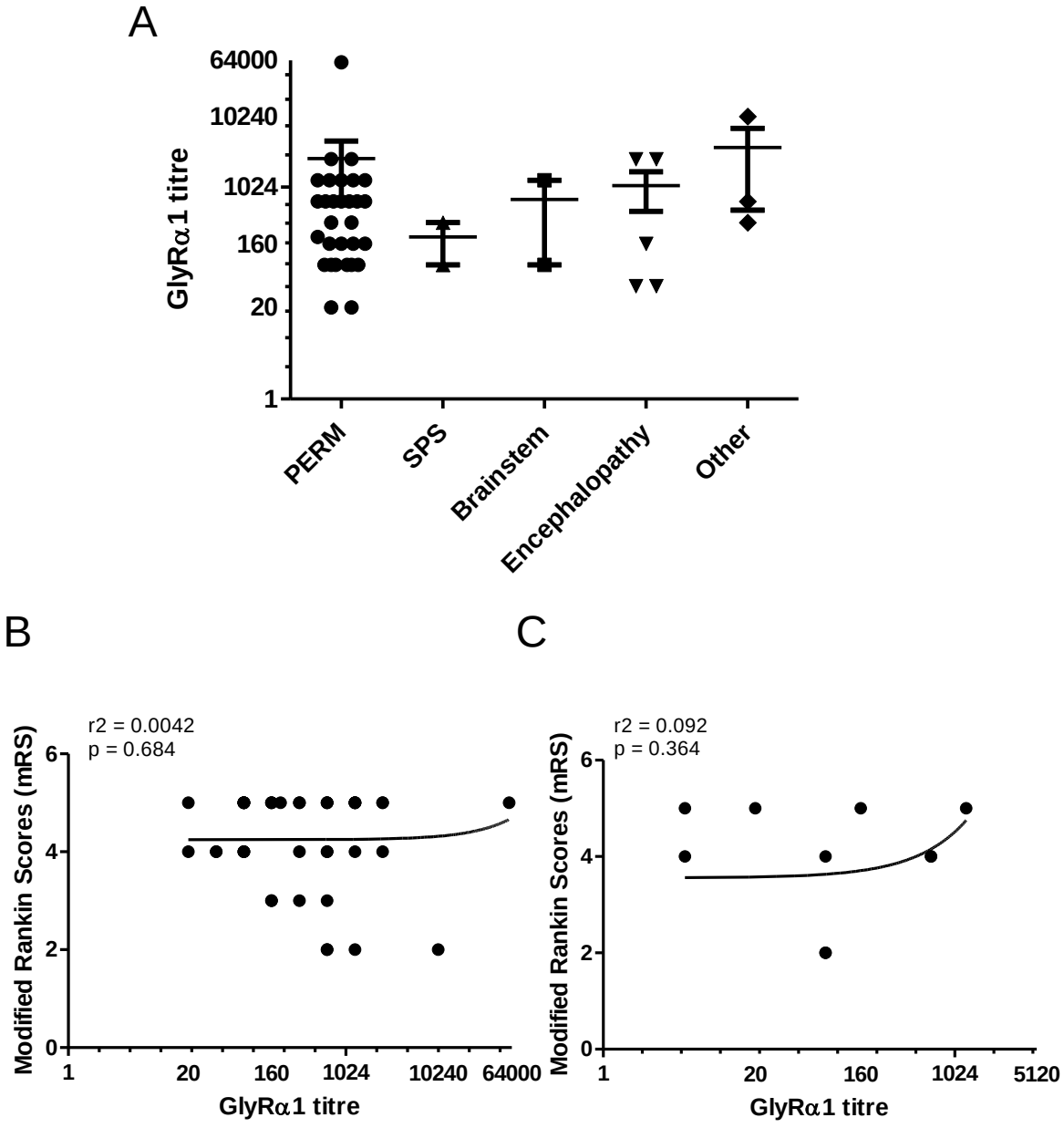

Fig. 3.8. GlyRα1 titres were similar in PERM or related syndromes and did not relate to disease severity. A. No differences in GlyRα1 titres were observed among clinical syndromes One way ANOVA (F= 0.081, df= 5, p = 0.988). No correlation between GlyRα1 titres in serum **(*B*)** or CSF **(*C*)** and modified Rankin scale scores was observed.

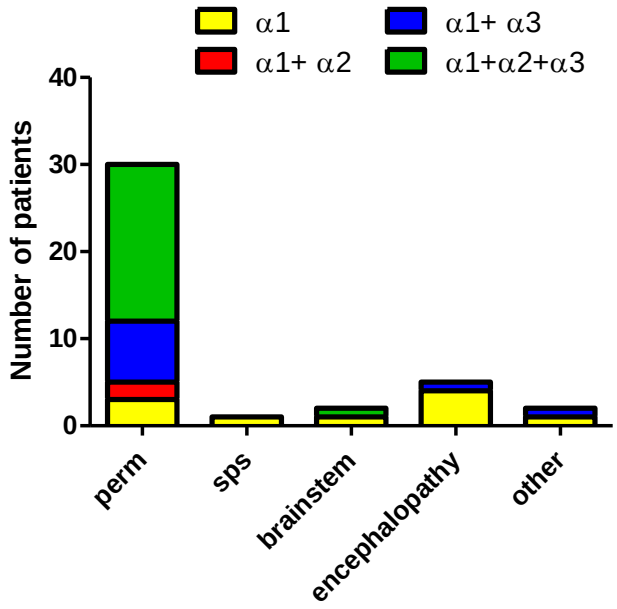

Fig. 3.9. Distribution of patients by clinical diagnosis and antibody subunit profile. Antibodies that bound to all the GlyRα subunits are present only in patients with PERM and brainstem symptoms, while antibodies that only bound to GlyRα1 subunit were present in all clinical syndromes.

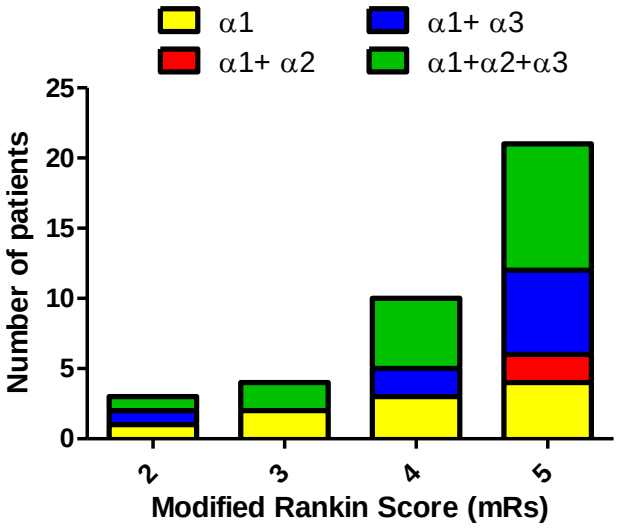

Fig. 3.10. Distribution of patients by disease severity and antibody subunit profile. Antibodies that bound to all the GlyRα subunits and the ones that only bind to GlyRα1 subunit were distributed in all clinical syndromes.

3.9). This generated an odds ratio of 39 (1.853 to 820.7) and a positive predictive value of 100% for having antibodies that bind to all GlyR subunits as a PERM predictor and a negative predictive value of 79.2%.

When GlyR-Ab profiling and disease severity was analysed (Fig. 3.10; Table 3.10), no clear relationship was observed as most of the GlyR-Ab profiles found in patients were distributed across their different disability mRS scores (Fisher´s exact test, p = 0.633; Table 3.11).

Additionally, in order to know if the improvement in disability scores after treatment was related to a decrease in the antibody titres, the change in mRS scores and the change in CBA scores in 25 patients who had GlyR-Ab testing at onset and at follow-up were analysed (Fig. 3.11 A,B). The mRS scores decreased by 62.2% from the initial value and the CBA scores decreased by 52.7% from the initial value (Fig. 3.11C). The decrease in mRS scores and CBA scores after treatment were not different (paired students t-test, p = 0.289) and there was no correlation between the percentage in change in mRS scores and the percentage of change in CBA scores; however, these results have to be interpreted cautiously since confounding factors such as follow-up time were not taken into account (Fig. 3.11D).

Table 3.8. Distribution of the antibody profile in the clinical syndromes

GlyRα antibody profile	PERM (N=30)	SPS (N=2)	Brainstem (N=2)	Encephalopathy (N=5)	Others (N=2)
α1	3 (10%)	1 (50%)	1 (50%)	4 (80%)	1 (50%)
α1+ α2	2 (6.7%)	0	0	0	0
α1+ α3	7 (23.3%)	0	0	1 (20%)	1 (50%)
α1+ α2 + α3	18 (60%)	0	1 (50%)	0	0

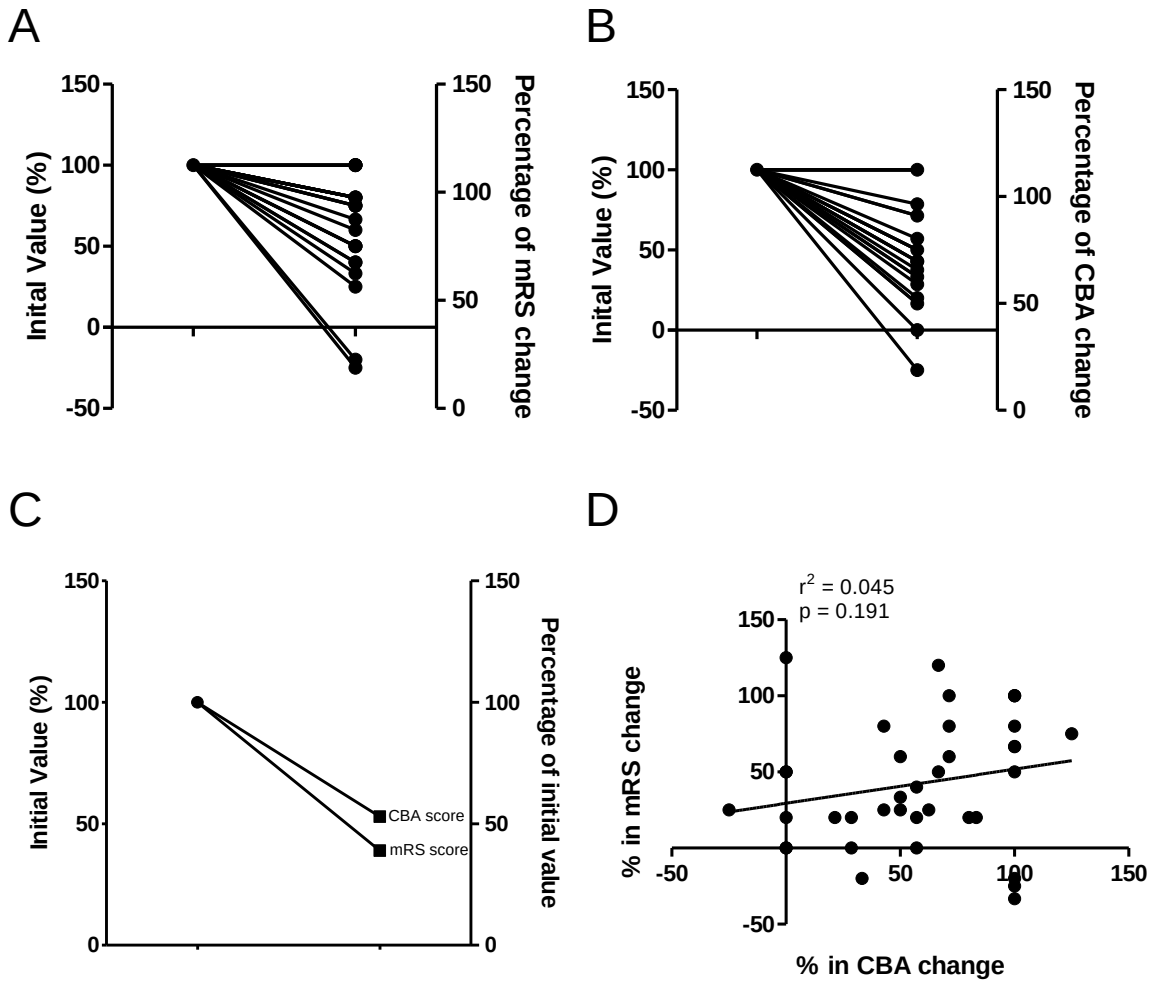

Fig. 3.11. Percentage of change in modified Rankin scale scores and cell based assays scores after treatment. A. Modified Rankin scores in general decreased after treatment but in two patients the mRS didn´t decrease. ***B.*** Cell based scores in general decreased after treatment but in two patients didn´t decrease. ***C.*** Decrease in Modified Rankin scores (62.2%) and CBA scores (52.8%) after treatment was similar (paired students t-test t=1.084, df=24, p = 0.289). ***D.*** No correlation was found between the percentage of change in the mRS scores and the percentage of change in the CBA scores.

Table 3.9. Comparison between the frequencies of GlyRα antibody profile with clinical syndrome

GlyRα antibody profile	Typical (PERM, SPS, Brainstem) N=24	Atypical (Encephalopathy, Other) N=10	P
GlyRα1	5 (20.8%)	5 (50%)	0.0021
GlyRα1+ GlyRα2+GlyRα3	19 (79.2%)	5 (50%)	

Table 3.10. Distribution of the antibody profile in the mRS disability scores

GlyRα antibody profile	mRS 2 (N=3)	mRS 3 (N=4)	mRS 4 (N=12)	mRS 5 (N=21)
α1	1 (33.3%)	2 (50%)	3 (25%)	4 (19%)
α1+ α2	0	0	0	2 (9.5%)
α1+ α3	1 (33.3%)	0	2 (16.7%)	6 (28.6%)
α1+ α2 + α3	1 (33.3%)	2 (50%)	5 (41.7%)	9 (42.6%)

Table 3.11. Comparison between the frequencies of GlyRα antibody profile with disability severity

GlyRα antibody profile	Low disability(mRS 2, 3) N=6	High disability (mRS 4, 5) N=21	P
GlyRα1	3 (50%)	7 (30.4%)	0.638
GlyRα1+ GlyRα2+GlyRα3	3 (50%)	14 (66.7%)	

3.3 Discussion

GlyR-Abs have only recently been recognised and the clinical and immunological characteristics of GlyR-Ab positive patients have not been characterised extensively. Until the publication of these data (Carvajal-González et al, 2014) most of the

information came from case reports and from two recently published retrospective cohorts, one in adults and the other one in children (McKeon et al 2013; Clardy et al 2013). This was the first prospectively diagnosed cohort of 45 patients with GlyR-Abs classifying the clinical syndromes and characterising their antibodies. Patients came from different European centres, and since GlyR-Abs are present in diseases with very low prevalence and incidence, it is very likely that this cohort is a good representation of the disease presentation in the general population in Europe.

The patients were identified by the presence of a positive GlyR-Ab but the final clinical classification was based principally on Meinck and Thompson (2002) and Espay and Chen (2006). PERM was defined as brainstem involvement in addition to the axial or limb rigidity typical of SPS or its varied forms (Brown and Marsden 1999). The patients had a varied clinical spectrum, with the majority of patients presenting with spinal cord hyperexcitability associated with brainstem features and compatible with a diagnosis of PERM. But a few patients presented only with spinal cord hyperexcitability or brainstem involvement compatible with a diagnosis of SPS or brainstem encephalitis (these patients had encephalopathic manifestations in addition to the brainstem features). In addition, there were five patients who only had encephalopathic manifestations with seizures, and three had unclear or other diagnoses, including one patient with optic neuritis similar to a previous report of a patient with immunoresponsive progressive visual loss (McKeon et al, 2012). These findings suggest that the clinical phenotype of GlyR autoimmunity can extend beyond the infratentorial involvement of the spinal cord and brainstem.

Patients were highly disabled during the course of the disease, some of them requiring intensive care due to autonomic disturbance and respiratory failure, which may have

contributed to two of the four hospital deaths. However, the majority of patients showed a good or very good response to treatments, despite the delay in a specific diagnosis in some cases, and the variable immunotherapies used. But relapses have occurred in some patients and seemed to be related to weaning of the immunosuppressive therapy, suggesting that long-term follow up and combined immunosuppressive therapy should be considered as is now the case in 27 patients.

GlyR-Abs were present in all the patients but four patients also had very high GAD antibody levels, typically associated with SPS; three of these patients had PERM (one in Iizuka et al 2012). The presence of both antibodies has also been reported in a proportion of archived adult and paediatric patients (McKeon et al 2013; Clardy et al 2013). Some authors have raised questions about the distinction between PERM and SPS, because SPS can evolve into PERM (Espay and Chen 2006), which may be the case in these four patients who had high levels of GAD antibodies and long histories. However, most of the patients in our prospective cohort had only GlyR-Abs and showed a more substantial and sustained clinical improvement with immunosuppressive therapies than usually expected in patients with typical SPS and GAD antibodies. GAD-Ab patients show a variable response to immunotherapy with infrequent recovery (Dalakas et al, 2001, McKeon et al, 2012); possibly due to T cell mediated cytotoxicity as observed in some post-mortem studies (Costa et al, 2002; Warren et al, 2002; Holmøy et al, 2009). The presence of GlyR-Abs in these patients may explain their better outcome, since neuronal cell surface antibodies usually define diseases that are responsive to immunotherapies (Vincent et al 2010; Lancaster and Dalmau 2012; Zuliani et al 2012). Another possibility is that physicians now have a higher confidence

and treat earlier patients with potentially pathogenic antibodies; comparative studies have not been reported yet.

The coexistence of GlyR and GAD antibodies in some patients suggests that neuronal surface antibodies, perhaps to different targets, could determine the clinical phenotypes of patients with GAD-Ab associated diseases which include cerebellar ataxia and a seizure-dominant form of limbic encephalitis (Saiz et al 2009; Malter et al 2010); indeed in an earlier paper it was reported that some SPS patients have additional antibodies to unidentified antigen(s) on the surface of GABAergic neurons (Chang et al 2013a).

The GlyR-Ab levels varied widely between individuals and between serum and CSF in those patients with paired samples, with intrathecal synthesis of the GlyR-Abs exceptionally high in three of six. It seems that high CSF levels are common in this condition, and may even be associated with undetectable serum values in patients with long histories as observed in previous retrospective cohorts (Clardy et al., 2013; McKeon et al., 2013; Carvajal-Gonzalez et al., 2014). However, we did not encounter this in our prospective patients, where the majority of paired samples studied showed that patients had higher serum levels; this does not exclude the possibility that in some patients with PERM or related syndromes there is an insidious onset with a maturing immune response that localises to the CNS and continues to produce GlyR-Abs there even if the peripheral immune response decreases spontaneously over time.

A high percentage of the GlyRα1-Ab positive patients had antibodies that also bind to other GlyRα subunits. This may be related to the high homology and similar secondary structures between the subunits which display 80 to 90% amino acid sequence identity (See Chapter 1, Fig. 1.2). Clinical correlations between the GlyRα subunit antibody

profile with the patient´s clinical presentation or their degree of disability are difficult since some of these patients had antibodies to other intracellular antibodies, and some clinical syndromes had low number of patients. However, PERM patients tended to have a higher prevalence of GlyR-Abs that bind to all the GlyRα subunits. The relevance of this finding has yet to be determined, since the clinical diagnosis is mainly supported by the presence of GlyRα1-Abs and no correlation of antibody specificity with the clinical outcome was observed.

3.4 Conclusions and limitations

The results in this chapter show that patients with symptoms and signs that include ocular motor and other brainstem dysfunction, hyperekplexia, stiffness, rigidity, myoclonus and spasms have GlyR-Abs and their detection supports the use immunotherapies that most likely will be clinically effective.

GlyR-Abs can also be detected in patients with encephalopathic syndromes or with limited brainstem features of auditory or vestibular dysfunction, suggesting their presence in more diverse phenotypes. GlyR-Abs present in the majority of the patients of this prospective cohort are not secondary to paraneoplastic syndromes but a complete investigation to rule out neoplasias such as thymomas and lymphomas must be performed in these patients.

GlyR-Ab positive patients have high disability during their clinical course, including the possibility of death due to autonomic and respiratory impairment, but respond well to immunotherapies; however, relapses may occur following successful treatment, indicating that long-term follow-up and maintenance immunosuppression should be considered.

Some of the results have to be interpreted cautiously since the atypical clinical presentations were present in a low number of patients, thus making difficult any extrapolations. Additionally, there were no consistent data of the immunotherapy timing or dosing, which could have had a major influence on the outcomes. And, there were two patients lost to follow-up which might affect the results given the rarity of the disease. Future analyses taking these factors into account are needed.

Finally, despite the detection of GlyRα1 antibodies in patients with brainstem/spinal cord hyperexcitability disorders, and also in some forms of autoimmune encephalitis, the presence of additional antibodies or other disease mechanisms cannot be excluded and required further studies.

The relationship between serum and CSF levels of surface antibodies and clinical status is complex in many of these antibody mediated CNS diseases. In order to have a better understanding of the role of the antibodies in the disease, in the following chapters the mechanisms of the GlyR-Abs present in the sera of PERM patients are evaluated using *in vitro* and *in vivo* studies.

CHAPTER 4. *In Vitro* Pathogenic Mechanisms of GlyR-Abs

4.1 Introduction

Some PERM patients have GAD antibodies and respond to immunosuppressive therapy, but these antibodies are not considered pathogenic as they are against an intracellular protein (Vincent, 2008; Alexopoulos and Dalakas, 2010; Lancaster and Dalmau, 2012). Moreover, a few post-mortem pathological studies on these patients showed inflammation with perivascular lymphocyte cuffing and neuronal loss in the brainstem and spinal cord, suggesting that there may be T cell-mediated damage (Whiteley et al, 1976; Turner et al 2011).

However, the finding that these patients have antibodies to glycine receptors (Hutchinson et al 2008), a ligand-gated ion channel expressed on the surface of inhibitory neurons in the spinal cord and brainstem, suggested that GlyR-Abs may be pathogenic. One of the criteria that needs to be met to prove the role of serum autoantibodies in autoimmune diseases is the demonstration of functional effects of antibodies using appropriate cell lines *in vitro* (Witebsky et al, 1957; revisited by Rose and Bona in 1993). Different mechanisms of antibody pathogenic mechanisms have been shown, such as increased turnover of the target after IgG binding to the receptor, morphological damage secondary to complement activation and lysis, and functional blocking of the receptor (See Chapter 1).

To date, *in vitro* effects of the antibodies have been demonstrated for very few antibodies, and in some the results are controversial. These antibodies include

acetylcholine receptor antibodies (Drachman et al, 1978), aquaporin-4 antibodies (Hinson et al, 2008), N-Methyl-D-aspartate antibodies (Dalmau et al, 2008), GAD antibodies (Ishida, Mitoma et al. 1999; Mitoma, Song et al. 2000) and MUSK antibodies (Viegas et al 2012). This chapter describes the characteristics of GlyR-Abs and examines the pathological role of these antibodies *in vitro*, before considering the *in vivo* approaches (Chapter 6).

4.2 Results

GlyR-Abs subclasses were determined by CBA as in Chapter 3, but using specific antibodies to human IgG subclasses instead of anti-human IgG. GlyR-Abs were all of the IgG1 subclass, some also had IgG3, and a few samples contained IgM antibodies (Fig. 4.1), mostly at low levels.

IgM and IgG1 and IgG3 subclasses are efficient at activating complement. Since GlyR-Abs antibodies were mainly IgG1 subclass, their ability to activate complement on the cell surface of transfected HEK cells was tested. C3b deposition, detected by fluorescent commercial antibody was observed on the surface of the HEK cells (Fig. 4.2A, 2B). There was a positive correlation between the C3b binding score and the IgG1 binding score $r2 = 0.321$, $p = 0.018$, $n = 17$ (Fig. 4.2C). These results suggest that Ig1 subtype GlyR-Abs, as expected, can activate complement *in vitro*. These analyses were performed before the start of the project.

Another pathogenic mechanism by which antibodies act is receptor internalisation (e.g. Hinson et al, 2007). To test this possibility four patient and four healthy control sera were chosen. Due to the wide range of titres among the chosen sera, it was necessary to

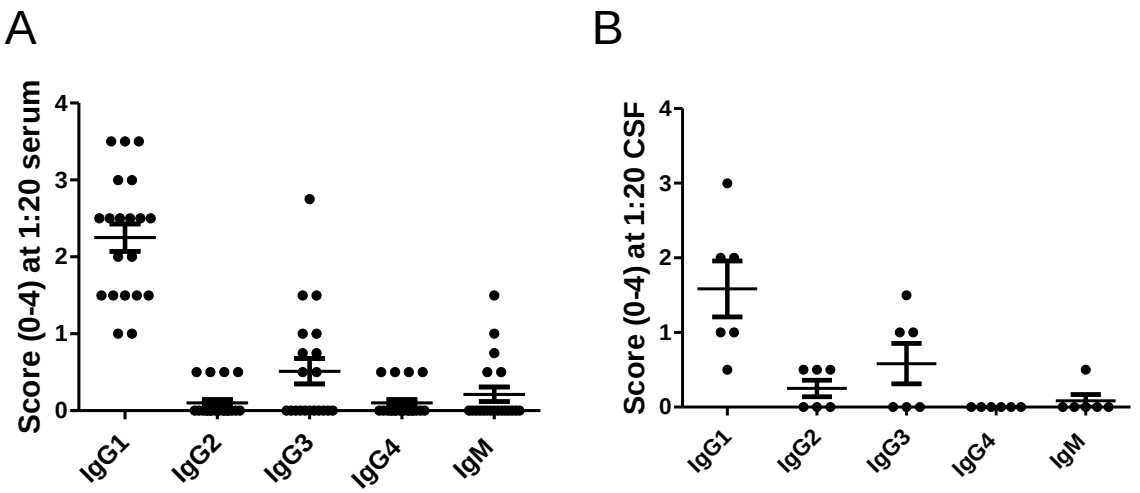

Fig. 4.1. IgG subtypes. CBA scores on GlyRα1-expressing HEK cells. The antibodies are mainly IgG1 and IgG3 subtypes in serum (***A***) and CSF (***B***).

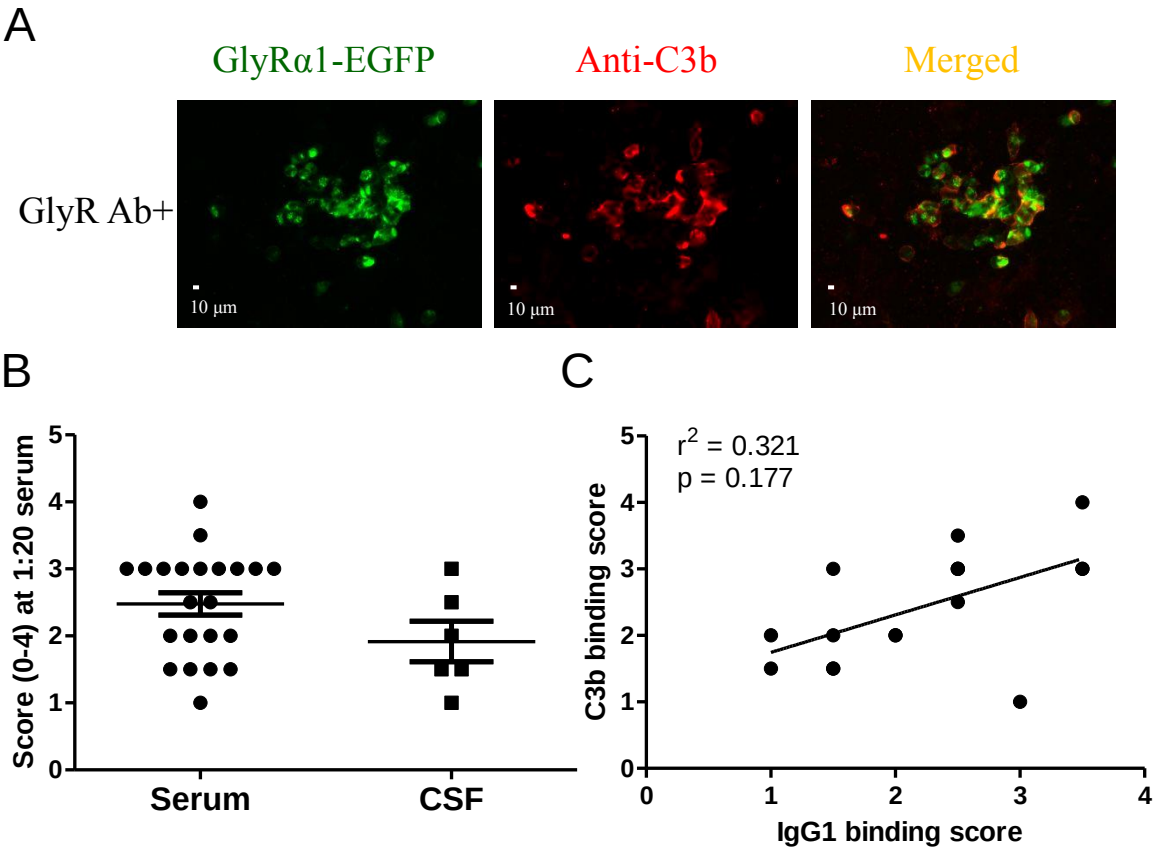

Fig. 4.2. Complement activation on GlyRα1-expressing HEK cells. A. Patient sera deposits C3b complexes on the surface of HEK cells. ***B.*** CBA scores of C3b deposition. ***C.*** There is a good correlation between IgG1-ab binding and complement activation in vitro.

use each serum at a dilution that would produce a similar fluorescence signal; therefore the limiting dilution point for each patient serum was first identified.

The end-point dilution was defined as the last dilution at which the binding scored 1; for the experiments, the dilution before the end-point dilution, which gave a visual score of at least 2 was chosen (limiting dilution point). In three patient sera the limiting dilutions were 1:80 to 1:160; in the fourth patient the end-point dilution was not reached (>1280) and this dilution was used (Fig. 4.3). For the internalisation experiments, the HEK cells expressing EGFP-tagged GlyRα1 were incubated with GlyR-Abs for different time periods (0 – 2 hrs.) at 37° C. The visual immunofluorescence scores increased over time when cells were incubated with patient sera, and there was no evident loss of IgG bound. Control sera did not produce a detectable signal (Fig. 4.4A,B).

Since the GlyR-Abs were present during the whole incubation period time, and the transfected cells were continuing to express GlyRs on the surface during the incubation, binding of the excess GlyR-abs could have obscured any internalisation. Therefore, the protocol was changed; dilutions giving a score of 3 were used to ensure sufficient GlyR-IgG to almost saturate the surface receptors and these were incubated with the cells for 1 hr. at 4°C, before washing the cells to remove excess GlyR-Ab and then raising the temperature to 37° C.

Live or fixed HEK cells expressing EGFP-tagged GlyRα1 subunit were incubated at 37ºC or 4°C with patient sera for different periods of time (0 to 16 hrs.). The bound antibody, as detected by anti-human IgG, decreased over time (average from 3.5 to 1.5 over 16 hours) in live cells incubated at 37ºC compared to live cells incubated at 4ºC or when the cells were fixed before incubation at 37ºC (Fig. 4.5A, 5C). Mean results of

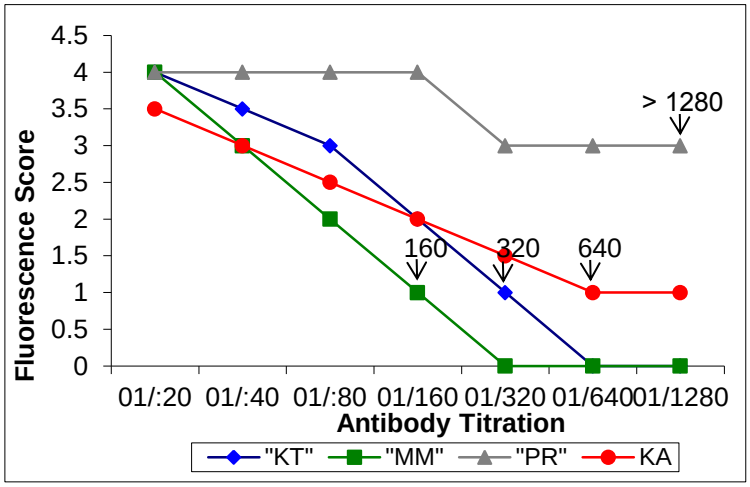

Fig. 4.3. Determination of glycine receptor antibody titres. Results of titrations of four sera based on visual scoring from 0 – 4, endpoints are showed.

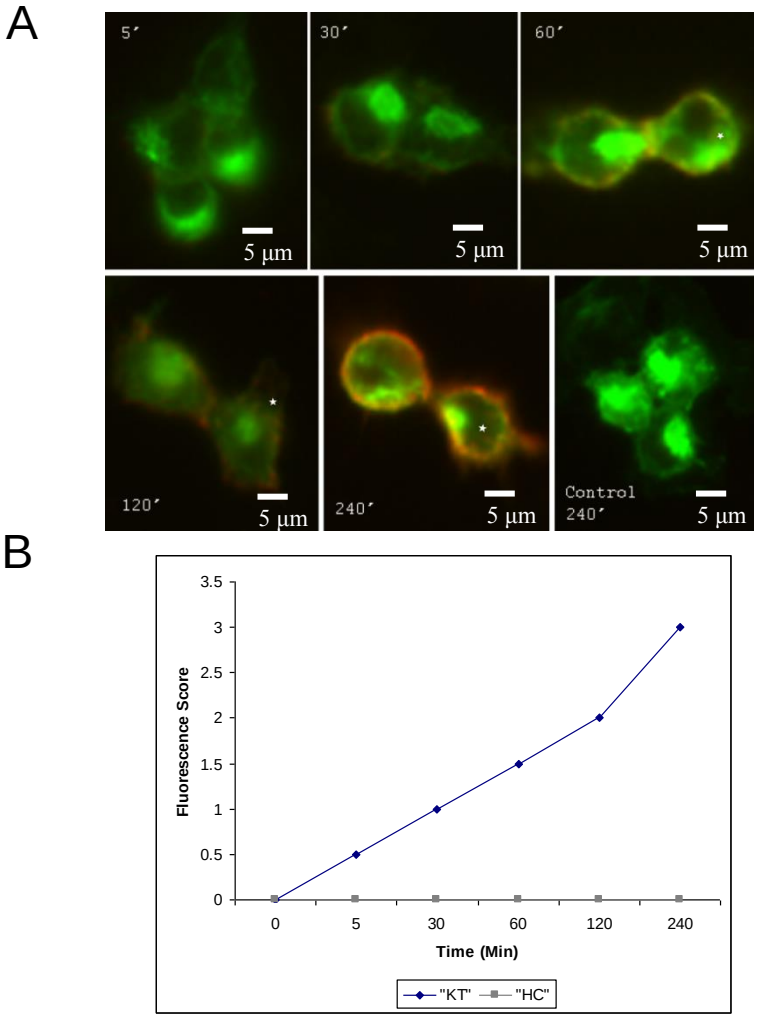

Fig. 4.4. Intensity of surface IgG binding scored as a function of time incubation. A. Merged images of HEK cells expressing GlyRα1 incubated with patient serum showed increased IgG binding over time. No binding is observed when HEK cells were incubated with healthy control serum. ***B.*** Fluorescence scores increased with increasing incubating periods.

the four sera were quantified and analysed using a two-way repeated measures ANOVA showing an effect of condition ($p < 0.0001$)] and time ($p < 0.0001$)], and an interaction between condition and time ($p = 0.0113$) (Table 4.1; Fig. 4.5B).

Post hoc analysis showed that the 37º C live cells had lower bound antibody at 2, 4, 8, 16 hrs of incubation ($p < 0.05$), with a decrease in fluorescence in the 37°C live cells from 0.5 hrs onwards compared to 0 hrs. No differences were found between the 4ºC live cells and 37ºC fixed cells. However, intragroup analysis of the 4ºC live and 37ºC fixed groups showed a decrease in fluorescence score at 16 hrs compared to 0 hrs ($p < 0.05$), suggesting the possibility of IgG dissociation. Healthy control sera showed no binding, as expected (Fig. 4.5A,B). These results suggest a loss of GlyR-Ab binding to the cell surface over time after incubation at 37°C, but also some loss by dissociation.

At higher magnification, in addition to the decrease in the surface binding, there was a change in the staining pattern. The IgG binding became more punctate, and at 2 hrs of incubation it was localised to one end of the cell, suggesting clustering and capping of the receptor (Fig. 4.6A). By contrast, when cells were fixed and incubated at 37ºC or at 4ºC, the surface binding remained constant, mainly on the surface, and the staining pattern did not indicate capping (Fig 4.6B,C).

To confirm that the loss of surface GlyR-Abs was due to internalisation, GlyRα1 subunit transfected HEK cells were treated with patient serum or healthy control serum, followed by 37ºC incubation (0 hrs to 2 hrs) as before; but in this case the cells were either fixed and incubated with anti-human IgG Alexa Fluor 488, or fixed, permeabilised and incubated with anti-human IgG Alexa Fluor 568. The intracellular clusters of red IgG were also quantified. There was an increase of intracellular clusters

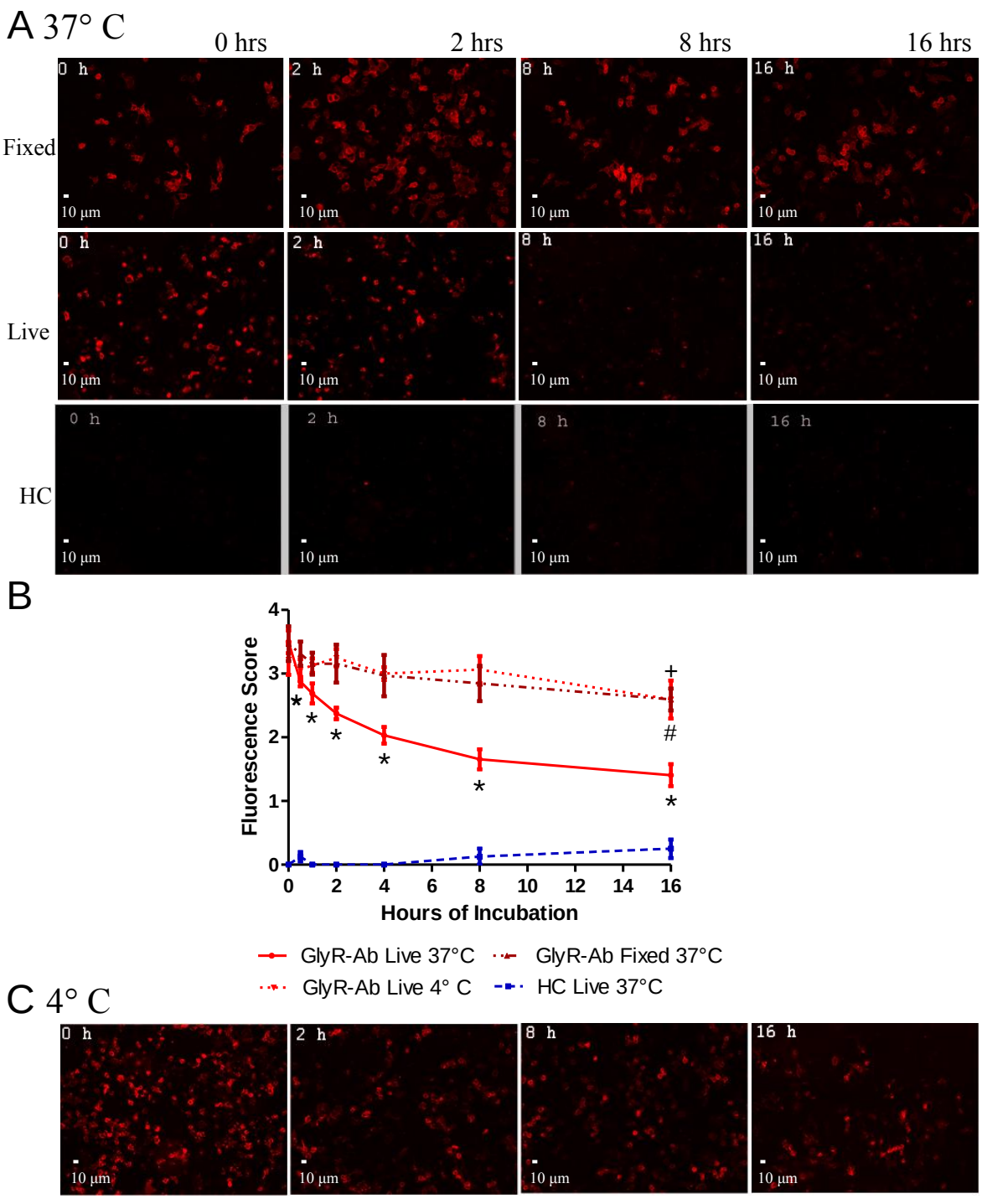

Fig 4.5. GlyR antibodies binding decreases after incubation at 37ºC. GlyR antibodies were labelled with AlexaFluor (568, red) anti-human IgG. ***A.*** There was a significant decrease in the detection of surface anti-human IgG when live HEK cells were exposed to patient serum over time (continuous line, middle panel) but not when they were fixed (dotted line, upper panel) . The score was negative when cells were incubated with healthy control serum (blue line, lower panel). ***B.*** Results from four GlyR antibody-positive sera compared with four healthy individuals' (HC) sera with the surface IgG binding scored after different incubation times. Mean ± SEM is displayed. Significant differences are marked with asterisks and plus signs. Two-way RM ANOVA ($F = 7.832$, $df = 20$, $p < 0.0001$). ***C.*** When incubated at 4ºC, the level of GlyR antibody binding remained constant over time (intermittent line).

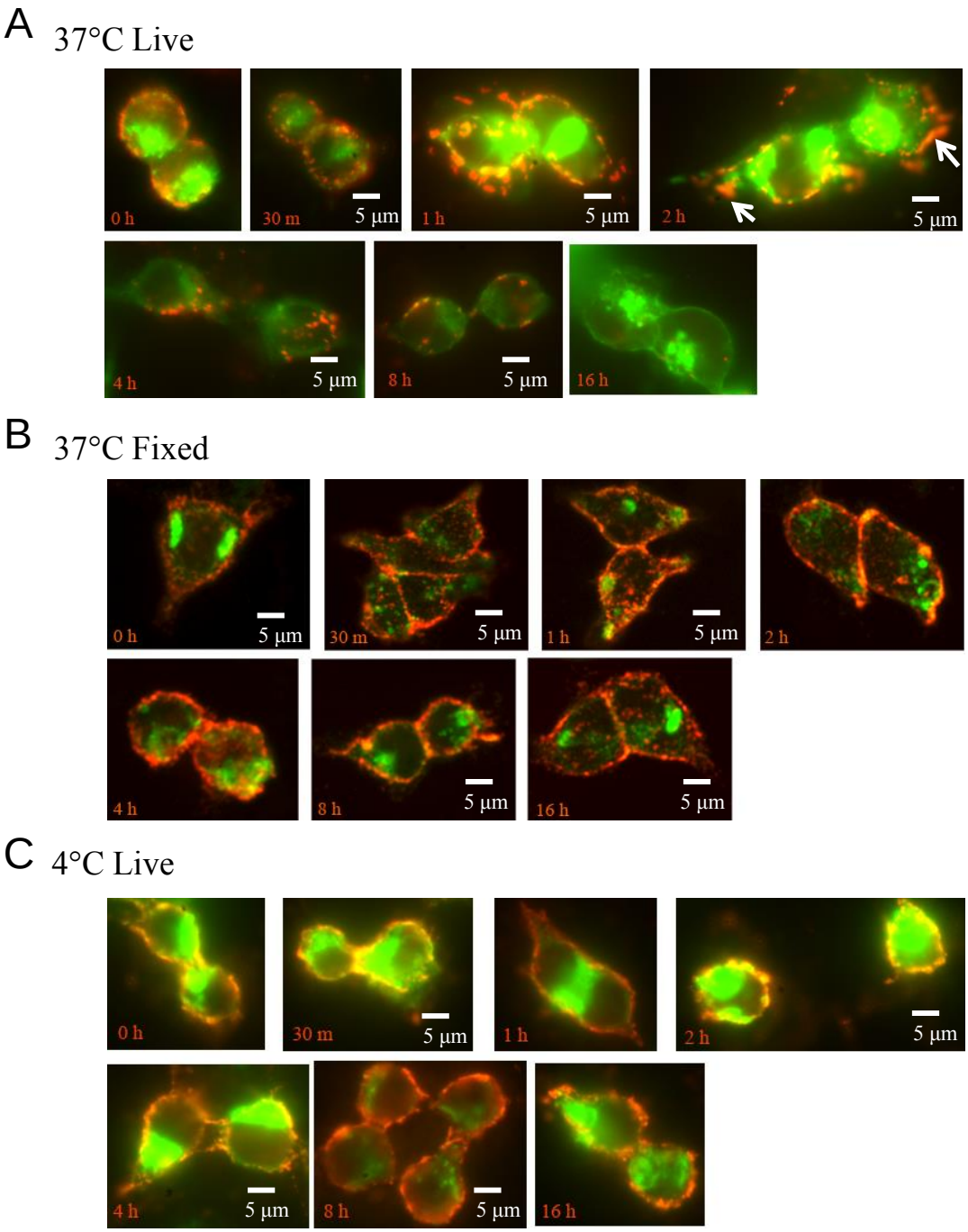

Fig. 4.6. Higher resolution of experiment in Figure 5 shows reduction in surface GlyR antibody binding follows capping and loss of GlyRs. A. Merged images of live HEK cells incubated with serum at 37ºC for different time periods. The surface binding and staining pattern changed, became punctate and was localized in the tail of the cell suggesting capping and clustering of the receptor (marked with arrows). ***B.*** The binding or staining pattern did not changed over time when cells were fixed during the incubation. ***C.*** Merged images of HEK cells incubated with serum at 4ºC for different time periods. The surface binding or staining pattern did not change, there was no evidence of capping and the binding remained constant mainly on the surface. These findings suggest that receptor internalization may be the underlying mechanism.

in the permeabilised cells compared with the unpermeabilised cells over time (Fig. 4.7A,B,C).

The experiment was then repeated, with other sera and over a longer period of time (0 hrs to 8 hrs). By 30 minutes of incubation at 37ºC, large intracellular clusters could be seen in the permeabilised cells (Fig. 4.8A) compared with the unpermeabilised cells (Fig. 4.8B); there was a decrease in the external binding over time in both, and an increase in internal binding 0 to 8 hrs from 3.6% to 60.97% of the cells. The percentage of cells with internal binding remained relatively constant (10%) over time when cells were not permeabilised (Fig. 4.8A,B). An unpaired two-tailed t-test showed that there was an increase in internal binding at 2 hrs compared to 0 hrs in the permeabilised group ($p < 0.0001$), and an increase in the internal binding when comparing the permeabilised and unpermeabilised groups at 2 hrs ($p < 0.0001$) (Table 1; Fig. 4.8C). These results confirmed that GlyR-Abs were internalised.

However, none of these experiments looked at the number of cell surface GlyR receptors. Figure 4.9 shows that the number of cells with GlyR on the surface increased over time during the incubation. The use of transfected cells, which overexpress the protein, may have made it difficult to observe a reduction of the surface receptor.

A preliminary experiment with the same incubation conditions was performed using different amounts of DNA (1µg, 2 µg and 3 µg of DNA), and the cells were treated with cycloheximide 50 µg/ml for 1 hour to prevent new protein synthesis. The percentage of green cells was analysed using a two-way repeated measures ANOVA showing an effect of condition ($p < 0.0001$), and time ($p < 0.0001$), with an interaction between them ($p < 0.0001$). In the cells transfected with 3 µg of DNA the average decrease of green cells was less pronounced (from 60% at 0 hrs of incubation to 43.8%

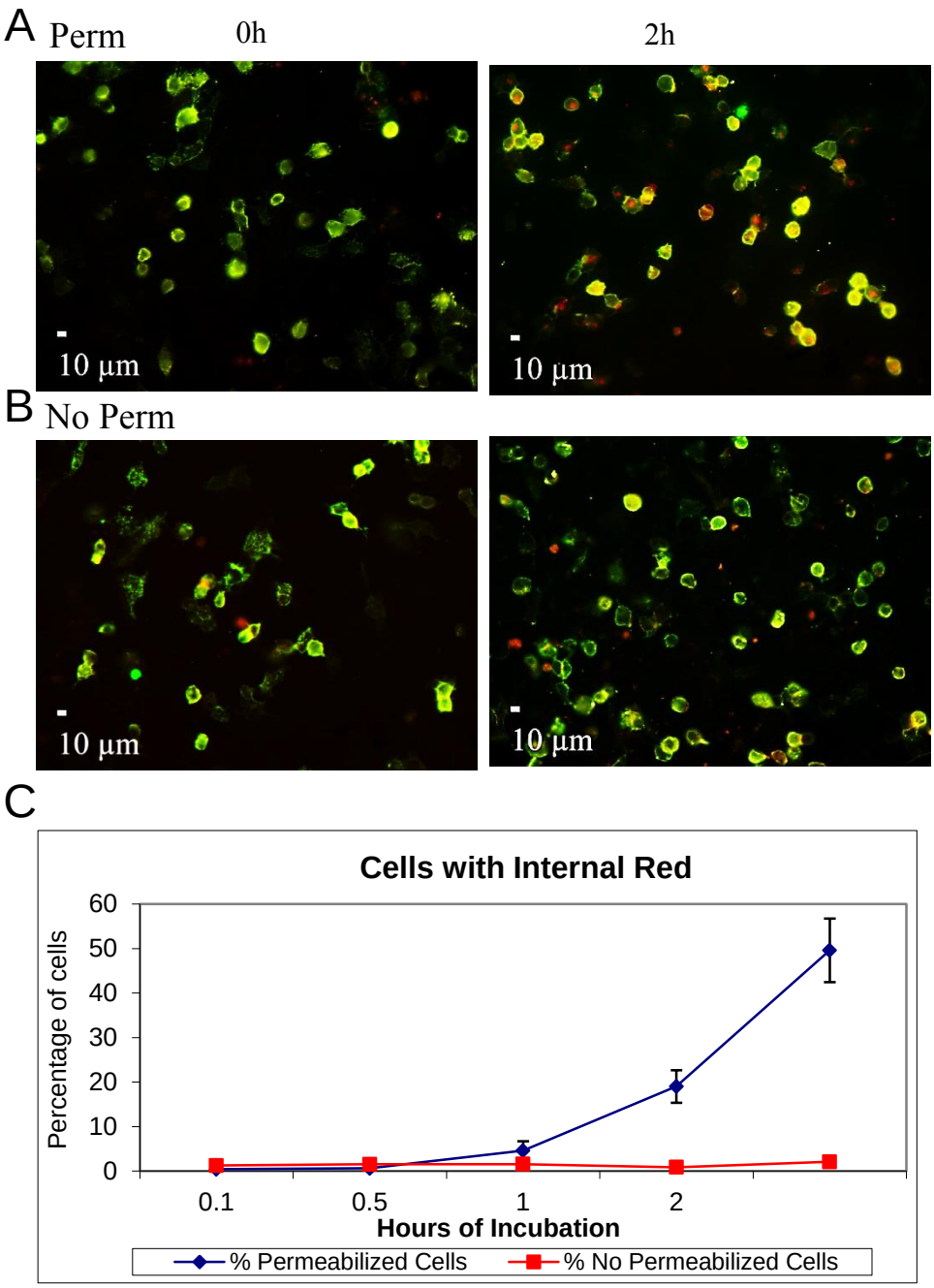

Fig. 4.7. Percentage of cells with internalised GlyR antibody. GlyR antibodies were double labelled with AlexaFluor (488, green and 568, red) anti-human IgG. ***A.*** Merged images of live permeabilised HEK cells incubated with serum at 37ºC at 0h and 2h. There is an increase of intracellular red IgG at 2h (arrows, blue line). ***B.*** Unpermeabilised cells incubated at 37°C don´t show increase in intracellular red IgG (red line). ***C.*** Results of the quantification of the percentage of cells with internal red IgG of one patient.

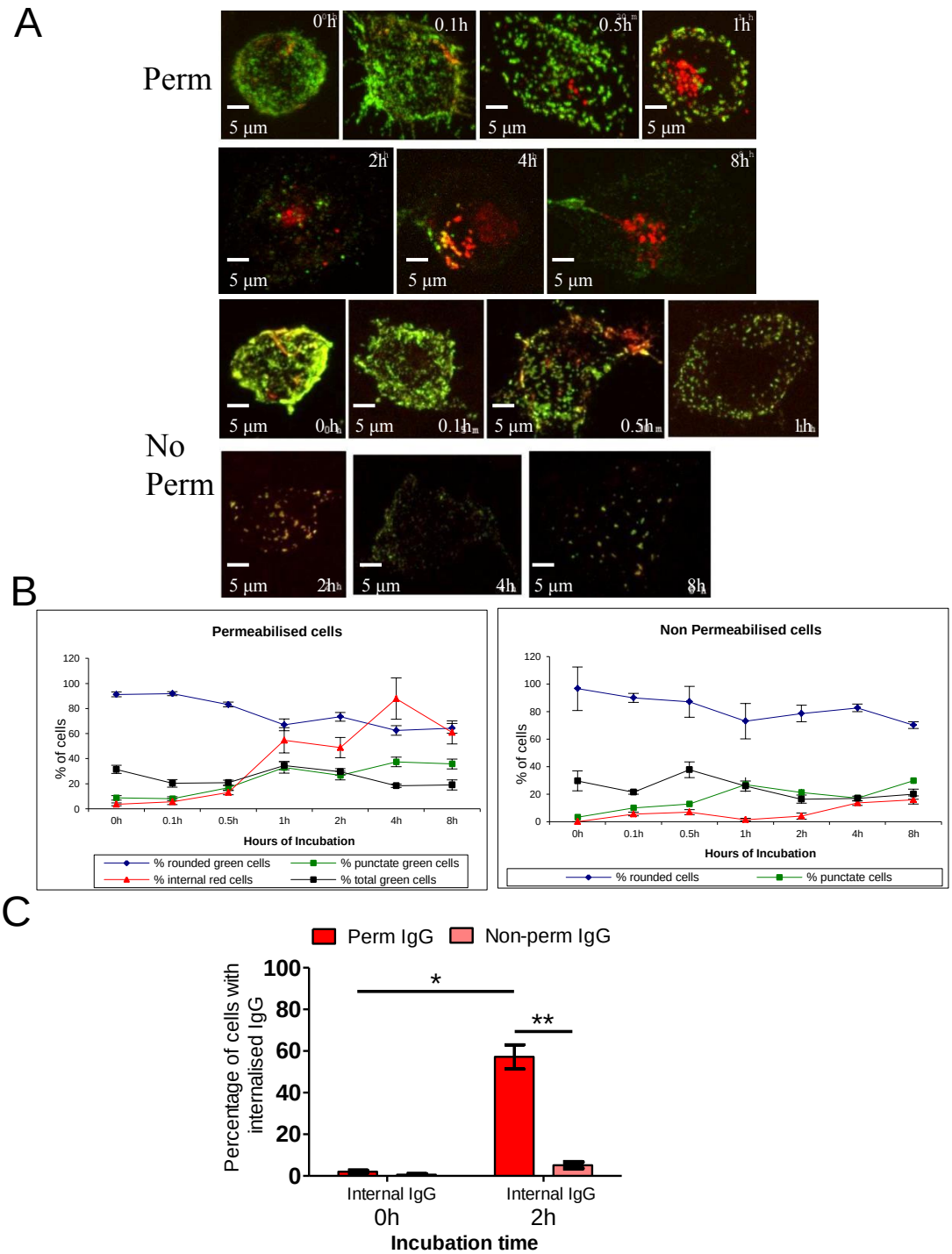

Fig. 4.8. Differential labelling of surface (green) and internal (red) antibodies in permeabilised cells confirm internalisation of GlyR antibodies over time. A. Merged confocal images of HEK cells incubated with serum at 37ºC for different periods of time and permeabilised to allow detection of intracellular IgG. There is a decrease in surface immunofluorescence (green) with a punctate pattern over time. The internalisation is demonstrated by increasing detection of intracellular IgG (red) when the cells are permeabilised. ***B.*** Non permeabilised cells also show decreased surface immunofluorescence but no intracellular IgG. Quantification showed that the ppercentage of green HEK cells and the percentage of punctate green HEK cells were similar in both groups. ***C.*** Results from two sera comparing the percentage of cells with internalized GlyR antibody at 0 and 2 h using a two-sided students (t-test ($t=8.707$, $df=18$, $p < 0.0001$).

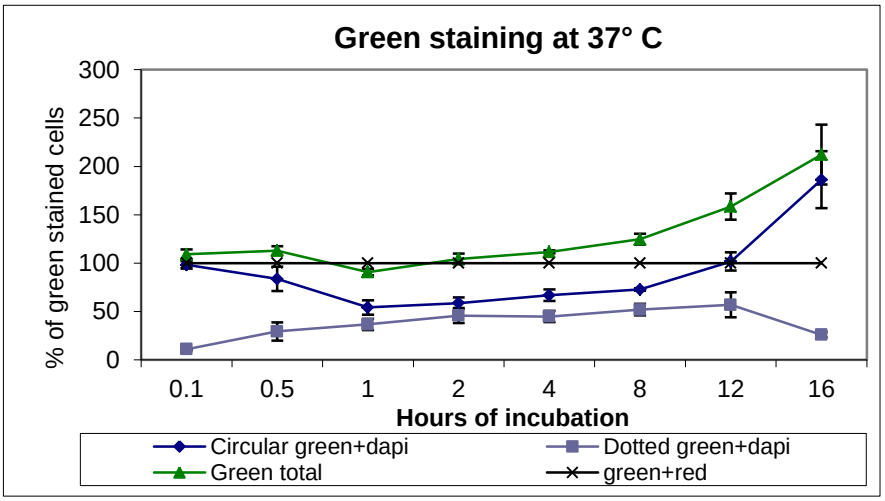

Fig. 4.9. Percentage of green stained cells after incubation with patient serum. Quantification in low magnification of merged images of live HEK cells expressing GlyR α1-EGFP incubated with serum at 37ºC and AlexaFluor 568 (red) for different time periods. Results show an increase over time of the percentage of green cells compared to the percentage of green cells with surface bound antibody in red.

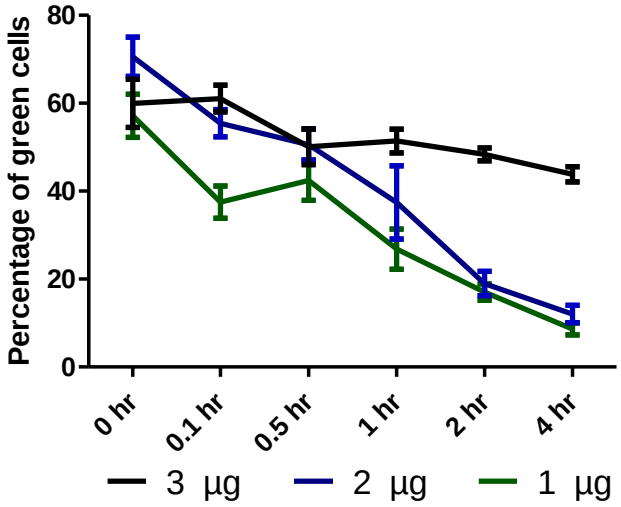

Fig. 4.10. Percentage of green cells incubated with patient serum decreased after treatment with cycloheximide. Live HEK cells transfected with 3, 2 or 1 µg GlyRα1-EGFP were treated with cycloheximide and incubated with serum at 37ºC for different time periods. Results show a decrease over time of the percentage of green cells in all groups that was more pronounced in the cells transfected with less amount of DNA.

after 4 hrs of incubation) than in those transfected with 2 and 1 μg of DNA (from 70.6% at 0 hrs of incubation to 12% after 4 hrs of incubation and from 57.1% at 0 hrs of incubation to 8.7% after 4 hrs of incubation respectively) (Table 4.1; Fig. 4.10)

The experiment was repeated using transfected HEK cells with 1μg of EGFP-tagged GlyRα1 DNA, and incubating the cells for different periods of time (0 hrs – 2 hrs) under the following conditions: a) Patient serum, b) Patient serum with cycloheximide, c) Healthy control serum with cycloheximide, and d) Cycloheximide alone without serum. When incubated with patient serum the percentage of cells expressing detectable EGFP-GlyRα1 fell from 37.1% at 0 hrs to 1.43% after 2 hrs of incubation, whereas the EGFP-GlyRα1 expression remained relatively constant when the cells were incubated with healthy control serum (about 60%) or no serum with cycloheximide (about 50%) (Fig. 4.11A,B).

Higher magnification of HEK cells confirmed the decrease in surface fluorescence over time and revealed that the EGFP-GlyRs became clustered when cells were exposed to patient serum in the presence of cyclohexamide, as previously indicated by detection of the bound IgG (Fig. 4.12). By contrast, when cells were exposed to healthy control serum in the presence of cycloheximide or exposed only to cycloheximide, the surface fluorescence remained constant and without any changes (Fig. 4.12G,H). In the absence of cycloheximide, the distribution of GlyR-EGFP was more uniform (Fig. 4.12F), suggesting restoration of surface GlyRα1 through new protein synthesis, and consistent with the lesser reduction of cells expressing GlyR-EGFP which fell from 49.45% at 0 hrs to 19.63% after 2 hrs (Fig. 4.12). An unpaired two-tailed t-test showed that there was a significant decrease of the percentage of HEK GlyRα1 expressing cells when cells were incubated with patient serum compared to incubation with healthy

A

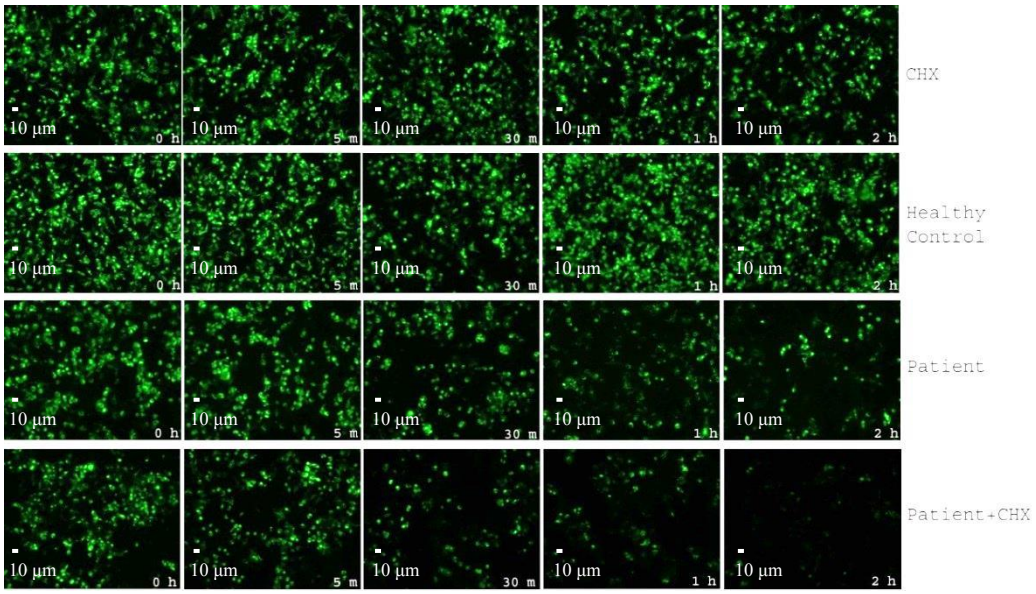

B

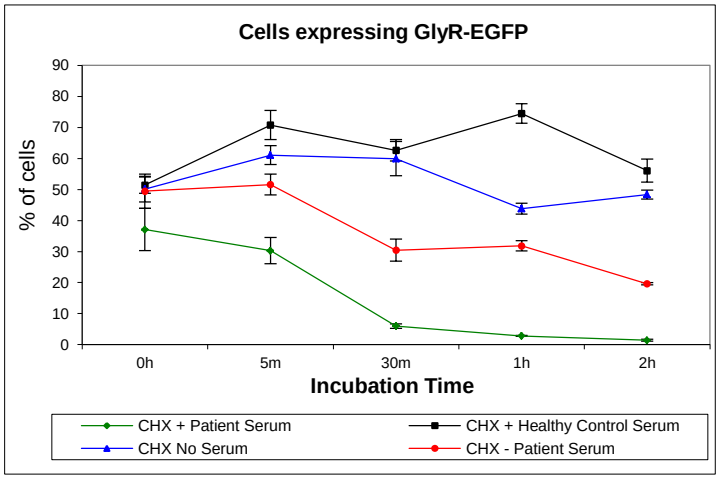

Fig. 4.11. Loss of GlyR antibody from the surface is accompanied by loss of GlyR surface expression. A. When cells were incubated at 37ºC with patient serum the percentage of cells expressing GlyR decreased with increasing periods of time (2 bottom panels). When cells were incubated with control serum the GlyR expression remained relatively constant (middle panel). Cycloheximide (CHX) + no serum (upper panel), These results suggest internalisation of GlyR. ***B.*** Quantification of cell surface expression of GlyR-EGFP

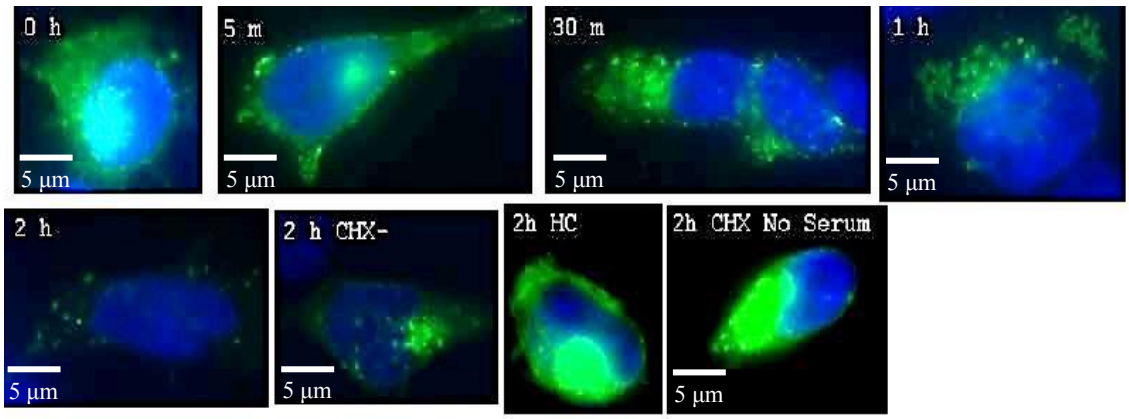

Fig. 4.12. Changes in cell surface expression of GlyR-EGFP after incubation in GlyR IgG. Merged images of HEK cells incubated with patient serum and CHX at 37ºC for different time periods. The surface fluorescence decreased over time and became a punctate pattern, suggesting receptor internalisation. The surface fluorescence remained constant and without changes when incubated with healthy control serum or with CHX and no serum (panels g and h). When cells were incubated with patient serum but not with CHX the staining pattern also changed to a punctate pattern but there is a restoration of surface fluorescence probably as a consequence of new protein synthesis (showed with arrows).

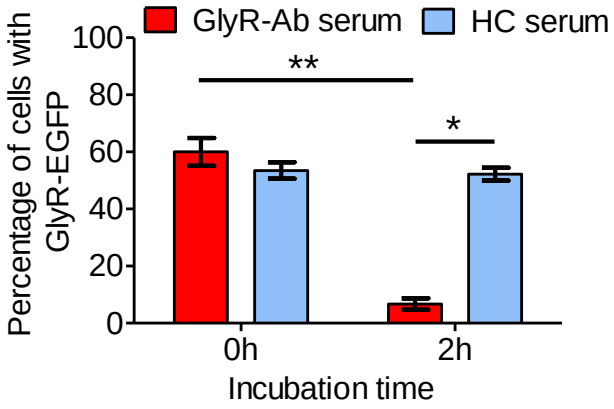

Fig. 4.13. Quantification of GlyR1-EGFP internalization. Results from two experiments with a single serum. Groups were compared using a two-sided Student's t-test (**t = 10.15, df = 18, p < 0.0001; *t = 15.01, df = 18, p < 0.0001).

control serum ($p < 0.0001$) and a significant decrease in the percentage of HEK GlyR α1 expressing cells at 2 hrs compared to 0 hrs in the patient serum group ($p < 0.0001$) (Table 4.1; Fig. 4.13). These results confirm that GlyR-Abs can lead to loss of GlyR cell surface expression.

Finally, to determine the fate of GlyRs internalised after exposure to patient's serum, specific antibodies to an early endosomal antigen (EE1) and to a late endosomal antigen (LAMP2) were used in co-localisation studies. Antibody binding increased the rate of GlyR internalisation, from 1 hrs to 4 hrs of incubation with patient serum. The percentage of cells showing colocalisation was approximately 90%. However in HEK cells exposed to healthy control serum the average percentage of cells also showed colocalisation rising from to 17.38% to 47.19% (Fig. 4.14A,B), suggesting that the GlyRs are constitutively internalised, even in the absence of GlyR-Abs.

Higher magnification of HEK cells showed that early endosomal vesicles (red) had little colocalisation with GlyR-EGFP when cells were exposed to the serum over a period of 30 min (Fig. 4.15A). But after 1h of incubation, the cells began to show large late endosomal vesicles (red) colocalising with GlyR-EGFP; these large late endosomal vesicles were not present in cells after incubation with healthy control serum (Fig. 4.15B). An unpaired two-tailed t-test showed that there was an increase of the percentage of cells with internalised GlyR α1-EGFP at 2 hrs compared to 0 hrs in cells treated with patient serum ($p < 0.0001$) and an increase in the percentage of cells with internalised GlyR α1-EGFP, when comparing the patient serum and healthy control treated cells at 2 hrs ($p < 0.0001$). In addition, there was a significant increase of the percentage of cells with internalised GlyR α1-EGFP at 2 hrs compared to 0 hrs in cells treated with healthy control serum ($p < 0.0001$), confirming that GlyRs are

A

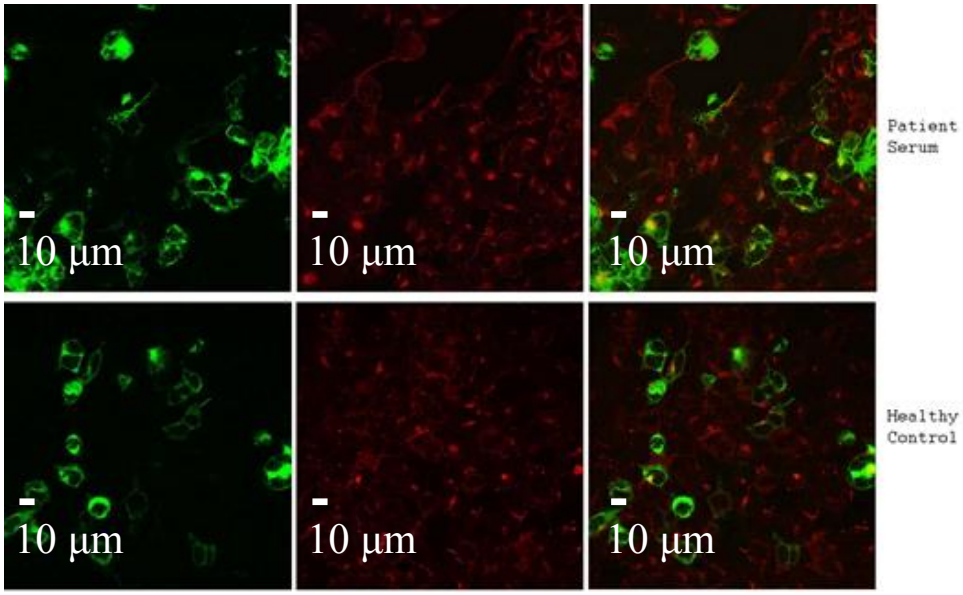

B

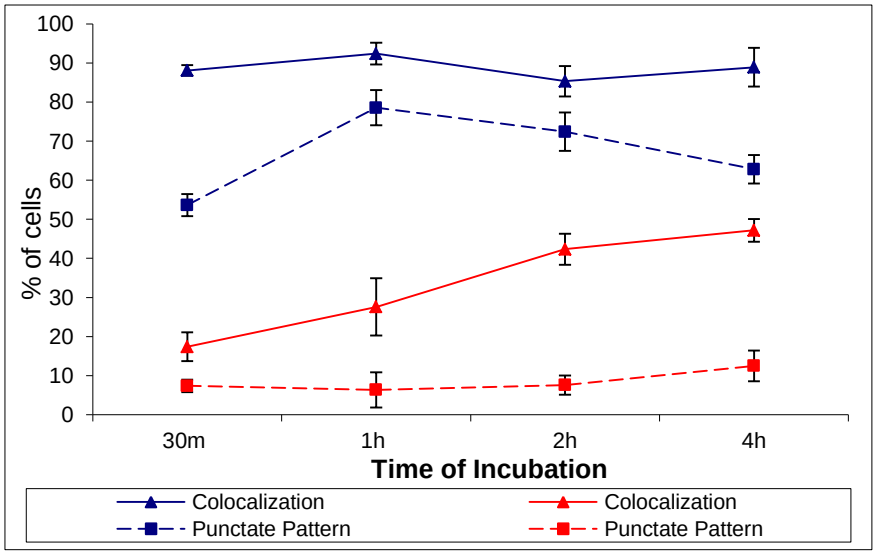

Fig. 4.14. GlyR antibodies binding to surface GlyR increases the rate of internalisation. A. HEK cells exposed to patient serum shows increased colocalisation of GlyR and late endosomal vesicles (yellow dots) than HEK cells exposed to healthy control serum. ***B.*** Quantification of the colocalisation extent and punctate pattern in HEK cells exposed to patient serum (blue line) and healthy control serum (red line). The average percentage of punctate cells rose from 53.64% to 62.83% in cells treated with patient serum but remained relatively constant (about 9%) in cells treated with healthy control serum.

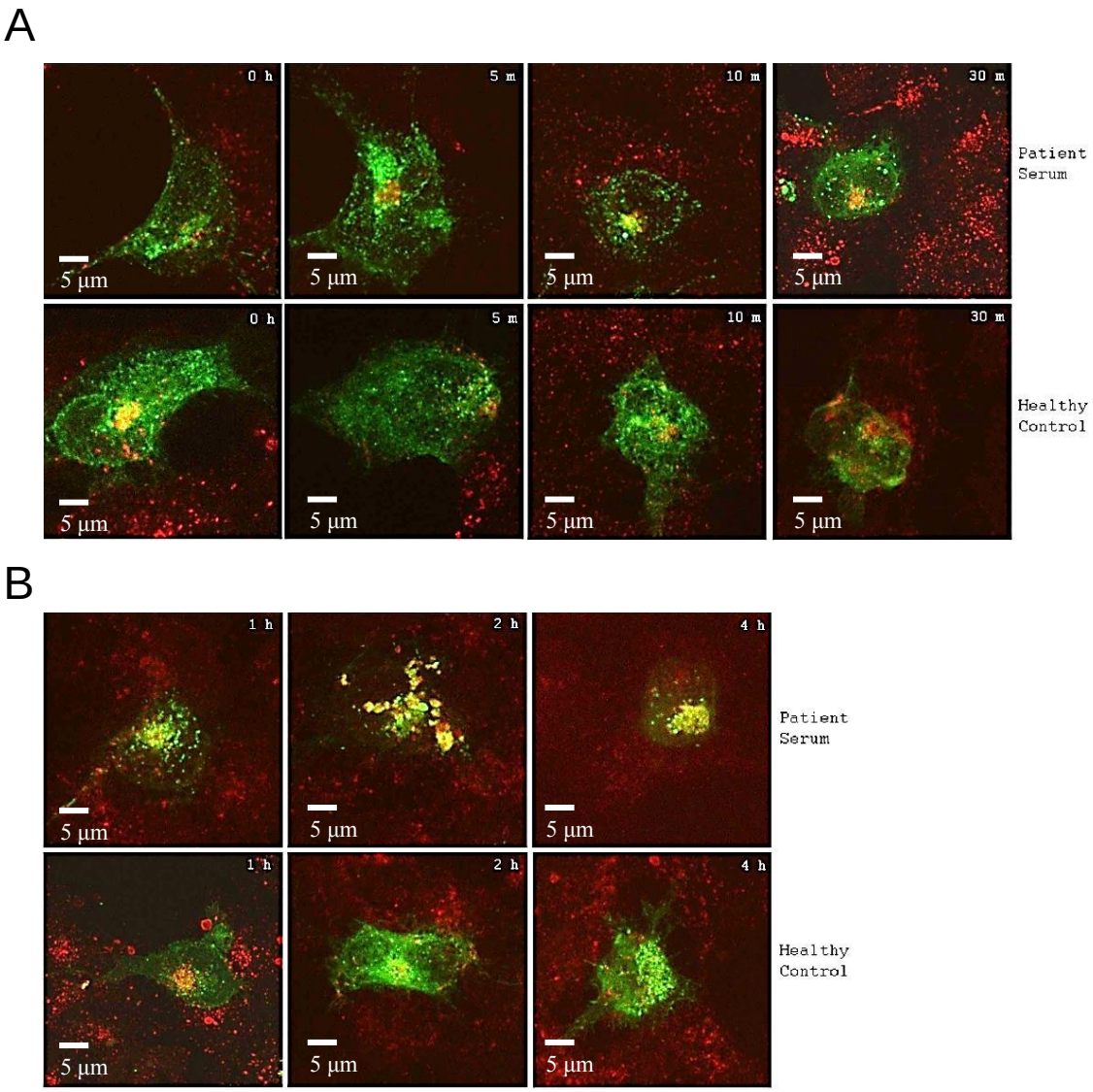

Fig. 4.15. Endocytosed GlyR's are targeted to the endolysosomal pathway. A. Merged confocal images of HEK cells shows little colocalisation of GlyR-EGFP (green) with EE1 vesicles (red) when they were exposed to patient or healthy control serum over a period of 30m. ***B.*** Merged confocal images of HEK cells shows big LAMP2 vesicles (red) which colocalise with GlyR-EGFP (green) when they were exposed to patient serum but not when they were exposed to healthy control serum.

constitutively turned-over (Table 4.1; Fig. 4.16). These results suggest that endocytosis, initiated by the crosslinking of GlyR after IgG binding at the cell surface, targets GlyR to the endolysosomal pathway where it is accumulated before its degradation.

Table 4.1. Statistical analysis of different in vitro experiments.

Experiment	Parameter evaluated	Statistical test	Factor or variables compared	Statistical value	P value
IgG internalisation	Fluorescence score	Two-way ANOVA	Condition	[F(2, 63)=28.36]	<0.0001
			Time	[F(6, 63)=11.78]	<0.0001
			Interaction	[F(12, 63)=2.44]	0.0113
IgG internalisation	Percentage of cells with internalised IgG	Student´s t-test	Perm 0hr vs 2hr	[t=9.448, df=18]	<0.0001
			Perm vs No perm 2hr	[t=8.707, df=18]	<0.0001
GlyR internalisation	Percentage of green cells	Two-way ANOVA	Condition	[F(2, 60)=19.53]	<0.0001
			Time	[F(5, 63)=52.09]	<0.0001
			Interaction	[F(12,63)=12.04]	<0.0001
GlyR internalisation	Percentage of cells with GlyR-EGFP	Student´s t-test	Patient vs HC 2hr	[t=15.01, df=18]	<0.0001
			Patient 0hr vs 2hr	[t=10.15, df=18]	<0.0001
GlyR colocalisation with endolysosomal pathway	Percentage of cells with internalised GlyR-EGFP	Student´s t-test	Patient 0hr vs 2hr	[t=13.73, df=18]	<0.0001
			Patient vs HC 2hr	[t=8.515, df=18]	<0.0001
			HC 0hr vs 2hr	[t=5.538 df=18]	<0.0001

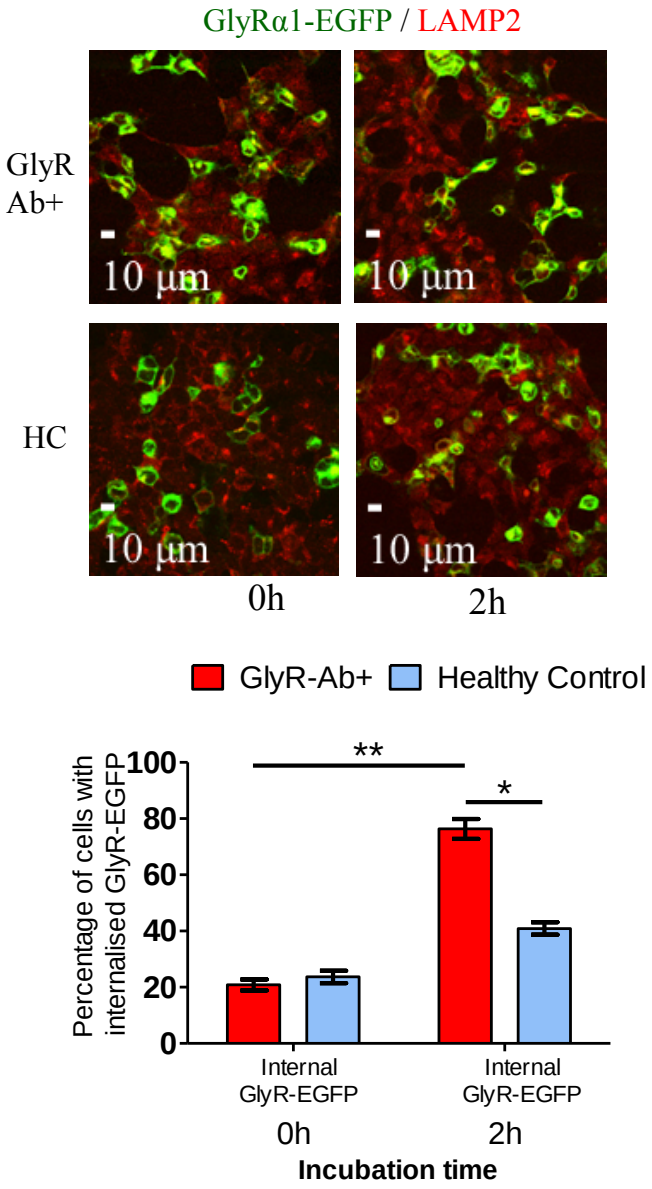

Fig. 4.16. Percentage of cells with co-localisation of GlyR1-EGFP and LAMP2. Results from two experiments with a single serum from two experiments with one serum from GlyR antibody and one healthy control. Groups were compared using a two-sided Students t-test (*t = 8.515, df = 18, $p < 0.0001$; **t = 13.73, df = 18, $p < 0.0001$).

4.3 Discussion

GlyR-abs found in the serum of GlyR-Ab patients have features of pathogenicity, similar to those observed for well-characterised pathogenic autoantibodies such as AChR-Ab in myasthenia gravis (Vincent and Newson-Davies, 1982), AQP4-Ab in neuromielitys optica (Hinson et al, 2007; Hinson et al, 2008) and NMDAR-Ab in encephalitis (Dalmau et al 2008).

GlyR-Abs were predominantly IgG1, and were shown to activate complement on the HEK cell surface; it is likely that complement-mediated destruction could be a mechanism *in vivo*. However, this mechanism may be determined by the amount of complement available in the relevant brain regions, or tissue specific differences in the modulation of complement regulators (Noris and Remuzzi, 2013). For instance, NMDAR antibodies do not appear to cause complement-mediated damage (Dalmau et al 2008, Tuzun et al 2009) even though they are also predominantly IgG1 (Irani et al 2010).

Another potential mechanism is the internalisation of the GlyRs. Here, over a period of 2 – 16 hrs GlyR-abs caused internalisation of the glycine receptors with the attached IgG. By the end of the 16 hour incubation, the human IgG was no longer detectable on the surface; the IgG was identified intracellularly, possibly in the endosomal pathway for proteolysis. The most likely process by which GlyR-Abs cause GlyR internalisation is antigenic modulation, where surface antigens are modulated by intermolecular cross-linking by bivalent IgG, as shown for other antibodies (de Petris et al, 1973 and Hinson et al, 2007). In fact, GlyR-abs could be seen to cause capping and clustering of the GlyRs, in a temperature dependent manner (Figure 4.6).

GlyR internalisation caused by GlyR-Ab binding occurred over several hours, which is slower than GlyR internalisation by agonist binding; this occurs by 30 min via clathrin-coat vesicles (Huang et al, 2007). This difference may be due to different mechanisms of endocytosis, as at least three endocytosis routes such as macropinocytosis, clathrin-coat vesicles and flask-shaped lipid microdomains called caveolae have been described (Alberts B, 2007). Here the GlyRs did not colocalise with the early compartment but with the late compartment of the endosome. Therefore antibody-induced internalisation may occur via different mechanisms from the classical clathrin-mediated endolysosomal pathway. Moreover, the time course of GlyRs internalisation in HEK cells is similar to that reported for other antibodies to cell surface antigens such as AChRs in muscle cell lines (Drachman et al 1978) although apparently faster than NMDAR antibodies acting on NMDARs in neuronal cultures (Dalmau et al 2008; Hughes et al 2010).

4.4 Conclusions and limitations

The results in this chapter show that serum and CSF GlyR-Abs cause complement activation and GlyR receptor internalisation *in vitro* and therefore should have pathogenic potential *in vivo*. The reduction of GlyR surface expression indicates a role for GlyR specific IgG as a cause of the complex symptomatology of GlyR-Ab patients. However, to demonstrate that the internalisation was only due to cross-linking of the GlyR by divalent antibodies, as in Stanley and Drachman (1978), it would be necessary to show a lack of effect of monovalent Fabs.

There may be some specific macromolecular complex occurring only in the cell membranes of the specific tissue cell types that could affect endocytosis efficiency. This was demonstrated for AQP4-abs, which did not produce internalisation of AQP4 channels in astrocytes either *in vitro* or *in vivo* (Ratelade et al 2011) although they had done so in HEK cells (Hinson et al, 2008). Therefore, to be more confident of the pathogenic role of GlyR-Abs these results would need to be replicated using neuronal cultures, the target cell affected in the CNS, and *in vivo* studies. However, that will be difficult, as cultured inhibitory neurons suitable for study are difficult to obtain in sufficient numbers for quantitative analysis.

Regardless of the pathogenic mechanisms involved, which could include a direct inhibition of function by the antibodies, the normality in the MRI images and the substantial recovery after immunotherapies in the majority of patients (Chapter 3) argues against a cell mediated destructive process and supports the possibility of a reversible internalisation as a major mechanism. The next step was to ask whether the GlyR-Abs bound to regions of the brain that were relevant to the clinical features of the diseases.

CHAPTER 5. Immunohistochemistry

5.1 Introduction

Previous reports have shown the presence of GlyR-Abs in PERM patients. Glycine receptor (GlyR) mediates inhibitory neurotransmission in the central nervous system (CNS), through binding of the amino-acid glycine. GlyR are pentameric proteins composed of two α and three β subunits. To date, based on its α subunit content, four different functional GlyR subtypes have been described (α1, α2, α3, α4); homomers of α subunits are also functional (Lynch, 2004 and 2009). Extracellular concentrations of glycine are regulated by the glycine transporters (GlyT1, GlyT2) (Legendre, 2001).

Several studies have been conducted to map the distribution of the glycine receptor system in rats using different techniques such as hybridisation histochemistry (Sato et al., 1991, Malosio et al, 1991), ligand binding (Frostholm and Rotter, 1985) and antibody labelling (Araki et al., 1988; Rampon et al, 1996). Also, mapping on human tissue has been performed (Nass et al, 1991; Baer et al, 2009). However, there are some discrepancies between the different studies which may be due to the existence of different forms of the glycine receptor (subunits, strychnine-sensitive or strychnine insensitive forms) and recognition by different probes, monoclonal antibodies and ligands.

This chapter describes the immunohistochemical localisation of the GlyR-Ab antigenic targets in rodent brain tissue, using four different antibodies specific to GlyR subunits. The cellular localisation of the GlyRs related to the staining of different neuronal, interneuronal and glial intracellular markers and their co-localisation with the patient antibody binding was studied in detail. Finally, the localisation of GlyTs, using two different antibodies to the each GlyT, was also examined.

5.2 Results

5.2.1 Glycine receptor expression in the CNS

Glycine receptor expression in rodent central nervous system was first examined using monoclonal antibodies to GlyRα1, GlyRα2, GlyRα3 and GlyRβ subunits, and a pan-GlyR monoclonal antibody that recognises all alpha and beta subunits. In order to find regional differences in the GlyR specific subunit expression, the staining obtained with each GlyR subunit antibody was compared among them and then compared with the stain obtained with the pan-GlyR monoclonal antibody.

Rat CNS frozen sections were incubated with the pan-GlyR monoclonal antibody and specific staining was observed widely, but unevenly, distributed throughout the CNS, including regions such as the hippocampus (CA regions and dentate gyrus), cerebellum (deep nuclei, granular, molecular and Purkinje cell layers), brainstem, thalamus, cortex, hypothalamus, caudate, white matter and spinal cord (Fig. 5.1A, 5.2; Table 5.1); little or no staining was observed with the negative control (Fig. 5.1B). The brainstem and spinal cord showed high immunoreactivity, the observed immunoreactive structures included cell bodies and fibres distributed regularly in all the parenchyma; whereas the GlyR-Ab immunoreactivity was lower in the cerebellum, diencephalon and telencephalon. In these areas, the immunoreactive structures did not include fibres as only cell bodies were observed with a patchy distribution within the parenchyma. Although, it was difficult to discriminate with this antibody between intracellular and extracellular staining.

GlyRα1 was strongly expressed in all major areas of the brainstem including medulla oblongata, pons and midbrain, and in the ventral and dorsal horns of the spinal cord, with expression in the thalamus, hypothalamus, colliculus, and deep nuclei of the cerebellum and no expression in the hippocampus, cerebral and cerebellar cortices (Fig. 5.2, Table 5.1). The

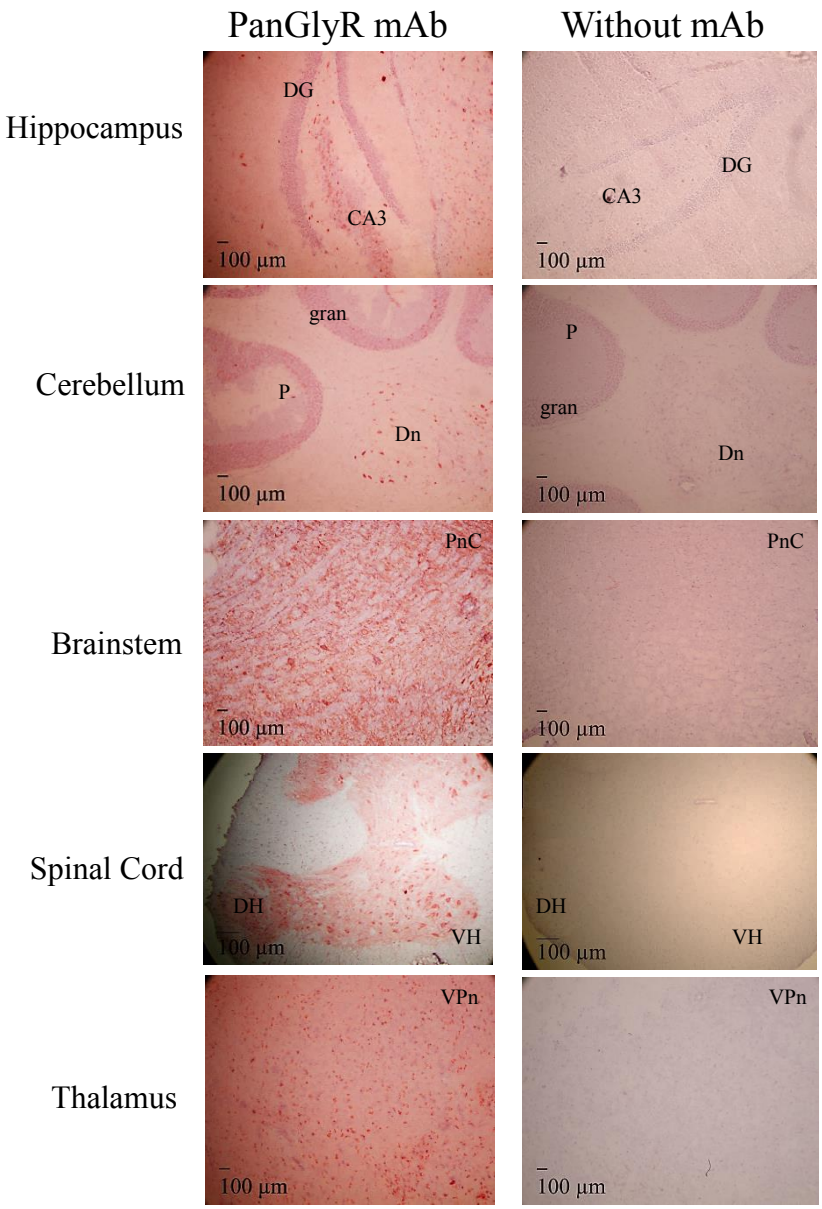

Fig. 5.1. Regional localisation of glycine receptors in the rat CNS. Microscopic images of the hippocampus, cerebellum, brainstem and thalamus for glycine receptors with monoclonal antibody to human GlyR (mAb4a), taken under light microscopy at 10x magnification. ***A.*** In the left panel, HRP staining with AEC chromogen was used (red), counterstain with haematoxylin, showing moderate immunoreactivity in the dentate gyrus (DG), CA2, CA3 region of the hippocampus, the Purkinje (P), granular layer (gran) and deep nuclei (Dn) in the cerebellum, the caudal reticular pontine nuclei (PnC) of the brainstem, the dorsal horn (DH), ventral horn (VH) of the spinal cord and the ventral posterior nucleus (VPn) nuclei in the thalamus. ***B.*** In the right panel, photographs of the same regions incubated without monoclonal antibody, but with secondary antibody showing no immunoreactivity.

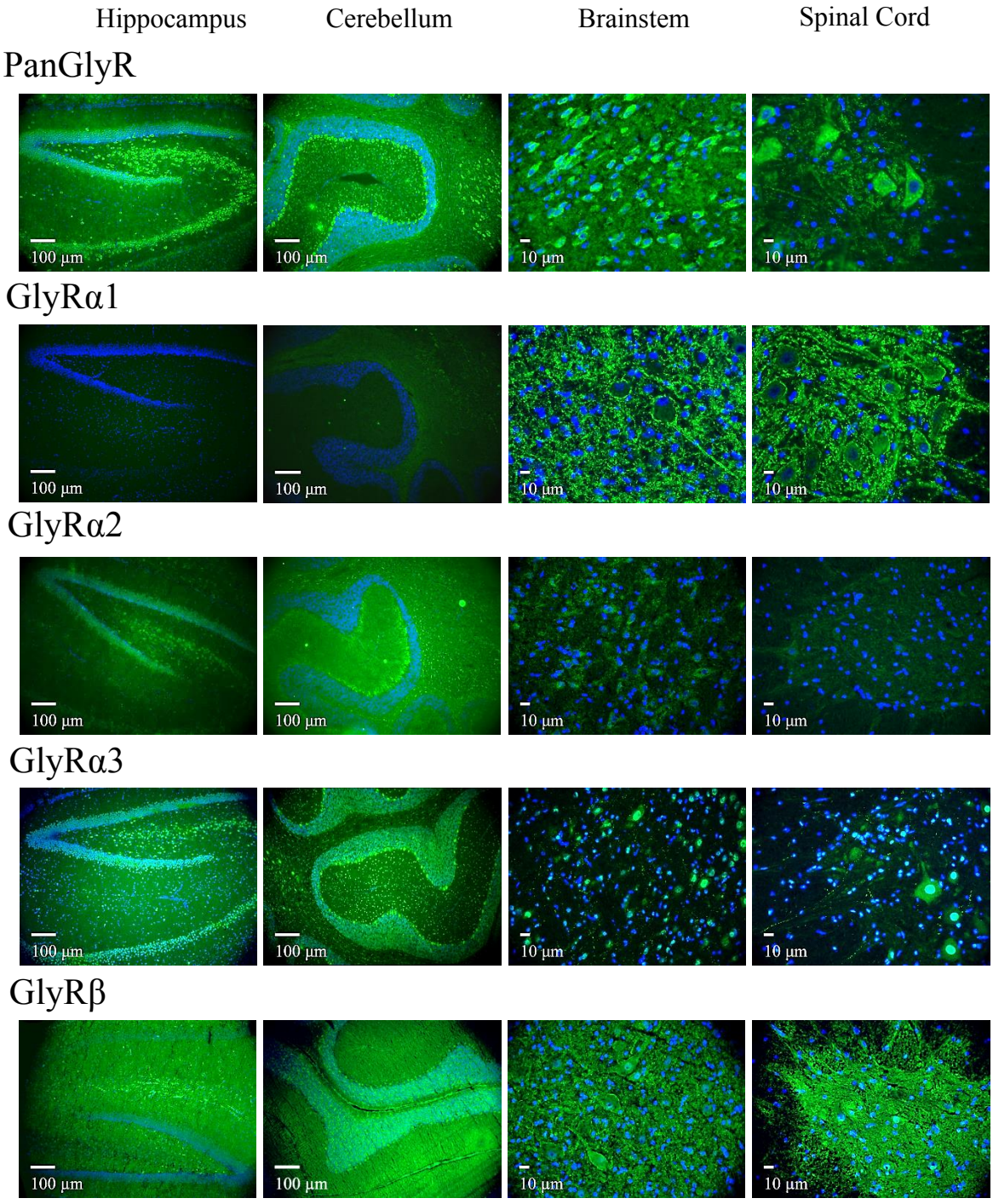

Fig. 5.2. GlyRs are widely expressed in the CNS with regional alpha and beta subunit differences. Pan GlyR shows that GlyRs are widely expressed in the CNS. GlyRα1 is strongly expressed in the brainstem and spinal cord, with no expression in the hippocampus and cerebellum, while, GlyRα2 and GlyRα3 are more strongly expressed in the hippocampus and cerebellum, although the staining pattern appears mainly intracellular. GlyRβ expression matches that of GlyRα1 distribution, but also shows some expression in regions where GlyRα2 and GlyRα3 are expressed but GlyRα1 is absent.

immunoreactivity had a punctate pattern observed on the surface of neuronal bodies and in the neuropil. No intracellular staining pattern was observed with this antibody.

GlyRα2 specific antibody showed expression in the hippocampus (CA regions and dentate gyrus), striatum, Purkinje cell layer of the cerebellum, cerebellar cortex, layers III-VI of the cerebral cortex, thalamus, caudate, white matter, with very low expression in the brainstem and spinal cord and no expression in the hypothalamus (Fig. 5.2, Table 5.1). However, most of the staining observed with this antibody appeared to be intracellular.

GlyRα3 expression was found extracellularly in the hippocampus (CA regions and dentate gyrus), the granular cell layer of the cerebellum, the dorsal horn of the spinal cord, the white matter and the hypothalamus. The immunoreactivity had a sparse punctate pattern that was less strong than that observed for the GlyRα1 subunit, and appeared to be extracellular. However, GlyRα3 was also widely observed intracellularly in several brain regions such as cerebral and cerebellar cortex, thalamus, hypothalamus, brainstem, and colliculus (Fig. 5.2, Table 5.1).

GlyRβ immunoreactive extracellular punctate clusters were found throughout the brainstem and the spinal cord. Less intense immunoreactivity was found in other areas of the brain such as the hypothalamus, thalamus, deep nuclei and granular cell layer of the cerebellum and in the molecular stratum of the hippocampus. No immunostainig was observed in the cerebral cortex. Some intracellular staining was observed with this antibody in the brainstem and spinal cord (Fig. 5.2, Table 5.1).

Since some antibodies recognised intracellular and extracellular epitopes and the intensity of immunoreactivity differed between the compartments, it was difficult to draw conclusions on the functional relevance of the staining observed. In order to show that some of the staining observed was located on the surface of the neurons, double immunolabelling studies using different monoclonal antibodies to intracellular proteins of neurons and glial cells (See Chapter 2, table 2.1) were used, in conjunction with a monoclonal antibody to GlyRα1. The

immunostaining obtained in the pontine caudal reticular nuclei (PnC) of the brainstem and in the ventral horns of the spinal cord was studied; since these regions are involved in the control of motor activity, particularly the startle response (Lee et al, 1996).

CNS sections incubated with gephyrin, MAP2 monoclonal antibodies (red), and GlyR monoclonal antibody mAb2 (green), showed discrete patches of GlyR aligned on the membrane of the neurons surrounding the cytoplasmic gephyrin and MAP2 immunoreactivity; the staining was observed on the surface of the soma and dendrites of the giant neurons of the PnC and in the neuropil (Fig. 5.3A). CNS sections incubated with GFAP monoclonal antibody (red) and GlyR monoclonal antibody mAb2 (green) showed GFAP staining surrounding the soma of neurons and in the neuropil without any colocalisation with GlyR immunoreactivity (Fig. 5.3A). The same staining pattern was observed when spinal cord sections were incubated with gephyrin, MAP2, GFAP monoclonal antibodies (red) and GlyR monoclonal antibody mAb2 (green). GlyR immunoreactivity was aligned on the surface of motoneurons and in the neuropil of the ventral horn of the spinal cord, as confirmed by incubation of spinal cord sections with CHAT monoclonal antibody (red) and GlyR monoclonal antibody mab2 (green) (Fig. 5.3B)

Additionally, in order to show that glycine receptor is also expressed on the surface of interneurons, double immunolabelling studies using monoclonal antibodies to interneuron markers (Table 5.2) were used in conjunction with a monoclonal antibody to GlyRα1; the staining was observed in the same brainstem and spinal cord areas.

CNS sections incubated with parvalbumin, calretinin, calbindin monoclonal antibodies (red), and GlyR monoclonal antibody mAb2 (green), showed the same GlyR immunostaining pattern, localised primarily in the neuropil and on the surface of neurons which did not have any interneuron immunoreactivity. However, there was also immunoreactivity in small interneurons in the PnC, with GlyR immunoreactivity on their surface (Fig. 5.4A). The same staining pattern was observed when spinal cord sections were incubated with parvalbumin, calretinin, calbindin monoclonal antibodies (red), and GlyRα1 monoclonal antibody mAb2 (green). GlyRα1

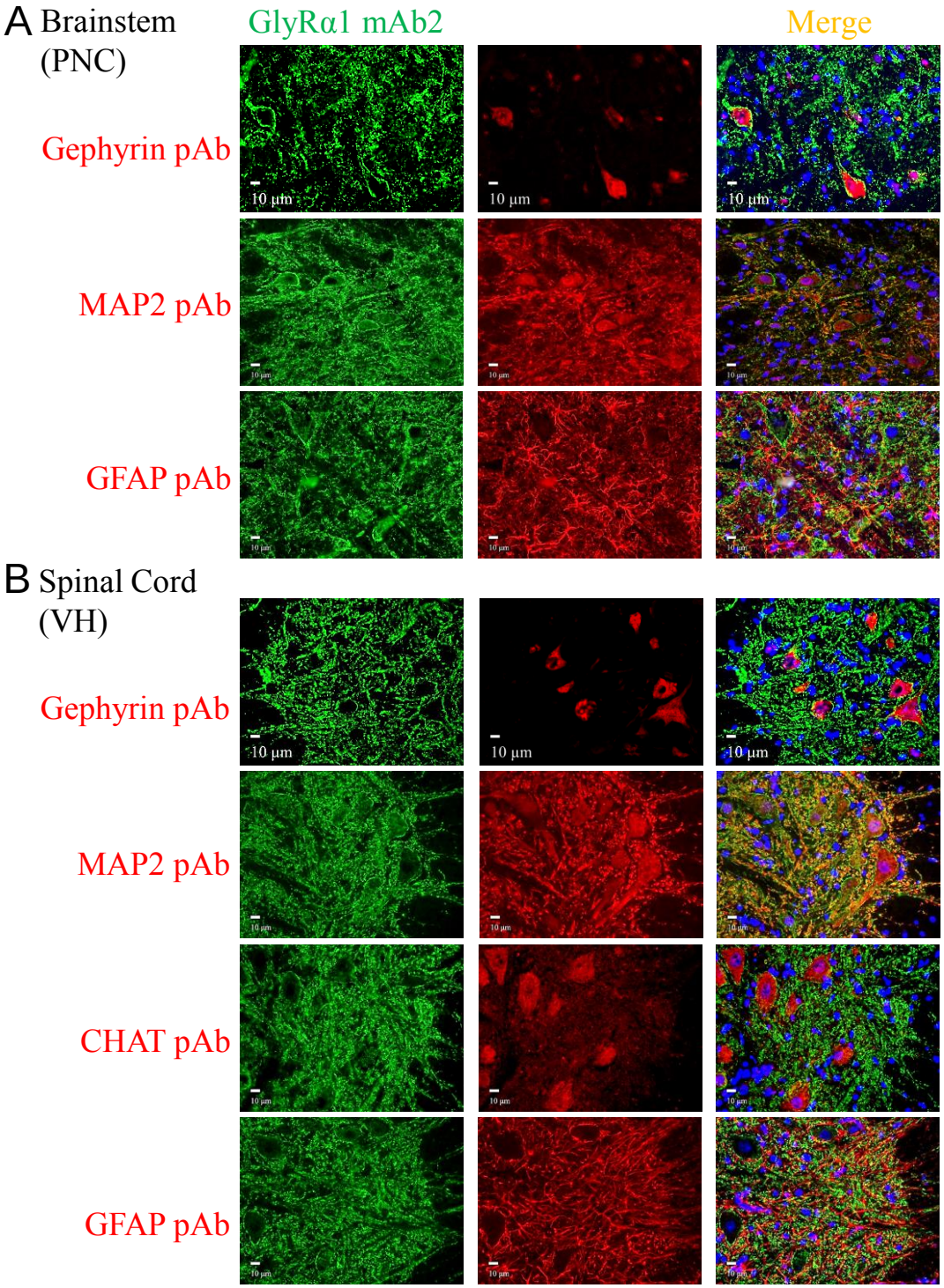

Fig. 5.3. GlyR is expressed in the neuropil and on the surface of neurons. Photographs were taken at 40x magnification. ***A.*** Double labelling of neurons in the PnC of the brainstem with monoclonal antibody mAb2 to GlyRα1 (green) and polyclonal antibodies to gephyrin and MAP2 (red) showed GlyR specific staining surrounding the surface of the neurons. GlyR immunoreactivity did not colocalise with GFAP polyclonal antibody (red). ***B.*** In the ventral horn of the spinal cord the same staining is observed surrounding the surface of the motoneurons as can be observed with the CHAT polyclonal antibody.

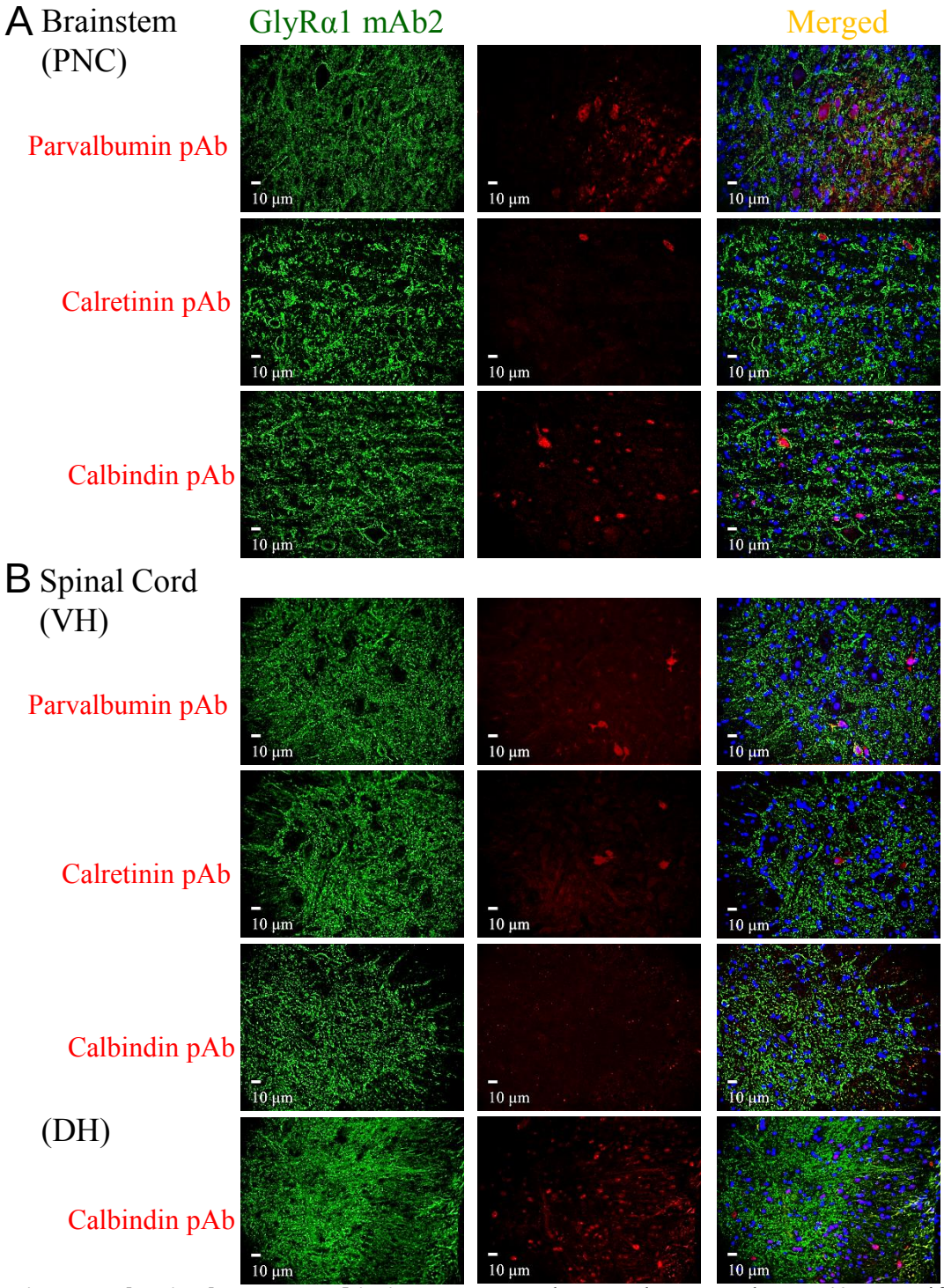

Fig. 5.4. GlyR is also expressed in interneurons. Photographs were taken at 40x magnification. ***A.*** Double labelling of neurons in the PnC of the brainstem with monoclonal antibody mAb2 to GlyR (green) and polyclonal antibodies to parvalbumin, calretinin and calbindin (red) showed the presence of small interneurons surrounded by GlyR specific staining in addition to the GlyR immunostaining observed in big neurons that did not have any interneuron marker. Some intereneurons did not have any GlyR immunostaining on their surface. ***B.*** Same staining is observed in the ventral horn of the spinal cord except that no calbindin positive interneurons were observed in the ventral horn but were observed in the dorsal horn of the spinal cord. Nuclei in blue (DAPI).

immunoreactivity in the ventral horn was observed mainly on the surface of motoneurons without any interneuron immunoreactivity, with some GlyR immunoreactivity surrounding a few small interneurons (Fig. 5.4B). Interestingly, calbindin immunoreactivity could not be observed in the ventral horn of the spinal cord, but was observed in the dorsal horn of the spinal cord and again it was surrounded by GlyR immunoreactivity (Fig. 5.4B). These results suggest that GlyR is expressed not only in the effector neurons but also in the regulating interneurons.

5.2.2 Glycine transporter expression in the CNS

Glycine transporter expression in rodent central nervous system was first examined using monoclonal antibodies to GlyT1 and GlyT2 transporters. GlyT2 was strongly expressed with a caudo-cephalic gradient in the brainstem and spinal cord, with some expression in the granular layer and deep nuclei of the cerebellum. No expression was found in other parts of the brain. The immunoreactivity had a punctate pattern distributed in the neuropil and formed big clusters surrounding neuronal bodies (Fig 5.5A, Table 5.1).

GlyT1 was widely expressed again with a caudalo-cepahlic gradient with strongest reactivity in the brainstem, spinal cord and the granular, molecular, Purkinje cell layers and deep nuclei of the cerebellum. Less intense immunoreactivity was found in the hippocampal dentate gyrus, CA regions, thalamus, hypothalamus, colliculus, caudate, cortex and white mater. The immunoreactivity had a more compacted pattern distributed in the neuropil and also formed big clusters surrounding neuronal bodies (Fig 5.5B, Table 5.1).

To confirm the specificity of the glycine transporter monoclonal antibodies, and further confirm the extracellular binding on the cellular surface of the GlyR-Ab, double immunolabelling studies of CNS sections incubated with monoclonal antibodies to GlyT1 and GlyT2 (red) and GlyR monoclonal antibody mAb2 (green) were performed. GlyT immunoreactivity (red) surrounding the GlyR immunoreactivity (green) was observed when brain and spinal cord sections were incubated with GlyT1 or GlyT2 monoclonal antibodies (Fig. 5.6A,B). Higher

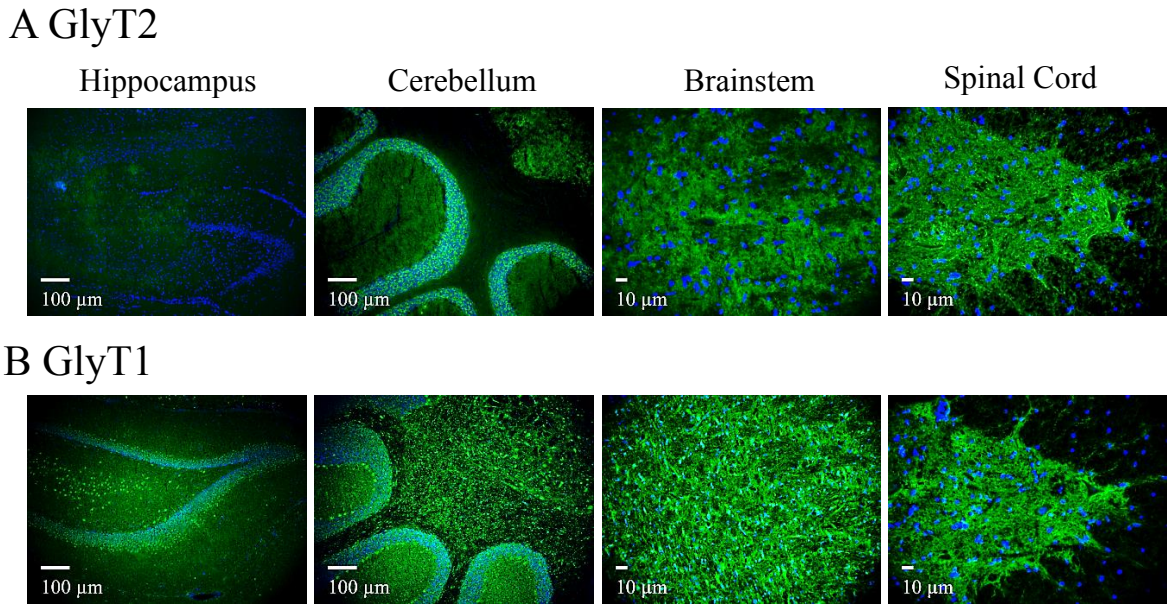

Fig. 5.5. GlyTs are widely expressed in the CNS with regional subtype differences. A. GlyT2 is strongly expressed in the brainstem and spinal cord, matching the GlyRα1 distribution with some expression in the cerebellum where GlyRα1 is not expressed. ***B.*** GlyT1 has a broader expression, matching not only the GlyRα1 distribution but also the GlyRα2 and GlyRα3 distribution.

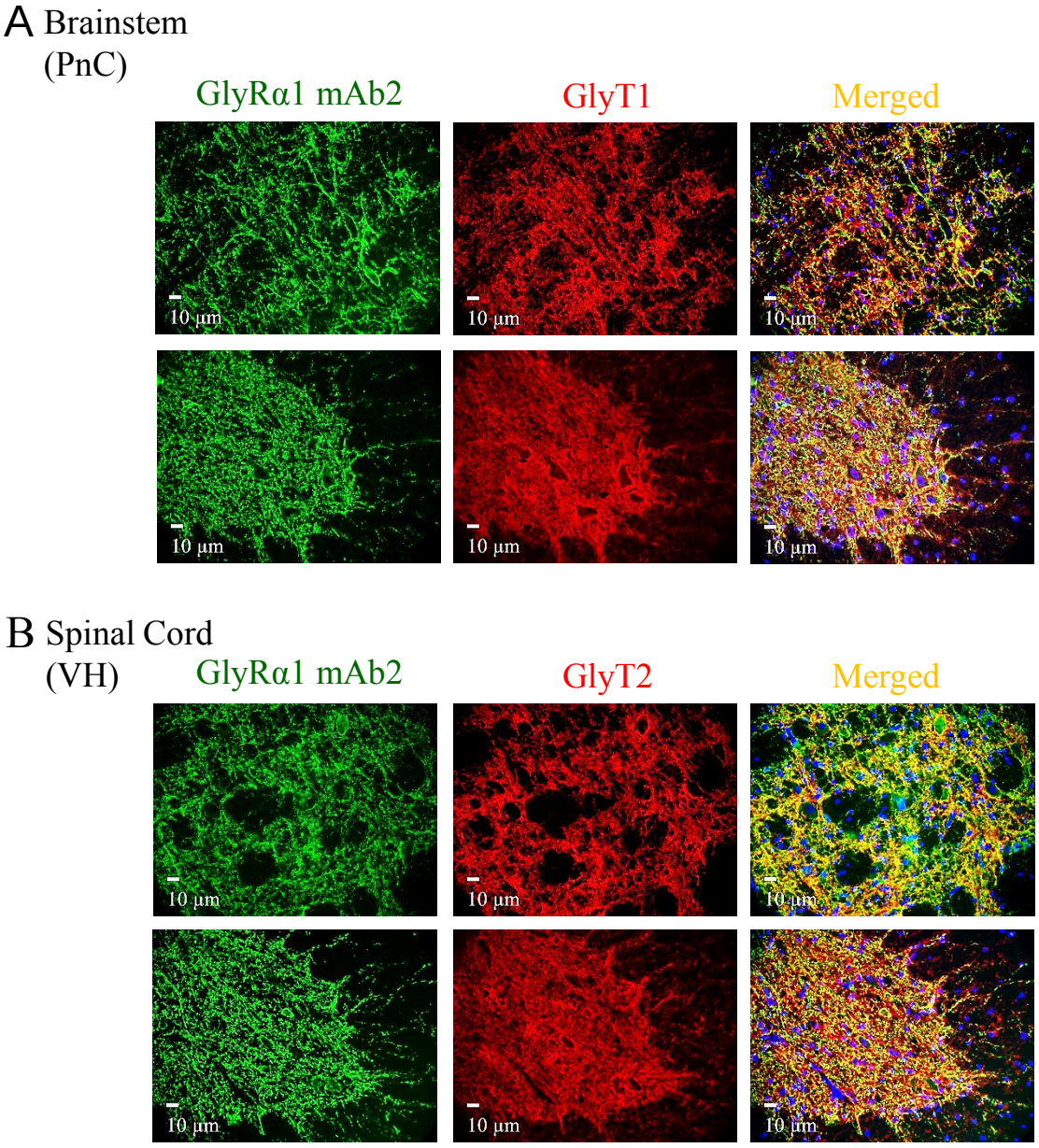

Fig. 5.6. GlyR is observed in close relationship with GlyT1 and GlyT2. Photographs were taken at 40x magnification. ***A.*** Double labelling of neurons in the PnC of the brainstem with monoclonal antibody mAb2 to GlyR (green) and polyclonal antibodies to GlyT1 and GlyT2 (red) showed GlyR specific staining in close association with GlyT1 (A) and GlyT2 (B). ***B.*** The same staining was observed in the ventral horn of the spinal cord. Nuclei in blue (DAPI).

Table 5.1. Specificities of commercial antibodies to glycine receptors and glycine transporters in rodent brain tissue

Pattern	Cellular Localization	Additional Staining	Spinal Cord and brainstem	Hippocampus	Cerebellum	Caudate and corpus callosum	Cortex and Thalamus
Glycine Receptors							
Pan α and β	Neurons and Neuropil	Intracellular	+++ both horns	++ dentate gyrus and CA regions	++ Deep nuclei, purkinje and granular cell layer	Caudate + Corpus callosum +	Cortex ++ Thalamus ++
α1	Neurons and Neuropil	None	+++ both horns	None	+ Deep nuclei	None	Cortex - Thalamus +
α2	Neurons and neuropil	Intracellular	+ both horns	++ dentate gyrus and CA regions	+ purkinje cell layer	Caudate + Corpus callosum +	Cortex + Thalamus +
α3	Neurons and Neuropil	Intracellular	+ mainly in the dorsal horn	++ dentate gyrus and CA regions	++ granular cell layer	Caudate + Corpus callosum +	Cortex + Thalamus +
β	Neurons and Neuropil	Intracellular	+++ both horns	+ Stratum layer	++ Deep nuclei, purkinje, granular and molecular cell layer	Caudate + Corpus callosum +	Cortex - Thalamus +
Glycine Transporters							
1	Presynaptic (surrounding neurons)	None	+++ both horns	+ dentate gyrus and CA regions	++ Deep nuclei, purkinje, granular and molecular cell layer	Caudate + Corpus callosum +	Cortex + Thalamus +
2	Presynaptic (surrounding neurons	None	+++ both horns	None	+ Deep nuclei and granular layer	None	None

magnification confocal images showed that the GlyT immunostaining was in close relation to the GlyR immunostaining without any colocalisation, suggesting a presynaptic localisation (Fig. 5.7).

5.2.3 Patient´s sera binding in the CNS

To confirm that GlyR-abs present in PERM patients sera bind to appropriate antigenic targets in central nervous system tissue, frozen rat brain and spinal cord sections were incubated with patient or healthy control sera (1:200 to 1:800) followed by incubation with Alexa Fluor 488 goat antihuman secondary antibody.

Initially it was difficult to assess the specificity of the immunostaining with patient serum as it appeared similar to the immunostaining obtained with control serum (Fig. 5.8). The following approaches were used to improve the immunostaining: a) Sections were incubated with different serum dilutions, in accordance to their GlyR-abs titres; b) Different incubation conditions were tested (RT for 1h, overnight incubation at 4°C) Preadsorption with guinea pig liver powder was tried to reduce non-specific nuclear staining.

With overnight incubation at 4°C and guinea liver powder preadsorption, specific staining could be observed in several brain regions when the sections were incubated with patient serum, including different hippocampal areas such as the granular layer of the dentate gyrus, the pyramidal layers of CA2, CA3, deep nuclei, granular and Purkinje layers in the cerebellum, and ventral and dorsal horns of the spinal cord (Fig. 5.9A). Under these conditions, no staining was observed when the sections were incubated with healthy control serum (Fig. 5.9B). Binding was seen in the brainstem at the pontine caudal reticular nuclei (PnC) and in the ventral horns of the spinal cord. The staining was observed on the surface of the soma as well as dendrites of neurons, and

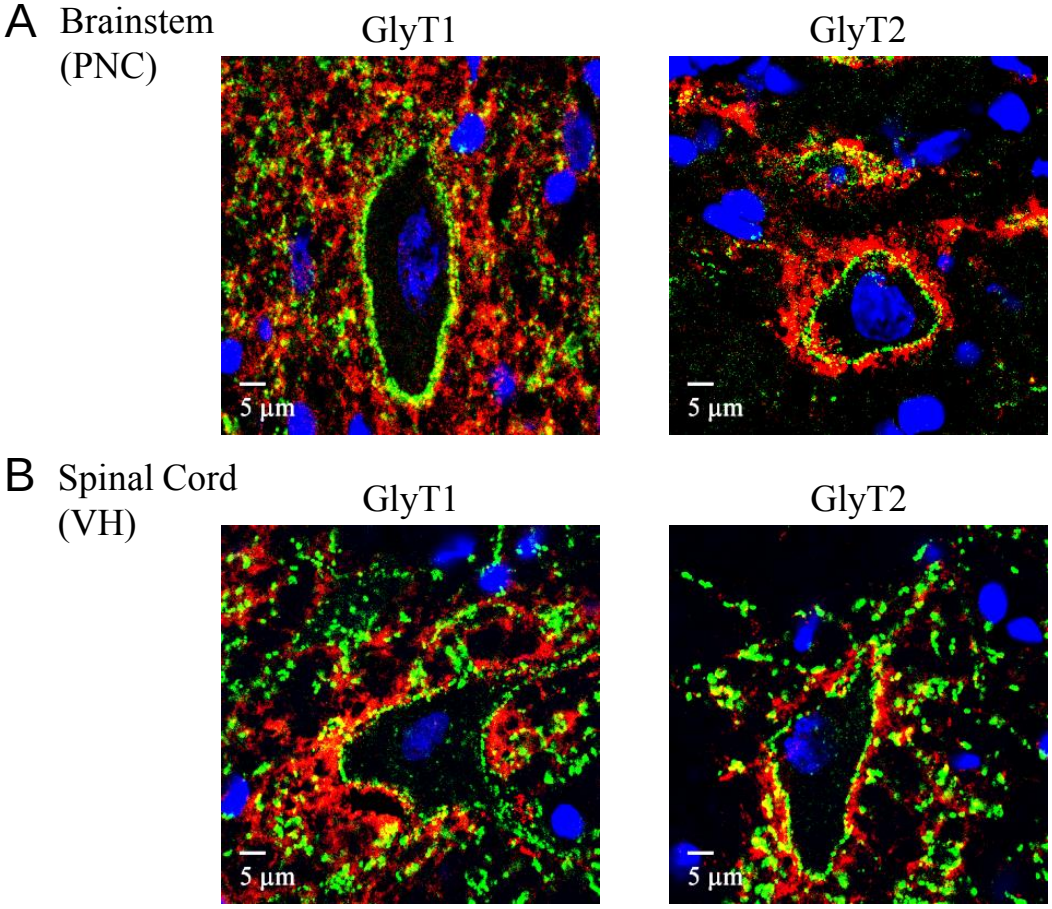

Fig. 5.7. Higher resolution images show that Glycine transporters in close apposition to GlyR´s. Confocal images were taken at 63x magnification. GlyT1 and GlyT2 specific staining (red) is surrounding the GlyR immunoreactivity (green) observed on the surface of neurons in the PnC of the brainstem ***(A)*** and in the ventral horn of the spinal cord ***(B)***, with very little colocalisation. Nuclei in blue (DAPI).

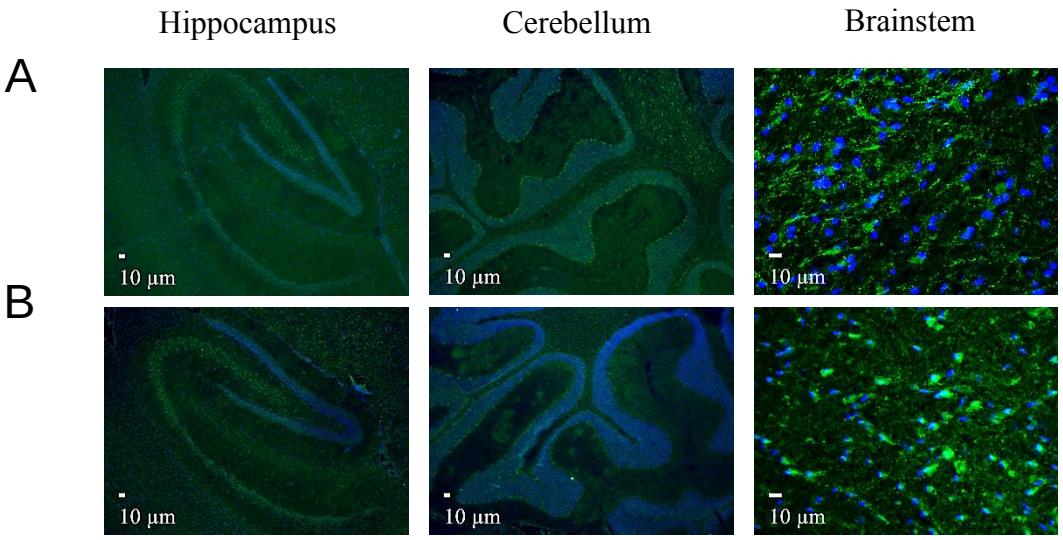

Fig. 5.8. Non-specific staining observed during the protocol optimization. Images were taken at 20x and 40x. ***A.*** Generalised unspecific staining is observed in the CA region, dentate gyrus of the hippocampus and in all layers of the cerebellum when brain sections were incubated with patient serum and healthy control. ***B.*** Higher magnification images of the PnC in the brainstem after incubation with patient serum and healthy control shows high background in the neuropil, making difficult to discriminate the specific staining of the patient serum from the non-specific staining of the healthy control. Nuclei in blue (DAPI).

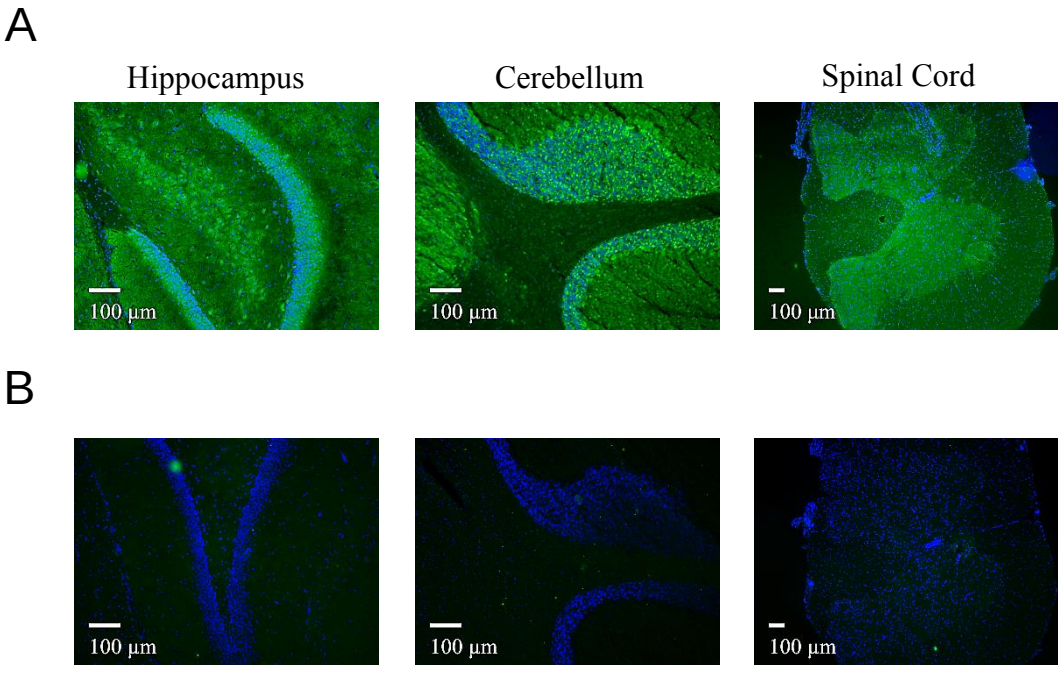

Fig. 5.9. Patient serum from PERM patients binds to rat CNS sections. Photographs were taken at 10x and 5x magnification. ***A.*** Immunostaining with patient serum (green) of fixed rat CNS sections show specific binding to the dentate gyrus, CA3, regions of the hippocampus, granular and Purkinje cell layer, and deep nuclei of the cerebellum, dorsal and ventral horns (DH, VH) of the spinal cord. ***B.*** No specific staining was observed in the same areas of the rat CNS when section were incubated with healthy control serum.

resembled the specific staining observed in the same areas using the monoclonal GlyRα1 antibody. It was different to the specific staining observed using the polyclonal antibody to glutamic acid decarboxylase (GAD), which binds intracellularly (Fig. 5.10A,B,C).

Double labelling of the brainstem at the PnC level and ventral horns of the spinal cord with patient serum (green) and GlyR monoclonal antibody mAb2 (red), showed colocalisation on the surface of the neurons (Fig. 5.11A,B upper panel), but no colocalisation was observed when healthy control was used (Fig. 5.11A, middle panel). When patient serum preadsorbed against HEK cells expressing GlyR α1 was used there was decreased staining on the surface of the neurons and a loss of the colocalisation (Fig. 5.11A,B lower panel), suggesting that the specific staining was due to presence of GlyR α1 in these regions.

To confirm further that the serum specific staining occurs on the surface of neurons in the PnC, and on the surface of motorneurons in the ventral horn of the spinal cord, triple labelling studies with patient serum (green), GlyR moclonal mAb2 (red) and MAP2 antibody in the brainstem or CHAT antibody in the spinal cord (purple) was tested. There was colocalisation of the GlyR α1 staining on the surface of PnC neurons surrounding the cytoplasmatic MAP2 immunoreactivity and on the surface of motorneurons surrounding the cytoplasmatic CHAT immunoreactivity (Fig. 5.12A). There was no colocalisation with healthy control serum as expected (Fig. 5.12B).

Forty-three sera were examined for binding to rat brain sections, and for co-localisation with commercial antibodies to GlyRα1. Forty-one of the forty-three sera bound to the tissue. For example all sera bound to the spinal cord and the brainstem where GlyRα1 is strongly expressed (Malosio et al, 1991), but some sera also bound to brain regions

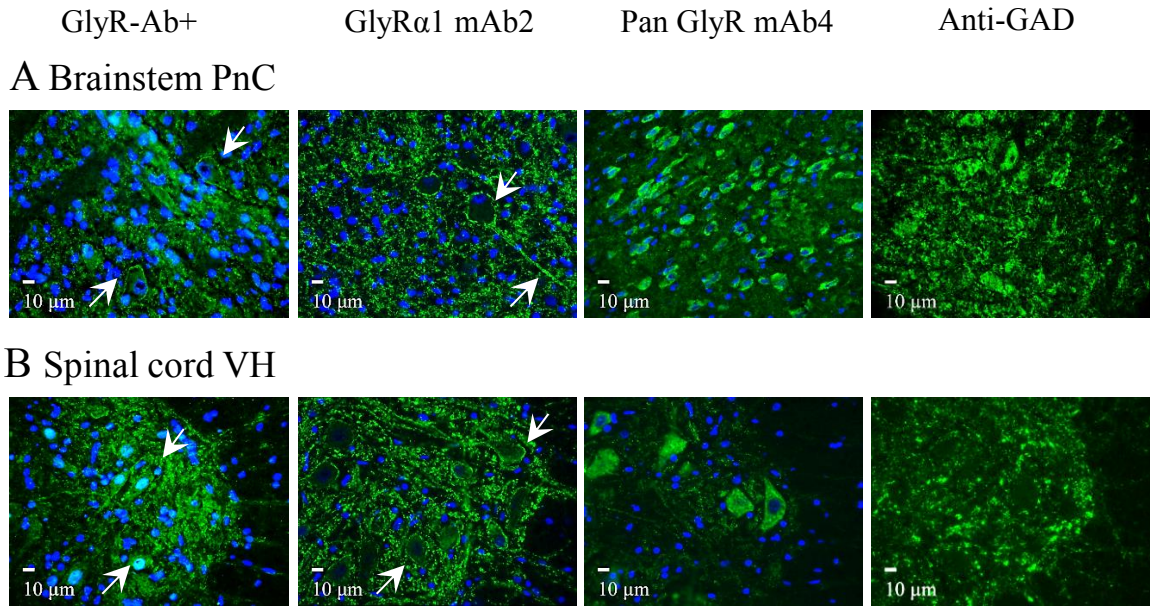

Fig. 5.10. Patient serum from GlyR-Ab patients binds to CNS regions involved in motor regulation. Photographs were taken at 40x magnification. Immunostaining with serum (green) of fixed rat CNS sections show specific binding to the surface of neurons in the caudal reticular pontine nuclei (PnC) (left upper panel) of the brainstem and motor neurons in the ventral horn of the spinal cord (left lower panel). The specific staining resembles that observed on the surface of neurons using GlyR antibody mAb2, in which is possible to observe the soma and dendrites of neurons (marked with arrows). In the right panel is shown the specific staining of neurons in the same areas with the GlyR antibody mAb4, showing a more cytosolic pattern. The specific staining is different to the specific staining observed with polyclonal antibody to GAD, which is mainly intracellular.

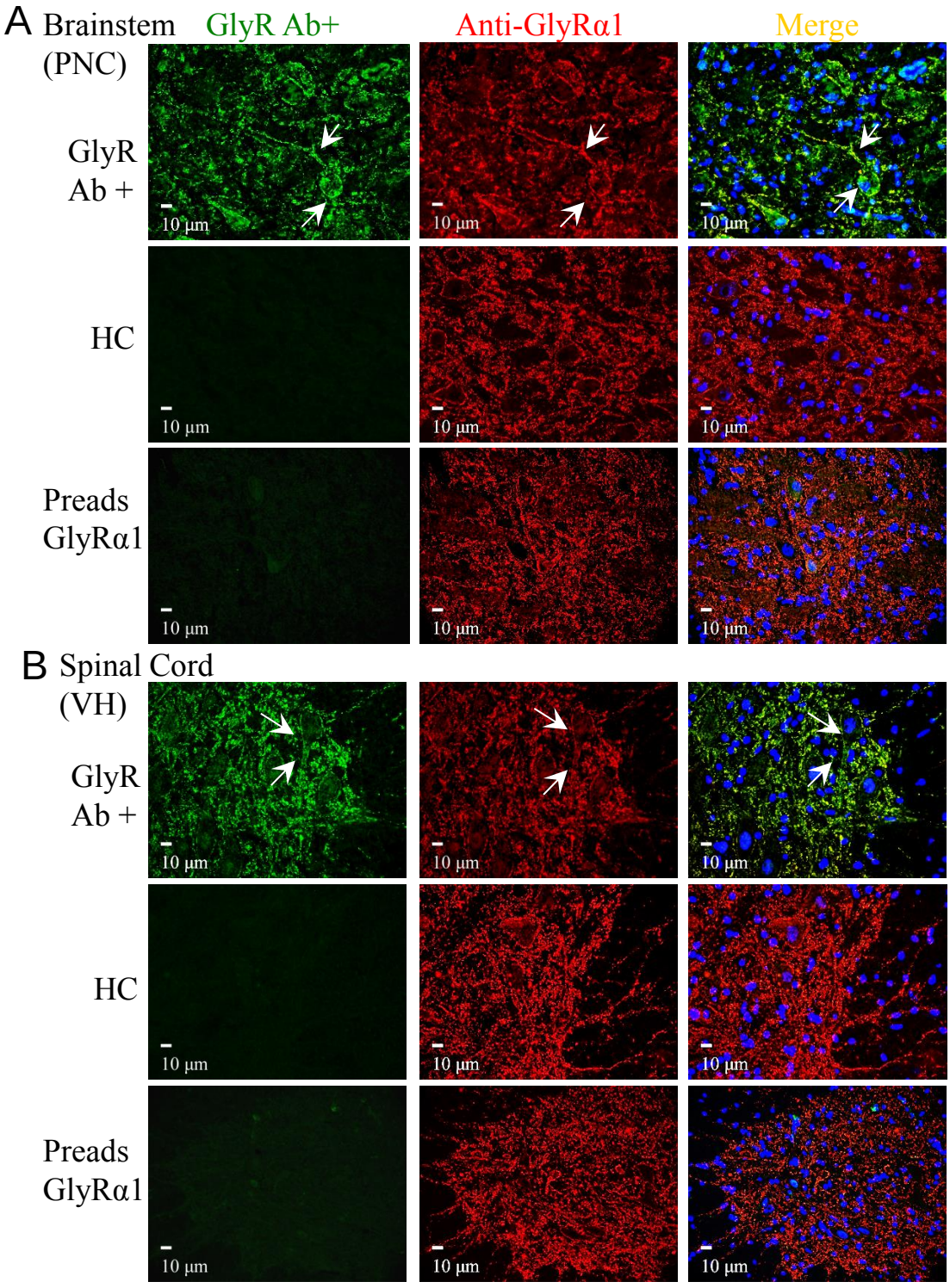

Fig. 5.11. Patient serum from PERM patients binds to CNS regions involved in motor regulation. Photographs were taken at 40x magnification. Double labelling of neurons in the pontine reticular nucleus (PnC) of the brainstem with patient serum (green) and monoclonal antibody to the GlyRα1 (red) show colocalisation on the neuronal soma and in the neuropil (arrows). Double labelling of the same neurons when incubated with healthy control serum showed no binding to the PnC and no colocalisation. After pre-adsorption against HEK-GlyRα1 cells there was a marked decrease in PnC staining with patient serum. ***B.*** The same staining findings were observed in the ventral horn of the spinal cord. Nuclei in blue (DAPI).

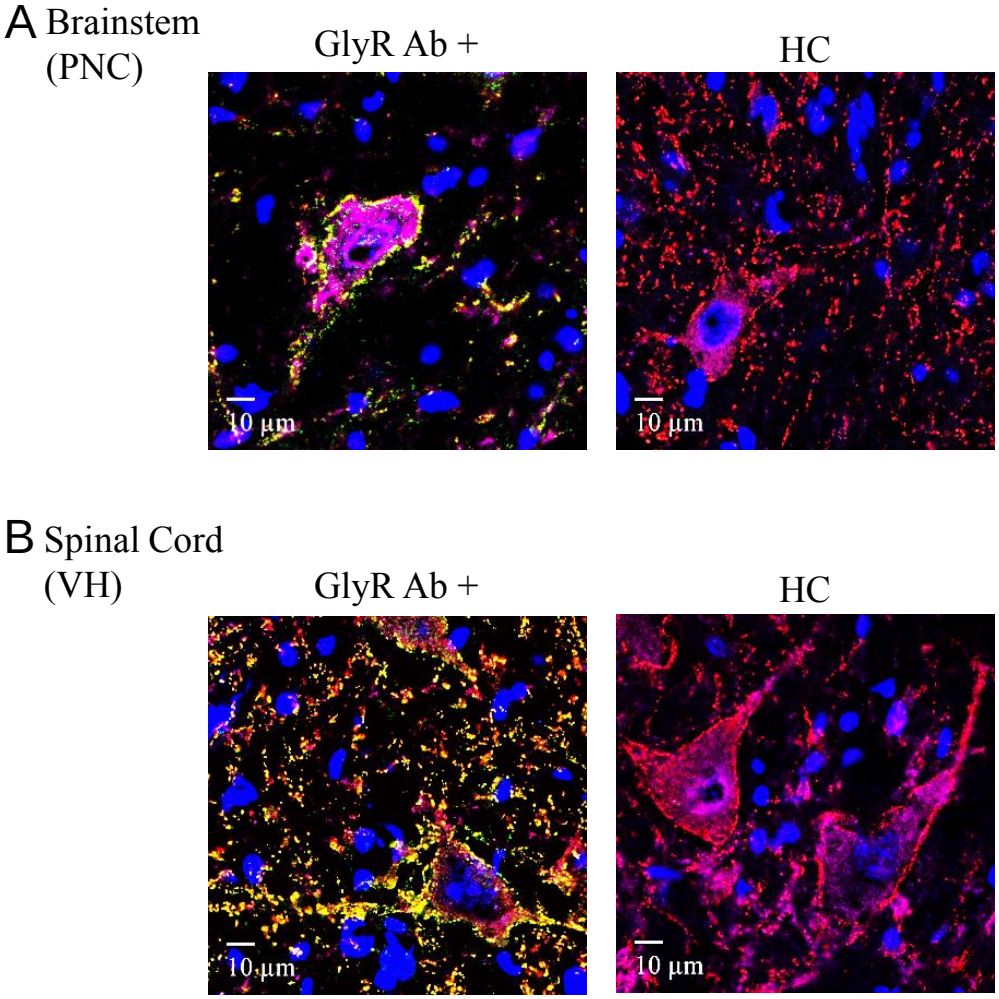

Fig. 5.12. Patient serum from PERM patients binds to the surface of neurons in the brainstem and spinal cord. Confocal images were taken at 63x magnification. ***A.*** Triple labelling of neurons in the PnC show the patient's serum (green) colocalising with GlyRα1 monoclonal antibody (red) on the surface of a large neuron labelled with the cytoplasmic neuronal marker anti-MAP2 antibody (purple). No colocalisation is observed when healthy control is used. ***B.*** Triple labelling of neurons in the ventral horn of the spinal cord show similar results with colocalisation of the patient's serum (green) and GlyRα1 monoclonal antibody (red) on the surface of a motor neuron labelled with motor neuron marker anti-choline acetyltranferase antibody (CHAT) (purple). Nuclei are stained with DAPI (blue).

where GlyRα1 is absent or weakly expressed such as the cerebellum, the hippocampus, the caudate and the white matter, suggesting the presence of other antibodies.

Five different staining patterns were described based on the antibody binding localisation, characterisitics and its colocalisation with GlyRα1 commercial antibody (Fig. 5.13, Fig. 5.14, Fig. 5.15A,B; Table 5.2):

- Pattern 1: Sera bound in a punctate manner to the cell bodies and neuropil of the brainstem and the spinal cord, co-localised with monoclonal antibodies to GlyRα1, and did not bind to the hippocampus, or the cerebellum. Nine patients' sera (21%) had this binding pattern.

- Pattern 2: Sera bound in the appropriate brainstem and spinal cord regions and co-localised with GlyRα1, but in addition also bound intracellularly to the dentate gyrus, CA regions of the hippocampus and granular and Purkinje cell layers and deep nuclei of the cerebellum. The additional binding was evenly distributed in the cell body, and did not co-localise with GlyRα1 monoclonal antibody. Twenty patients´sera (46%) had this binding pattern.

- Pattern 3: Sera bound in the appropriate brainstem and spinal cord regions co-localised with GlyRα1, but in addition also bound in an uneven punctate distribution to deep nuclei, the molecular and granular cell layer of the cerebellum and in the molecular and pyramidal stratum of the CA regions of the hippocampus and in the cerebral cortex. The binding did not colocalise with GlyRα1 monoclonal antibody. Seven patients´sera (16%) had this binding pattern.

- Pattern 4: Sera bound intracellularly to the brainstem, the spinal cord, the dentate gyrus, CA regions of the hippocampus and granular, Purkinje cell layers and deep nuclei of the cerebellum. This binding did not colocalise with GlyRα1 monoclonal and resembled an astrocytic pattern; two patients´sera (5%) had this binding pattern.

- Pattern 5: Sera bound intracellularly to the brainstem, the spinal cord, the dentate gyrus, CA regions of the hippocampus and granular and Purkinje cell layers and deep nuclei of the cerebellum. The binding did not colocalise with GlyRα1 monoclonal and resembled a nuclear pattern; three patients´sera (7%) had this binding pattern.

In two patients (5%) it was impossible to detect serum binding despite trying with different serum dilutions. Overall patterns 1, 2 and 3 colocalised with GlyRα1 monoclonal antibody whereas patterns 4 and 5 did not. The CSF staining patterns were similar to those observed with sera (Fig. 5.15). These results strongly suggested the presence of antibodies to additional antigens in 10/38 (26.4%) of the sera.

The intracellular binding observed in some of these patients appeared to correspond to antibodies to glutamic acid decarboxylase (GAD65). Previous studies have reported the existence of GAD antibodies in SPS and PERM patients (Meinck et al, 2001). In order to corroborate this, preadsorption studies and double immunolabelling studies using GAD65 commercial antibody, in conjunction with GlyRα1 antibody were performed in the same regions. Sera from pattern 3 bound to the previously described regions and were adsorbed by soluble GAD (Fig. 5.16A). The binding observed in these regions was similar to that observed after incubation with GAD polyclonal antibody. Healthy serum did not show any binding in these regions (Fig. 5.16A). In addition, sera from pattern 3

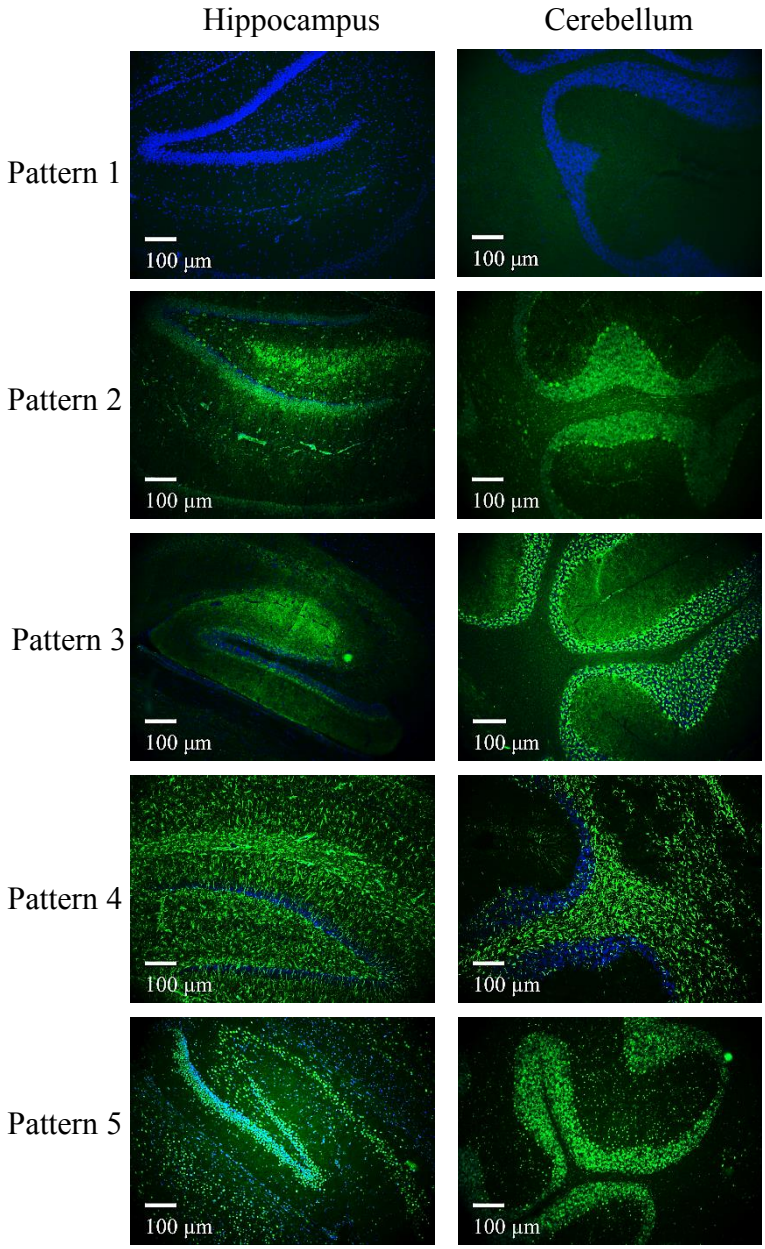

Fig. 5.13. Sera from PERM patients bind to the hippocampus and cerebellum with different patterns. Images were taken at 10x magnification. ***A.*** Patients from pattern 1 did not bind to these regions, but the rest of the patients sera did bind to different areas in these regions with different staining patterns. In patterns 2, 3 and 5 appeared mainly intracellular but was more homogeneous in pattern 2, more patchy in pattern 3, and pattern 5 resembled a nuclear staining. While pattern 4 resembled an astrocytic staining. Nuclei are stained with DAPI (blue).

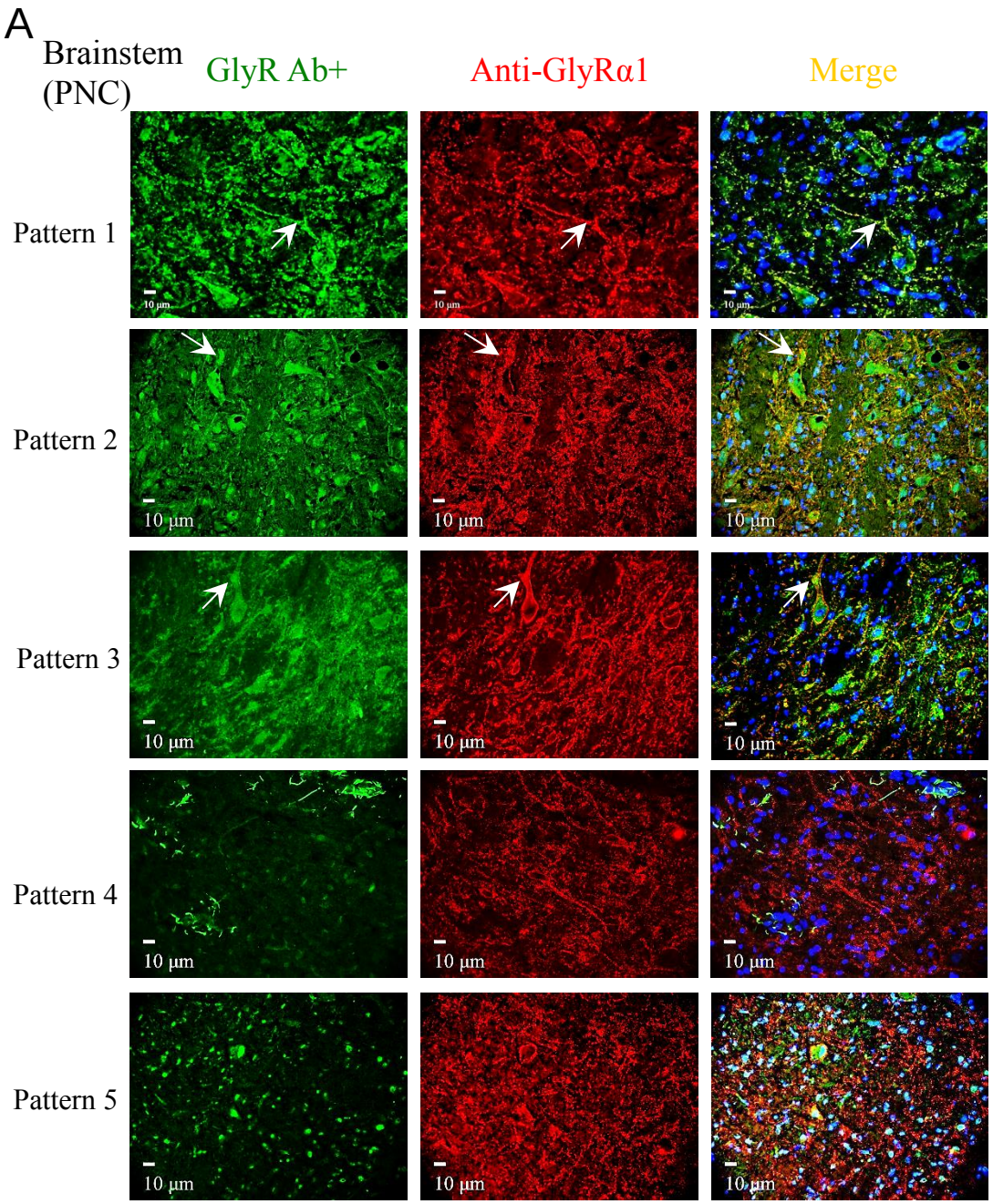

Fig. 5.14A. Sera from PERM patients bind to the brainstem with different patterns. Photographs were taken at 40x magnification. Double labelling of neuron in the pontine reticular nucleus (PnC) of the brainstem with patient serum (green) and monoclonal antibody to the GlyRα1 (red) show colocalisation on the neuronal soma and in the neuropil (arrows) in patterns 1, 2, 3, while no colocalisation is observed in patterns 4 and 5. Additionally, in patterns 2 and 3 an intracellular staining can be observed, more homogenous in pattern 2, more patchy in pattern 3. Serum in pattern 4 resembles an astrocytic pattern and in pattern 5 there is nuclear staining. Nuclei are stained with DAPI (blue).

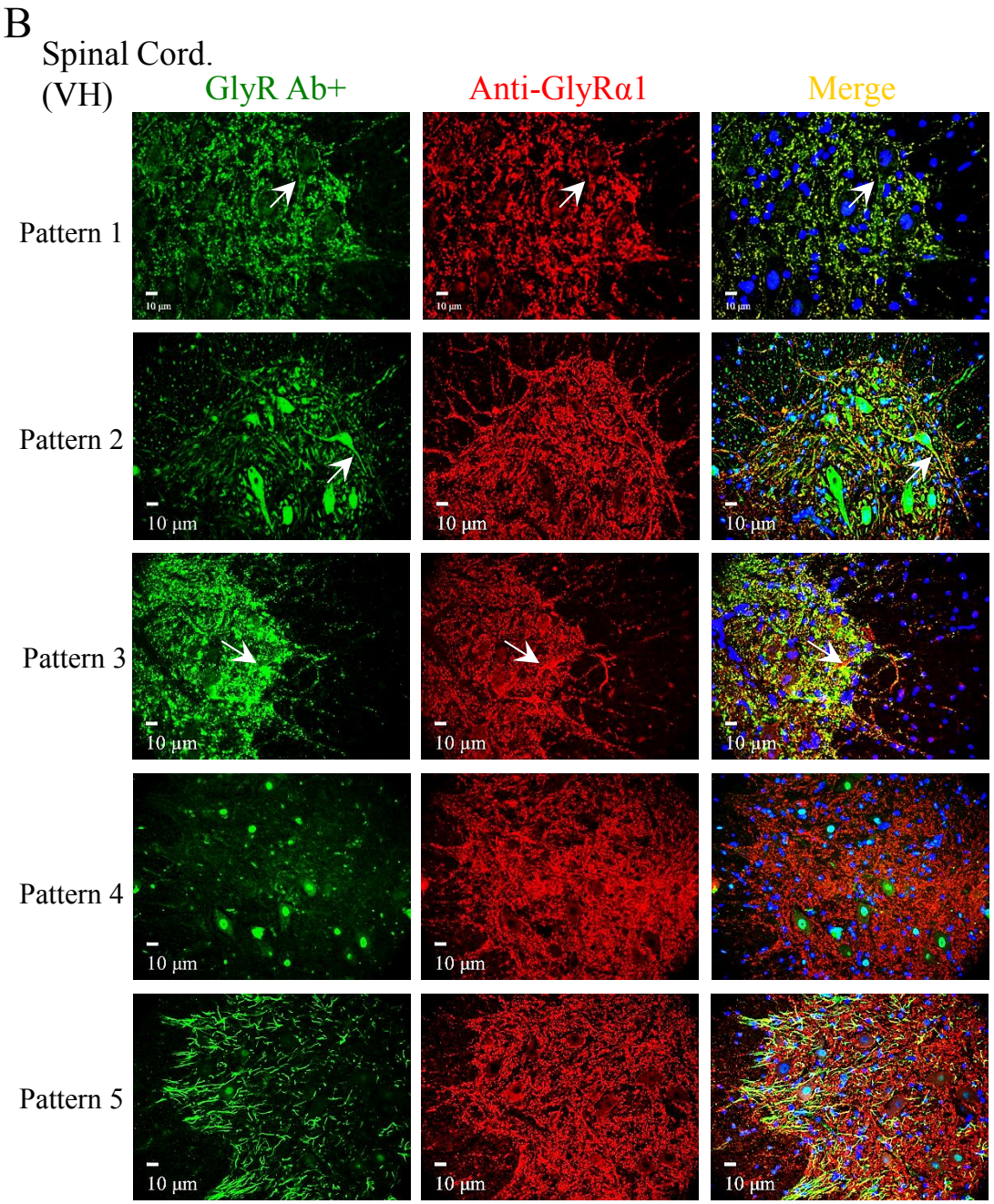

Fig. 5.14B. Patient sera from PERM patients bind to the spinal cord with different patterns. Photographs were taken at 40x magnification. Double labelling of neurons in the ventral horn of the spinal with patient serum (green) and monoclonal antibody to the GlyRα1 (red) showed similar results with colocalisation on the neuronal soma and in the neuropil (arrows) in patterns 1, 2 , 3; while no colocalisation is observed in patterns 4 and 5. Additionally, in patterns 2 and 3 an intracellular staining can be observed, more homogenous in pattern 2, more patchy in pattern 3. Serum in pattern 4 resembles an astrocytic pattern and in pattern 5 there is nuclear staining. Nuclei are stained with DAPI (blue).

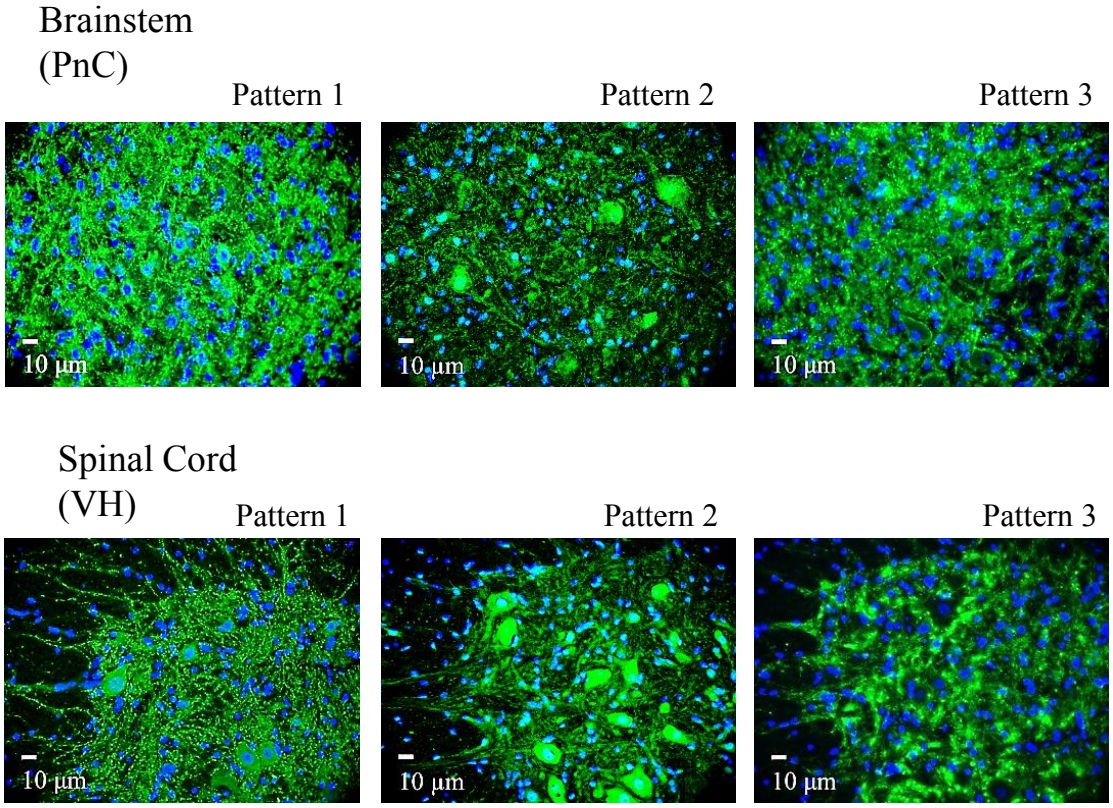

Fig. 5.15. CSF from patients binds in a similar pattern to the serum. Images were taken at 40x magnification. PNC of the brainstem (upper panel) and ventral horn of the spinal cord (lower panel). CSF form pattern 1 is mainly extracellular with no intracellular staining while pattern 2 has extracellular staining with an even intracellular staining, and pattern 3 has extracellular staining with an uneven intracellular staining. Nuclei are stained with DAPI (blue).

Table 5.2. Main patterns of patients' antibodies binding to rodent brain tissue and GlyR subunit binding

Number of patients N=43	Cellular localization	Co-localisation with GlyRα1 Ab	Spinal cord and brainstem binding	Hippocampus	Cerebellum	Other brain areas	Additional staining	GlyR Subunits at 1:80 serum dilution	Conclusion
Pattern 1 9 (21%)	Extracellular Neurons and neuropil	Yes	100%	0%	55.6% Granular cell layer (dendrites)	Caudate 100% Corpus callosum 28.2% Cortex 11.1%	Absent	α1+ α2+ α3 55.6% α1+ α3 28.2% α1 only 11.1%	Mainly α1 but some reactivity with other subunits on brain sections
Pattern 2 20 (46%)	Extracellular neurons and Neuropil	Yes	100%	100% Intracellular Dentate gyrus and ca regions	100% Intracellular all layers and deep nuclei	Caudate 100% intracellular Corpus callosum 55% Cortex 20%	Intracellular Evenly distributed in the cell body	α1+ α2+ α3 45% α1+ α3 30% α1 only 25%	Mainly α1 and other generalized cytoplasmic antigen
Pattern 3	Extracellular neurons and Neuropil	Yes	100%	100% Intracellular Dentate gyrus and molecular	100% Molecular layer and deep nuclei	Caudate 100% extracellular Corpus	Intracellular Uneven punctate	α1+ α2+ α3 28.6% α1+ α3	α1 and intracellular antigen (GAD-Ab)

7 (16%)				layer		callosum 28.6% Cortex 100%	clusters	28.6% α1+ α2 14.2% α1 only 28.6%	
Pattern 4 2 (5%)	Intracellular	No	100%	100% intracellular Dentate gyrus and ca regions	100% Intracellular All layers and deep nuclei	Caudate 100% intracellular Corpus callosum 50% Cortex 0%	Absent	α1+ α2+ α3 50% α1+ α2 50%	Other intracellular antigen, astrocityc pattern
Pattern 5 3 (7%)	Intracellular	No	100%	100% Intracellular Dentate gyrus and ca regions	100% Intracellular All layers and deep nuclei	Caudate 100% intracellular Corpus callosum 0% Cortex 100%	Absent	α1 only 100%	Other intracellular antigen, nuclear pattern

*In two patients it was not possible to detect serum binding to brain sections.

showed colocalisation of serum IgG (green) with commercial anti-GAD-65 antibody (red) in both the brainstem and the spinal cord (Fig 5.16B). Double labelled higher magnification images from this patients´ serum showed extracellular colocalisation of the patients´s antibodies with GlyRα1 monoclonal antibody, and some intracellular staining which did not colocalise. Preadsorption of the patient serum with GlyRα1 transfected HEK cells lead to a decrease of the extracellular specific staining without affecting the intracellular staining, whereas preadsorption with soluble GAD lead to a decrease in the intracellular staining without affecting the extracellular staining (Fig. 5.16C,D).

These results confirm the presence of both GlyRα1 and GAD antibodies in some PERM patients. This serum and four other sera had high GAD antibody titres (>2000 U/ml).

The binding of some sera to intracellular antigens was not adsorbed by GlyR-HEK, untransfected HEK cells or soluble GAD, suggesting the presence of antibodies to other intracellular antigens. One of those intracellular antigens may correspond to antigens present in glial cells based on an empirical observation of the staining. Therefore, double labelling studies using GFAP commercial antibody, in conjunction with GlyR α1 antibody were performed as above. Sera from pattern 4 showed colocalisation of serum IgG (green) with commercial anti-GFAP antibody (red) in both the brainstem and the spinal cord (Fig 5.17).

Another possibility was the presence of antibodies against other GlyRα subunits; this possibility was strengthened by the finding that PERM patients' sera bind to HEK cells expressing GlyRα2 and GlyRα3, as shown in chapter 3. Surprisingly, when the sera were preadsorbed against each GlyRα subunit, the immunostaining observed in different brain areas disappeared, including the specific staining of the brainstem and

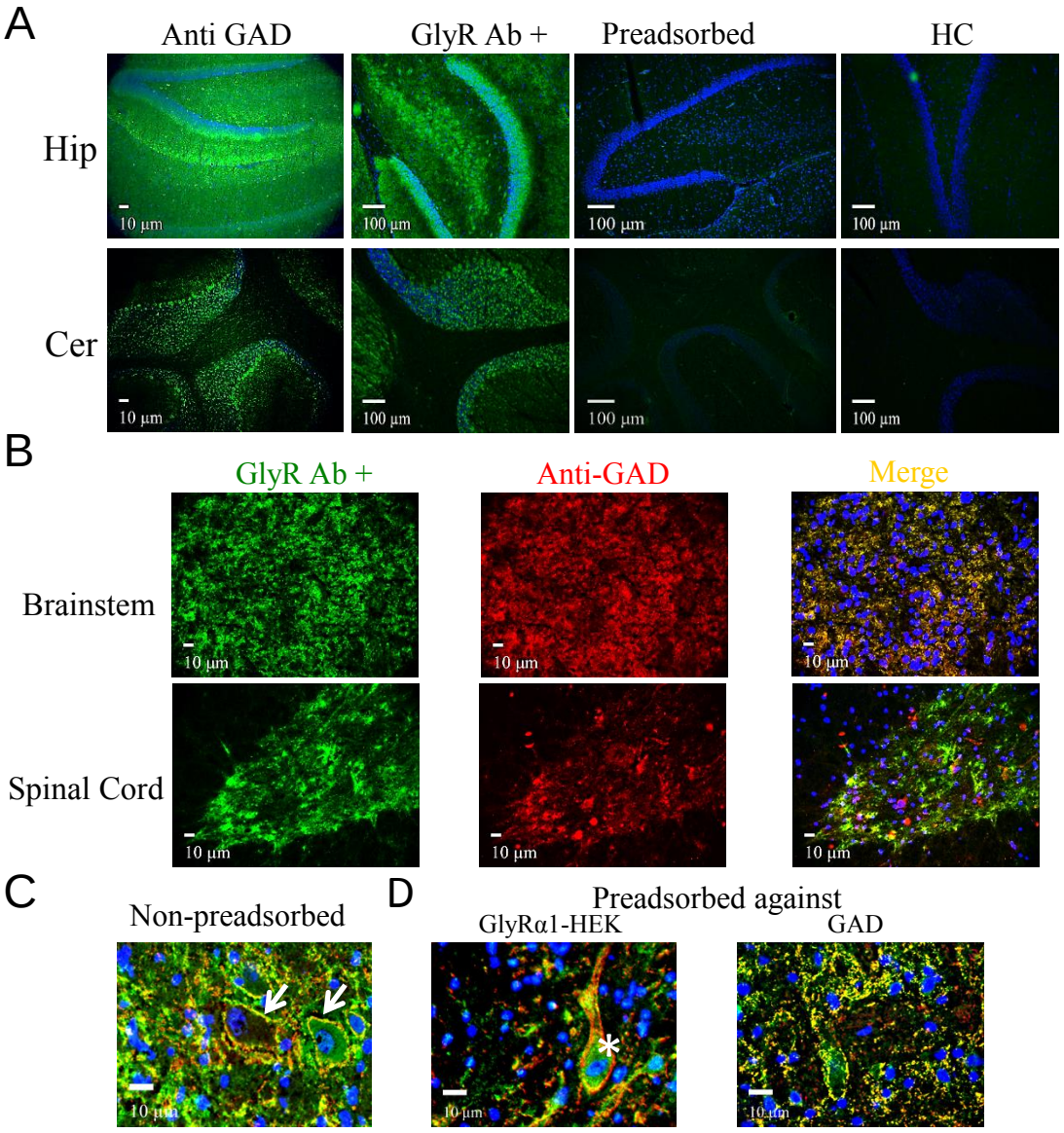

Fig. 5.16. Some patient sera contain other antibodies that bind intracellularly. Confocal images were taken at 63x magnification. ***A.*** Immunostaining with a patient serum (green) on fixed rat CNS sections (second panels) shows specific binding to the dentate gyrus, CA3 and other regions of the hippocampus and the granular and Purkinje cell layers and deep nuclei of the cerebellum, where GlyRα1 binding is not observed, matching the immunostaining observed with the anti-GAD commercial antibody. (upper panels). The immunolabelling of the hippocampus and cerebellum was greatly reduced when the serum was adsorbed against GAD (third panels). No specific staining was observed when sections were incubated with control serum (HC, lower panels)***B.*** Double immunolabelling with this patient's serum (green) colocalises with anti-GAD commercial antibody (red), in the brainstem and spinal cord as shown in the Merge. ***C.*** Higher resolution images, double-labelled with another patient IgG (green) and monoclonal anti- GlyRα1 (red), demonstrates colocalisation (arrows) and also neuropil binding which did not colocalise (asterisks) and was not adsorbed by mock-transfected HEK cells. ***D.*** Immunolabelling with this patient's serum pre-adsorbed against HEK-GlyRα1 cells shows a loss of the colocalisation, leaving intact the intracellular staining (left panel). Conversely, when preabsorbed with soluble GAD, the intracellular staining was reduced leaving intact the extracellular staining (right panel).

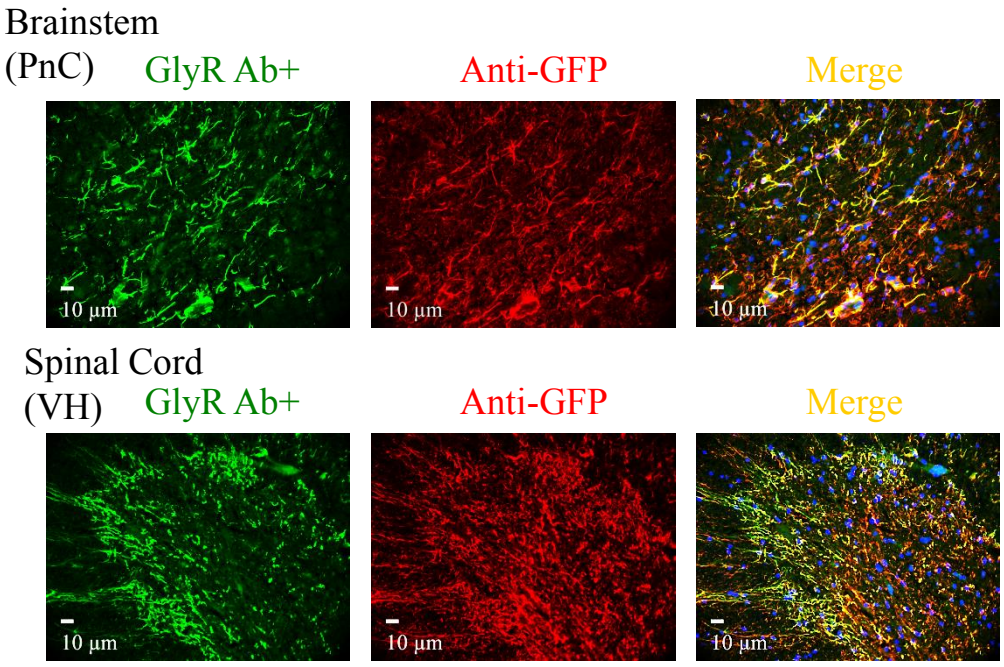

Fig. 5.17. Some patient sera contain other antibodies that bind intracellularly. Images were taken at 40x magnification. Nuclei are stained with DAPI (blue). Double labelling of fixed rat CNS sections with patient's serum (green) colocalises with glial fibrillary acidic protein (GFAP) commercial antibody (red) in the brainstem (upper panel) and spinal cord (lower panel).

the spinal cord where GlyRα1 is strongly expressed (Fig. 5.18), and was confirmed when the serum binding to HEK GlyRα1 was lost after serum preadsorption with each GlyRα subunit (Fig. 3.5). These results suggest that most of the PERM patients IgG cross-react with the different GlyR subunits.

However, a few PERM patients have more than one antibody to different GlyR subunits. Preadsorption studies of HEK cells expressing either GlyRα1 or GlyRα3 subunits showed serum binding to both expressing HEK cells but the serum binding was lost when the serum was preadsorbed against HEK cells expressing GlyRα1 leaving intact the binding to GlyRα3 HEK cells. The opposite was observed when the serum was preadsorbed against HEK cells expressing GlyRα3, losing the GlyRα3 binding and leaving intact the GlyRα1 binding (Fig. 5.19B).

5.2.3.1 Patient´s sera binding to the dorsal horn of the spinal cord

Double labelling studies of the dorsal horns of the spinal cord with patient serum (green) and GlyR monoclonal antibody mAb2 (red) showed two different binding patterns. The first was specific staining of the neuropil in lamina II, III, IV of the spinal cord; this staining colocalised with monoclonal antibody to GlyRα1 in laminas III, IV without colocalisation in the lamina II. By contrast, the second binding pattern was staining only in the laminas III, IV of the spinal cord colocalising with the monoclonal antibody with no staining observed in the lamina II of the spinal cord (Fig. 5.19A). Patients with the first binding pattern had antibodies to GlyRα1 and GlyRα3 subunits, as demonstrated by the loss of the specific staining in the lamina II of the spinal cord when the serum was preadsorbed with HEK cells expressing GlyRα3, whereas the staining was preserved when the serum was preadsorbed with untransfected HEK cells (Fig. 5.19C) Patients with the second binding pattern had antibodies only to GlyRα1

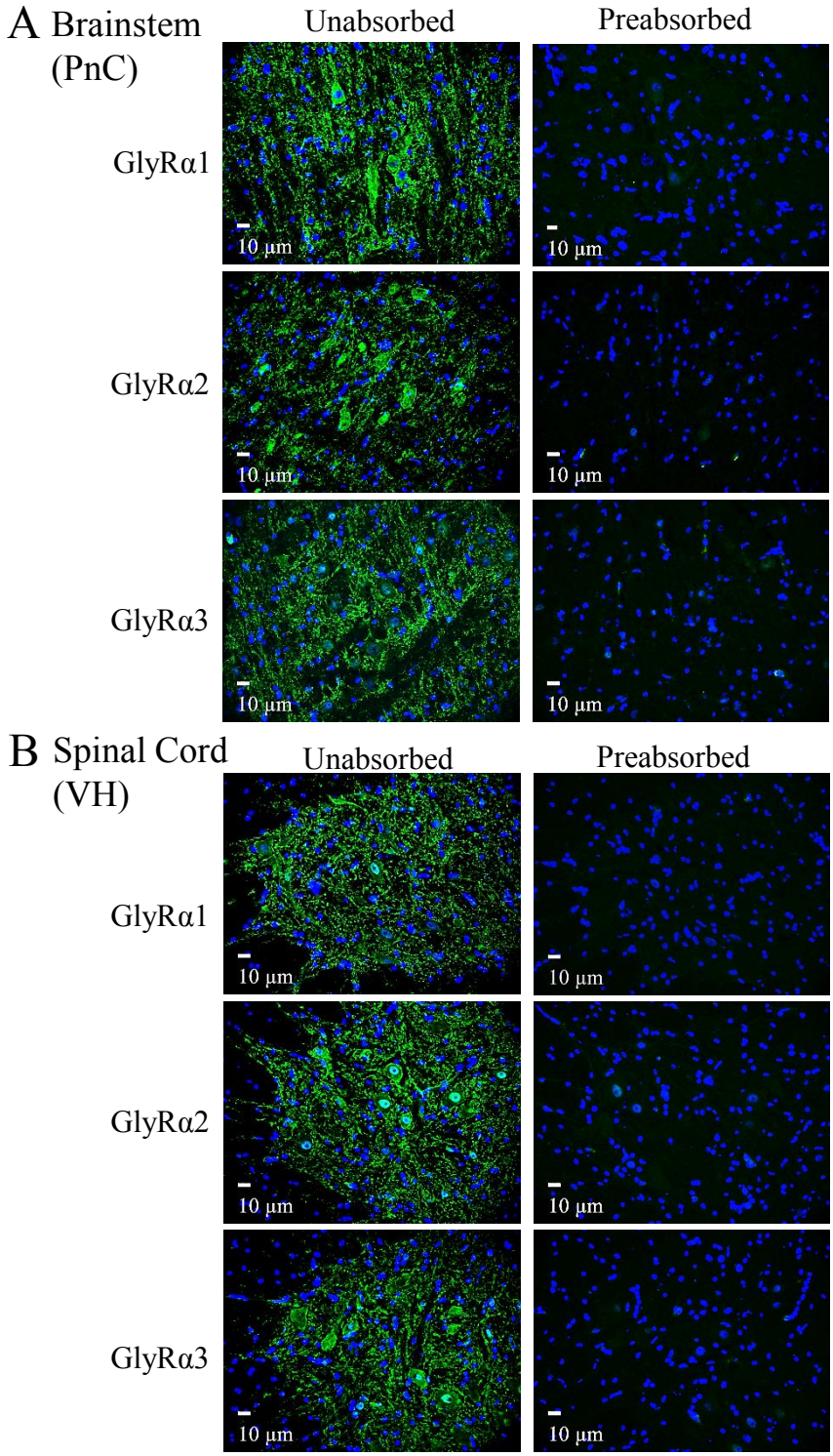

Fig. 5.18. Patient sera binding is lost after preasdorption of patient's IgG with the different GlyR subunits. Images were taken at 40x magnification. Nuclei are stained with DAPI (blue). ***A.*** Patient's serum (green) immunoreactivity in the PNC of the brainstem is loss after serum preadsorption with HEK cells expressing either GlyRα1, GlyRα2 or GlyRα3 ***B.*** Same results are observed in the ventral horn of the spinal cord with loss of serum immunoreactivity after serum preadsoprtion with HEK cells expressing either GlyRα subunit.

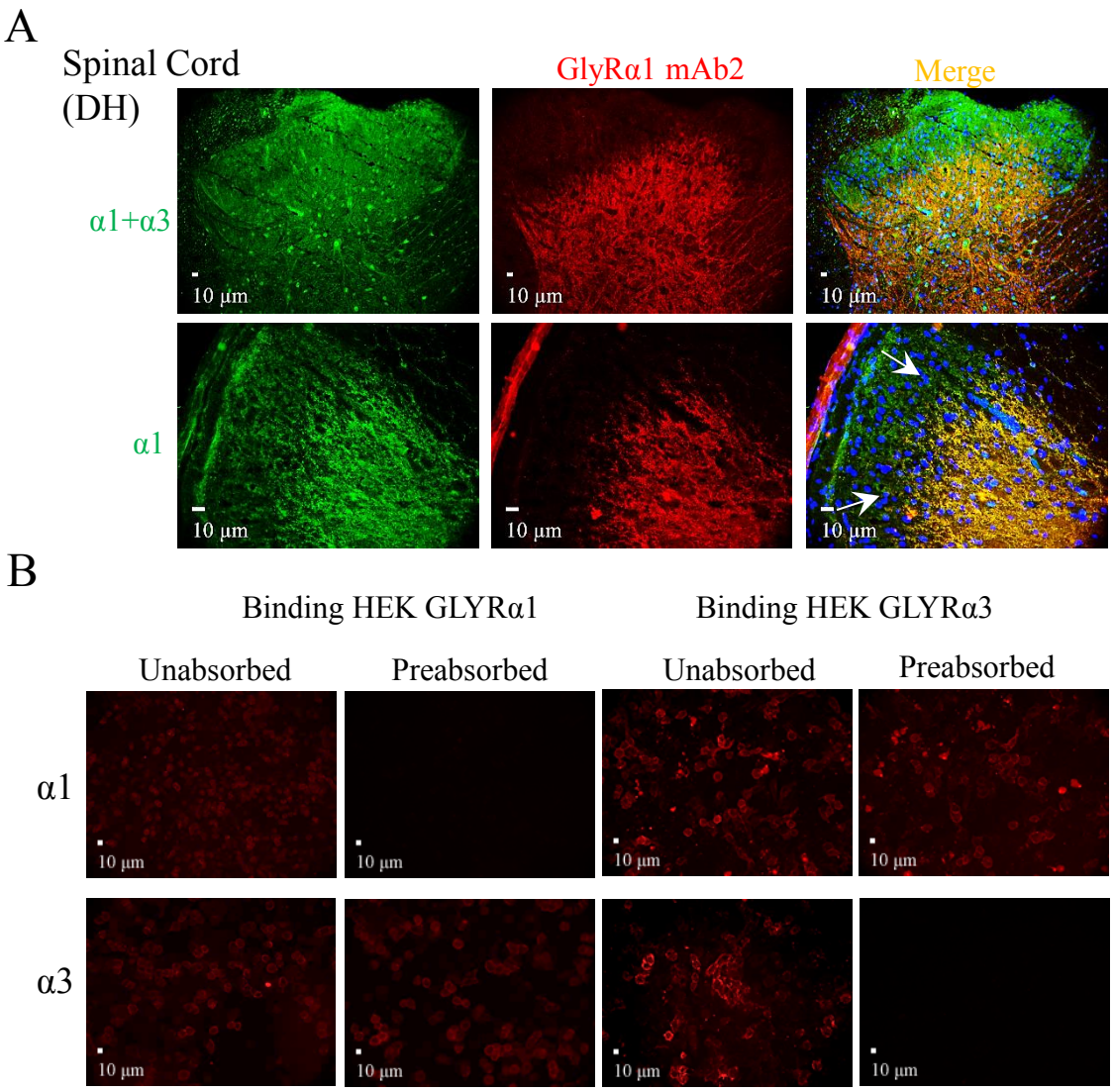

Fig. 5.19. A few PERM patients have antibodies to different GlyR subunits. Images were taken at 40x magnification. Nuclei are stained with DAPI (blue). ***A.*** Double labelling of neurons in the dorsal horn of the spinal cord with patient serum known to bind to HEK cells expressing GlyRα1 or GlyRα3 subunits (green) and monoclonal antibody to the GlyRα1 (red) showed immunoreactivity on the neuropil in laminas II, III and IV, which colocalises with the monoclonal antibody in laminas III and IV, no colocalisation is observed in lamina II (arrows). ***B.*** Cell based assays using HEK cells expressing either GlyRα1 subunit or GlyRα3 show patient serum binding (α1 1:40) which was lost after serum preadsorption with HEK cells expressing GlyRα1 but not after serum preadsorption with HEK cells expressing GlyRα3 (upper panels). Conversely, other patient serum (α3 1:160) GlyRα3 subunit also show serum binding which was lost after serum preadsorption with HEK cells expressing GlyRα3 but not after serum preadsorption with HEK cells expressing GlyRα1.

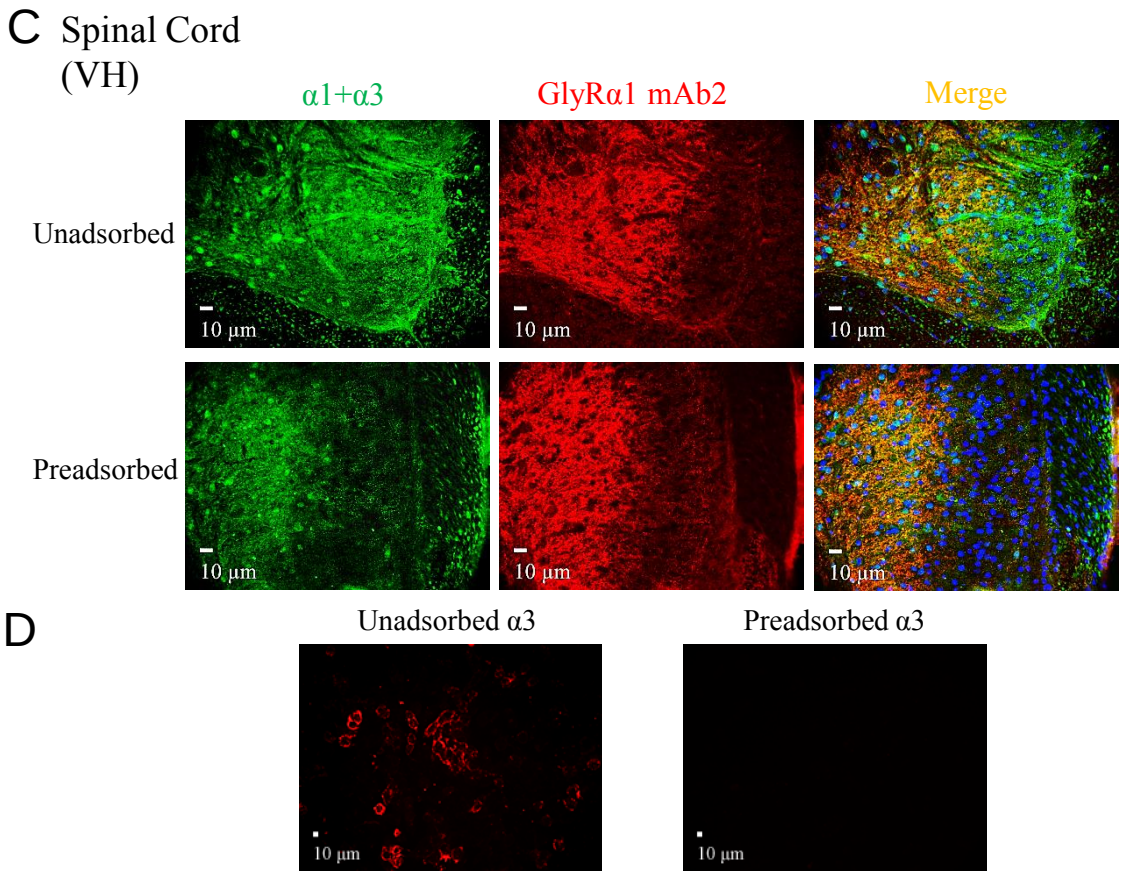

Fig. 5.19. (cont) Patient sera immunoreactivity in the lamina II of the spinal cord is lost after serum preadsorption with GlyRα3 subunit. Images were taken at 40x magnification. Nuclei are stained with DAPI (blue). ***C.*** Double labelling of neurons in the dorsal horn of the spinal cord with a patient serum known to bind HEK cells expressing GlyRα1 or GlyRα3 subunits (green) and monoclonal antibody to the GlyRα1 (red) showed loss of immunoreactivity in lamina II after serum preadsorption with HEK cells expressing GlyRα3, leaving intact the immunoreactivity in laminas III and IV which colocalises with the monoclonal antibody. ***D.*** Images were taken at 20x. Patients IgG binding to HEK cells expressing GlyR α3 (red) was lost after serum preasdorption with HEK cells expressing GlyRα3 subunit.

subunits. The serum binding to HEK cells expressing GlyRα3 after preadsoprtion with mock HEK cells or HEK GlyRα3 expressing cells is shown in figure 5.19D.

5.2.4 Clinical correlation

To see if the GlyR-Ab staining pattern had any relationship with the patient´s clinical presentation of the disease, the staining of 40 patients was segregated by clinical syndrome and disability mRS scores. PERM sera showed all binding patterns, whereas the other clinical presentations did not (Table 5.3). No clear correlation between GlyR-Ab serum binding pattern and clinical presentation was found, but it was evident that sera with the second binding pattern were present in most of the clinical presentations except in the SPS group and interestingly sera with the first binding pattern was present only in patients with PERM (Fisher´s exact test, $p = 0.529$; Fig. 5.20; Table 5.4); whether this observation has any clinical relevance is difficult to determine as other intracellular antibodies are involved in some of the staining patterns. A similar finding was observed with patient sera with the second binding pattern distributed across the different disability mRS scores, but sera with the first binding pattern was present only in patients with high disability mRS scores (Fig. 5.21). In addition, patients who had low disability scores did not have all the sera binding patterns, whereas patients with high disability mRS scores had most of the staining patterns (Table 5.5). It is difficult to draw conclusions from these observations due to the presence of other antibodies in some of the staining patterns (Fisher´s exact test, $p = 0.268$; Table 5.6).

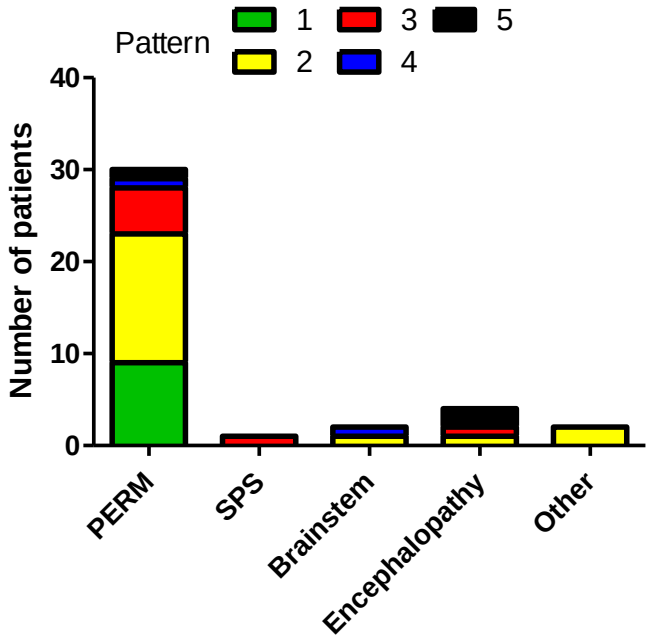

Fig. 5.20. Distribution of patients by clinical diagnosis and immunostaining pattern. Immunostaining pattern 1 is present only in PERM patients, while immunostaining pattern 2 is present in all clinical syndromes.

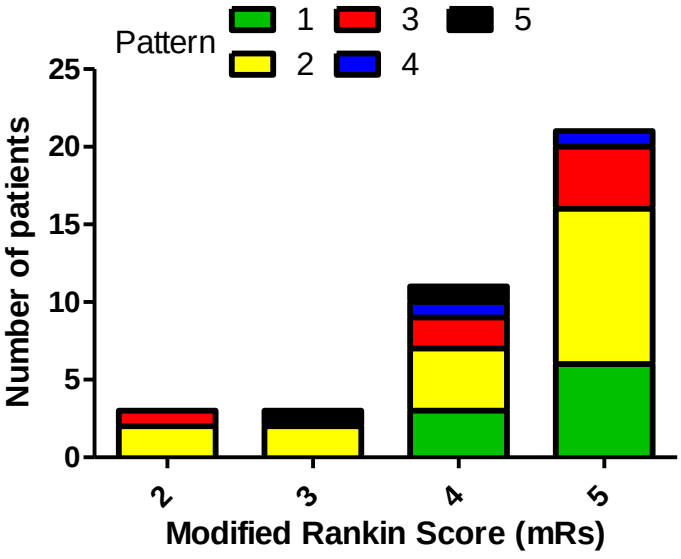

Fig. 5.21. Distribution of patients by disease severity and immunostaining pattern. Immunostaining pattern 1 is present only in patients with high disability mRS scores, while immunostaining pattern 2 is present in all disability mRS scores

Table 5.3. Distribution of the immunostaining patterns in the clinical syndromes

Immunostaining Pattern	PERM (N=30)	SPS (N=2)	Brainstem (N=2)	Encephalopathy (N=5)	Others (N=2)
1	9(30%)	0	0	0	0
2	14(46.7%)	1(50%)	1(50%)	1(20%)	2(100%)
3	5(16.7%)	1(50%)	0	1(20%)	0
4	1(3.3%)	0	1(50%)	0	0
5	1(3.3%)	0	0	2(40%)	0

Table 5.4. Comparison between the frequencies of immunostaining patterns 1 and 2 with clinical syndrome

Immunostaining Pattern	Typical (PERM, SPS, Brainstem) N=24	Atypical (Encephalopathy, Other) N=3	P
1	9 (37.5%)	0 (0%)	0.529
2	15 (62.5%)	3 (100%)	

Table 5.5. Distribution of the immunostaining patterns in the mRS disability scores

Immunostaining Pattern	mRS 2 (N=3)	mRS 3 (N=3)	mRS 4 (N=12)	mRS 5 (N=21)
1	0	0	3 (25%)	6 (28.6%)
2	2 (66.6%)	2 (66.6%)	4 (33.3%)	10 (47.6%)
3	1 (33.3%)	0	2 (16.6%)	4 (19%)
4	0	0	1 (8.3%)	1 (4.8%)
5	0	1 (33.3%)	1 (8.3%)	0

Table 5.6. Comparison between the frequencies of immunostaining patterns 1 and 2 with disability severity

Immunostaining Pattern	Low disability(mRS 2, 3) N=4	High disability (mRS 4, 5) N=23	P
1	0 (0%)	9 (0%)	0.268
2	4 (62.5%)	14 (100%)	

5.3 Discussion

Glycine receptors identified by highly specific antibodies were widely expressed in the central nervous system with regional differences depending on the GlyR subunit studied. Their distributions were similar to those previously reported in other immunohistochemistry studies of GlyR in the rat and human CNS with some minor discrepancies (Araki et al, 1988; Naas et al, 1991, Baer et al, 2009). The important finding here was the very good co-localisation of the patients´sera binding with the monoclonal antibody to GlyRα1 binding, confirming GlyRα1 as the main antigenic target.

GlyRα1 was strongly expressed in the upper and lower brainstem and the spinal cord with some expression in different regions of the forebrain such as the thalamus, hypothalamus and the colliculus. These findings are in agreement with those obtained using antibody binding (Araki et al, 1988), and those obtained using in situ hybridization with GlyR α1 mRNA (Malosio et al, 1991). In addition, these findings resemble the distribution of the GlyR determined by autoradiographic studies with [^{3}H] strychnine as a ligand (Zarbin et al, 1981) which confirms that the α1 subunit is a component of the adult strychnine-sensitive GlyR (Betz and Becker, 1988). However, minor discrepancies were found in the cerebellum, contrary to the findings of Araki et

al, 1988, since these authors did not find binding in the molecular layer, but there was staining in the deep cerebellar nuclei.

GlyRα1 was found on the surface of both effector neurons and interneurons, which suggest that inhibitory glycinergic networks may be more complicated than initially thought (Harvey and Rigo, 2010). Glycine could be exerting a fine control of the overall motor network activity, regulating both the excitatory and inhibitory outputs of the circuitry. For instance, in the hippocampus, glycine has been shown to act as an agonist of both the inhibitory GlyRs and the excitatory NMDARs, and also to regulate the inhibitory GABAARs (Xu and Gong, 2010). Similar to the complex involvement of GABARs in network activity, where GABAR mediates tonic inhibition through extrasynaptic receptors and phasic inhibition through intrasynaptic receptors in both inhibitory and excitatory cells (Walker and Semyanov, 2008).

The distribution of GlyRα2 and GlyRα3 subunits in the brain tissue, by contrast, was less clear. Previous reports suggested that GlyRα2 is widely expressed in the immature central nervous system with a developmental switch to GlyRα1 as the CNS matures (Becker et al., 1988, Akagi et al., 1991). However, this idea has been challenged lately with recent reports using in situ hybridization, RT-PCR studies, and electrophysiological recording in slices showing the presence of GlyRα2 postnatally (Malosio et al, 1991, Garcia-Alcocer et al, 2008, Chatipakkorn et al, 2002). In this study, GlyRα2 was found mainly in the hippocampus, cerebellum and cerebral cortex, similar to the results obtained by in situ hybridization with GlyRα2 mRNA (Malosio al, 1991), RT-PCR techniques (Garcia-Alcocer et al, 2008), and antibody labelling (Brackmann et al, 2004). Some mismatches were found with the findings of the study of

Malosio et al, 1991; as here GlyRα2 was only expressed intracellularly in the ventral horn spinal cord, and the colliculus, and not in the hypothalamus.

GlyRα3 was found extracellularly expressed in the hippocampus, the granular cell layer of the cerebellum, spinal cord and white matter, again showing concordance with previous reports using in situ hybridization (Malosio et al, 1991), RT-PCR techniques (Guadalupe et al, 2008), and antibody labelling (Harvey et al, 2004). However, GlyRα3 was also widely observed intracellularly in several brain regions such as the cerebral cortex, thalamus, hypothalamus, brainstem and colliculus; whether this finding is relevant or just the product of unspecific binding remains to be proven. The main discordance in the findings here compared to the findings of Malosio et al, 1991 was the expression of GlyRα3 in the spinal cord but this result agreed with the results obtained by Harvey in 2004.

GlyRβ was found mainly in the spinal cord and brainstem with less expression in regions like the cerebellum, hippocampus, thalamus and hypothalamus. These findings agree with the findings obtained by Weltzien et al, 2012, but no expression in the cerebral cortex was found here. In the hippocampus there was only expression in the striatum, and in the granular and Purkinje cell layer of the cerebellum.

The overall distribution of the GlyRβ subunit was similar to the distribution of the GlyRα1 subunit, which has been shown to co-assemble with GlyRβ subunits to form the major type of synaptic GlyRs in the adult CNS (Betz and Laube, 2006; Lynch, 2009). However, GlyRβ subunit was also found in other regions where GlyRα1 is not expressed such as the hippocampus and the cerebellum, which could imply the co-assembly of GlyRβ subunit with GlyRα2 and GlyRα3 subunits that are expressed in these brain regions, as has been shown in the retina (Weltzien et al, 2012). Moreover,

functional inhibitory glycinergic currents have been identified in the cerebellum and hippocampus (Dieudonne, 1995; Song et al, 2006, Kubota et al., 2010; reviewed by Xu and Gong 2010). However, these currents could be secondary to the presence of functional homomeric GlyRs which do not require co-assembly with GlyRβ, such as those found on mossy fibre terminals in the hippocampus (Kubota et al., 2010); further studies are required to elucidate the different types of functional GlyRs in these regions.

GlyT2 expression was found mainly in the midbrain, hindbrain, spinal cord and cerebellum; these results are in agreement with previous findings (Jursky and Nelson, 1995). GlyT1 expression included the midbrain, hindbrain, spinal cord, cerebellum and several areas of the prosencephalon such as the hippocampus, cerebral cortex, thalamus and hypothalamus; these results are in agreement with previous findings (Zafra et al, 1995).

GlyT1 and GlyT2 have been implicated in the termination of glycinergic neurotransmission, which correlates with the high expression levels of GlyT1 in the spinal cord and the brainstem and the high correspondence between the GlyT2 and GlyRα1 immunoreactivity distribution. Interestingly, GlyT2 immunoreactivity was also found in the granular layer of the cerebellum where GlyRα1 subunit is not expressed and possibly suggests the involvement of GlyT2 in terminating glycine neurotransmission involving GlyRα2 and GlyRα3 subunits, since GlyT1 is also present.

On the other hand GlyT1 has a wider expression distribution which includes areas where GlyRα1 subunit and GlyT2 are not expressed; suggesting that in these areas GlyT1 is not involved in glycinergic synaptic transmission. In fact, it is believed that in these regions glycine receptors are located extrasynaptically and may play a role in regulating the firing activity of neurons (Danglot et al, 1994; Song et al, 2006). In

addition, it has been shown that GlyT1 is closely associated with NMDAR and regulates the concentration of glycine, which is required as a co-agonist at NMDAR excitatory synapses (Cubelos et al, 2005, Betz et al, 2006).

Overall, the results obtained in this study agree with previous immunolabelling studies but show some differences with the results of studies that examined the GlyR transcripts. The differences between the GlyR transcripts and the protein levels observed in the different immunolabelling studies could be due to posttranscriptional mechanisms which regulate the translation of GlyR transcripts in different regions of the CNS. For instance, N-glycosylation has been shown to be required for GlyRα1 assembly and transport between the endoplasmic reticulum and the Golgi apparatus (Griffon et al, 1999). Another possibility may be that in some regions the GlyRs are not clustered at the postsynaptic sites remaining diffusely distributed in extrasynaptic regions, making their detection by immunostaining more difficult.

The patients' antibodies showed good co-location with GlyRα1 monoclonal antibody, Immunohistochemistry on brain sections showed that patient sera binds to the surface of brainstem and spinal cord neurons co-localising with monoclonal antibodies to GlyRα1 and neuronal markers, confirming the specificity and likely targets of the pathogenic antibodies. However it was curious that although patient antibody binding disappeared after preadsorption with HEK cells expressing GlyRα2 and α3 subunits, implying cross-reactivity of the IgG with the different α subunits, none of the sera co-localised with the intracellular binding of polyclonal antibodies to GlyRα2 and α3, making it difficult to assess whether they are targets in the hippocampus and the cerebellum where the binding was demonstrated. In addition, despite absence of GlyRα1 in the hippocampus, the possibility of low functional levels cannot be discounted as some of these patients

presented mainly with an encephalopathic/seizures clinical phenotype and other reports have shown a possible association with glycine antibodies and epilepsy (Ekizoglu et al, 2014, Zuliani et al, 2014).

A few patients had antibodies to GlyRα1 and GlyRα3, as shown by antibody binding to neurons and neuropil in the dorsal horns of the spinal cord where nociceptive afferents terminate and may correlate with some of the sensory symptoms found in the patients, such as pain that is not always associated with muscle spasms (Clerinx et al 2011). These symptoms may be associated with reduced control of nociceptive pathways regulated by GlyRα3 (Harvey et al, 2004).

A number of sera also bound to other brain regions, notably the cerebellum, basal ganglia and hippocampus where the monoclonal anti-GlyRα1 did not bind. In four patients this staining was due to coexisting GAD antibodies but in others there could be novel intracellular antigen(s), although antibodies against intracellular antigens are unlikely to be pathogenic.

It was difficult to make any clinical correlation between the CNS regions where the GlyR-Abs bound, the immunostaining pattern and the patients´ clinical presentation or their degree of disability. This could be related to the presence of antibodies to other intracellular antigens in the serum of some patients, the heterogeneity of the antibody penetration among different brain regions, the site of antibody penetration to the brain after blood brain barrier damage, the degree of intrathecal antibody synthesis, and the time elapsed before the beginning of the immunosuppressive therapy.

Nevertheless, all patient´s serum bound to the brainstem and spinal cord, where impairment in glycinergic activity is likely to underlie the predominant clinical

manifestations in these patients. Also, the broader clinical spectrum seen in these patients could be related to the action of GlyR-Abs in other brains regions. For instance, GlyRs have also been shown to have a role in visual and auditory processing (Wässle et al, 2009; Dutertre et al 2012), perhaps explaining the dizziness or deafness in two patients, and possibly involved in the visual disturbance in two who were consider to have demyelinating syndromes (see also McKeon et al 2012).

GlyRs are also expressed in regions known to regulate autonomic function such as the locus coeruleus, nucleus solitarius, and the rostral ventrolateral medulla (Cabot et al., 1992; Rampon et al., 1996; Waldvogel et al., 2010); in these sites a reduction in GlyR control of sympathetic activity by the GlyR-Abs could be responsible for the increased sympathetic tone found in the patients, e.g. tachycardia and urinary retention and, as the rostral ventrolateral medulla is involved in generating the rhythmic respiratory pattern, the respiratory failure observed in some patients (Paton and Ritcher, 1995).

5.4 Conclusions and limitations

GlyRα1 is highly expressed in the spinal cord and hindbrain, with less expression in the midbrain and very little expression in the forebrain. Other subunits are expressed more widely with predominant expression in the forebrain and cerebellum with less expression in the hindbrain and spinal cord.

Patient serum and CSF GlyR-Abs bind in a similar fashion mainly to the spinal cord and brainstem co-localising with monoclonal anti-GlyRα1-Ab which confirms their antigenic target. The dysfunction of the glycinergic pathways in these brain regions may underlie the clinical manifestations in GlyR-Ab patients.

However, many patient sera also bind intracellularly to other brain regions such as the cerebellum and hippocampus where GlyRα1 is not visibly expressed, implying the presence of additional antibodies to GAD or other antigens in these patients, making the relationship between immunostaining findings and clinical presentation complex, as can be observed for other cell surface antibodies.

The functional relevance of some of the immunostaining observed in these study is limited by the epitope against the commercial antibodies are raised and therefore needs to be assessed in the light of further electrophysiological studies.

CHAPTER 6. *In vivo* pathogenic mechanisms of GlyR-Abs

6.1 Introduction

The presence of circulating antibodies against neuronal antigens does not necessarily indicate pathogenicity or autoimmune disease, as self-reactive antibodies can be observed in healthy individuals. However, circumstantial evidence such as clinical improvement with plasma exchange, or maternal to foetal passive transfer of disease, suggests a pathogenic role for the autoantibodies. In order to prove the role of serum autoantibodies in autoimmune diseases, the criteria established by Witebsky in 1957, and revisited in 1993 by Rose and Bona need to be met (Chapter 1). One of the criteria is the passive transfer of the disease into experimental animals.

Passive transfer studies that demonstrate the pathogenic role of the antibodies in peripheral nervous system diseases, such as myasthenia gravis and Lambert-Eaton syndrome, have been successful (Toyka et al., 1975; Lang et al., 1983; Mossman et al 1986). However, similar studies looking at the role of pathogenic antibodies in central nervous system disease have been more difficult to establish, probably because the CNS is protected from circulating antibodies by the blood-brain barrier (BBB). Therefore in order to overcome this difficulty, the blood-brain barrier has to be compromised allowing the antibodies to reach the CNS, or the antibodies can be injected into the cerebrospinal fluid or directly into the brain parenchyma. For blood brain barrier disruption several methods have been used such as systemic injections of

lipopolysaccharides (LPS) (Ichikawa and Ito, 2011) or encephalotogenic T-helper (Th) cells (Sommer et al, 2005).

This chapter describes the results of two experimental designs attempting to transfer PERM into mice, using purified IgG from patients. Systemic injections of IgG in conjunction with LPS injections and icv injections of IgG were both tried. After extensive behavioural and motor tests, the immunohistochemical localisation of the transferred IgG in the CNS tissue of the mice given systemic IgG was studied in detail, in order to see if the IgG had been deposited in those regions known, from Chapter 5, to bind GlyR-Abs.

6.2 Results

IgG was purified from plasmapheresis samples of two patients from the prospective cohort (Carvajal-González et al 2014) who had PERM. The main patient was male, aged 40, with motor symptoms including rigidity, spasms, hyperekplexia, brainstem symptoms (dysphagia, gaze palsy) and respiratory failure and a diagnosis of PERM. Healthy control purified IgG was obtained from pooled plasma of healthy individuals obtained from the blood bank.

The PERM purified IgG showed strong antibody binding to the transfected HEK cells, and the purified control IgG was negative (Fig. 6.1A). The preparation was titrated to determine the endpoint dilution and the purified IgG concentration was determined by western blotting (Fig. 6.1B); PERM patient IgG concentration was 12.3 mg/ml and healthy control IgG concentration was 14.6 mg/ml. The end-point titration value of the

A

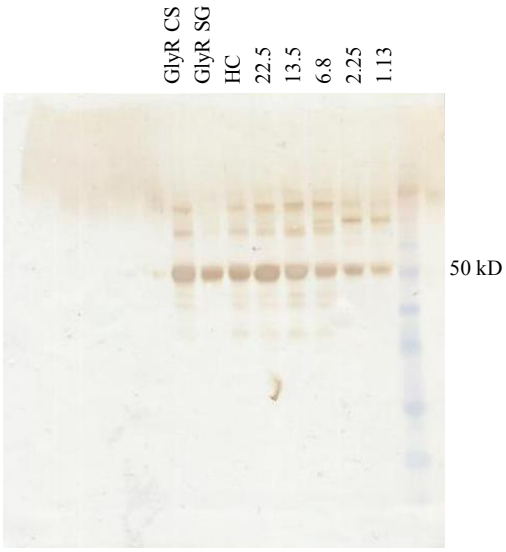

B

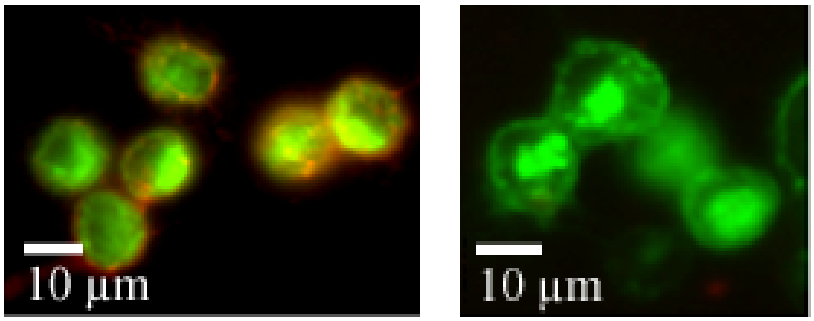

C

Patient	CBA Score (serum)	Endpoint titre	CBA Score (IgG prep.)	Endpoint titre	[ ] mg/ml
GlyR (SG)	1.5	1/60	2.5	1/320	12.3
HC (pooled)	0.5	0	0.75	0	14.6
GlyR (CS)	2.5	1/160	3	1/640	17.9

Fig. 6.1. IgG purification. A. Purified IgG bands from a PERM patient and a healthy control were detected and quantified by western blotting. ***B.*** Purified patient IgG sera bind to HEK 293 cells expressing GlyRα1-EGFP (green); the IgG binding is detected with anti-human IgG (red). Purified control IgG does not bind to the GlyRα1-EGFP expressing cells. ***C.*** Summary of the IgG preparation.

PERM IgG was 1:320, as summarised in figure 6.1C. The second patient's IgG preparation gave similar results.

In order to allow IgG penetration into the CNS, the blood-brain barrier was disrupted using systemic injections of lipopolysaccharides (LPS) (3 mg/kg). However, LPS is known to cause physiological and behavioural alterations (sickness behaviour) secondary to the immune response (Bison et al, 2009), and thus is likely to interfere with the possible behavioural results obtained after systemic IgG injection. The first experiment was designed to study this so that confounding results induced by LPS were avoided.

In the first experiment, the animals were allowed to become familiar with the tasks on two occasions, one day apart, before the start of the tests. The results from these two "base-line" tests were averaged and the test results normalised to them. In order not to interrupt presentation of the results, the statistical analyses used are provided in the Figure legends and in Tables 6.1, 6.2, 6.3 and 6.4.

6.2.1 Intraperitoneal injection of LPS

This was to test the effects of LPS and included three groups of six animals: a) Mice injected with LPS, b) Mice injected with saline, c) Un-injected mice. Motor behaviour, anxiety-like behaviour and weight were measured after the injection of LPS (3 mg/kg) at 2, 6, 24 and 48 hours. Measures of general health and motor performance were taken, to see the extent and duration of effects of LPS, and were analysed using a two-way repeated measures ANOVA (Fig. 6.2).

After injection of LPS the mice showed a clear dip in body temperature compared to either saline or un-injected mice at 2, 6 and 24 hours (Fig 6.2A). Moreover, by 48

hours, the LPS injected mice had lost 13.8% of their initial weight compared with the other two groups that did not differ ($p = 0.0052$; Fig. 6.2B). LPS injected mice also showed reduced number of peripheral crosses compared to baseline in the open field ($p < 0.0001$; Fig. 6.2C), which had reversed by 48h. The narrow beam, designed to measure motor coordination, was also different between the LPS-injected and control-injected mice (Fig. 6.2D), with the LPS injected mice requiring more steps to cross the narrow beam compared to saline injected or un-injected mice at 6 and 24 hours ($p < 0.0001$), with reversal of the effect by 48 hours. Finally, to evaluate anxiety-like behaviour, a dark/light box was used. In this case, both the LPS and saline showed fewer crosses between the two compartments compared to the un-injected mice at 6, 24 and 48 hours ($p < 0.0001$; Fig. 6.2E).

Overall, these results indicated that mice injected with LPS had significant alterations in their physiology and behaviour compared to mice treated with saline or un-injected mice, but that most of these changes had reversed by the end of 48 hours. In addition, even the manipulation of the mice required to give intraperitoneal injections of saline increased their anxiety-like behaviour that was not seen in the un-injected animals.

6.2.2 Intraperitoneal (IP) passive transfer experiments of GlyR-Abs

a) Experiment 1

Based on the results of the pilot study, an experiment evaluating the motor and anxiety-like behaviour 48 hours after the LPS injection was performed. In addition, it was decided to manipulate the un-injected mice to simulate the injection procedure that involved immobilisation and insertion of a syringe needle into the peritoneal cavity. The experiment consisted of 6 animals in each group injected with a) GlyR-IgG + LPS;

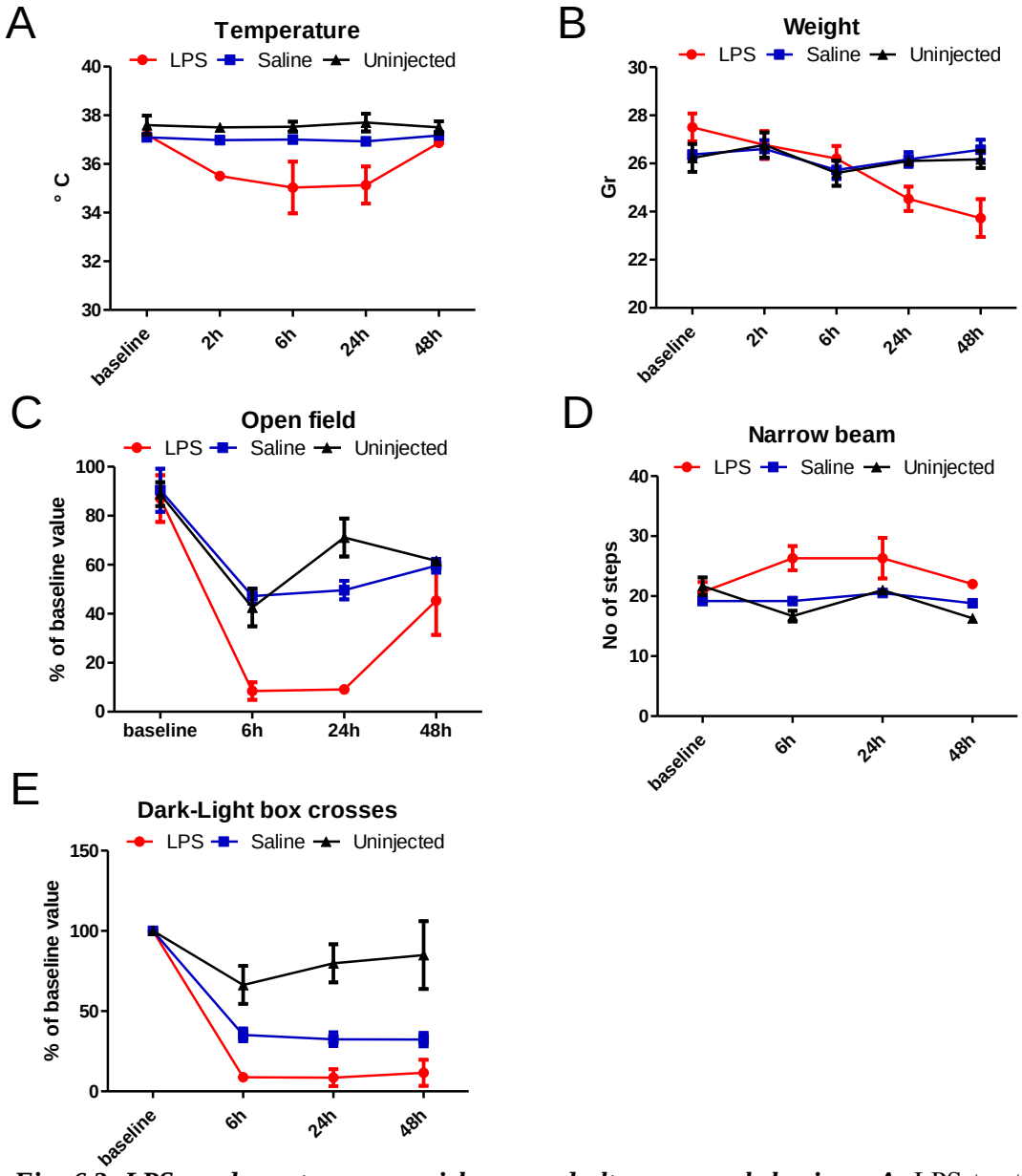

Fig. 6.2. LPS produces temporary sickness and alters mouse behaviour. A. LPS treated mice had a significant decrease in temperature which lasted 48 hrs. No alterations in temperature were found in saline and uninjected mice (Two-way ANOVA F (2, 45) = 36.24; $p < 0.0001$). ***B.*** LPS treated mice had a progressive decrease in weight that was significant after 48 hrs., while saline and uninjected mice did not have ant alterations in weight (Two-way ANOVA F (4, 45) = 34.91; $p = 0.0052$). ***C.*** LPS treated mice had a bigger decrease in the percentage of peripheral crosses compare to decrease in saline and uninjected mice. The effect lasted 48 hrs. ***D.*** LPS treated mice required a significant higher number of steps to cross the narrow beam; the effect lasted 48 hrs. Saline and uninjected mice crossed the narrow beam using the same number of steps (Two-way ANOVA F (2, 36) = 25.14; $p < 0.0001$). ***E.*** LPS and saline treated mice had a significant decrease in the percentage of crosses between the dark and the light compartment in the dark-light box compared to uninjected mice. The effect persisted after 48 hrs. (Two-way ANOVA F (2, 36) = 52.23; $p < 0.0001$).

b) HC IgG + LPS; and c) Saline + LPS and d) Un-injected. The experiments were conducted with each of the mice coded and mice distributed randomly between the cages by Dr Jacobson. All results were tabulated on Excel files and submitted to the supervisor before decoding for the final analyses; data were analysed using a two-way ANOVA repeated measures ANOVA or a one-way ANOVA.

The three groups injected with LPS had lower weights throughout the experiment than the un-injected group ($p < 0.0001$), with no differences in weight between the three LPS treatment groups (Fig. 6.3A). A similar effect of LPS was seen when the open field behaviour was measured, with clear reductions in the number of crosses between squares ($p < 0.0001$; Fig. 6.3B). There was no additional effect in the GlyR-IgG mice that might have indicated a specific effect of the GlyR-Abs. Passive transfer of GlyR-IgG without LPS did not appear to affect the activity in the Dark/Light box or in the closed alleys, which are tests of anxiety (Table 6.2; Fig. 6.4A, B, C, D). These results suggest that passive transfer of GlyR-IgG did not induce anxiety-like behaviour in the mice over and above that related to the LPS.

To see if there was any effect of GlyR-IgG treatment on motor performance, tests of coordination, strength, sensorimotor function and forced walking ability were evaluated. The rotarod is the classic test of forced motor ability. There was a significant difference between the GlyR-Ab + LPS injected mice and the other three groups (Fig 6.5A). This was clear whether the raw data were analysed ($p < 0.0001$; Fig 6.5A top) or the data for each animal was normalised to their pre-injection (baseline) results ($p < 0.0001$; Fig 6.5A bottom). GlyR IgG + LPS injected mice had a significant lower latency to fall, which was observed two days after the first LPS injection and was sustained until four days after the second LPS injection; although the IgG was injected

A

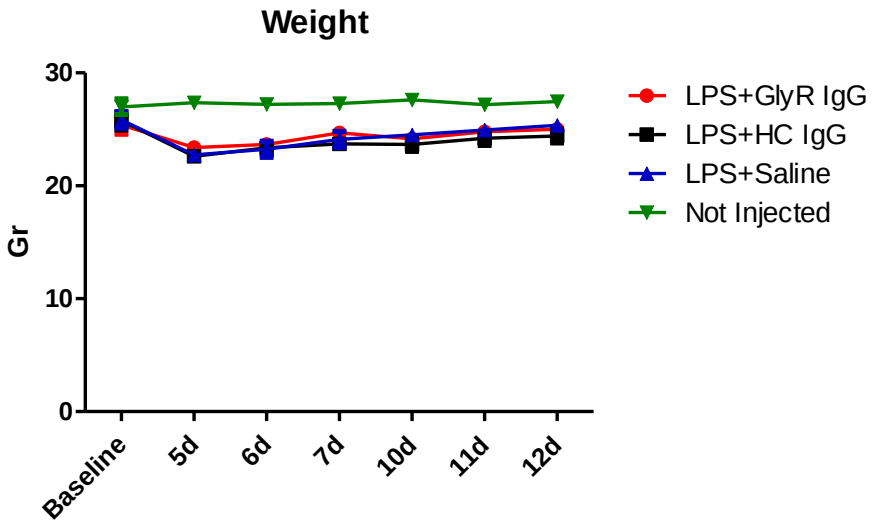

B

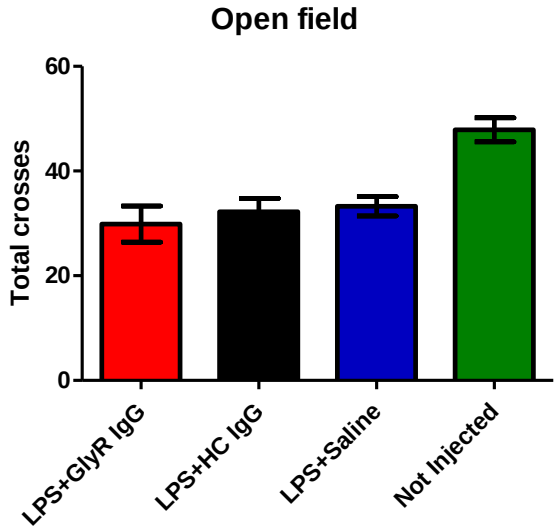

Fig. 6.3. Injected animals were equally affected by LPS. A. LPS treated groups had a significant decrease in weight compared to uninjected mice. The weight loss lasted throughout the whole experiment with a slight recovery towards the end (Two-way ANOVA $F= 6.033$ $df=134$ $p < 0.0001$). ***B.*** Although no significant differences in the number of square entrances were found among LPS treated mice, untreated mice had a significant higher locomotor activity (One-way ANOVA $F= 9.810$ $df=3$ $p < 0.0001$).

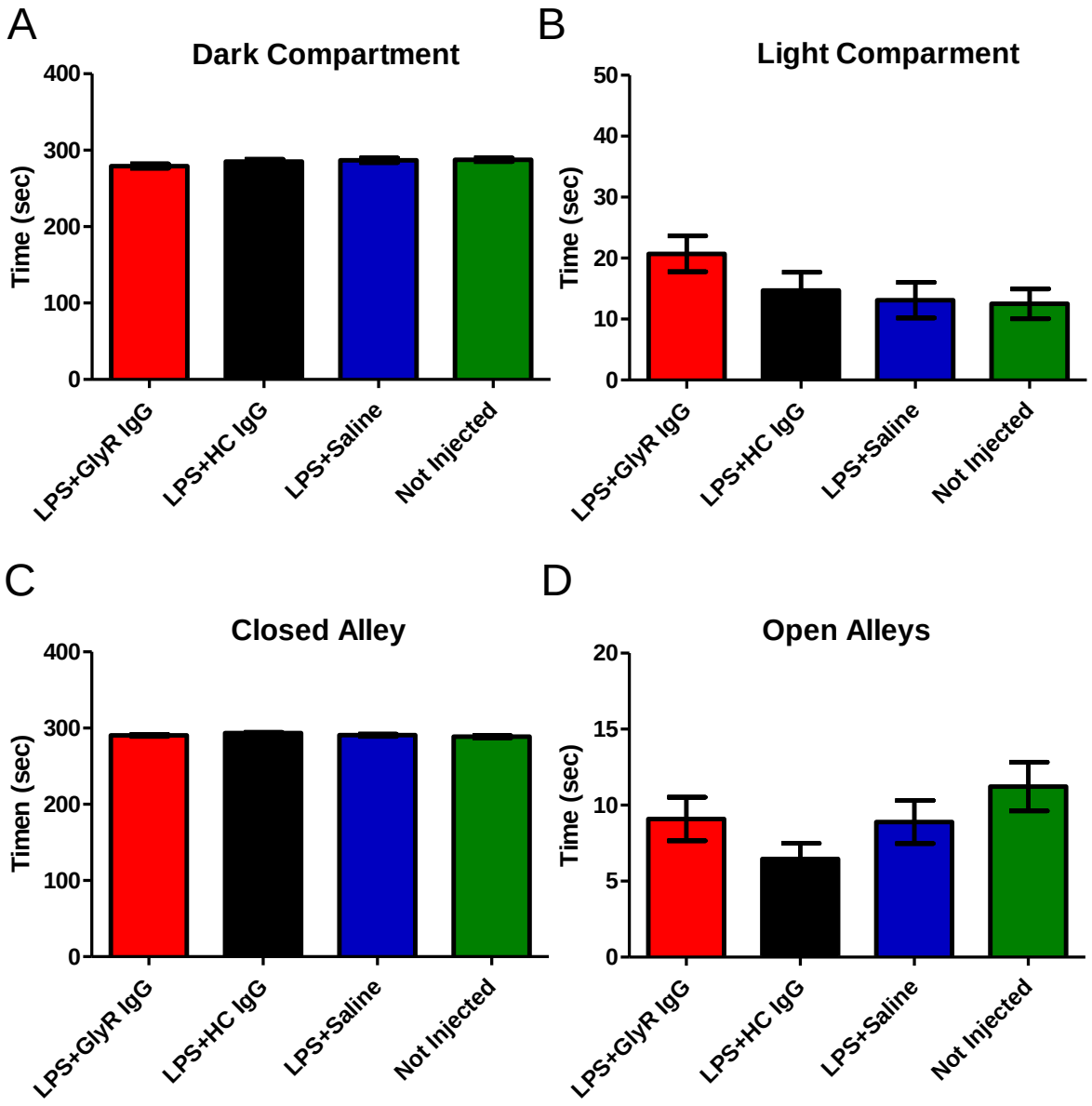

Fig. 6.4. Passive transfer of GlyR-IgG from patient 1 did not induce anxiety-like behaviour in mice. Anxiety-like behaviour was evaluated in the Dark-Light box and in the successive alleys apparatus. ***A.*** No significant differences between the experimental groups were observed in the amount of time spent in either the dark compartment (One-way ANOVA F= 1.837 df=2 p = 0.193) or the light compartment (One-way ANOVA F= 1.7501 df=2 p = 0.189). ***B.*** No significant differences between groups were found in the amount of time spent either the closed (Kruskall Wallis p = 0.1137) or open alleys (Kruskall Wallis p = 0.1416).

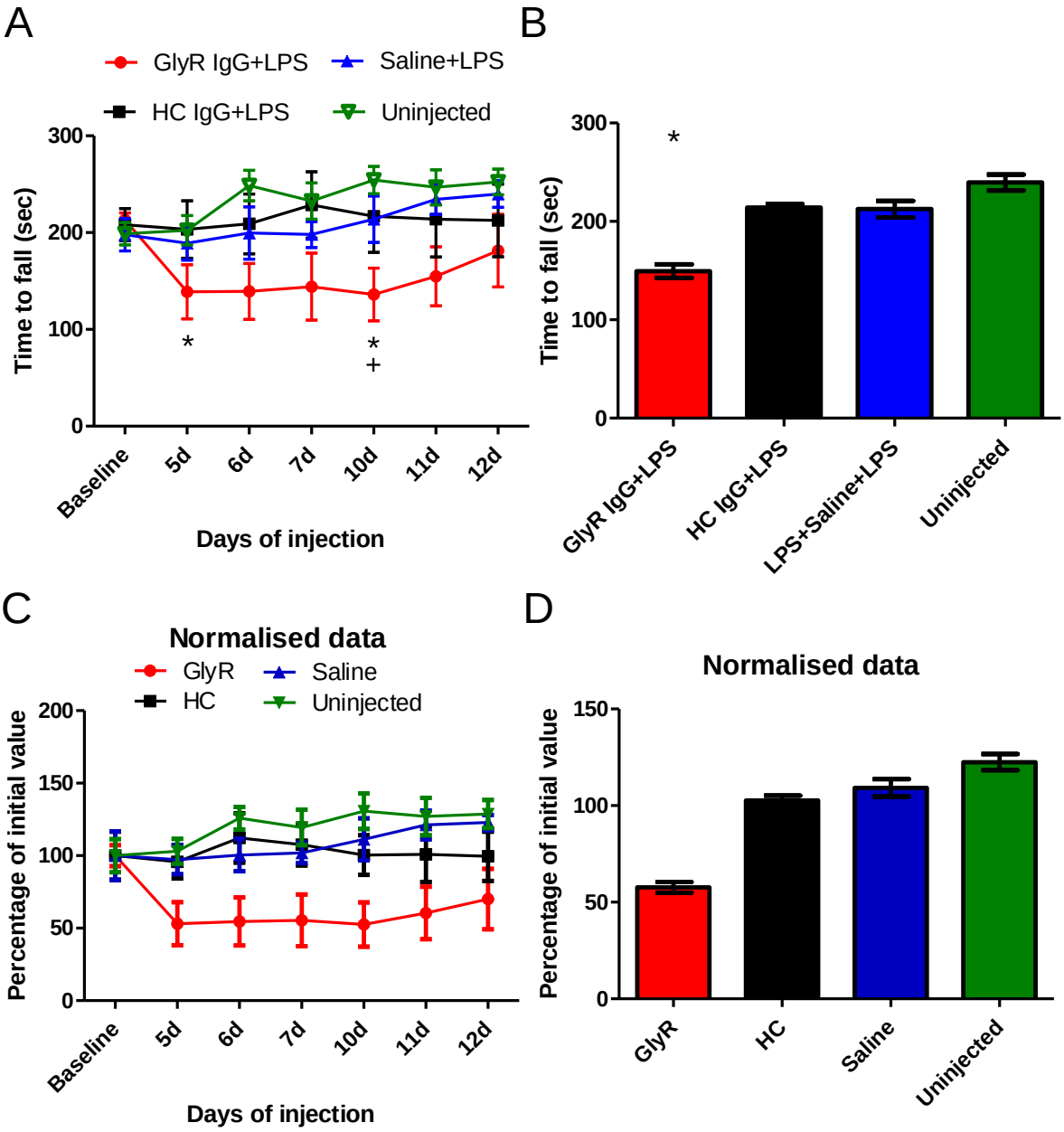

Fig. 6.5. Passive transfer of GlyR-IgG affects forced walking ability. A. Mice treated with GlyR-Ab i.p. showed a significant decrease on the time spent on the rotarod compared to mice treated with HC IgG, saline or untreated mice. The effect was clearly observed at day 10 of injection (+). When compared to baseline the GlyR-IgG treated mice spent significantly less time on the rotarod at days 5 and 10 of injection (*). Mean + SEM from 6 mice is displayed. (Two-way ANOVA F= 17.24 df=162 $p < 0.0001$). ***B***. Summary of the data during the injected days. One-way ANOVA (F=30.0 df=23 $p < 0.0001$). ***C***. With data normalisation the effect is shown clearer. (Two-way ANOVA F= 38.84 df=114 $p < 0.0001$). ***D.*** Sumarised data. (One-way ANOVA F=61.62 df=23 $p < 0.0001$) Not injected mice spent significantly higher time in the rotarod compared than baseline than LPS injected groups.

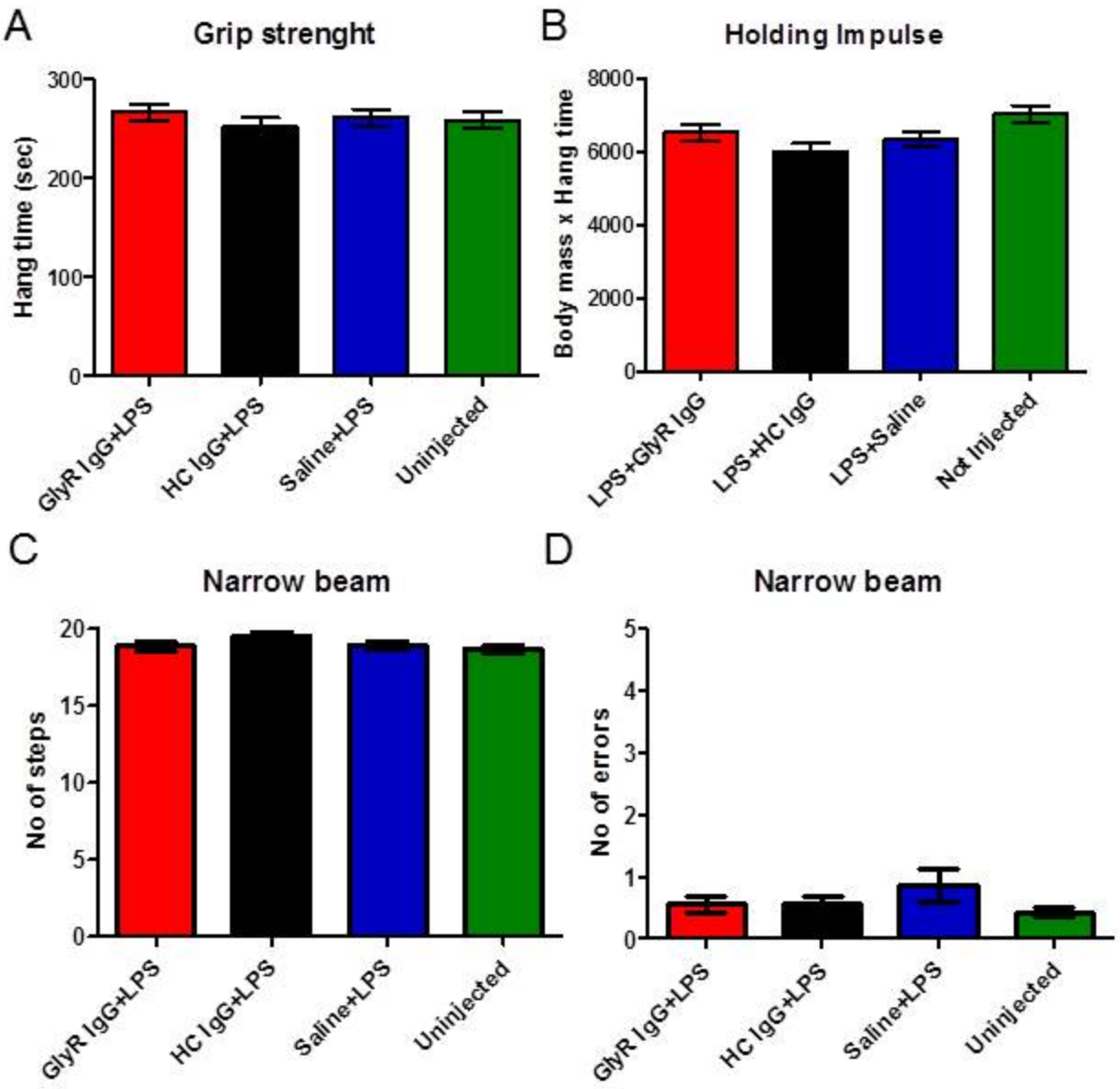

Fig. 6.6. Motor induced dysfunction in GlyR IgG treated mice was not related to alterations in grip strength or to alterations in coordination and balance. Animals were placed hanging in an inverted mesh grid. ***A.*** No significant differences between groups were found in grip strength One-way ANOVA ($F=0.285$ $df=161$ $p = 0.752$). ***B.*** This was evident even when the differences in weight were taking into account One-way ANOVA ($F=1.109$ $df=161$ $p = 0.334$). Animals were placed in an elevated narrow beam, and monitored while crossing it to a safe platform. ***C.*** No significant differences between groups were found in the number of steps needed to cross the narrow beam One-way ANOVA ($F=1.568$ $df=161$ $p = 0.199$). ***D***. No significant differences between groups were found in the number of errors made while crossing the narrow beam Kruskall-Wallis test ($p = 0.617$).

daily, the effects were not significant by 12 days. The average time to fall from the rotarod over the full time period was also different (Figure 6.5B). In this analysis, the un-injected controls performed slightly better ($p < 0.0001$; Fig. 5C) than the other groups.

To see if the impairment in motor performance was due to muscle strength, or coordination, balance or sensorimotor functioning problems, the animals' performance on the inverted mesh grid and on the narrow beam was tested. Grip strength, measured by the time that the mice could hang on an inverted mesh screen, was not different between the groups, nor was the number of steps or errors made in traversing the narrow beam Figure (6.6A, B, C, D).

However, there was a trend towards GlyR IgG + LPS injected animals having lower walking scores compared to un-injected mice ($p = 0.075$; Fig. 6.7A). Also, analysis of the time to turn on the elevated narrow beam before walking showed that all groups improved their performance over the course of the tests, but the GlyR-Ab injected mice improved less than the other groups, only attaining 60% of the baseline time values compared with 40% in the control groups ($p = 0.0024$; Fig. 6.7B). These results suggest that treatment with GlyR IgG can impair the sensorimotor function in mice.

In addition, gait analysis was performed by means of foot prints obtained when animals crossed the wide runway There were no differences between groups in the total time to cross the wide runway or the total number of steps required (Table 6.2; Fig. 6.8A, B). The total number of errors made crossing was also not different between the groups (Table 6.2; Fig. 6.8C).

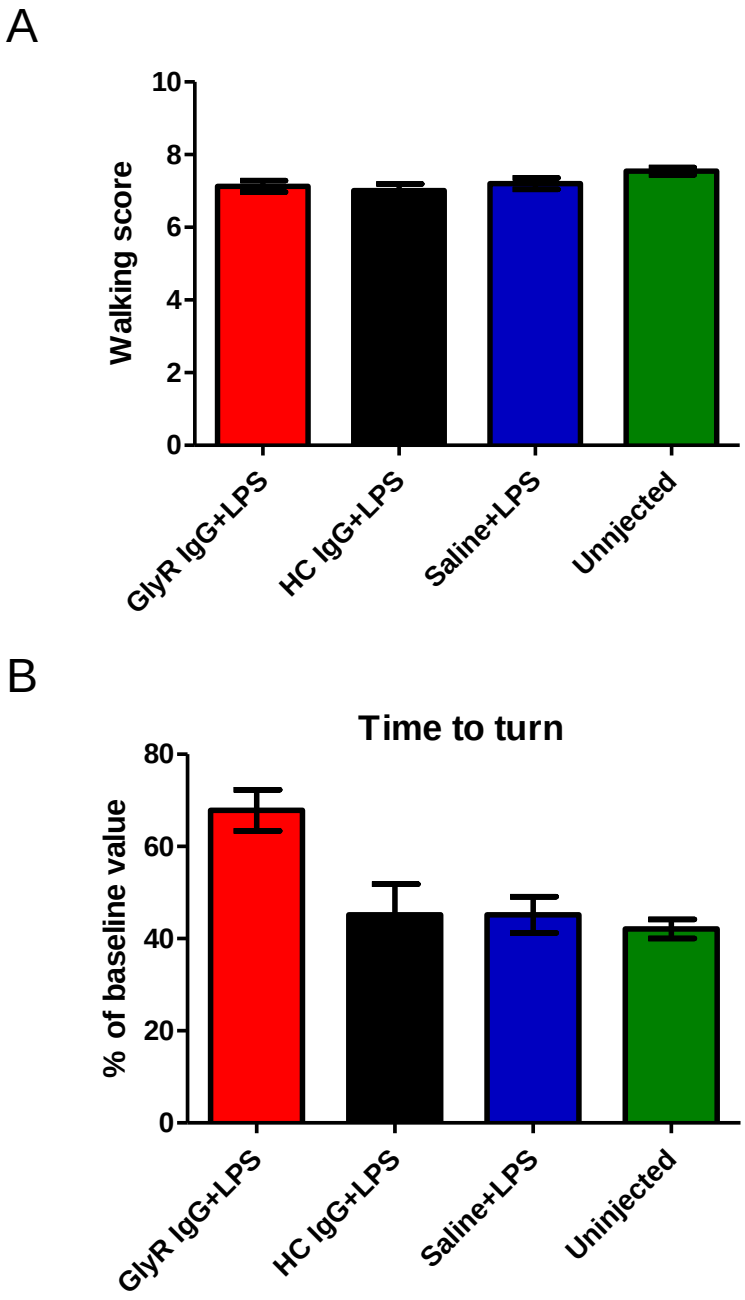

Fig. 6.7. Passive transfer of GlyR-IgG has a subtle effect on sensorimotor function on narrow beam. Animals were placed in an elevated narrow beam, and monitored while crossing it to a safe platform. ***A.*** No significant differences between groups were found in the walking score while crossing the narrow beam One-way ANOVA ($F=2.345$ $df=161$ $p = 0.075$). ***B***. GlyR-IgG treated mice spent significantly more time turning into the right direction in the narrow beam One-way ANOVA ($F=6.791$ $df=23$ $p = 0.0024$).

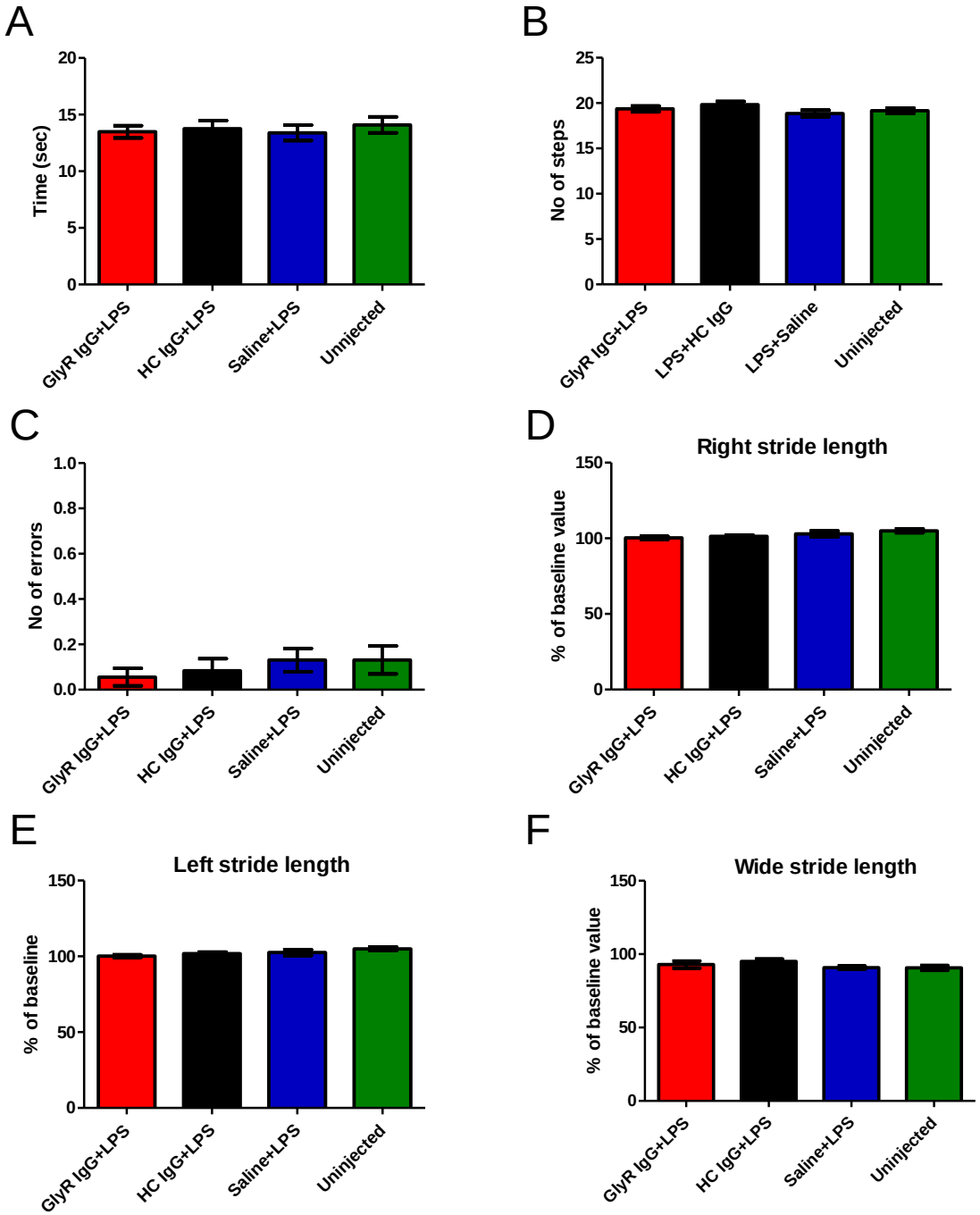

Fig. 6.8. No alterations in gait on mice treated with GlyR IgG were found in the wide runaway. Animals were placed in an elevated wide runaway and monitored while crossing it to a safe platform. No significant differences between groups were in time to cross ***(A)*** One-way ANOVA ($F=0.219$ $df=161$ $p = 0.882$), number of steps need to cross ***(B)*** One-way ANOVA ($F=1.506$ $df=161$ $p = 0.215$), or number of errors made ***(C)*** while crossing Kruskall-Wallis ($p = 0.543$). No significant differences between groups were found in stride length (RSL: Right ***(D)*** One-way ANOVA ($F=2.283$ $df=161$ $p = 0.110$), LSL: Left ***(E)*** One-way ANOVA ($F=2.290$ $df=161$ $p = 0.109$), WSL: Wide ***(F)*** One-way ANOVA ($F=1.359$ $df=161$ $p = 0.284$).

Other parameters that were analysed included the right stride length, left stride length, and wide stride length. The analyses did not show any differences between the groups in these parameters (Table 6.2; Fig. 6.8D, E, F). These results suggest that there were no gait alterations in the animals treated with GlyR IgG.

b) Experiment 2

To try to replicate the results, the same experiment was repeated using a purified IgG from a different patient with a different purified pool of HC IgG. For this experiment, the un-injected group was omitted and the successive alleys test was not performed, as this had been uninformative in Experiment 1. The rest of the experimental design was the same as in the previous experiment. However, the experiment had to be stopped at day 10 as there were some mouse deaths after the second LPS injection. This was found, on decoding, to be only in the control IgG injected mice, and was thought to be due to serum sickness as a result of using a pool of normal fresh sera for the IgG preparation which may have contained immune complexes. Only the behavioural analysis after the first LPS injection could be assessed.

Again all groups showed a significant decrease in weight over time, of between 14 and 16%. There were no differences between groups (Table 6.3; Fig. 6.9A) in the open field though these were more variable compared to Experiment 1, possibly related to differences in the behaviour of the new batch of animals or differences in the effect of the new LPS batch. Grip strength analysis showed that HC-IgG injected mice fell faster compared to the other two groups ($p = 0.0398$; Fig. 6.9C) and analysis of the dark-light box parameters showed that HC-IgG injected mice spent significantly more time in the dark box ($p = 0.0003$; Fig. 6.9D). These results confirm that HC IgG injected mice

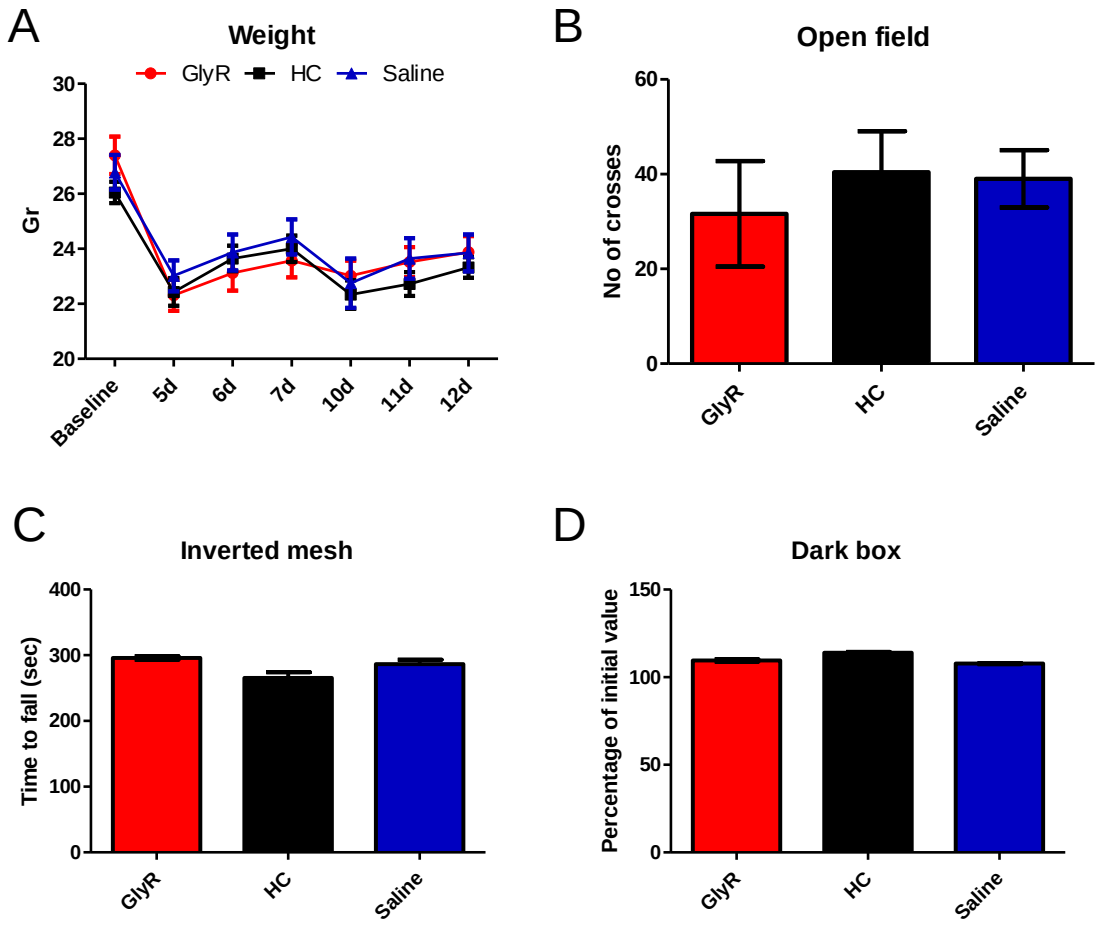

Fig. 6.9. HC-IgG injected mice displayed a more accentuated sickness behaviour not related to LPS injection. A. No significant differences in loss weight among LPS treated groups was observed. (Two-way ANOVA F= 1.398 df=126 p = 0.251). ***B.*** No significant differences in the number of square entrances were found among LPS treated mice (One-way ANOVA F= 0.287 df=11 p = 0.757). ***C.*** HC-IgG treated mice hung less time in the inverted mesh grid compared to GlyR-IgG treated mice or saline (One-way ANOVA F= 5.783 df=8 p = 0.0398). ***D.*** HC-IgG treated mice spent significantly more time in the dark box compared to GlyR-IgG treated mice or saline (One-way ANOVA F= 42.42 df=8 p = 0.0003).

displayed a slightly altered behaviour not related to the LPS injections, but most likely due to serum sickness.

The behavioural analyses showed no differences between the GlyR IgG treated group and the HC IgG or saline treated groups in most of the tests, including the rotarod (Fig. 6.10A, B), except for a significant effect in the number of steps needed to cross the narrow beam ($p = 0.045$; Fig. 6.11A, B). These results indicated that the passive transfer of GlyR IgG may affect coordination in mice, but the lack of a rotarod effect was disappointing.

The analysis of the other narrow beam parameters (Fig. 6.12) or the wide runway parameters did not show any significant differences between groups (Fig. 6.13).

6.2.2.1 IgG quantification

Sera taken before perfusion of the mice were tested for human GlyR-Ab using the cell-based assay with the serum diluted 1:10. Only a score of 1 was observed in the GlyR-IgG treated mice from the first experiment (Fig. 6.14A, F) with no binding in the HC-IgG or in the other three groups (Fig. 6.14B, C, D). When a secondary anti-mouse IgG was used instead of the anti-human IgG, no binding was found as expected (Fig. 6.14E).

To measure quantitatively the IgG content of the sera, the IgG concentration was determined by western blotting (Fig. 6.15A) on bleeds during the course of the experiment. At day 7, the human IgG levels in the GlyR-IgG and HC IgG treated mice were between 0 and 5 mgs/ml and day 14 between 3 and 8 mgs/ml. (Fig. 6.15B). These levels of human IgG in the mouse sera were achieved by daily intraperitoneal injections of 6.2 mg/ml of IgG (73.8 mg in total. The injected material with a titre of 320 contained 12.5 mgs/ml of total IgG; whereas in the mouse sera a titre of only 20 (score

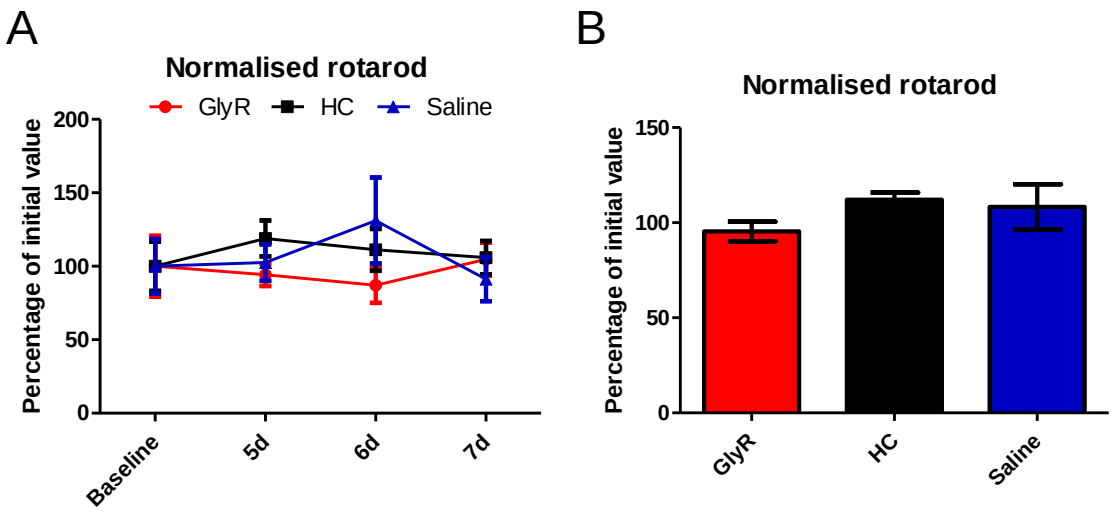

Fig. 6.10. No replication of the effects on forced walking ability was observed in GlyR-IgG treated mice with serum from patient 2. A. No significant differences between groups were observed in the time spent on the rotarod. ***B***. Summary of all data during the injected days. One-way ANOVA (F=1.258 df=11 p = 0.350).

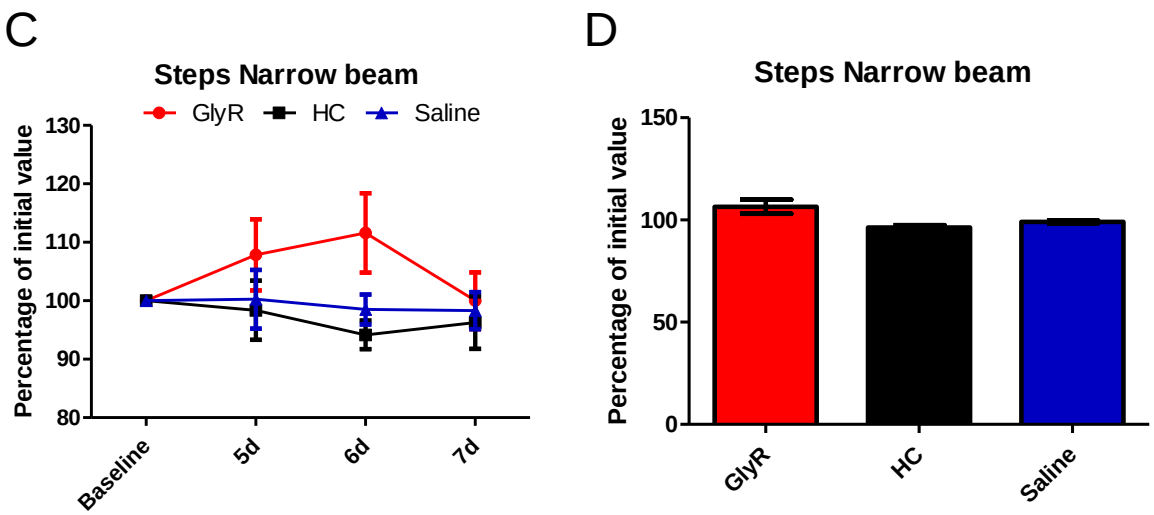

Fig. 6.11. Passive transfer of GlyR-IgG from patient 2 affects coordination. Animals were placed in an elevated narrow beam, and monitored while crossing it to a safe platform. ***A.*** Mice treated with GlyR-Ab i.p showed an increase in the number of steps needed to cross the narrow beam compared to mice treated with HC IgG or saline. The effect was clearly observed at day 6 of injection (*). Mean + SEM from 6 mice is displayed. Two-way ANOVA (F= 3.28 df=54 p = 0.045)**.** ***B***. Summary of the data during the injected days. One-way ANOVA (F=6.206 df=8 p = 0.035).

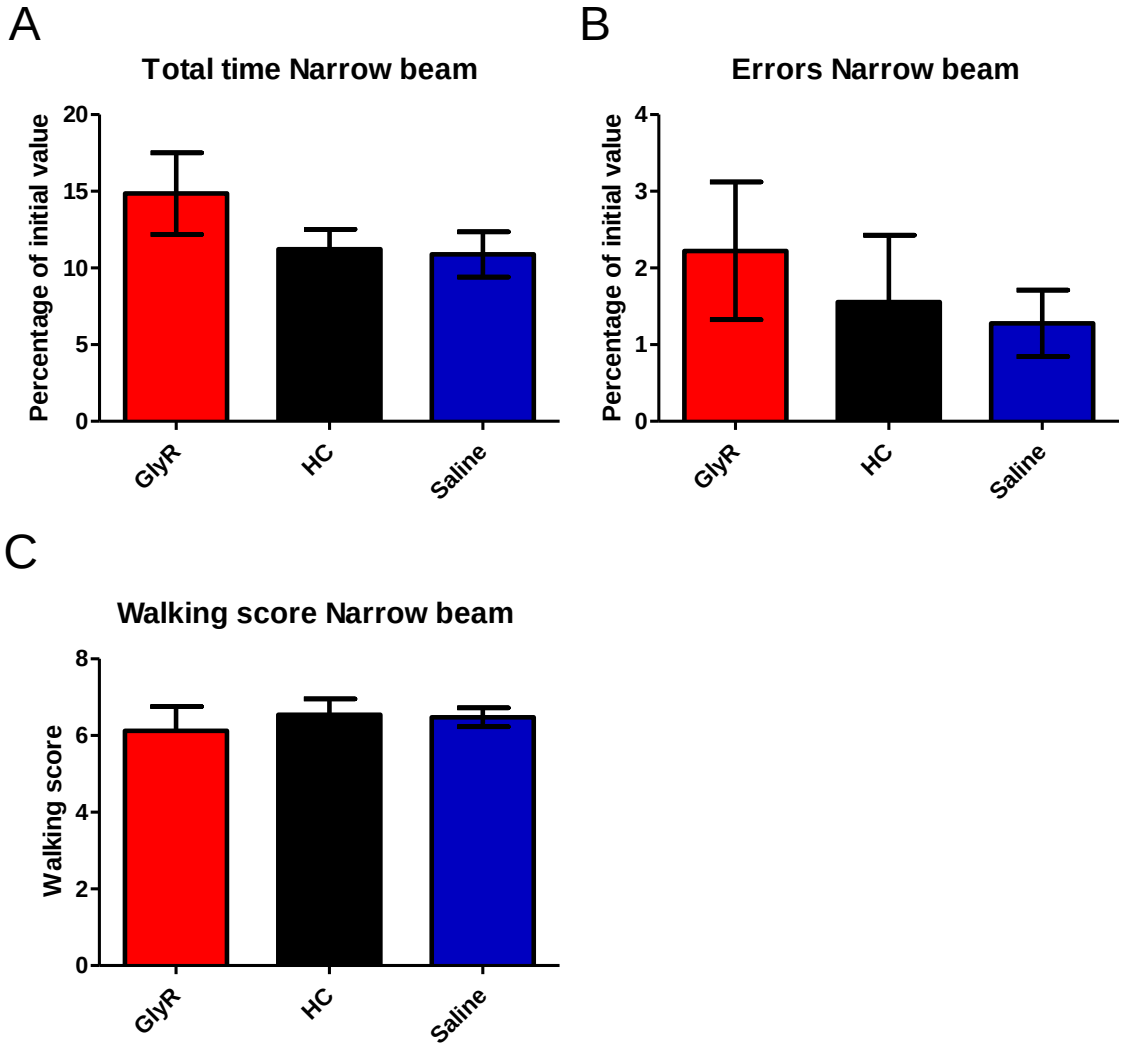

Fig. 6.12. No major alterations in balance or sensorimotor function were found in mice treated with GlyR-IgG. Animals were placed in an elevated narrow beam, and monitored while crossing it to a safe platform. ***A.*** No significant differences between groups were found in the time to cross the narrow beam (One-way ANOVA F=0.402 df=8 p = 0.686). ***B***. No significant differences between groups were found in the number of errors made while crossing the narrow beam (One-way ANOVA F=1.396 df=8 p = 0.309). ***C***. No significant differences between groups were found in the walking score (One-way ANOVA F=0.609 df=8 p = 0.574).

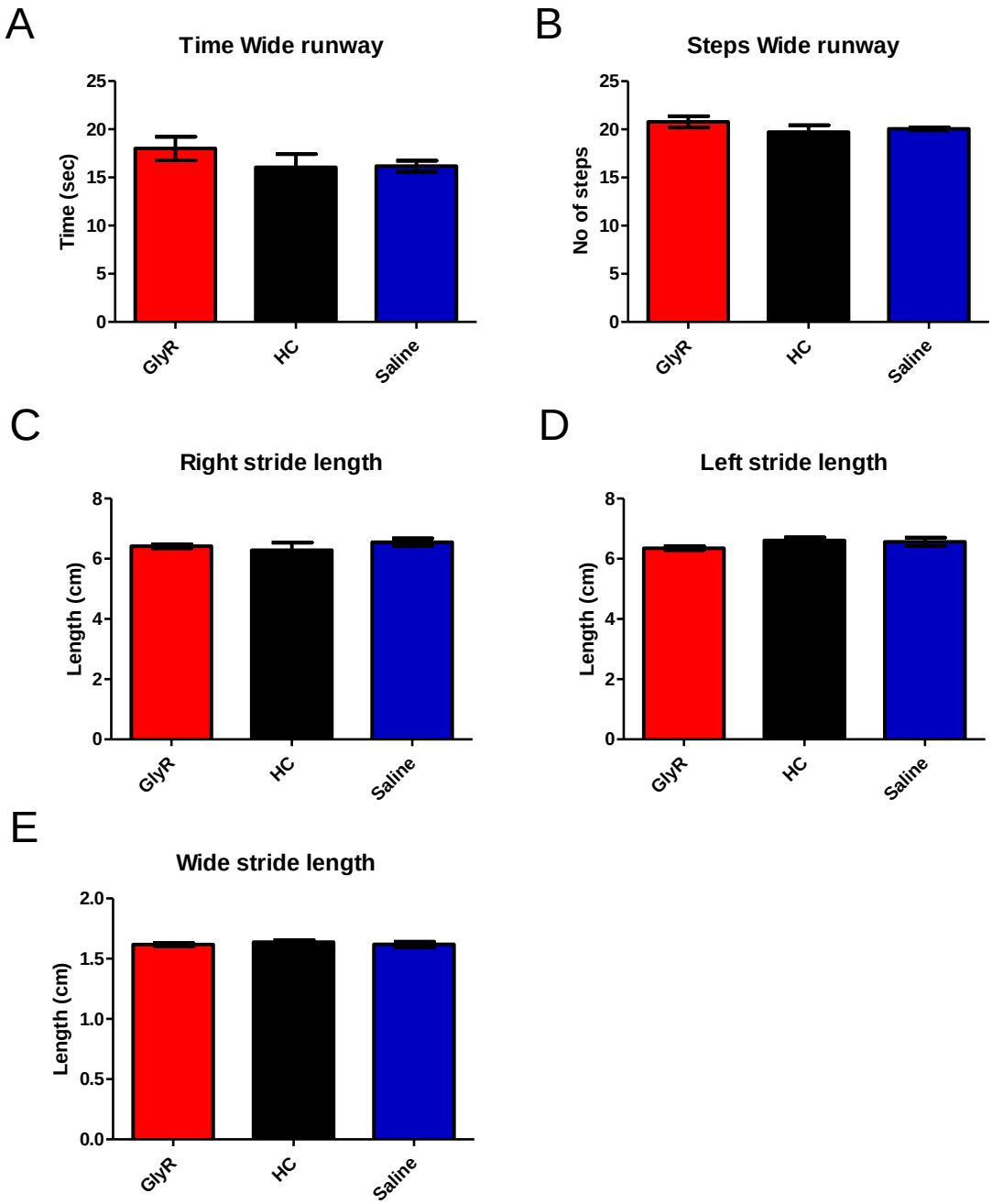

Fig. 6.13. No alterations in gait on mice treated with GlyR IgG were found in the wide runaway. Animals were placed in an elevated wide runaway and monitored while crossing it to a safe platform. No significant differences between groups were in time to cross ***(A)*** One-way ANOVA ($F=0.434$ $df=8$ $p = 0.962$), number of steps need to cross ***(B)*** One-way ANOVA ($F=1.004$ $df=8$ $p = 0.421$). No significant differences between groups were found in stride length (RSL: Right ***(C)*** One-way ANOVA ($F=0.641$ $df=8$ $p = 0.559$), LSL: Left ***(D)*** One-way ANOVA ($F=1.704$ $df=8$ $p = 0.259$), , WSL: Wide ***(E)*** One-way ANOVA ($F=0.435$ $df=8$ $p = 0.666$).

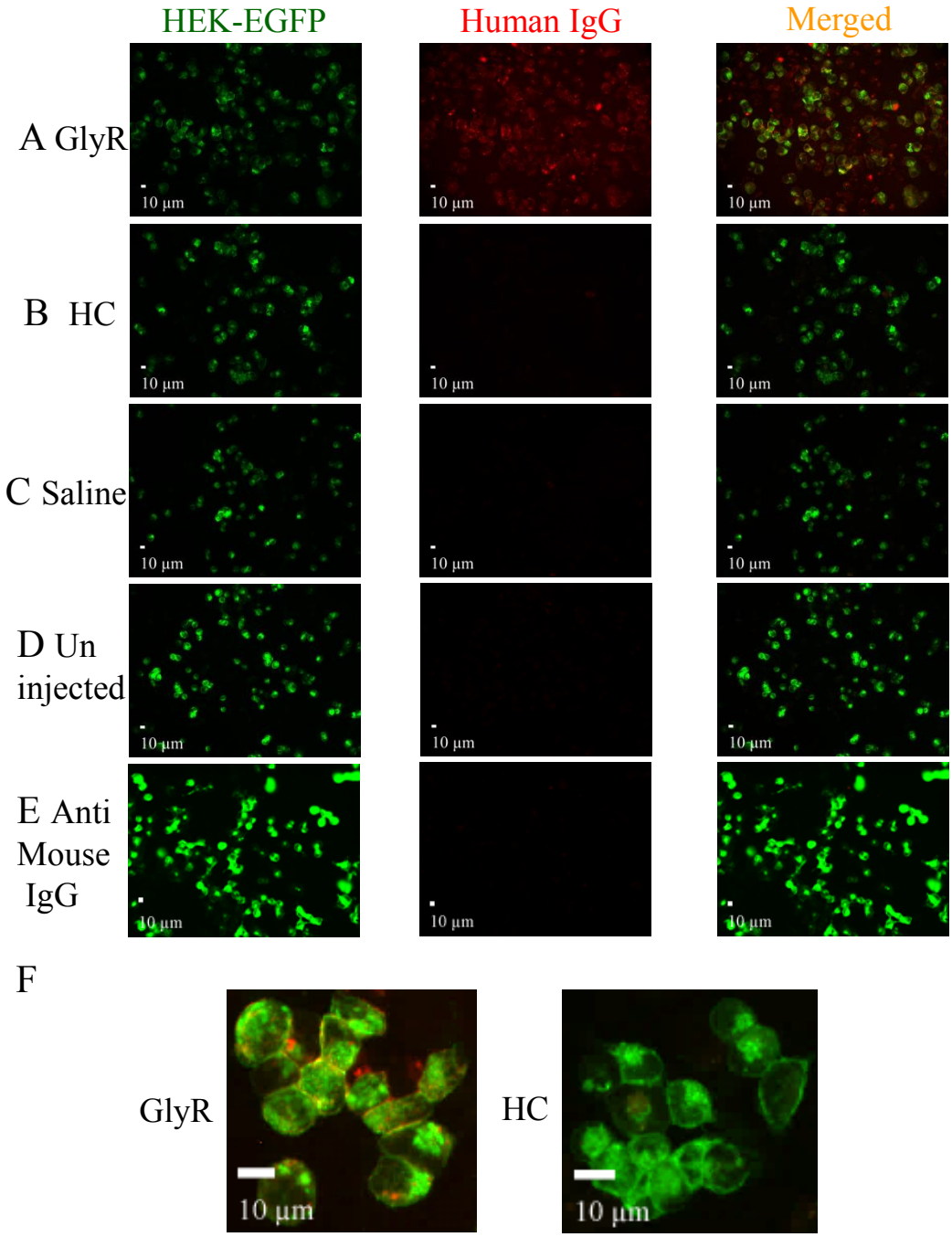

Fig. 6.14. GlyR Abs were present in mice serum after passive transfer. CBAs were performed at 1:10 dilution. ***A.*** Sera from GlyR-IgG treated mice bind to HEK 293 cells expressing GlyRα1-EGFP (green); the IgG binding is detected with anti-human IgG (red). Sera from HC-IgG treated mice ***(B)***, saline injected mice ***(C)*** or not injected mice ***(D)*** do not bind to the GlyRα1-EGFP expressing cells***. E.*** When the sera from GlyR-IgG treated mice was tested with a anti-mouse secondary antibody no antibody binding was detected. ***F.*** Higher magnification images of CBAs incubated with GlyR-IgG and HC-IgG.

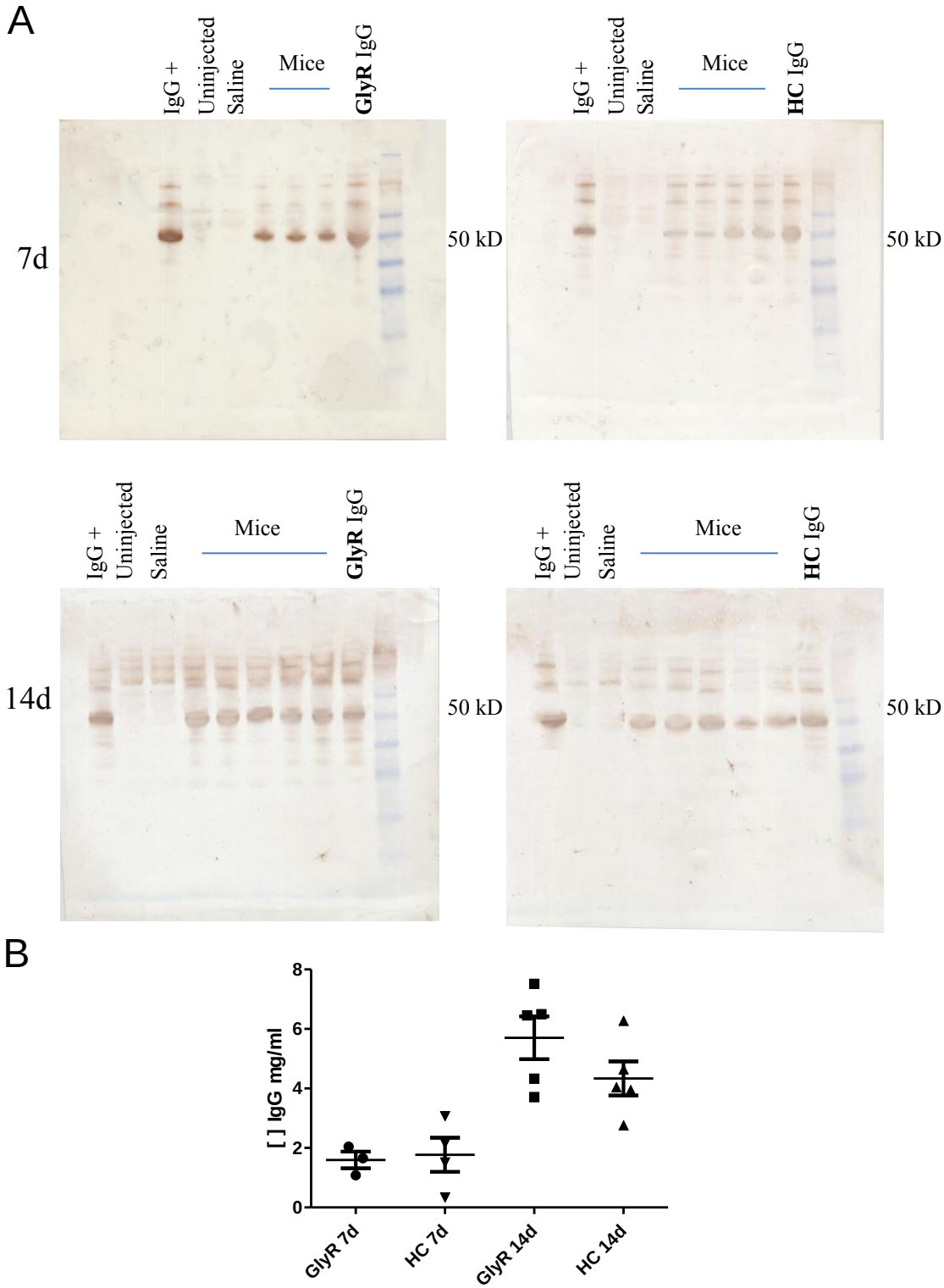

Fig. 6.15. IgG quantification in mice sera after passive transfer. Sera from GlyR-IgG (left) and HC-IgG (right) treated mice were taken at day 7 (upper panel) and 14 (lower panel). ***A.*** IgG bands were detected and quantified by western blotting. ***B.*** No significant differences in the transferred human IgG between GlyR-IgG and HC-IgG treated mice groups at days 7 or 14 were found after comparison with two sided Students t-test ($t=0.2427$, $df=5$; $p = 0.8179$); ($t=1.486$, $df=8$; $p = 0.1755$).

1 at 1:20) was associated with 5.7 mg/ml at termination. These results confirm that human IgG was effectively transferred into both groups of mice but the GlyR-Ab levels in the GlyR-Ab injected mice were lower than expected.

6.2.2.2 Immunohistochemistry

In order to determine if transferred IgG can be found in the CNS tissue of mice, IgG deposits were examined in tissue from one animal of the first experiment, using a highly cross-absorbed anti-human IgG monoclonal antibody. In order to improve the staining the following measures were used: a) highly cross-adsorbed antibodies were used to reduce background; b) overnight incubation at 4°C; c) fresh frozen tissue was fixed with formaldehyde 3% for 5 minutes.

IgG deposits were found in many brain regions which included the brainstem (midbrain, pons and medulla oblongata), the spinal cord (ventral and dorsal horns), the hippocampus (CA regions and dentate gyrus) and the cerebellum (white matter, granular and molecular layer) in both the GlyR IgG treated mice and the HC IgG treated mice. No IgG deposits were found in the CNS tissue of saline treated and un-injected groups (Fig. 6.16A,B,C,D).

It was difficult to assess differences in the IgG distribution between the GlyR IgG treated and the HC IgG treated mice groups, as much of the IgG had a capillary distribution and was present in both groups, as expected. However, in the GlyR IgG CNS tissue it was possible to observe in addition a more diffuse staining pattern. Therefore, in order to discriminate between the intravascular IgG and the IgG deposited in the tissue, double immunolabelling studies with a monoclonal antibody to Von-Willebrand factor was used in conjunction with the anti-human IgG monoclonal

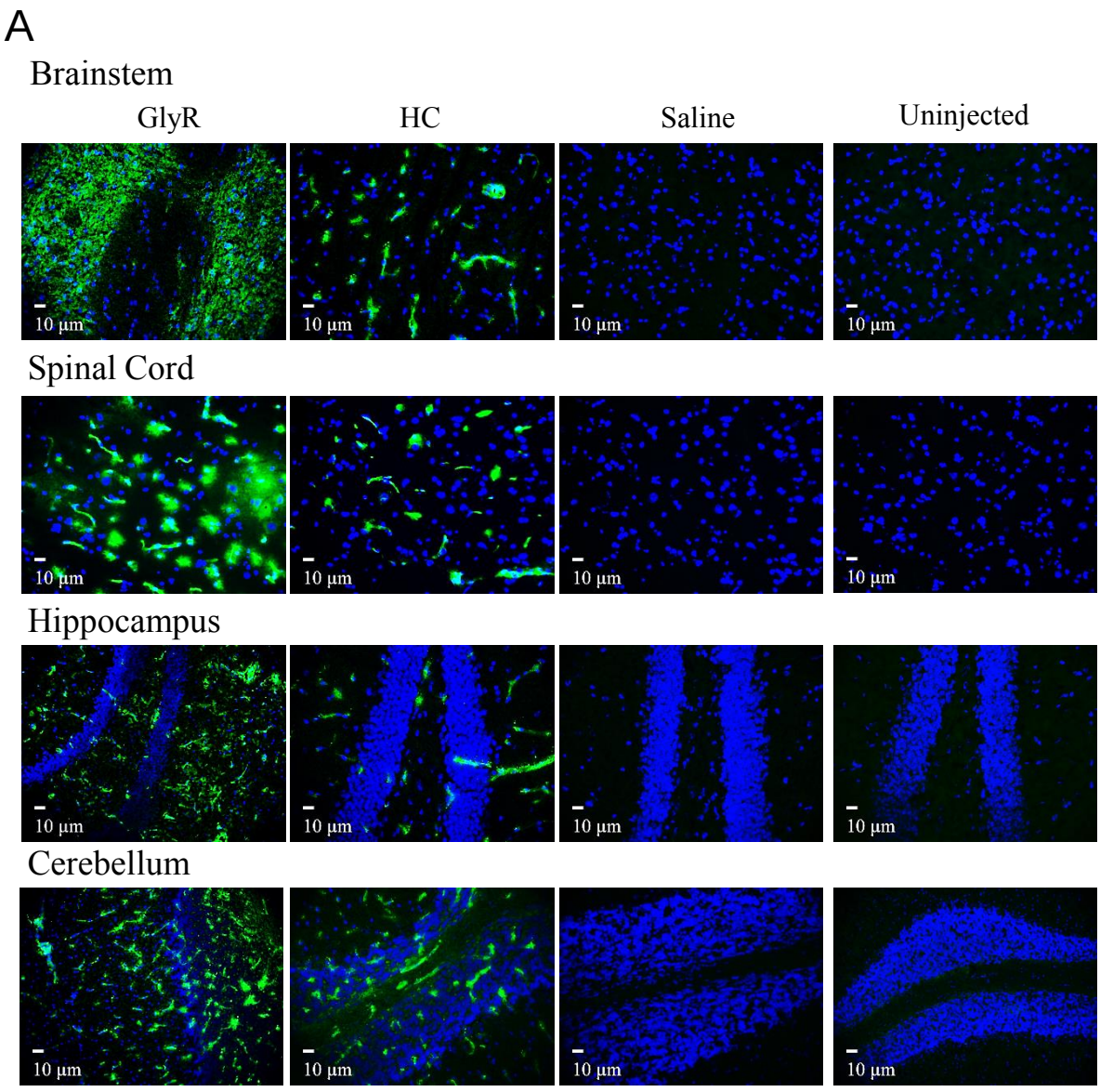

Fig. 6.16. IgG was transferred to mice and deposited in several brain regions. A. Human IgG is observed in the brainstem, the spinal cord, the hippocampus and the cerebellum of mice injected with purified GlyR IgG and HC IgG. The staining pattern of the human IgG resembles that of the capillaries, with some diffuse staining mainly in the GlyR IgG injected mice. No human IgG is detected in those areas when the mice were injected with saline or when they were not injected.

antibody. IgG was observed in the brainstem at the pontine caudal reticular nuclei (PnC), the ventral horns of the spinal cord, the hippocampus at the dentate gyrus and the cerebellum at the molecular, purkinje, granular cell layers and white matter (Fig. 6.17, 18, 19, 20).

Double labelling of CNS sections incubated with Von-Willebrand monoclonal antibody (red), and anti-human IgG monoclonal antibody (green), demonstrated binding in the PnC of the brainstem and in the ventral horns of the spinal cord, regions with a high level of GlyR expression. The staining showed linear patches of human IgG co-localising with the Von-Willebrand immuno-reactivity in both HC and GlyR-IgG injected mice, but there was also diffuse IgG reactivity without any co-localisation with the Von-Willebrand immuno-reactivity in the GlyR IgG treated mice (Fig. 6.17A, 18A). Interestingly in the spinal cord the IgG staining was sometimes in cytoplasmic distribution, around the nuclei (Fig. 6.18A). In the HC IgG treated mice, the human IgG had a similar linear distribution co-localising with the Von-Willebrand immuno-reactivity without any diffuse IgG reactivity, except for small clusters of human IgG observed surrounding some of the vessels (Fig. 6.17B, 18B). In the saline and the un-injected groups, only the Von-Willebrand reactivity was observed (Fig. 6.17C, 17D, 18C, 18D).

In order to see if the transferred human IgG also deposited in other brain regions with less GlyR expression, the co-localisation studies were also examined in the hippocampus, the cerebellum and the caudate. In the cerebellum and caudate of GlyR IgG treated mice the anti-human IgG immuno-reactivity was observed not only inside the vessels co-localising with Von-Willebrand immuno-reactivity but also in the tissue without any co-localisation (Fig. 6.19A, 20A). The HC IgG treated group only had anti-

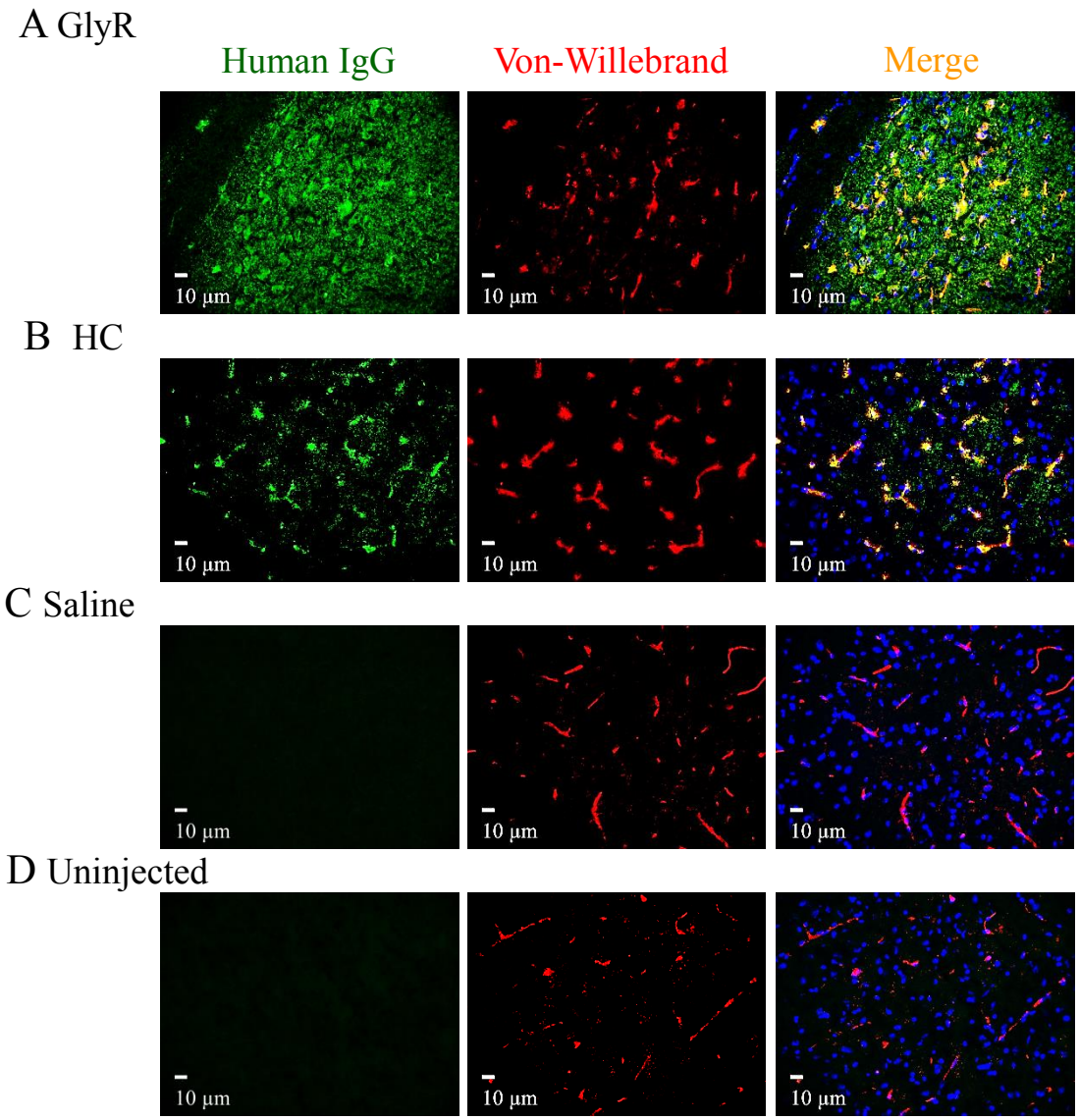

Fig. 6.17. IgG deposits were found in brain regions involved in motor control . Double labelled photographs were taken at 40x magnification at the brainstem in the PnC. ***A.*** In GlyR-IgG treated animals human IgG (green) is located inside the vessels colocalising with Von-Willebrand factor antibody (red) and also in the tissue without any colocalisation. ***B.*** In healthy control treated animals the human IgG (green) is located only in the vessels. ***C.*** In saline treated animals and untreated animals ***(D)***, human IgG deposits are not detectable. nuclei are stained with DAPI (blue).

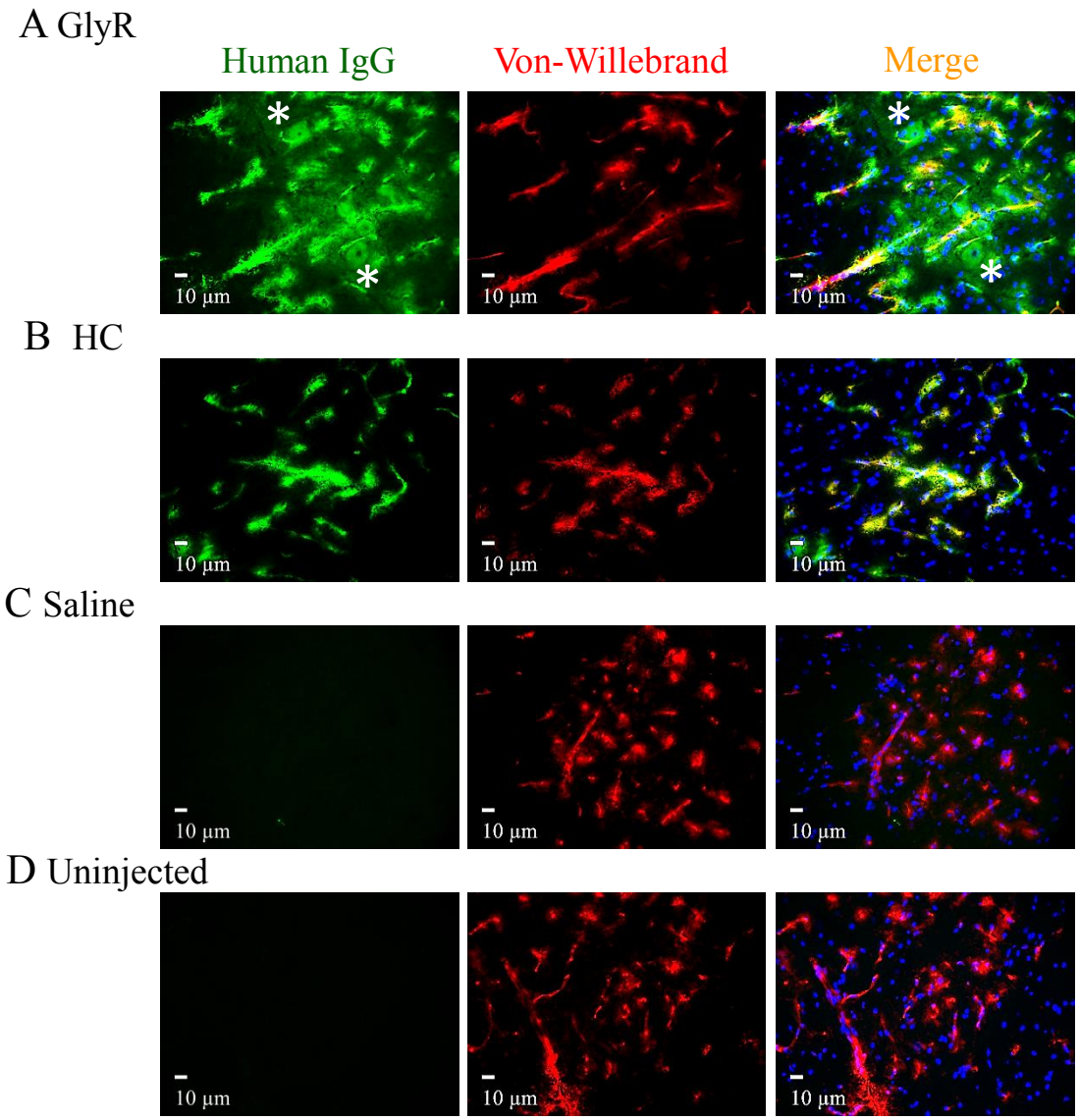

Fig. 6.18. IgG deposits were found in brain regions involved in motor control . Double labelled photographs were taken at 40x magnification at the spinal cord in the ventral horns. ***A.*** In GlyR-IgG treated animals human IgG (green) is located inside the vessels colocalising with Von-Willebrand factor antibody (red) and also in the tissue without any colocalisation; possible cellular cytoplasms are marked with asterisks. ***B.*** In healthy control treated animals the human IgG (green) is located only in the vessels. ***C.*** In saline treated animals and untreated animals ***(D)***, human IgG deposits are not detectable. nuclei are stained with DAPI (blue).

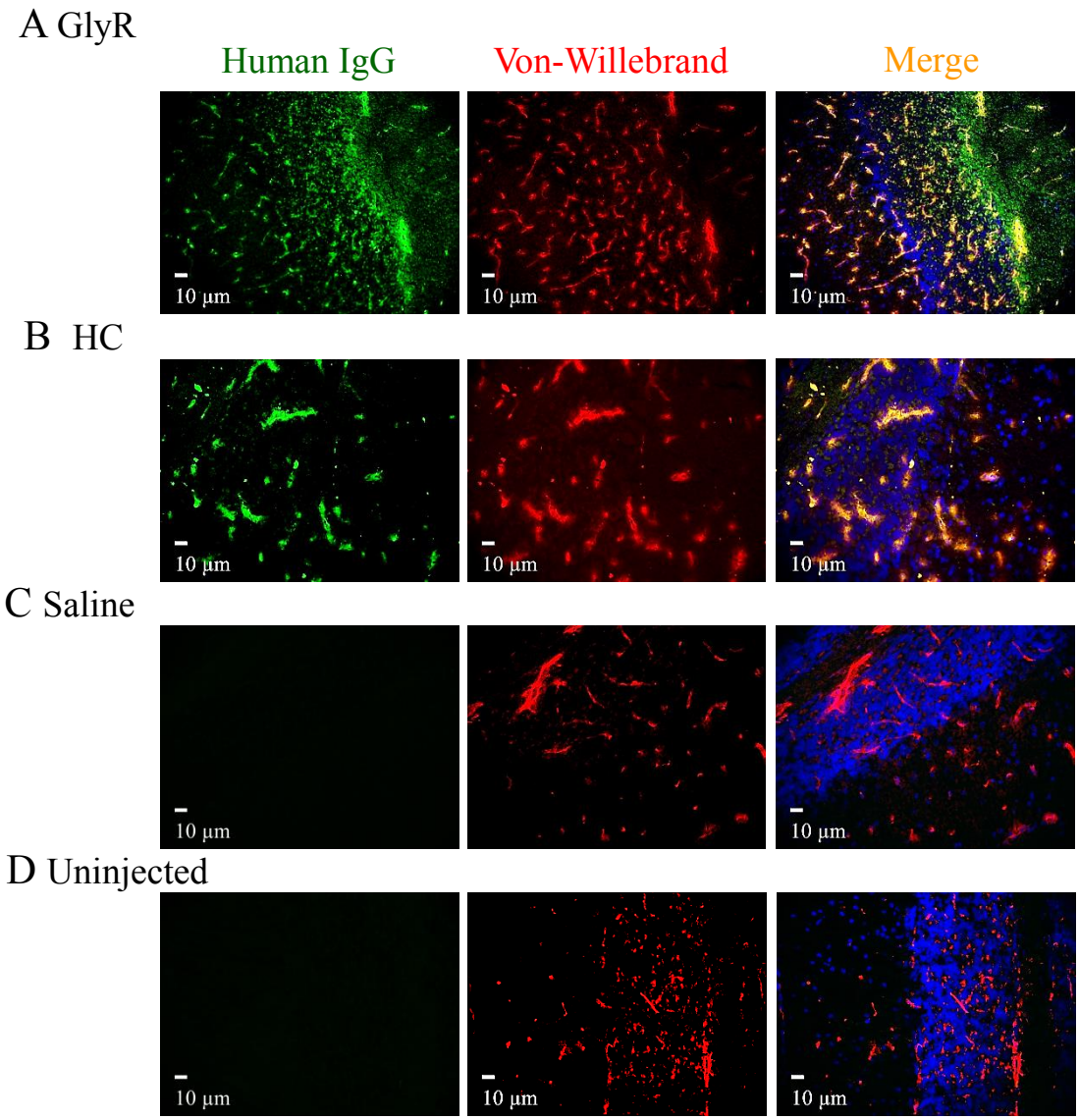

Fig. 6.19. IgG deposits were found in brain regions involved in motor control . Double labelled photographs were taken at 40x magnification at the cerebellum. ***A.*** In GlyR-IgG treated animals human IgG (green) is located inside the vessels colocalising with Von-Willebrand factor antibody (red) and also in the tissue without any colocalisation. ***B.*** In healthy control treated animals the human IgG (green) is located only in the vessels. ***C.*** In saline treated animals and untreated animals ***(D)***, human IgG deposits are not detectable. nuclei are stained with DAPI (blue).

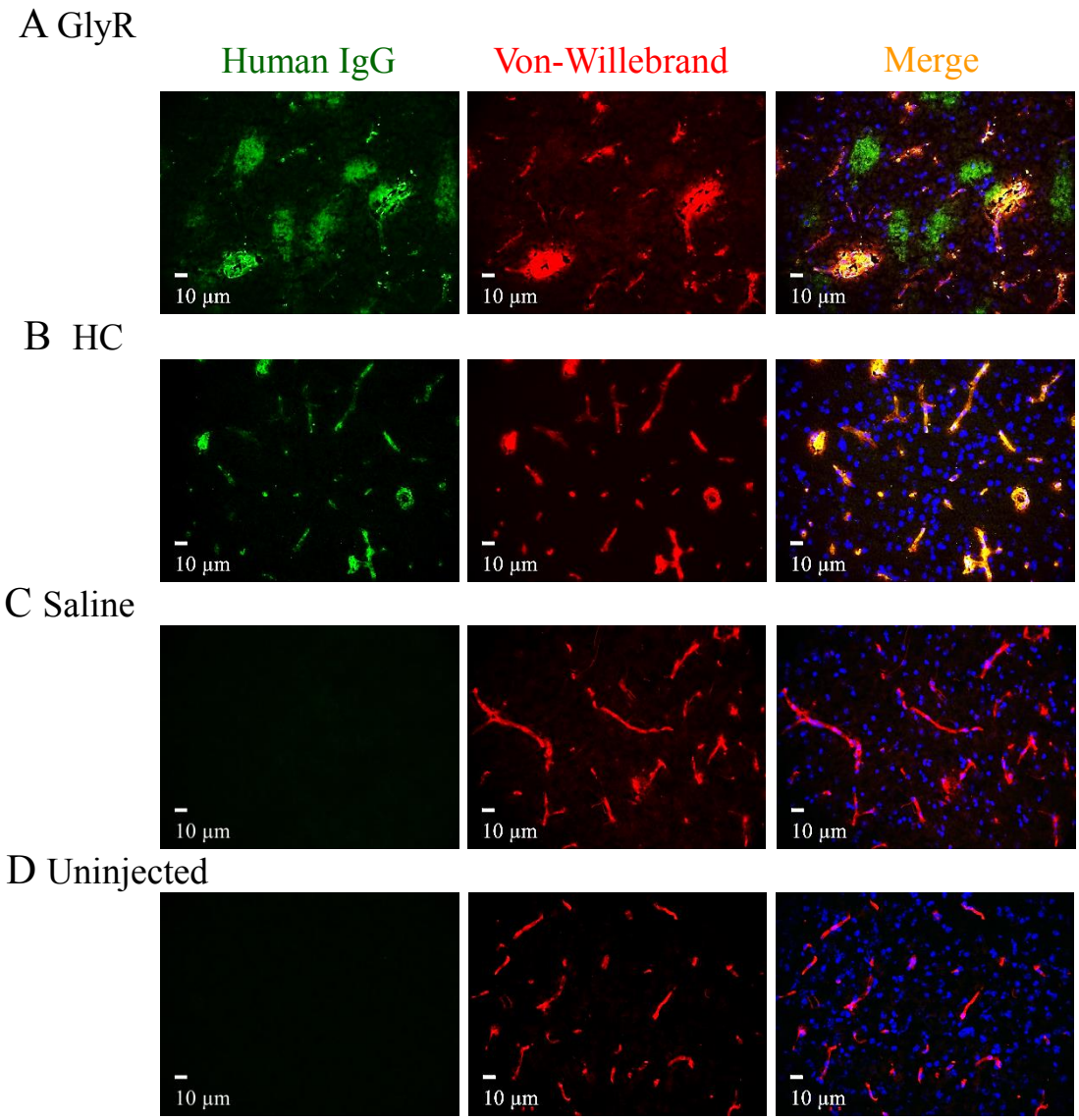

Fig. 6.20. IgG deposits were found in brain regions involved in motor control. Double labelled photographs were taken at 40x magnification at the caudate. ***A.*** In GlyR-IgG treated animals human IgG (green) is located inside the vessels colocalising with Von-Willebrand factor antibody (red) and also in the tissue without any colocalisation. ***B.*** In healthy control treated animals the human IgG (green) is located only in the vessels. ***C.*** In saline treated animals and untreated animals ***(D)***, human IgG deposits are not detectable. nuclei are stained with DAPI (blue).

human IgG inside the vessels (Fig. 6.19B, 20B), with again none in the saline and un-injected groups (Fig. 6.19C, 19D, 20C, 20D).

In the hippocampus, by contrast, there was no anti-human IgG immuno-reactivity except in the vessels in the GlyR IgG (Fig. 6.21A) or HC IgG (Fig. 6.21B) mice. The saline and un-injected groups were negative for anti-human IgG immuno-reactivity as elsewhere (Fig. 6.21C, D). These results suggest that transferred human GlyR IgG was only deposited in brain regions involved in motor function.

To see if human IgG deposits co-localise with GlyR, similar experiments were performed comparing anti-human IgG monoclonal (green) and polyclonal antibody to GlyRα1 (red). These showed double labelling and co-localisation in the PnC, the ventral horns of the spinal cord and cerebellum in the GlyR IgG treated mice; the human IgG localised inside the vessels did not show any co-localisation as expected (Fig. 6.22A, 23A, 24A). In the HC IgG treated mice, the anti-human IgG only showed the capillary pattern (Fig. 6.22B, 23B, 24B), and the saline and un-injected groups only showed the GlyRα1 staining (Fig. 6.22C, 22D, 23C, 23D, 24C, 24D).

In the hippocampus, since there was no GlyRα1 staining, only the capillary IgG deposits were found in the mice that had received human IgG (Fig. 6.25A, B) and none in those that had not (Fig. 6.25C, D). These results suggest that transferred human GlyR IgG was deposited in regions where GlyR is expressed.

Higher magnification confocal images of the brainstem and the ventral horn of the spinal cord demonstrated in more detail the localisation of the human IgG. GlyRα1 immunoreactivity was on the surface of the neurons as seen in (Fig. 3.13, chapter 3) but the human IgG staining was mainly intracellular, with some IgG also found between

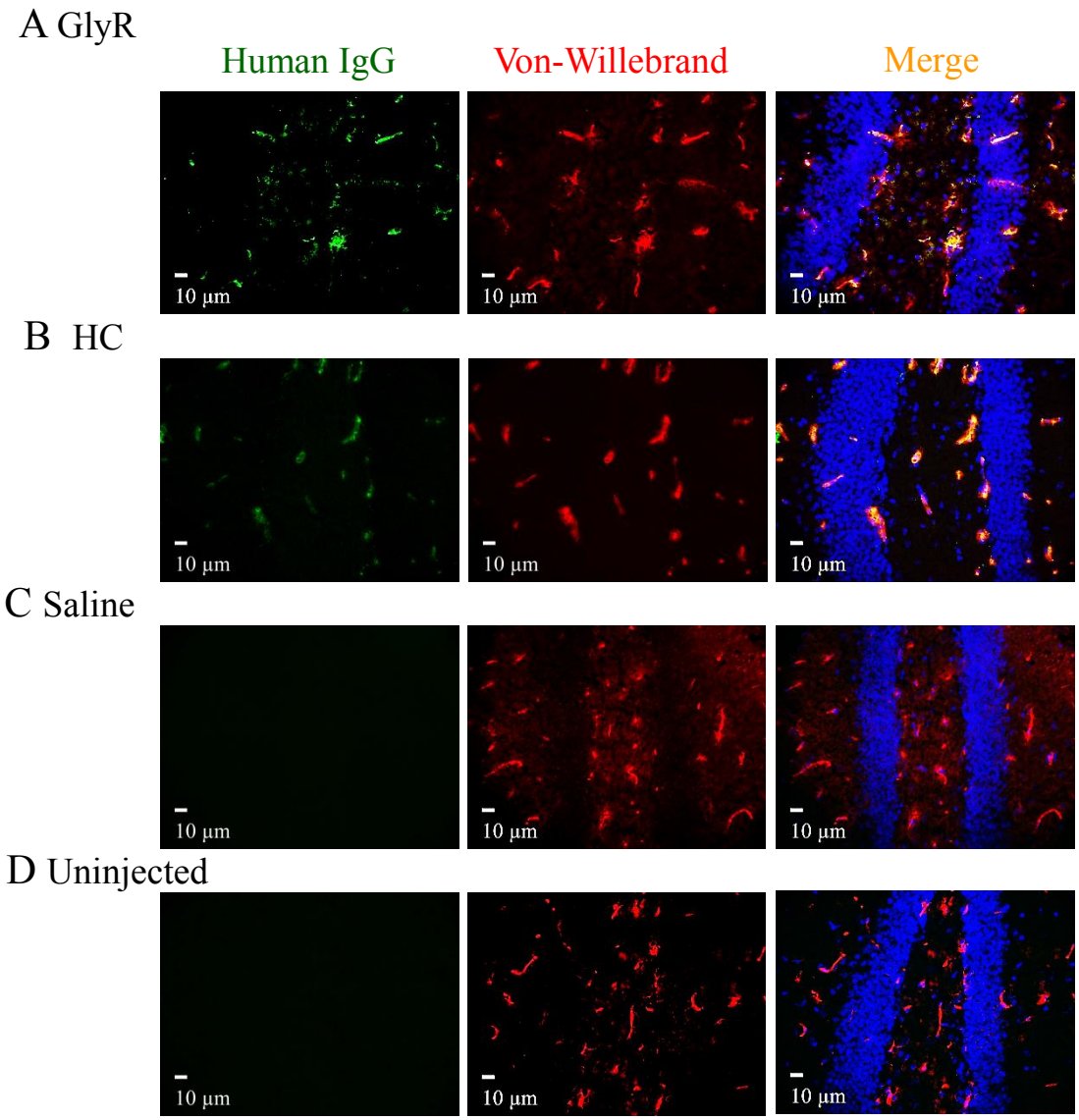

Fig. 6.21. IgG deposits were not found in brain regions not involved in motor control. Double labelled photographs were taken at 40x magnification at the híppocampus. ***A.*** In GlyR-IgG treated animals human IgG (green) is located inside the vessels colocalising with Von-Willebrand factor antibody (red), without any IgG deposited in the tissue. ***B.*** In healthy control treated animals the human IgG (green) is located only in the vessels. ***C.*** In saline treated animals and untreated animals ***(D)***, human IgG deposits are not detectable. nuclei are stained with DAPI (blue).

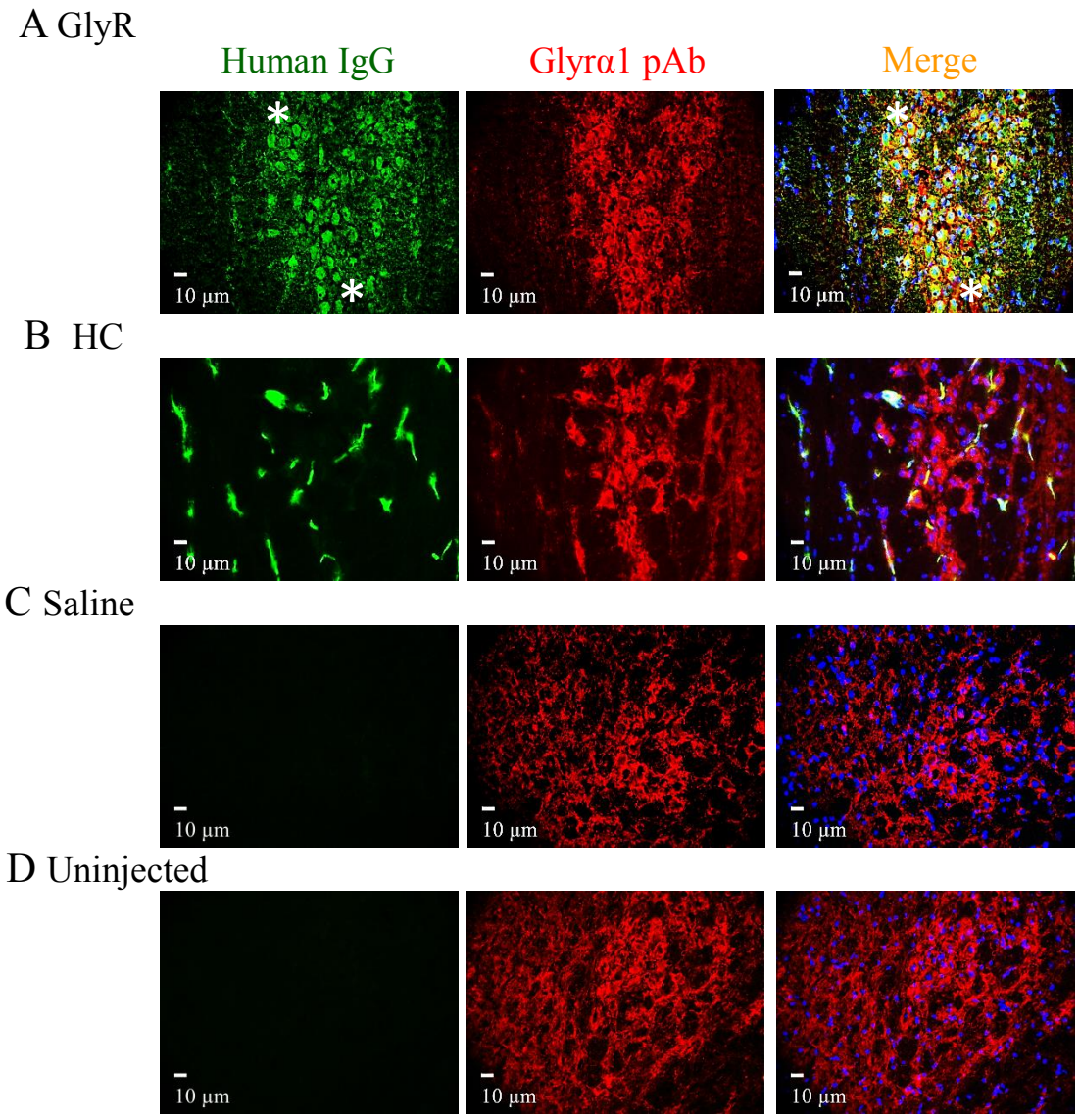

Fig. 6.22. IgG deposits were found in brain regions that express GlyRα1. Double labelled photographs were taken at 40x magnification at the brainstem in the PnC. ***A.*** In GlyR-IgG treated animals human IgG (green) colocalises with GlyRα1 antibody (red); possible cellular cytoplasms are marked with asterisks. ***B.*** In healthy control treated animals the human IgG (green) is located only in the vessels and don´t colocalise. ***C.*** In saline treated animals and untreated animals ***(D)***, human IgG deposits are not detectable. nuclei are stained with DAPI (blue).

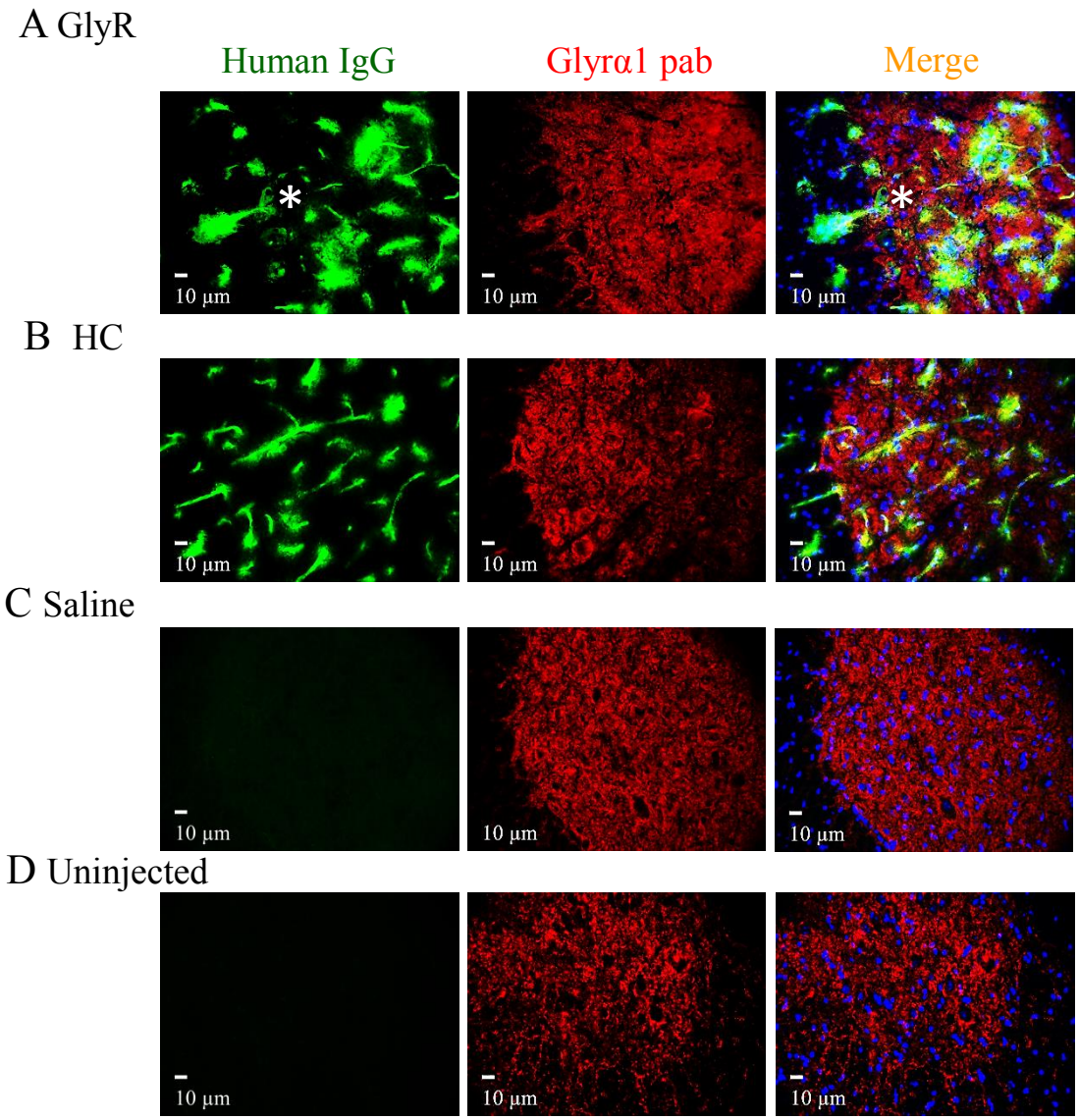

Fig. 6.23. IgG deposits were found in brain regions that express GlyRα1. Double labelled photographs were taken at 40x magnification at the spinal cord in the ventral horn. ***A.*** In GlyR-IgG treated animals human IgG (green) colocalises with GlyRα1 antibody (red); possible cellular cytoplasms are marked with asterisks. ***B.*** In healthy control treated animals the human IgG (green) is located only in the vessels and don´t colocalise. ***C.*** In saline treated animals and untreated animals ***(D)***, human IgG deposits are not detectable. nuclei are stained with DAPI (blue).

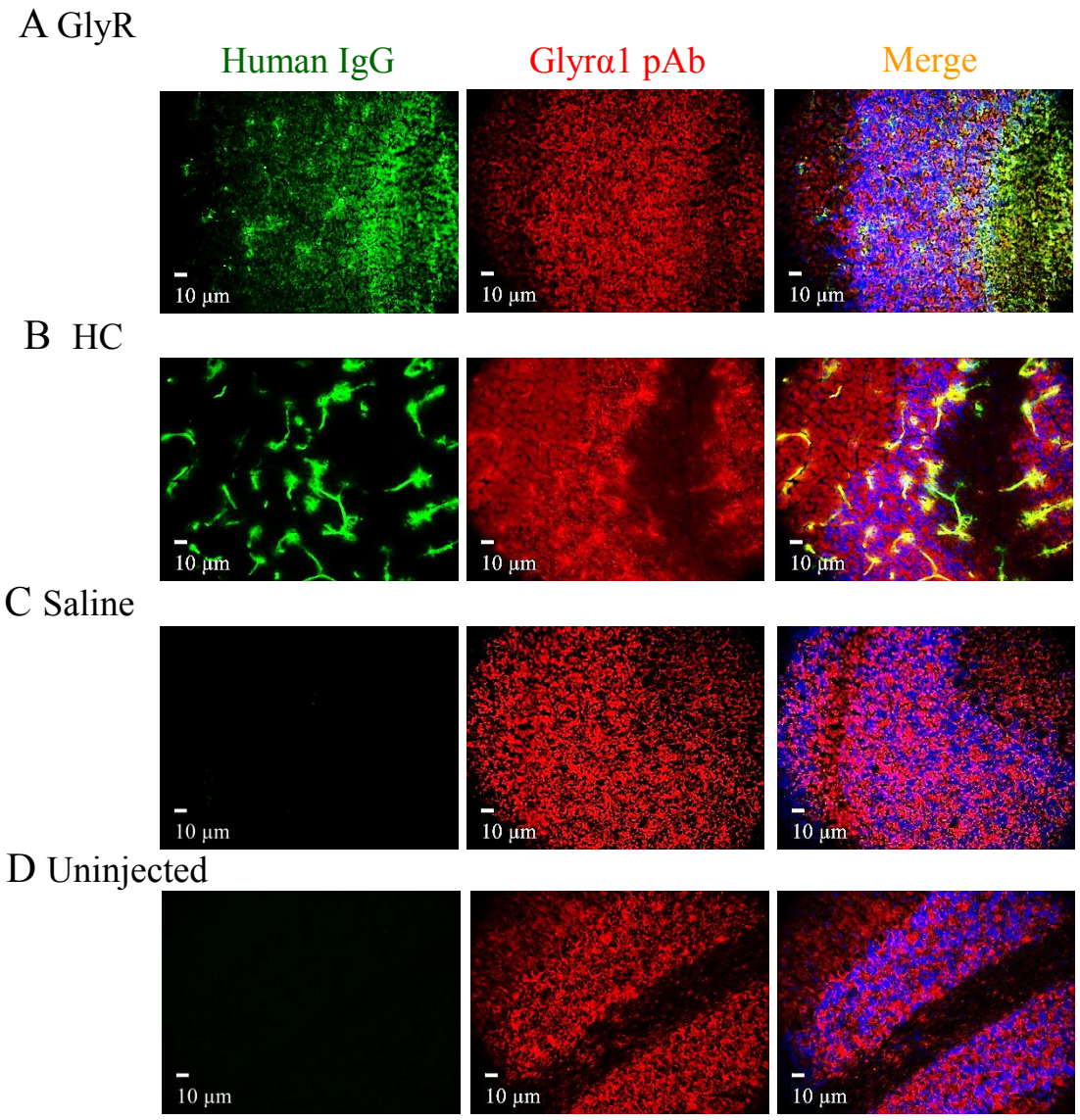

Fig. 6.24. IgG deposits were found in brain regions that express GlyRα1. Double labelled photographs were taken at 40x magnification at the cerebellum. ***A.*** In GlyR-IgG treated animals human IgG (green) colocalises with GlyRα1 antibody (red). ***B.*** In healthy control treated animals the human IgG (green) is located only in the vessels and don´t colocalise. ***C.*** In saline treated animals and untreated animals ***(D)***, human IgG deposits are not detectable. nuclei are stained with DAPI (blue).

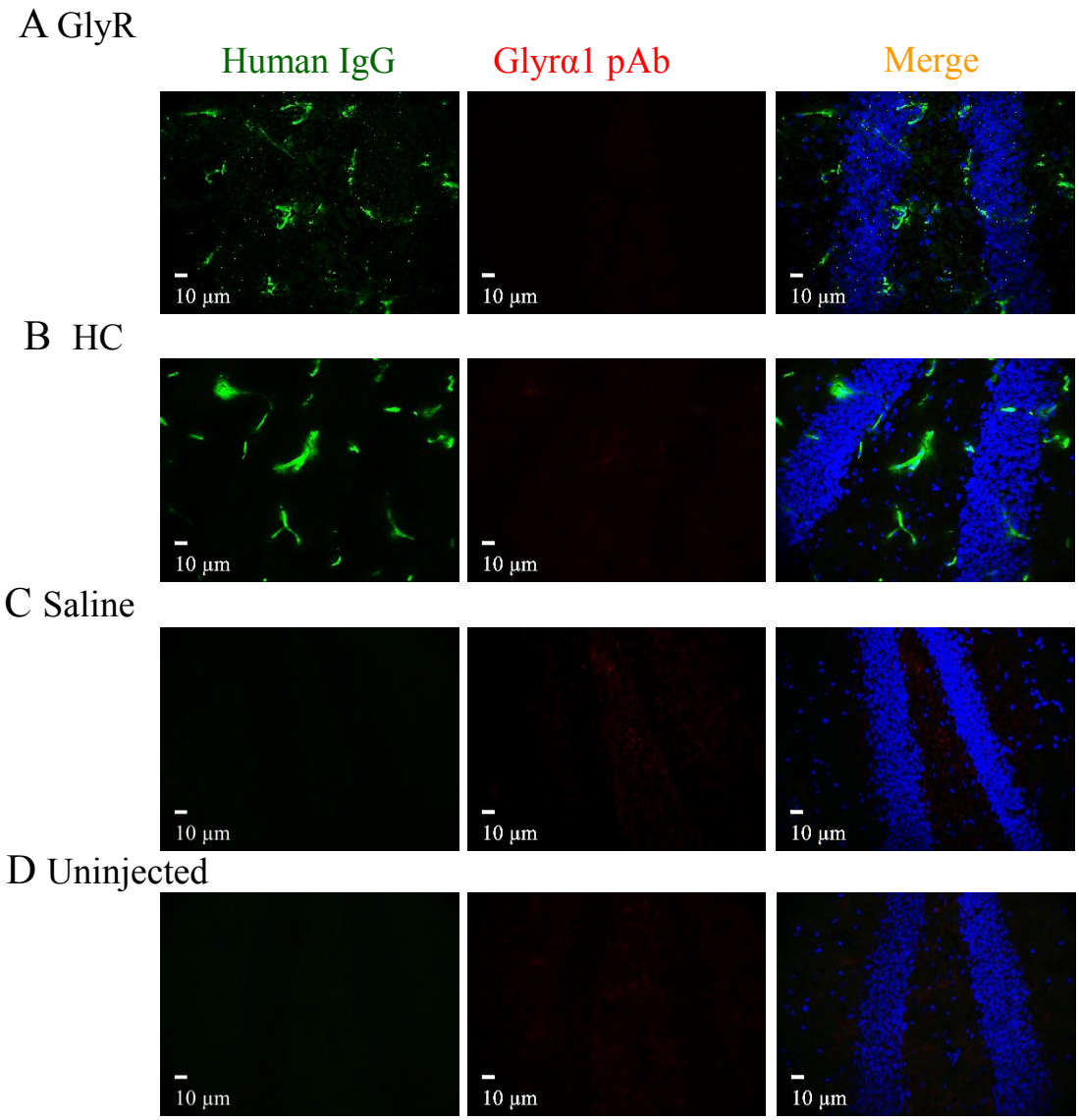

Fig. 6.25. IgG deposits were not found in brain regions that do not express GlyRα1. Double labelled photographs were taken at 40x magnification at the hippocampus. ***A.*** In GlyR-IgG treated animals no human IgG deposits were found, the human IgG (green) is located only in the vessels and don´t colocalise with GlyRα1 antibody (red). ***B.*** In healthy control treated animals the human IgG (green) is located only in the vessels and don´t colocalise. ***C.*** In saline treated animals and untreated animals ***(D)***, human IgG deposits are not detectable. nuclei are stained with DAPI (blue).

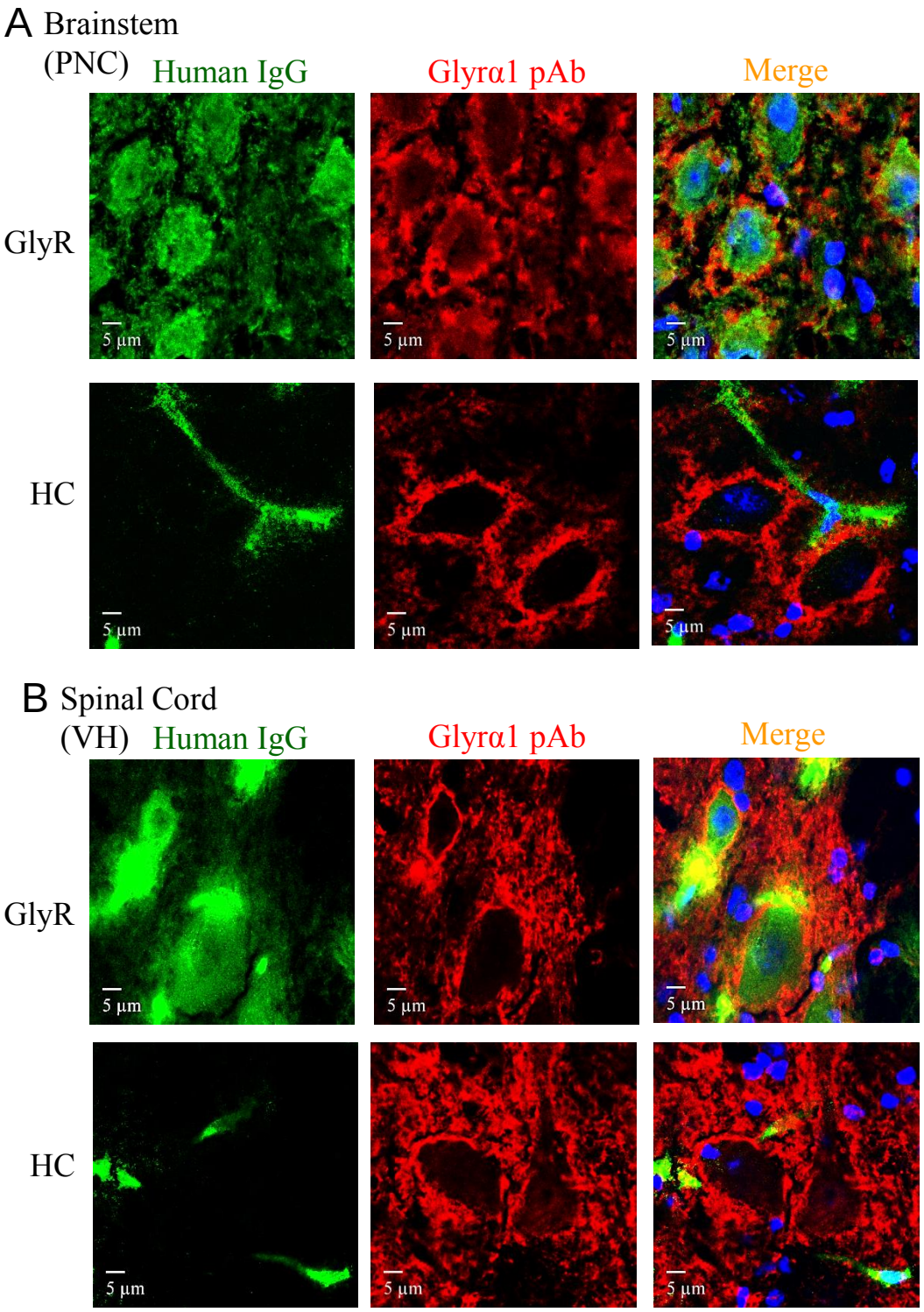

Fig. 6.26. Higher resolution of experiment in Figure 5 shows that IgG deposits are localised intracellularly. Confocal photographs were taken at 63x magnification at the brainstem in the PnC and at the spinal cord in the ventral horn. ***A.*** In GlyR-IgG treated animals human IgG cytoplasmic deposits (green) are surrounded by the surface GlyRα1 (red), with some of the IgG located extracellularly as well. ***B.*** In healthy control treated animals the human IgG (green) is located extracellularly near the cells resembling a capillary strucuture. nuclei are stained with DAPI (blue).

cells (Fig. 6.26A, C) in the GlyR IgG treated mice. This was not seen in the HC IgG treated animals (Fig. 6.26B, 26D). The staining observed in these experiments was consistent as IgG deposits were located in the same brain regions with the same pattern.

6.2.3 Intracerebroventricular (icv) passive transfer experiment

The clinical evaluation of the mice did not demonstrate very striking differences except in a few parameters, despite the apparently successful transfer and deposition of IgG antibodies in relevant brain regions of the GlyR-Ab injected mice. To see whether a greater and quicker effect could be shown with antibodies injected into the CSF, a passive transfer experiment was performed using 8 µl (0.1 mg) of purified IgG injected icv. Only the GlyR-Ab and HC IgG groups were used, with six animals in each group.

For this experiment, only one baseline was performed because of time constraints, followed 24 hours later by a single injection of the purified IgG into the third ventricle; the animals were then studied for three consecutive days. Then, after another 48h without any test, the animals were tested again for two days. The behavioural analyses did not show differences between the GlyR IgG treated group and the HC IgG treated groups, except for an effect on the anxiety-like behaviour and in the time needed to cross the wide runway. In this case, as there were only two groups of mice, students t-tests were used to assess any differences found.

The number of crosses between the light and dark compartment were lower in the GlyR-IgG injected mice ($p = 0.0182$; Fig. 6.27A), as was the time spent in the light box ($p = 0.0428$; Fig. 6.27B). There was also a trend towards a higher number of crosses in the open field in the GlyR-IgG mice compared to the HC-IgG injected mice ($p = 0.056$;

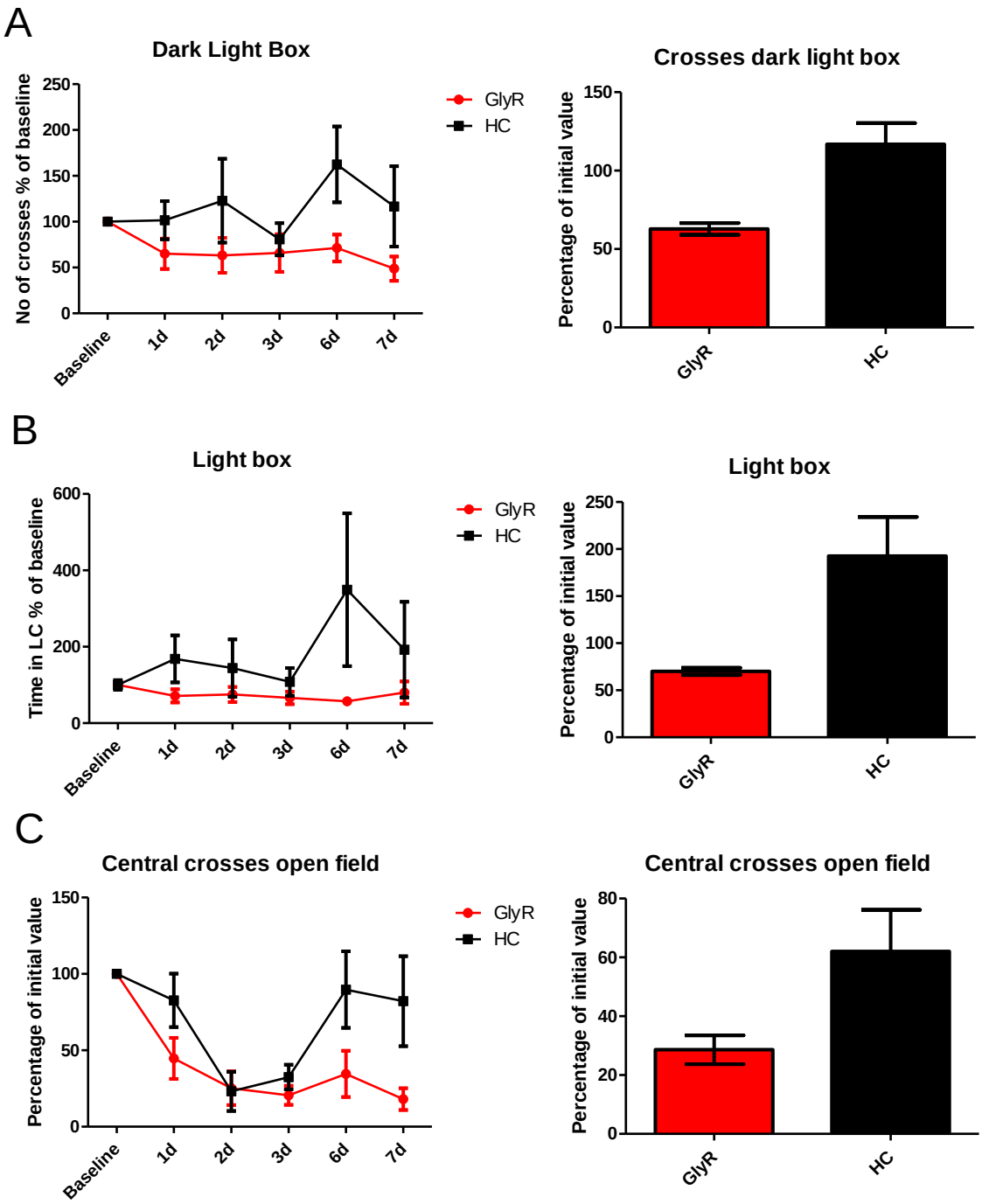

Fig. 6.27. Intracerebroventricular injection of GlyR-Abs caused an anxious-like behaviour in mice. Anxiety-like behaviour was evaluated in the Dark-Light box and in the open field. ***A.*** GlyR-Ab injected mice did significantly less crosses between the light and the dark compartments compared to HC-IgG injected mice (t= 3.854 df= 4 P = 0.0182). ***B.*** GlyR-Ab injected mice spent significantly less time in the light compartment compared to HC-IgG injected mice (t= 2.931 df= 4 P = 0.0428). ***C.*** GlyR-Ab injected mice did almost significantly less entrances to the central squares in the open field compared to HC-IgG mice (t= 2.237 df= 4 P = 0.056).

Fig. 6.27C). These results suggest icv injection of GlyR-Abs caused an anxious-like behaviour in mice.

The GlyR-Ab injected mice needed significantly more time to cross the wide runway compared to HC-IgG injected mice ($p = 0.0385$; Fig. 6.28A). The Student´s t-test analysis of the other wide runaway parameters did not show any differences in number of steps (Fig. 6.28B), right, left or wide stride length (Table 6.4; Fig. 6.28C, D, E). These results suggest that GlyR-Abs impaired gross motor performance in mice.

Interestingly, the latency to fall from the rotarod during the first three days showed a trend towards a less improvement in performance in the GlyR IgG injected mice compared to the HC-IgG injected mice ($p = 0.053$; Fig. 6.29A) which was significant at the first day of testing (Fig. 6.29B; $p = 0.048$), but no differences were found by 6 and 7 days (Fig. 6.30A). However, univariate general linear intragroup analysis of the GlyR-IgG treated mice and the HC-IgG treated mice showed differences in the latency to fall over time ($p < 0.05$). In the GlyR-IgG treated mice the latency to fall was significantly higher at day 7 after IgG injection compared to baseline while in the HC-IgG treated mice the latency to fall was significantly higher at days 6 and 7 after IgG injection compared to baseline (Table 6.4; Fig. 6.29A). These results suggest that icv injections of GlyR-Abs could have affected motor performance during the first 24 hours after injection.

To see whether these changes could be reflections of a more general effect of the surgery and injections, other features were also analysed. There was a slight decrease in weight at day 1 after surgery in both groups; 8.1% in the GlyR-IgG injected group and 7.4% in the HC-IgG injected group with complete recovery of weight during the following days of the experiment (Table 6.4; Fig. 6.30A). There were no differences in

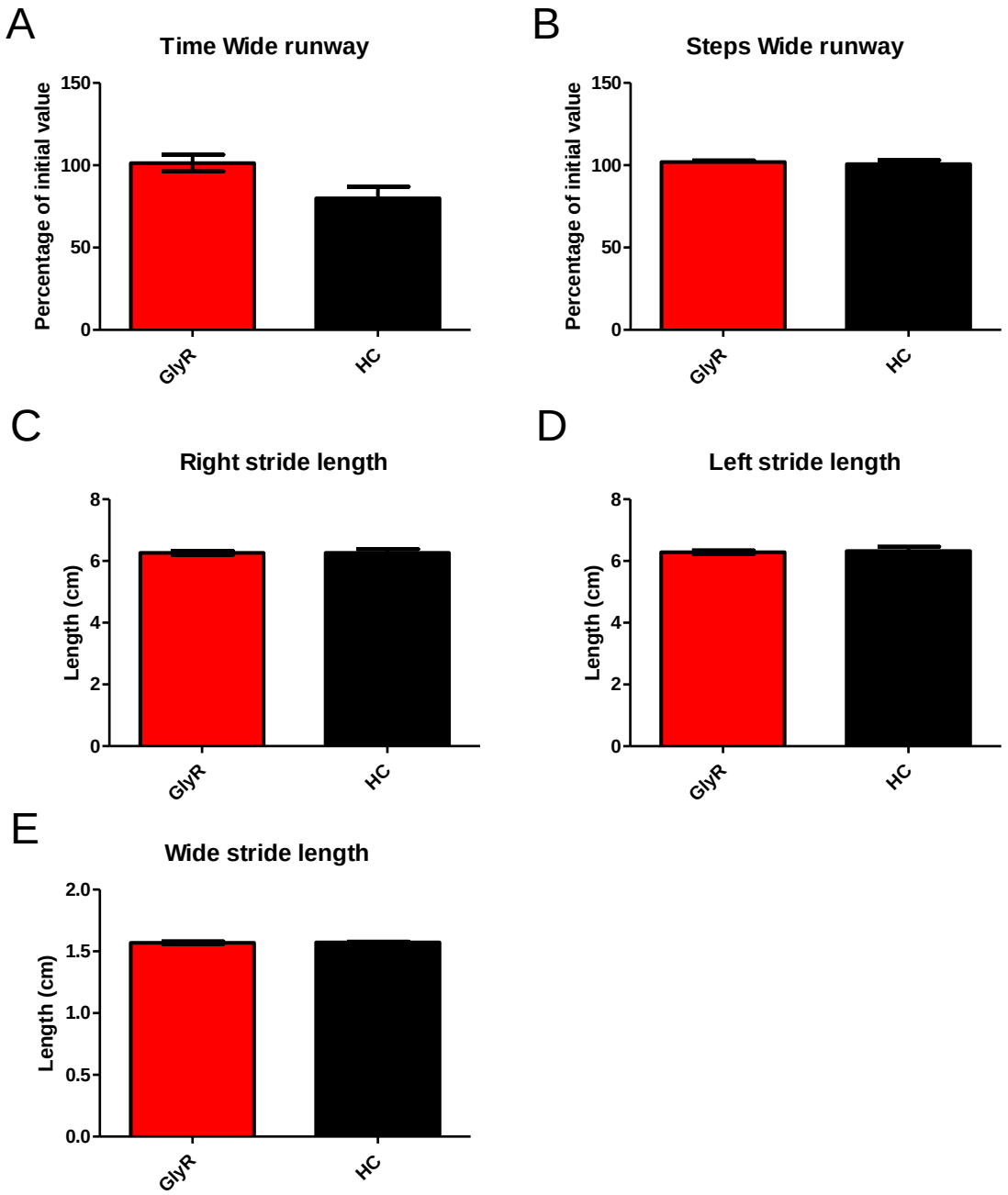

Fig. 6.28. Intracerebroventricular injection of GlyR-Abs caused impairment in motor learning in the wide runaway without affecting their gait. Animals were placed in an elevated wide runaway and monitored while crossing it to a safe platform. ***A.*** Mice treated with GlyR-Ab nedeed a significant higher time to cross the wide runaway compared to mice treated with HC IgG (t= 2.473, df= 8, p = 0.0385). ***B.*** No significant differences between groups were found in the number of steps (t= 0.474, df= 8, p = 0.648). No significant differences between groups were found in stride length (RSL: Right ***(C)*** Student´s t-test (t= 0.018, df= 10, p = 0.986), LSL: Left ***(D*** Student´s t-test (t= 0.265, df= 10, p = 0.797) , WSL: Wide ***(E)*** Student´s t-test (t= 0.168, df= 10, p = 0.870).

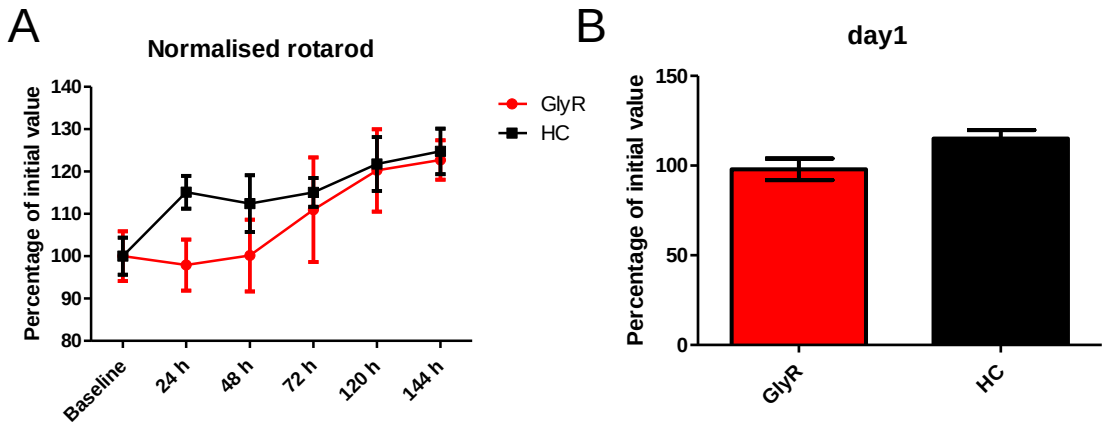

Fig. 6.29. Intracerebroventricular injection of GlyR-Abs could have affected forced walking learning ability during the first 24h. A. Mice treated with GlyR-Ab showed during the first three days an almost significant decrease in the time spent on the rotarod compared to mice treated with HC IgG (t=2.712, df=4; p = 0.053). By the end of the experiment both groups spent significantly higher time on the rotarod compared to baseline. ***B***. The effect was clearly observed at day 1 after injection (t=2.244, df=10; p = 0.048).

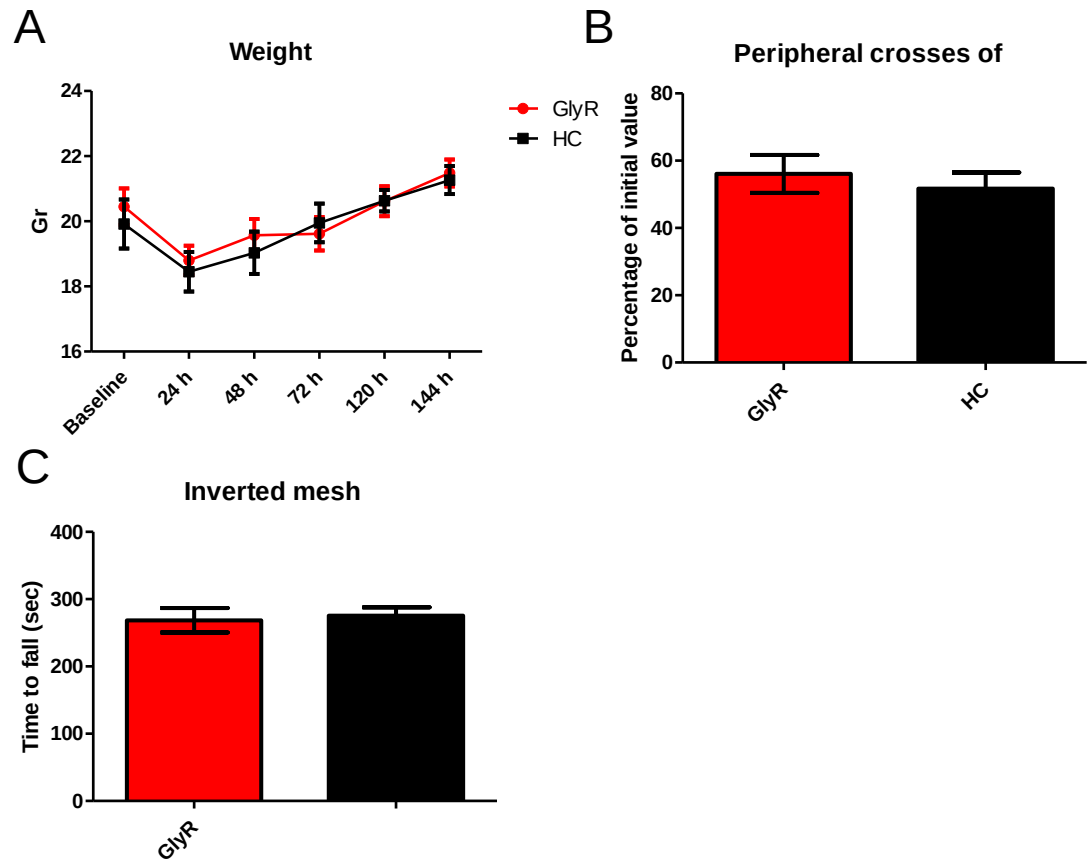

Fig. 6.30. Surgery and intrathecal of human IgG had a minimal effect on mice. A. Mice had a slight decrease in weight 24 hrs. after surgery which was recovered by the end of the experiment (t= 0.375, df= 10, p = 0.716). No significant differences in the number of peripheral crosses in the open field (t= 0.594, df= 8, p = 0.569) ***(B)*** and in the muscle strength (t= 0.322, df= 10, p = 0. 0.754) ***(C)*** were found between groups.

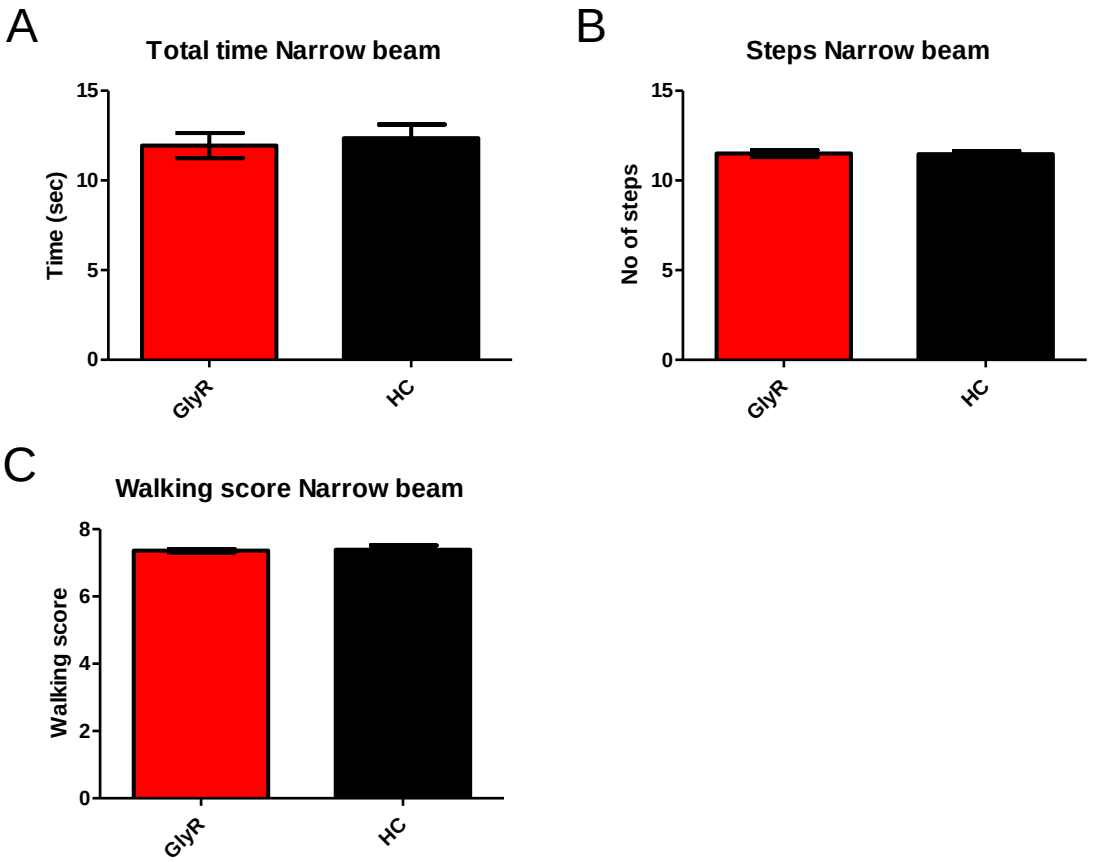

Fig. 6.31. No alterations in balance, coordination or sensorimotor functioning after intrathecal injection of GlyR-Abs into mice were found in the narrow beam. Animals were placed in an elevated narrow beam, and monitored while crossing it to a safe platform. No significant differences between groups were found in the time to cross ($t= 0.405$, $df= 10$, $p = 0.695$) ***(A)***; number of steps needed to cross ($t= 0.110$, $df= 10$, $p = 0.915$) ***(B)*** or the walking score while crossing) ($t= 0.203$, $df= 10$, $p = 0.843$) ***(C)***.

exploratory behaviour (crosses in the peripheral squares of the open field), grip strength or narrow beam activity comparing with the base-line tests between groups (Table 6.4; Fig. 6.30B, C, 31A, B, C). These results suggest that the surgery had a minimal impact on the mice behaviour.

Table 6.1. Statistical analysis of different parameters evaluated in the preliminary study

Parameter evaluated	Statistical test	Factor or variables compared	Statistical value	P value
Weigth	Two-way ANOVA	Condition	[F (2, 45) = 36.24]	<0.0001
		Time	[F (4, 45) = 10.26]	0.006
		Interaction	[F (8, 45) = 17.15]	0.034
Temperature	Two-way ANOVA	Condition	[F (2, 20) = 1.60]	0.2202
		Time	[F (4, 20) = 34.91]	0.0052
		Interaction	[F (4,20) = 4.15]	0.0132
Exploratory behaviour	Two-way ANOVA	Condition	[F (2, 36) = 20.65]	<0.0001
		Time	[F (3, 36) = 38.63]	<0.0001
		Interaction	[F (6, 36) = 4.16]	0.0028
Movement coordination	Two-way ANOVA	Condition	[F (2, 36) = 25.14]	<0.0001
		Time	[F (3, 36) = 5.49]	0.0033
		Interaction	[F (6, 36) = 4.57]	0.0015
Anxiety-like behaviour	Two-way ANOVA	Condition	[F (2, 36) = 52.23]	<0.0001
		Time	[F (3, 36) = 54.01]	<0.0001

		Interaction	[F (6, 36) = 6.26]	0.0001

Table 6.2. Statistical analysis of different behavioural test from the first IP passive transfer experiment

Behavioural test	Parameter evaluated	Statistical test	Statistical value	P value
Dark-light box	Time spent in dark compartment	One-way ANOVA	[F (3, 23) = 1.837]	0.193
	Time spent in light compartment	One-way ANOVA	[F (3, 23) = 1.750]	0.189
Successive alleys	Time spent in the closed alley	One-way ANOVA	[F (3, 161) = 2.036]	0.111
	Time spent in open alleys	Kruskall-Wallis	5.451	0.142
Narrow beam	Number of steps	One-way ANOVA	[F (3, 161) = 1.568]	0.199
	Number of errors	Kruskall-Wallis	1.791	0.617
Wide runaway	Time to cross	One-way ANOVA	[F (3, 161) = 0.219]	0.883
	Number of steps	One-way ANOVA	[F (3, 161) = 1.506]	0.215
	Number of errors	Kruskall-Wallis	2.144	0.543
	Left stride length	One-way ANOVA	[F (3, 161) = 2.290]	0.109

	Right stride length	One-way ANOVA	[F (3, 161) = 2.283]	0.110
	Wide stride length	One-way ANOVA	[F (3, 161) = 0.169]	0.284
Inverted mesh grid	Grip strength	One-way ANOVA	[F (3, 161) = 0.450]	0.745
	Holding impulse	One-way ANOVA	[F (3, 161) =1.827]	0.175

Table 6.3. Statistical analysis of different behavioural test from the second IP passive transfer experiment

Behavioural test	Parameter evaluated	Statistical test	Statistical value	P value
Open field	Exploratory behaviour	One-way ANOVA	[F (2, 11) = 0.287]	0.757
Dark-light box	Time spent in light compartment	One-way ANOVA	[F (2, 8) = 0.777]	0.501
Narrow beam	Number of errors	One-way ANOVA	[F (2, 8) = 0.402]	0.686
	Time to cross	One-way ANOVA	[F (2, 8) = 1.396]	0.309
	Walking score	One-way ANOVA	[F (2, 8) = 0.609]	0.574
Wide runaway	Time to cross	One-way ANOVA	[F (2, 8) = 0.434]	0.962
	Number of steps	One-way ANOVA	[F (2, 8) = 1.004]	0.421
	Left stride length	One-way ANOVA	[F (2, 8) = 1.704]	0.259
	Right stride length	One-way ANOVA	[F (2, 8) = 0.641]	0.559

	Wide stride length	One-way ANOVA	[F (2, 8) = 0.435]	0.666
Rotarod	Time to fall	One-way ANOVA	[F (2, 11) = 1.258]	0.350

Table 6.4. Statistical analysis of different behavioural test from the ICV passive transfer experiment

Behavioural test	Parameter evaluated	Statistical test	Statistical value	P value
Weight		Student´s t-test	(t= 0.375, df= 10)	0.716
Open field	Exploratory behaviour	Student´s t-test	(t= 0.594, df= 8)	0.569
Inverted mesh grid	Time to fall	Student´s t-test	(t= 0.150, df= 8)	0.884
Dark-light box	Time spent in dark compartment	Student´s t-test	(t= 0.930, df= 8)	0.379
Narrow beam	Time to cross	Student´s t-test	(t= 0.256, df= 8)	0.804
	Number of steps	Student´s t-test	(t= 0.167, df= 8)	0.872
	Walking score	Student´s t-test	(t= 0.408, df= 8)	0.694
Wide runaway	Number of steps	Student´s t-test	(t= 0.474, df= 8)	0.648
	Left stride length	Student´s t-test	(t= 0.211, df= 8)	0.838
	Right stride length	Student´s t-test	(t= 0.042, df= 8)	0.968
	Wide stride length	Student´s t-test	(t= 0.144, df= 8)	0.889

6.3 Discussion

Glycine receptor antibodies from one PERM patient were effectively transferred into mice after systemic injections over 12 days and were associated with motor dysfunction. The analysis of brain tissue suggests that systemic injections can lead to deposition of IgG in those regions that express GlyRs, and the cytoplasmic location of the antibodies suggests that they have bound to the GlyRs on the neurons and been internalised. Although these experiments did not achieve a clinical phenotype of startle or rigidity, they are the first to show that circulating GlyR-Ab can access some regions of the brain involved in motor control and regulation, and that this is associated with motor dysfunction and anxiety symptoms that might be due to receptor dysfunction in these brain regions.

The human IgG levels reached similar levels to the normal levels of mouse IgG observed in serum (2-5 mg/ml), although by the end of the experiment the human IgG levels were higher possibly related to the accumulation of IgG over time since the mouse IgG half-life is 7.5 to 9 days (Bonilla, 2008). Compared to the injected IgG, the levels of human IgG in the mouse sera at the end of the experiment was very low, with a 13 fold decrease in IgG levels, but this drop in the IgG levels was similar to that observed in other passive transfer experiment where neonatal animals were given intraperitoneally 16 mg per gram per 5 days and obtained IgG sera levels of 6.4 mg/ml (Anhalt et al, 1982).

The antibodies had to reach their antigenic targets in the CNS if they were to induce PERM-like manifestations and, therefore, the blood-brain barrier was artificially disrupted to allow access of GlyR-Abs to the brain. In the literature there are very few studies of passive transfer of antibodies mediating CNS diseases via systemic injection,

and most of the examples are for neuromyelitis optica (Bennett et al, 2009; Bradl et al, 2009; Kinoshita et al, 2009), stiff person syndrome (Sommer et al, 2005) and paediatric autoimmune neuropsychiatric disorders associated with streptococcal infection (Yaddanapudi et al, 2010). These studies are demanding and the injection of substances to disrupt the blood-brain barrier can introduce noise in the results. In fact it is well-known that LPS injection into rodents induces behavioural changes, called sickness behaviour, secondary to the neural effects of cytokynes such as interleukin 1 produced by the immune system stimulation (Bison et al, 2009, Kent et al, 1992). To see to what extent these effects of LPS might compromise the experiments reported here, the extent and duration of LPS effects on mice behaviour were investigated. LPS injection affected exploratory behaviour, motor coordination, caused anxiety-like symptoms, hypothermia and induced weight loss in mice, similar to previous findings of physiological and neuropsychological effects induced by LPS injection (Yirmiya et al, 1994; Bison et al, 2009). The dip in performance during the first 24-48 hours after LPS confirmed how important it is to take these changes into account when attempting to transfer human IgG antibodies to experimental animals, and demonstrate the need to avoid behaviour experiments during this time period.

Passive transfer of GlyR-Abs produced a pattern of motor dysfunction characterised by impaired forced walking ability, coordination and sensorimotor dysfunction, but other typical PERM manifestations such as stiffness, exaggerated startle response or muscle spasms were not present. Interestingly no differences in anxiety-like symptoms were found in mice after systemic injection of GlyR-Abs, but it is possible that LPS masked the anxiety-like features of the GlyR-Abs, or that the IgG did not gain access to the relevant brain regions when injected systemically as after the icv injection, signs of

anxiety-like behaviour were observed. The observed motor dysfunction is likely caused by a local action of the injected IgG on supra-spinal and spinal motor pathways, since IgG deposits were observed in brain regions that express glycine receptors and are involved in motor regulation, such as the brainstem, caudate, cerebellum and spinal cord.

IgG deposits found in these regions co-localised with commercial antibody to GlyRα1 subunit and no IgG deposits were found in regions that do not express glycine receptors such as the hippocampus and the cortex. Interestingly, confocal images of these regions showed that IgG deposits were located intra-cellularly supporting the internalisation of GlyR as one possible pathogenic mechanism by which GlyR-Abs affect the glycinergic neuron function (Chapter 4 and Carvajal-González et al, 2014).

Disruption of glycinergic neurotransmission in transgenic mice expressing a dominant mutation of the GlyRα1 subunit causes motor symptoms similar to the symptoms observed in patients with PERM and hyperekplexia (Becker et al, 2002), and alters in vitro the pattern of the alternating rhythms in the spinal cord (Hinckley et al, 2005). There are no studies in the literature addressing the pathogenic role of the GlyR-Abs, but supra-spinal disinhibition has been demonstrated in SPS and PERM with GAD autoimmunity (Koerner et al, 2004). However, since GAD in an intracellular antigen it is unlikely that GAD autoantibodies are pathogenic; in fact various in vivo and in vitro studies of GAD-Abs evaluating their pathogenic actions have yielded inconsistent experimental evidence (Raju et al, 2005; Geis et al, 2011; Manto et al, 2011; Hansen et al, 2013; Chapter 1). Additionally, SPS can be associated with other intracellular (amphiphysin) and extracellular antigens which may influence the clinical phenotype in these patients (Sommer et al, 2005, Geis et al, 2011, Chang et al, 2013).

Icv injection of GlyR-Abs into mice, by contrast to systemic injection, caused anxiety-like behaviour and a slight impairment in motor performance which may be related to the more anxiety-like state of the mice; neuropsychological studies have shown that persons with high anxiety levels adopt a more conservative gait pattern on the treadmill compared to persons with low-anxiety level conditions (Nibbeling et al, 2012). Although we did not find a large proportion of patients with anxiety symptoms, they have been reported in other studies (Henningsen and H-M Meinck, 2003; Alexopoulos et al, 2013). Disappointingly, there were no clear motor abnormalities in the mice injected icv, although the GlyR-Ab IgG injected mice did not function as well on the rotarod. The differences between the two passive transfer results could be due to a variety of reasons: a) Since the GlyR-Abs were injected directly into the CNS, there was no need to inject LPS, and this may have avoided the masking of anxiety that could have obscured the results in the intraperitoneal injections; b) It is possible that the lack of a full motor symptomatology was the result of using only a single injection of a small amount of IgG into the third ventricle which would have diffused widely and may not have been taken up adequately by the brainstem, spinal cord, and other brain structures involved in motor regulation. For instance, a previous passive transfer study of GAD antibodies found that supra-spinal GABAergic dysfunction, rather than spinal GABAergic dysfunction, caused motor dysfunction in mice (Geis et al, 2011); c) More relevantly, in previous successful passive transfer studies using intrathecal injections of IgG, the antibodies were injected repeatedly or infused continuously (Geis et al, 2010; Geis et al, 2011, Hansen et al, 2013), while here only a single icv IgG injection was performed because of the Home Office restrictions on Dr Lang's licence existing at the time. The trend towards a temporary effect of GlyR-Abs on rotarod performance indicates a need for further icv models in the future.

6.4 Conclusions and limitations

The results in this chapter show that passive transfer of GlyR-Abs may cause motor dysfunction and anxiety-like behaviour in mice, and in particular that the IgG can be shown bound to supra-spinal and spinal structures involved in motor regulation after systemic injection. This in itself is an important finding. Moreover, IgG deposits colocalised with GlyR commercial antibody and were found intracellularly suggesting internalisation of the antibodies with reduced GlyR expression and disruption in glycinergic neurotransmission, as suggested by the results in Chapter 4. On the other hand, it is possible that since the whole plasma IgG was used, there could have been other antibodies to unknown antigens in the IgG preparations that might have been responsible for the clinical features. However, the localisation of the IgG in cells that express the GlyR on their surface in regions involved in motor regulation strongly suggests that the GlyR-Abs were responsible for the deficits observed.

However, the full spectrum of clinical manifestations of PERM patients was not demonstrated in these passive transfer experiments and doubtless there could be improvements to the experimental protocols; these could include transferring more IgG, from a patient with a higher titre of antibodies, systemically in order to obtain higher levels of circulating antibodies, or chronic infusions of IgG into the ventricles. The need to take great care not only with the patient IgG preparations but also with the control IgG preparations was evident after the second experiment which was compromised by use of a pool of very fresh, unheated, plasmas that might have contained immune complexes, responsible for the serum sickness that appeared in the mice.

Another aspect that might have explained the apparent failure of the second experiment, with a different IgG preparation, could be differences in epitope recognition between the IgG preparations of the patients used and the relatively low titre of GlyR-Abs in the purified plasma (1:320 and 1:640) (Dinkel et al, 1998; Manto et al, 2011). Optimising the concentrations of the injected material and assessing the serum levels more comprehensively in the systemic injections could be helpful.

Finally there were experimental design differences between the systemic and the ICV passive transfer experiments which prevent comparison of the results, but it will be of great interest to compare the immunostaining results between these two approaches. Time limitations meant that they could not be pursued in time for this Thesis, but further studies with IgG preparations of other PERM patients are required to confirm the results of these experiments.

CHAPTER 7. General Discussion

PERM and related disorders are rare but provide yet another example of conditions in which an antibody specific to a neurotransmitter receptor plays an important role. The work in this Thesis describes for the first time the characteristics of the patients and their antibodies, and one of the potential mechanisms by which the antibodies lead to loss of inhibitory function. The results show that PERM is a treatable autoimmune disease but that some patients with GlyR-Abs have clinical phenotypes, such as epileptic encephalopathies or restricted brainstem disorders, that extend beyond the major motor manifestations characteristically associated with PERM. Importantly, it was shown that antibodies in the patients bind principally to brain regions known to express GlyR and to modulate and control motor functions, and that injection of the antibodies into mice produces some evidence of motor dysfunction and anxiety-like behaviour, associated with IgG deposition in the same regions.

GlyR-Abs can be a useful guide to the aetiology and diagnosis in patients with a range of motor features of stiffness and spasms, and the presence of the antibodies implies a treatable autoimmune disease. PERM is, at its worst, a highly disabling disease where autonomic and respiratory failures can be missed and lead to fatal outcomes if not anticipated and the patient adequately observed. Unexpectedly some patients with apparently the same GlyR-Abs have relatively mild motor symptoms but can still be at risk of respiratory difficulties. Equally the motor dysfunction can be focussed on the brainstem with no clear spinal features of rigidity and muscle spasms. Encephalopathic manifestations such as seizures, cognitive disturbances and loss of consciousness were also, surprisingly, found in some patients at onset and were a more common feature in all patients if the disease was allowed to progress. In some cases this could be due to

additional antibodies (such as NMDAR-Abs in Turner et al, 2011) but in many cases there was no evidence for co-existing targets except for the four patients who had GAD-Abs at high levels. In all patients, as with any autoimmune neurological disease, tumours should be searched for, but in patients with GlyR-Abs relatively few patients had new evidence of tumours, and they were thymomas and lymphomas, and only one had a recurrence of a breast cancer, whereas breast and lung cancers are more often found in SPS with GAD-Abs (Murinson 2004).

PERM is another example of an "autoimmune channelopathy". The clinical features observed in PERM patients such as muscle spasms, cramps, myoclonus, muscle stiffness and tightness, stimulus-evoked startle and respiratory failure are similar to those seen in syndromes caused by mutations in genes coding for proteins involved in glycinergic neurotransmission such as hereditary hyperekplexia which is caused by mutations in GLRA that encodes the GlyRα1 subunit or SLC6A5, the gene for the GlyT2 (Harvey et al, 2008). Poisoning with the alkaloid strychnine, which is a GlyR antagonist, causes similar manifestations including agitation, heightened awareness and responsiveness, stimulation-evoked seizures, myoclonus, respiratory failure, and sometimes death (Porter and Kaplan, 2011). Moreover, other members of the same superfamily of five subunit, ligand-gated ion channels such as GABA receptors, and muscle AChRs, are also targets for either mutations or autoimmune attack leading to receptor-specific disorders (Vincent et al, 2010, Zuliani et al, 2012, Irani et al, 2014).

An autoimmune basis for SPS and related disorders has long been recognised because of the association with high titres of GAD or amphiphysin antibodies and often evidence of autoimmunity in the patient or their families. However, GAD antibodies are intracellular and thus inaccessible to circulating antibodies. By contrast, GlyR-Abs

found in PERM patients target the extracellular domain of the ligand-gated membrane protein and thus are more likely to be pathogenic. This Thesis provides the first *in vitro* and *in vivo* evidence that GlyR-Abs are pathogenic. GlyR-Abs were shown to be mainly IgG1 and IgG3 subclasses and to activate complement in vitro on the surface of GlyR-expressing HEK cells. To what extent complement activation contributes to the PERM physiopathology in vivo, however, is unclear but it may not be a major factor since most of the patients recovered after immunosuppressive therapies and were left with restricted or very little disability. Neuroimaging and CSF studies for inflammation were often normal at onset or during the disease, but it could be informative to do structural and functional analysis of the patients after recovery to see if there are persistent changes, as have been described in patients with NMDAR-Ab or LGI1-Ab diseases (Finke et al 2012; Malter et al 2014). However, such studies would be more challenging since the areas involved, the brainstem and spinal cord will be much harder to study.

Most antibodies are divalent (except for IgG4) and if they can bind to at least two epitopes on adjacent receptors they will induce internalisation of their target, as was very clear with AChR antibodies in myasthenia gravis (Drachman et al 1981). Since the GlyR-Abs were IgG1 and IgG3, and the GlyRs contain at least two a1 subunits, it was not unexpected that the antibodies could act in a similar manner. This mechanism is thought to be sufficient to cause disease, appears to produce little cellular damage and can be reversible once the antibodies are removed as shown in myasthenia gravis and NMDAR encephalitis patients (Drachman et al, 1978, Tuzin and Dalmau, 2008).

The *in vitro* results on GlyRs expressed in HEK cells, were reinforced by immunohistochemistry results obtained in other parts of this Thesis; GlyR-Abs present

in PERM patients were highly specific, binding to rat brain regions known to express GlyRs, related to motor control such as the brainstem and spinal cord and colocalising in these regions with commercial monoclonal antibodies to GlyRα1 subunit. This specific binding was lost after serum adsorption with HEK cells expressing GlyRα1 subunit.

Although these clinical and experimental findings imply a pathogenic role of self-reactive GlyR-Abs present in PERM patients, asserting a causal link between autoantibodies and disease requires fulfilling other established criteria, specifically modelling the disease in healthy animals by passive transfer of IgG present in affected patients. This Thesis provides preliminary *in vivo* evidence of behavioural alterations after passive transfer of purified IgG from PERM patients. Mice injected systemically with GlyR IgG after BBB disruption with LPS showed altered motor performance with IgG deposits observed in brain regions known to express GlyRs and to coordinate motor behaviour. A further single intra-ventricular passive transfer study also showed evidence of behavioural alterations, but the mice developed anxiety-like behaviour, and motor manifestations were not convincing. The lack of motor alterations in this experiment may be the result of a very short exposure to IgG (24 hrs), as most passive transfers have used several days of injections or continuous infusion (Geis 2010; Geis et al, 2012; Hansen et al, 2013).

Although it was not possible to reproduce the clinical core features of PERM patients such as stiffness, muscle spasms and excessive startle, this is not uncommon in passive transfer studies where most studies have failed to model completely all the features of the human disease in animals. For example, passive transfer studies of SPS also failed to reproduce the core features, only inducing motor performance alterations and

anxiety-like behaviour in mice (Geis et al, 2010; Geis et al, 2012; Hansen et al, 2013), except for an initial study using amphiphysin antibodies where the authors reported stiffness in rats (Sommer et al, 2005) (Table. 7.1). However, the latter was short-lived and may have been confounded by the effect of intraperitoneal injections that can cause such behaviour in mice (L Jacobson, A Vincent unpublished observations).

Table 7.1. Overview of in vivo experiments in CNS mediated diseases.

Antigen and disease	Species	Method for passive transfer of IgG	Findings	Author
Glutamic acid decarboxylase (GAD) SPS	Rat Rat	Intrathecal chronic injections Intrathecal chronic injections	Anxiety-like behaviour Motor dysfunction	Geis et al, 2011 Hansen et al., 2013
Amphiphysin (SPS)	Rat Rat	Systemic chronic IP injections Intrathecal chronic injections	Stiffness Motor dysfunction	Sommer et al, 2005 Geis et al, 2010
N-methyl-D-Aspartate receptor (NMDAR) Encephalitis	Rat Rat Rat Mouse	Chronic intrahippocampal injection Acute intrahippocampal injection Acute intracortical injection Acute intracortical injection	Reduction in MDAR expression in the hippocampus Increased extracellular glutamate Increased excitability of motor cortex Disruption of NMDAR´s interaction with B2 adrenergic receptor	Hughes et al, 2010 Manto et al, 2010 Manto et al, 2011 Mikasova et al, 2012
Aquaporin4 Neuromyelitis optica	Rat	Systemic chronic IP injections (EAE)	Astrocyte loss and perivascular deposition of IgG and	Kinoshita et al, 2009

			complement	
	Rat	Systemic chronic IP injections (EAE)	Astrocyte loss and perivascular deposition of IgG and complement	Bradl et al, 2009
	Mouse	Chronic injections into the optic nerve and retina	Astrocyte depletion, myelinosis, complement activation	Asavapanum as et al, 2014
MGluR1	Mouse	Acute intrathecal injection	Cerebellar ataxia	Sillevis et al, 2000

The difficulties in reproducing all the clinical features may also be related to differences in how effectively and in which brain regions the antibodies access their targets in the CNS, which could be due to regional differences in BBB disruption. It is not uncommon in autoantibody mediated diseases of the CNS that antigens are ubiquitously expressed in the CNS, yet the antibodies show very little regional antigenic preference and therefore cannot be the determining factor of disease phenotype. This is the case in neuromyelitis optica where aquaporin 4 is expressed in stomach and renal tissue, but there are no consistent gastrointestinal or renal manifestations (Lennon et al, 2005). It has been suggested that different agents used to disrupt the BBB can influence the brain regions made vulnerable to antibodies. For example, in both patient and control passive transfer experiments, human IgG was found in the hippocampus and the brainstem – suggesting that certain areas are more leaky than traditionally thought (Chang et al 2013). In one study where epinephrine was used to open the BBB, the anti-NMDAR epitope IgG deposits were observed in the amygdala (Huertas et al, 2006). In the experiments reported here, there were no major IgG deposits in the hippocampus, while in a previous passive transfer studies of antibodies to an NMDAR epitope, IgG deposits

were found mainly in the hippocampus (Kowal et al, 2004); this is reassuring since in the latter case, the antibody target was expressed in the hippocampus whereas GlyRs are poorly expressed in this region as shown in Ch. 5. By contrast, IgG was clearly deposited mainly in the PnC of the brainstem and in the spinal cord, which is where the GlyRs are most strongly expressed.

7.1 An integrative perspective

The fact that most of the patients in this cohort responded very well to immunotherapy contrary to the often poor response of SPS patients, suggests that PERM may be a different type of autoimmune disease, where the neuronal cell death mediated by T cell cytotoxicity observed in SPS (Costa et al., 2002; Warren et al., 2002; Holmøy et al., 2009) is limited. Instead GlyR-Abs are likely to reduce GlyR functions as a consequence of the antigenic modulation that occurred in vitro and was apparent by internalised IgG in the brains of injected mice. Although only 10% of the patients had high GAD-Abs, it is clinically relevant to appreciate that other antibodies, such as GlyR-Abs, may be responsible for the clinical features with which GAD-Abs are often associated, such as cerebellar ataxia and a seizure-dominant form of limbic encephalitis (Malter et al., 2010; Saiz et al., 2008). Thus the presence of GAD-Abs in syndromes with brainstem and spinal cord hyperexcitability, should not exclude a search for other neuronal surface antibodies that might determine the clinical phenotypes of these patients.

How is it possible that two autoimmune diseases with possible different causative antibodies can cause largely similar clinical manifestations? One possible explanation

may be related to the co-localisation of GABA and Glycine which are co-released from the same presynaptic terminal buttons (Chaudhry et al, 1998; Dumoulin et al, 1999; Dumoulin et al, 2000) and, therefore, autoantibody targeting either of these molecules could affect the function of both at mixed synapses. There are also reports of specialised GABAergic or glycinergic neurotransmission from mixed presynaptic inhibitory neurons (e.g.: Golgi cells in the cerebellum), where the differential expression of $GABA_A$ and glycine receptors in the postsynaptic terminals segregates with specific inhibitory signalling (Duqué et al, 2005).

Indeed, GlyRs observed by immunohistochemistry were located in interneurons of the ventral horn which express GlyRs in high amounts. Thus GlyR-Abs could be affecting the fine-tuning inhibitory control that these neurons exert on the excitatory outputs. This hypothesis is supported by some reports of a cross-linked fine-tuning inhibition of GABAergic inhibition by GABAergic and glycinergic interneurons in the spinal cord of the dorsal horn (Takazawa and MacDermott, 2010). Whether there are other examples of fine-tuning of gabaergic interneurons on glycinergic interneurons, or glycinergic interneurons on other glycinergic interneurons is unclear. At the network level little is known about how GABAergic and glycinergic networks interplay and mediate fast inhibitory neurotransmission in different CNS areas. Growing evidence suggests that fast inhibition in presynaptic and postsynaptic terminals is required to fine-tune and to limit the excitability of the network. This mechanism is proposed to facilitate spatial and temporal discrimination of sensory stimuli in the dorsal horn of the spinal cord (Zeilhofer et al, 2012) and in the hippocampus it is postulated that glycinergic neurotransmission regulates hippocampal neuronal activity through cross-inhibition of

gabaergic inhibition, and through the modulation of excitatory NMDARs by the glycine binding site (Xu and Gong, 2010).

Another relevant question is why patients with GlyR-Abs had a wider clinical spectrum than can be inferred by extrapolation of GlyRs expression in the brain. Some patients with GlyR-Abs presented mainly with symptoms of supratentorial involvement which does not correlate with the expression of GlyRs mainly in the brainstem and spinal cord. One possible explanation may be that glycine receptors with subunit profiles different from the traditional α1 (α2 and α3 subunits) were found in supratentorial regions such as the hippocampus, the cerebral cortex and caudate among others. However, the IgG staining seemed more intracellular raising questions about their potential to be antigenic targets for the antibodies in vivo. Nevertheless, a high proportion of GlyR-Abs found in PERM patients cross-reacted with all three subunits raising the possibility of antibody binding in these regions. Supporting this hypothesis, GlyT1, a glial transporter, in highly expressed and regulates the inhibitory action of glycine in these regions (Sipilä et al, 2014), as was here shown here by immunohistochemistry. There are also electrophysiological reports of glycinergic neurotransmission in the hippocampus and the cerebellum (Danglot et al, 2004; Dieudonne et al, 1995), but these indicated that GlyRs in these regions are located extra-synaptically and their functions are not clear.

Based on this evidence, GlyR-Abs may act by down-regulating the amount of GlyRs present on the presynaptic and postsynaptic sites at the glycinergic synapse, affecting not only the regulatory inhibition of the excitatory neuron but also the fine cross-inhibition of the inhibitory neuron and leading to the symptomatology observed in

PERM patients (Fig. 1). Differences in the clinical picture observed in these patients may also be due to differences in the influence of compensatory gabaergic networks.

Finally, an unresolved issue from the immunological perspective is how GlyR-Abs reach their target in the CNS. Are they produced outside of the CNS or are they produced intrathecally? In the great majority of patients, the serum levels are persistently higher than CSF levels of the specific antibody. Not many patients in this cohort had paired serum-CSF samples, and in the six patients with adequate sample volumes this was the case, although in three patients the CSF titres were extremely high and there was very substantial intrathecal synthesis of GlyR-Abs, as found in all antibody-mediated CNS diseases (Vincent et al 2011), although not necessarily in every individual. For instance, here, the index patient (Hutchinson et al 2008) during a relapse had very high serum levels and very little in the CSF, with no intrathecal synthesis. These observations indicate that initially the immune response must be systemic, and it is only under certain conditions that the antibodies cross the BBB (Poduslo et al, 1994), probably after local inflammatory reactions that increase its permeability (Cutler et al., 1970). This would allow an increased diffusion of antibodies and lymphocytes from the general circulation into the CNS (Martinez-Martinez et al., 2013), and may be critical not only for initiating the disease but also for determining which regions are involved.

7.2 Future perspectives

The results obtained in this research generated interesting questions that need to be addressed in future experiments. At the cellular level, there are other possible pathogenic mechanisms that were not explored, like a possible direct effect on the

glycine ion channel of the GlyR-Abs by either blockage or allosteric modulation. Further in vitro confirmation of the antigenic modulation of GlyRs induced by GlyR-Abs in neurons needs to be performed since they are the natural cellular targets of the antibodies in the CNS and some of the effects seen in the artificial in vitro systems may not be reproducible in neurons; this was found with AQP4-Abs on astrocytes (Ratelade et al, 2011). Also, it is important to know whether the complement activation observed in vitro also occurs in vivo. Mouse complement does not act very well with human IgG (Saadoun et al, 2010) and addition of human complement might be much more effective in inducing a passive transfer model, as they showed with intra-parenchymal injection of AQP4 antibodies. Additionally, it will be important to know if antibodies against other proteins involved in glycinergic neurotransmission are present in these or other patients such as GlyT or against the GlyRβ subunit, which are co-expressed in most functional GlyRs.

PERM associated with GlyR-Abs now meets three of the four modified Witebsky's criteria for autoimmune diseases. In order to complete the fourth criteria the induction of some of the clinical features by active immunisation against glycine receptors is needed. In addition, a pivotal question not only in PERM but in all CNS autoantibody mediated diseases is what initiates and sustains the immune response, and what determines the relapsing remitting or monophasic course of the disease.

At the clinical level this research suggest that PERM patients respond well to immunotherapy in contrast to SPS patients, but no comparative studies have been performed so far to confirm or refute this assumption. Also, it will be important to continue increasing the number of GlyR-Ab positive patients to confirm if combined immunosuppressive therapy is more effective than monotherapy and to confirm if the

presence of antibodies that bind to all GlyR α subunits is a good predictor for presenting PERM as suggested by data in this Thesis.

Finally, the supratentorial symptoms observed in these patients may be a consequence of GlyR-Abs exerting their effect in GlyRs present in these regions, but a better characterisation of roles of GlyRs in areas other than the brainstem and spinal cord is needed, and will require both better commercial antibodies to the different GlyRα subunits, and further electrophysiological experiments.

Appendix 1

Questionnaire for referring clinicians

	Your patient	
Our invoice number		
Initials of patient		
Are you the appropriate neurologist?		
Email		
Country of origin		
Has consent been obtained if required?		
General features: please describe		
Gender		
age at onset (years) females		
age at onset (years) males		
Disease presentation		
Acute		
Subacute		
subacute with acute exacerbation		
chronic/insidious		
chronic with acute exacerbation		
Duration at time of serum sample		
Course of disease		
Monophasic		

Recurrent/relapsing		
chronic progressive		
Follow-up too short or unknown		
Severity of disease - use mRs if you can or other score - at onset		
Treatments given		
Final outcome - use mRs if you can or other score		
YOUR DIAGNOSIS - please give your clinical diagnosis. Eg SPS, PERM, Hyperekplexia or other		
Which clinical picture does your patient fit best? Please check one of the following		
1. Severe acute brain and brain stem involvement		
2. Brainstem followed by generalised rigidity and myoclonus ie Classical PERM		
3. Bulbar and oculomotor dysfunction with touch sensitive myoclonus		
4. Spinal cord involvement predominantly with later brainstem		
5.Pain and sensory symptoms followed by brainstem and rigidity		
6. Other features or diagnosis		
Clinical Features please describe	**At onset**	**At maximum severity**
Spasms /Stiffness/Rigidity (neck, trunk or limb muscles)		
Oculomotor disturbance: nerve or gaze palsy (eyelid ptosis, diplopia, nystagmus, slow/jerkey movements)		
Trigeminal, facial and bulbar motor disturbance (dysphagia, dysarthria, difficulty chewing, facial numbness, trismus)		

Excessive startle (spontaneous or triggered by noise or touch)		
Sensory symptoms/Pain		
Cognitive impairment /encephalopathy /seizures /sleep disorders		
Limb or gait cerebellar ataxia		
Walking difficulties/falls (mostly related to stiffness/rigidity/spams)		
Limb paresis / Pyramidal signs		
Autonomic disturbances (hyper/hypohidrosis, dry mouth, brad/tachyc, hypo/hyper blood pressure, bladder, bowel or sexual dysfunction)		
Respiratory failure (admission in ICU/ventilation)		
Sudden death		
Associated conditions		
Tumours from past medical history or other significant PMH		
Autoimmune disorders; family history of spasms, stiffness etc		
Investigations	**At onset**	**At maximum severity**
Brain MRI		
Spinal cord MRI		
Chest CT/whole body PET scan		
EMG		
EEG		
CSF any abnormality		
CSF pleocytosis		
CSF protein		

CSF IgG or OCBs		
anti-GAD		
onco-neuronal abs		
other autoantibodies		

Appendix 2

doi:10.1093/brain/awu142 Brain 2014: Page 1 of 15 | 1

BRAIN
A JOURNAL OF NEUROLOGY

Glycine receptor antibodies in PERM and related syndromes: characteristics, clinical features and outcomes

Alexander Carvajal-González,[1,*] M. Isabel Leite,[1,*] Patrick Waters,[1,*] Mark Woodhall,[1,*] Ester Coutinho,[1] Bettina Balint,[2] Bethan Lang,[1] Philippa Pettingill,[1] Aisling Carr,[3] Una-Marie Sheerin,[4] Raomand Press,[5] Michael P. Lunn,[6] Ming Lim,[1] Paul Maddison,[7] H.-M. Meinck,[2] Wim Vandenberghe[8] and Angela Vincent[1]

1 Nuffield Department of Clinical Neurosciences, John Radcliffe Hospital, Oxford OX3 9DU, UK
2 Department of Neurology, INF 400, 69120 Heidelberg, Germany
3 Department of Clinical Neurology, Royal Victoria Hospital, Belfast, Northern Ireland, BT12 6BA
4 Department of Clinical Neurosciences, Charing Cross Hospital, Imperial College, London UK
5 Clinical Neuroscience, Karolinska Institute, Department of Neurology, Karolinska University Hospital Huddinge, Stockholm, Sweden
6 Centre for Neuromuscular Disease, National Hospital for Neurology and Neurosurgery, Queen Square, London, WC1N 3BG, UK
7 Department of Clinical Neurology, Queen's Medical Centre, Nottingham, NG7 2UH, UK
8 Department of Neurology, University Hospitals Leuven; Department of Neurosciences, KU Leuven, Leuven, Belgium

*These authors contributed substantially to this work.

Correspondence to: Prof. Angela Vincent,
Nuffield Department of Clinical Neurosciences,
John Radcliffe Hospital,
Oxford OX3 9DU, UK
E-mail: angela.vincent@ndcn.ox.ac.uk

See doi:10.1093/brain/awu153 for the scientific commentary on this article.

The clinical associations of glycine receptor antibodies have not yet been described fully. We identified prospectively 52 antibody-positive patients and collated their clinical features, investigations and immunotherapy responses. Serum glycine receptor antibody endpoint titres ranged from 1:20 to 1:60000. In 11 paired samples, serum levels were higher than ($n = 10$) or equal to ($n = 1$) cerebrospinal fluid levels; there was intrathecal synthesis of glycine receptor antibodies in each of the six pairs available for detailed study. Four patients also had high glutamic acid decarboxylase antibodies (>1000 U/ml), and one had high voltage-gated potassium channel-complex antibody (2442 pM). Seven patients with very low titres (<1:50) and unknown or alternative diagnoses were excluded from further study. Three of the remaining 45 patients had newly-identified thymomas and one had a lymphoma. Thirty-three patients were classified as progressive encephalomyelitis with rigidity and myoclonus, and two as stiff person syndrome; five had a limbic encephalitis or epileptic encephalopathy, two had brainstem features mainly, two had demyelinating optic neuropathies and one had an unclear diagnosis. Four patients (9%) died during the acute disease, but most showed marked improvement with immunotherapies. At most recent follow-up, (2–7 years, median 3 years, since first antibody detection), the median modified Rankin scale scores (excluding the four deaths) decreased from 5 at maximal severity to 1 ($P < 0.0001$), but relapses have occurred in five patients and a proportion are on reducing steroids or other maintenance immunotherapies as well as symptomatic treatments. The glycine receptor antibodies activated complement on glycine receptor-transfected human embryonic kidney cells at room temperature, and caused internalization and lysosomal degradation of the glycine receptors at 37° C. Immunoglobulin G antibodies bound to rodent spinal cord and brainstem co-localizing with monoclonal antibodies to glycine receptor-α1. Ten glycine receptor antibody

positive samples were also identified in a retrospective cohort of 56 patients with stiff person syndrome and related syndromes. Glycine receptor antibodies are strongly associated with spinal and brainstem disorders, and the majority of patients have progressive encephalomyelitis with rigidity and myoclonus. The antibodies demonstrate *in vitro* evidence of pathogenicity and the patients respond well to immunotherapies, contrasting with earlier studies of this syndrome, which indicated a poor prognosis. The presence of glycine receptor antibodies should help to identify a disease that responds to immunotherapies, but these treatments may need to be sustained, relapses can occur and maintenance immunosuppression may be required.

Keywords: stiff person syndrome; progressive encephalomyelitis with rigidity and myoclonus; autoimmune encephalitis; glycine receptor; autoantibody

Abbreviations: GAD = glutamic acid decarboxylase; GlyR = glycine receptor; HEK = human embryonic kidney cells; NMDAR = *N*-methyl-D-aspartate receptor; PERM = progressive encephalomyelitis with rigidity and myoclonus; VGKC = voltage-gated potassium channel

Introduction

Antibodies to receptors, ion channels or related proteins have become important markers for diseases that often improve substantially with immunotherapies (Vincent *et al*., 2011; Lancaster and Dalmau, 2012; Zuliani *et al*., 2012). *N*-methyl-D-aspartate antibodies are associated with anti-NMDA receptor (NMDAR) encephalitis and antibodies to leucine-rich, glioma inactivated 1 protein and contactin-associated protein 2 [components of the voltage-gated potassium channel (VGKC)-complex], with limbic encephalitis, Morvan's syndrome or peripheral nerve hyperexcitability. Antibodies to other CNS receptors have also been found in limbic encephalitis (Lancaster and Dalmau, 2012), and to dopamine receptors in children with a rare form of basal ganglia encephalitis (Dale *et al*., 2012). In addition, antibodies to the glial protein aquaporin 4 are an established cause of neuromyelitis optica (Jarius and Wildemann, 2010). Because each of these antibodies can bind to antigenic epitopes that are exposed on the surface of the cell they are likely to be pathogenic.

Stiff person syndrome is another antibody-associated syndrome, often with antibodies to glutamic acid decarboxylase (GAD; reviewed by Brown and Marsden, 1999; Meinck and Thompson, 2002; Alexopoulos and Dalakas, 2010). This enzyme, however, is intracellular rather than on the cell surface. Many patients do not respond well to immunotherapies but there are reports of clinical improvement with intravenous immunoglobulins or plasma exchange (reviewed by Alexopoulos and Dalakas, 2010), and recent reports of experimental transfer of disease to experimental animals with GAD or amphiphysin antibodies (Geis *et al*., 2010, 2012; Hansen *et al*., 2013).

A proportion of patients with GAD antibodies have a syndrome called stiff person syndrome plus or progressive encephalomyelitis with rigidity and myoclonus (PERM). PERM is similar to stiff person syndrome with rigidity, stimulus-sensitive spasms, myoclonus, hyperekplexia and autonomic disturbance, but with additional brainstem or other neurological defects. In general, PERM has been described as more severe, progressive and more often fatal compared with stiff person syndrome (Brown and Marsden, 1999; Meinck and Thompson, 2002). In a few cases, pathological findings on post-mortem have confirmed inflammation in PERM (Whiteley *et al*., 1976; Turner *et al*., 2011), suggesting that there may be T cell-mediated damage in both diseases.

In 2008, however, we described a patient with PERM, without GAD antibodies, who made a delayed but substantial recovery after receiving steroids, plasma exchange, intravenous immunoglobulin and cyclophosphamide. Retrospectively, the patient's sera, at onset and peak of disease, contained antibodies that bound to GlyRα1 subunits (now known as GLRA1) expressed on the surface of transfected human embryonic kidney cells, and also immunoprecipitated GlyRα1 (Hutchinson *et al*., 2008). Since then, further patients with glycine receptor (GlyR) antibodies have been described (Clerinx *et al*., 2011; Mas *et al*., 2011; Turner *et al*., 2011; Ituka *et al*., 2012; Peeters *et al*., 2013; Piotrowicz *et al*., 2011; Damasio *et al*., 2013; Stern *et al*., 2014; Bourke *et al*., 2014) with combinations of stiffness, rigidity, excessive stimulus-evoked startle, brainstem and autonomic signs. GlyR antibodies have also been found in retrospective cohorts of adults or children (Alexopoulos *et al*., 2013; Clardy *et al*., 2013; McKeon *et al*., 2013), with or without GAD antibodies. Here we describe the clinical spectrum of 52 GlyR antibody-positive patients (including those reported previously, see above), and the treatment responses, antibody characteristics and immunohistochemical localization of target antigens in rodent brain tissue.

Materials and methods

Patients

We identified 52 patients prospectively from 779 samples (including 55 serum/CSF pairs) referred to the Oxford Neuroimmunology service for GlyR antibody screening from 2008 to March 2012. Consent forms and questionnaires were sent to the neurologists (the glycine receptor antibody study group, see Appendix 1) who referred positive samples, and the data collated and analysed in Oxford. The study was performed with consent from the Regional Ethics Committee Ref: 07/Q1604/28. Sera positive for NMDAR or aquaporin 4 antibodies were used as serum controls, and six archived multiple sclerosis CSFs were used as CSF controls. We also examined GlyR antibodies in a retrospective cohort of 56 patients (35 females, 21 males) with stiff person syndrome, PERM or related disorders that had been collected in Heidelberg, Germany.

Detection of glycine receptor-bound antibodies for diagnosis

For screening we used immunofluorescence cell-based assays on human embryonic kidney (HEK) 293 cells transfected to express homo-pentamers of GlyRα1 tagged with enhanced green fluorescent protein, as previously described (Hutchinson *et al.*, 2008) and used in the Oxford clinical diagnostic service (see Supplementary material for details). Serum was tested at 1:20 and CSF at 1:2. The intensity of the staining was assessed visually by two independent observers, using a semiquantitative score (0 = no binding; 1–2 = low level binding; 2–4 = increasing strength of binding) as described previously (Leite *et al.*, 2008; Waters *et al.*, 2008). All sera and CSFs with positive binding were retested and checked for negativity against a second antigen to confirm specificity. When sufficient sample was available, GlyR antibody-positive sera and CSFs were also tested at serial dilutions to identify the concentration at which binding was scored as 1 ('endpoint' dilution). All of the available first samples were also tested for NMDAR and GAD antibodies by routine tests; 28 had VGKC-complex antibodies requested previously by the referring neurologists.

The subclass of the GlyR antibodies was determined by use of specific anti-subclass antibodies to IgG1, IgG2, IgG3, IgG4 and IgM (Invitrogen). Their ability to fix complement was demonstrated on the transfected HEK293 cells. After the addition of the patient serum (1:20) and washing, fresh human complement was added at 37°C for 1 h. Surface-bound C3b was detected with a fluorescent commercial antibody (Dako) as previously described (Leite *et al.*, 2008; Waters *et al.*, 2008). To determine subunit specificity, all positive samples were also screened against the other α subunits of the GlyR, α2 and α3 (see Supplementary material for details).

Blood–brain barrier integrity and antibody index

Full details are given in the Supplementary material. The six serum/CSF pairs with sufficient volumes were used to determine the integrity of the blood–brain barrier and the intrathecal synthesis of specific GlyR antibodies. Western blotting was used to measure total levels of IgG in paired sera (1:300) and undiluted CSF and for the albumin content of the sera (1:300) and CSFs, comparing with IgG and albumin standard curves. The IgG index was calculated according to:

$$[\text{CSF IgG (mg/ml)}/\text{serum IgG (mg/ml)}]/[\text{CSF albumin (mg/ml)}/\text{serum albumin (mg/ml)}];$$

and the intrathecal synthesis of GlyR antibody by calculating:

$$[\text{CSF GlyRα1 endpoint titre}/\text{CSF total IgG}]/[\text{serum GlyRα1 endpoint titre}/\text{serum total IgG}].$$

Effects of antibody binding to glycine receptor expressed on HEK cells

Full details are given in Supplementary material. To see whether GlyR antibodies were associated with internalization of the GlyRs, sera (1:80 to 1:160) were incubated with GlyRα1 expressing HEK cells for 1 h at 4°C and washed. Fixed or live cells were then incubated at either 4°C, or 37°C for 5 min to 16 h. After fixation of all cells, surface-bound human IgG was detected and the coverslips scored as for the diagnostic assay (see above). To see if the loss of surface GlyR antibody IgG was due to internalization, surface bound GlyR antibody was visualized (green) and scored at different times and compared with cells fixed and permeabilized in 0.3% Triton™ X-100 so that internal IgG could be visualized with Alexa Fluor® goat anti-human IgG (red). The results were quantified and data analysed with ImageJ software.

To examine the levels of surface GlyRα1, rather than bound IgG, the same procedure was carried out using GlyR-EGFP (enhanced green fluorescent protein) transfected cells, and cycloheximide to prevent new GlyR-EGFP synthesis. The percentage of cells with GlyR-EGFP on the surface or internalized was analysed. Finally to look at the endosomal location of internalized GlyR-EGFP, mouse antibodies to the late endosomal antigen (1:250; SantaCruz) were used, detecting with Alexa Fluor® 568 goat anti-mouse IgG (Invitrogen).

Binding to rat brain tissue sections

Full details are given in the Supplementary material. Indirect single and double immunofluorescence staining was performed on 11-μm cryostat sections of fresh frozen adult rat brain. The sections were fixed, blocked and incubated overnight at 4°C with human sera (1:200 to 1:800) and mouse monoclonal antibodies to the GlyRα1 subunit (1:500; Synaptic Systems) or rabbit polyclonal antibody to GAD (1:500; Sigma). The sections were washed, and bound patient or commercial antibodies detected with the appropriate secondary antibodies. Slides were photographed under a Leica fluorescence microscope (DM 2500) with a digital camera (QImaging, Rolera XR, Fast 1394). Four sera were pre-adsorbed against HEK cells expressing GlyRα1, GlyRα2, Glyα3 or untransfected HEK cells, or with recombinant GAD (12.5 μg/ml; RSR Ltd), overnight at 4°C before applying to the rat brain sections. To identify the neurons by confocal microscopy, sections were incubated with human sera (1:200 to 1:800), mouse monoclonal antibody to glycine receptor (as above) and either rabbit polyclonal antibody to microtubule-associated protein 2 (MAP2; 1:1000; Sigma) or rabbit polyclonal antibody to choline acetyltransferase (ChAT; 1:100; Millipore). Images were taken with a Zeiss confocal microscope (LSM 710).

Statistics

Kruskal–Wallis test and Dunn's multiple comparisons were used to assess the immunotherapy responses. Two-way ANOVA and two-sided Students *t*-tests were used to analyse the internalization experiments.

Results

The prospective cohort was identified from samples referred for testing from 2008 to March 2012. Images of patient and healthy control sera binding to GlyRs expressed on HEK cells are shown in Fig. 1A and the initial scores for each patients' serum and, when provided, CSF in Fig. 1B and C. For disease controls, we used samples identified as positive for NMDAR or aquaporin 4 antibodies, and multiple sclerosis CSFs. Only 1% of sera with aquaporin 4 antibodies, and none of those with NMDAR antibodies, bound to the GlyR cells at a score of >1 (Fig. 1B), and none of the control CSFs bound detectably (Fig. 1C). Therefore, we studied consecutive patients with GlyR antibody scores of >1 in serum and >0 in CSF. Forty-one sera and 11 serum/CSF pairs were positive. The remaining 727 patients, including 52 with

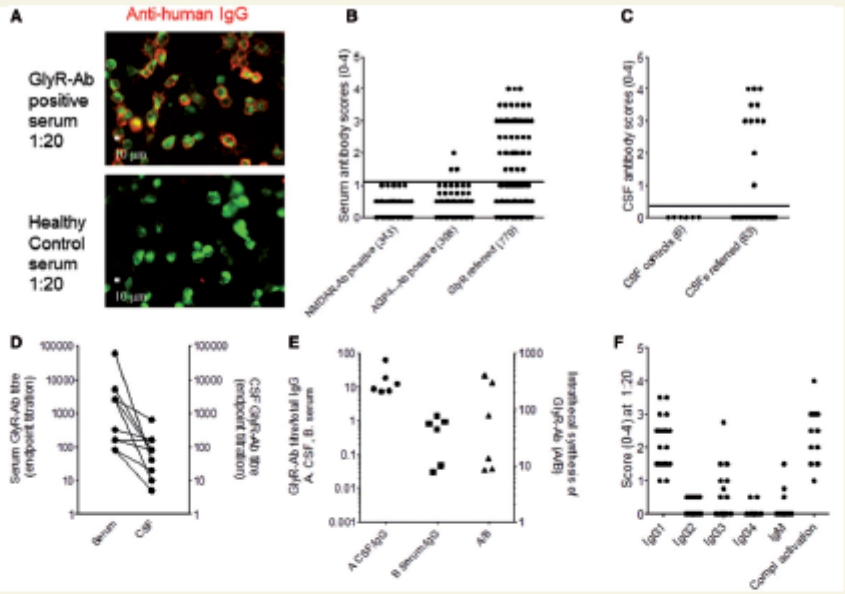

Figure 1 GlyR antibodies (Ab) in PERM and related disorders. (A) A patient's serum IgG binding to HEK293 cells expressing GlyRα1-EGFP (green); the IgG binding is detected with anti-human IgG (red). No IgG binding is observed with serum from a healthy individual. (B) Visual scores of sera (diluted 1:20) referred for routine GlyR antibody testing compared with scores in sera positive for NMDAR or aquaporin 4 (AQP4) antibodies studied as neurological controls. (C) Scores of referred CSF samples (diluted 1:1) compared with multiple sclerosis control CSFs. (D) Endpoint titrations for sera and paired CSFs; the CSF titres are generally lower than serum titres but in three patients are equal or only a dilution lower. (E) Calculation of intrathecal synthesis in six paired CSFs. GlyR antibody titres (from D) divided by IgG concentration for sera (serum/IgG) or for CSFs (CSF/IgG). Intrathecal synthesis rates are given as the ratio between these values as described above, and are raised in all patients, particularly in three. (F) Scores for each IgG subtype and for the deposition of complement C3 on the GlyRα1-expressing HEK cells. The antibodies are mainly IgG1 and IgG3 subtypes and activate complement on the surface of the GlyRα1-transfected cells.

serum/CSF pairs and five unpaired CSF samples were negative (median 0).

The endpoint dilution titres in sera (1:40 to 1:60 000) and CSFs (1:5 to 1:640) varied widely (eg, Fig. 1D), but some patients had CSF levels equal to ($n = 1$) or very similar to serum levels suggesting marked intrathecal synthesis of the specific GlyR antibody. To asses this quantitatively, we measured serum and CSF IgG and albumin in each of six patients with sufficient remaining samples. The ratios of serum:CSF IgG (138-592) and albumin (187 to 403) were within normal limits with Q_{Ab} of 0.6 to 1.4 (normal 0.7 to 1.3), indicating no general blood–brain barrier breakdown. By contrast, the antibody index for the GlyR antibody ranged from 8 to 400 (normal <1.4). These values represent substantial intrathecal synthesis of the specific GlyR antibodies, particularly in the three patients with values >50 (Fig. 1E).

Clinical data of patients with glycine receptor antibody-positive referred samples

For the 52 prospectively-referred GlyR antibody-positive patients, questionnaires were sent to the referring neurologists. Seven patients with very low GlyR antibodies (not titrating beyond 1:40) were excluded from the cohort because they had minimal symptoms and were lost to follow-up ($n = 2$), the clinician did not respond ($n = 1$) or the patients received a different diagnosis: one with Creutzfeldt-Jakob disease (Angus-Leppan *et al.*, 2013), one with confirmed hereditary myoclonus dystonia (Patient DYT_11), one with a motor polyneuropathy and one with possible psychogenic movement disorder.

References

Ahmadi, S., U. Muth-Selbach, et al. (2003). "Facilitation of spinal NMDA receptor currents by spillover of synaptically released glycine." Science **300**(5628): 2094-2097.

Akagi, H., K. Hirai, et al. (1991). "Cloning of a glycine receptor subtype expressed in rat brain and spinal cord during a specific period of neuronal development." FEBS Lett **281**(1-2): 160-166.

Alberts, B et al. (2008). "Molecular biology of the cell". 5th Ed. Garland Science.

Alexopoulos, H., S. Akrivou, et al. (2013). "Glycine receptor antibodies in stiff-person syndrome and other GAD-positive CNS disorders." Neurology **81**(22): 1962-1964.

Anhalt, G. J., R. S. Labib, et al. (1982). "Induction of pemphigus in neonatal mice by passive transfer of IgG from patients with the disease." N Engl J Med **306**(20): 1189-1196.

Araki, T., M. Yamano, et al. (1988). "Localization of glycine receptors in the rat central nervous system: an immunocytochemical analysis using monoclonal antibody." Neuroscience **25**(2): 613-624.

Atkinson, M. A., M. A. Bowman, et al. (1994). "Cellular immunity to a determinant common to glutamate decarboxylase and coxsackie virus in insulin-dependent diabetes." J Clin Invest **94**(5): 2125-2129.

Asavapanumas, N., J. Ratelade, et al. (2014). "Experimental mouse model of optic neuritis with inflammatory demyelination produced by passive transfer of neuromyelitis optica-immunoglobulin G." J Neuroinflammation 11: 16.

Back, T., G. Stoltenburg-Didinger, et al. (1997). "A new variant of progressive encephalomyelitis with rigidity associated with cerebellar ataxia and dementia: correlation of MRI and histopathological changes. A case report." Neurol Res 19(2): 187-191.

Baer, K., H. J. Waldvogel, et al. (2009). "Localization of glycine receptors in the human forebrain, brainstem, and cervical spinal cord: an immunohistochemical review." Front Mol Neurosci **2**: 25.

Bakker, M. J., J. G. van Dijk, et al. (2006). "Startle syndromes." Lancet Neurol **5**(6): 513-524.

Barker, R. A., T. Revesz, et al. (1998). "Review of 23 patients affected by the stiff man syndrome: clinical subdivision into stiff trunk (man) syndrome, stiff limb syndrome, and progressive encephalomyelitis with rigidity." J Neurol Neurosurg Psychiatry **65**(5): 633-640.

Becker, C. M., W. Hoch, et al. (1988). "Glycine receptor heterogeneity in rat spinal cord during postnatal development." EMBO J **7**(12): 3717-3726.

Becker, L., J. von Wegerer, et al. (2002). "Disease-specific human glycine receptor alpha1 subunit causes hyperekplexia phenotype and impaired glycine- and GABA(A)-receptor transmission in transgenic mice." J Neurosci **22**(7): 2505-2512.

Bell, E and Bird, L (2005). "Autoimmunity". Nature **435**(7042):583.

Bennett, J. L., C. Lam, et al. (2009). "Intrathecal pathogenic anti-aquaporin-4 antibodies in early neuromyelitis optica." Ann Neurol **66**(5): 617-629.

Betz, H. and C. M. Becker (1988). "The mammalian glycine receptor: biology and structure of a neuronal chloride channel protein." Neurochem Int **13**(2): 137-146.

Betz, H., J. Gomeza, et al. (2006). "Glycine transporters: essential regulators of synaptic transmission." Biochem Soc Trans **34**(Pt 1): 55-58.

Betz, H. and B. Laube (2006). "Glycine receptors: recent insights into their structural organization and functional diversity." J Neurochem **97**(6): 1600-1610.

Bison, S., Carboni, L, et al. (2009). "Differential behavioral, physiological, and hormonal sensitivity to LPS challenge in rats". International J Interferon, Cytokine and Mediator Res **1**(1): 1–13.

Bonilla, F. A. (2008). "Pharmacokinetics of immunoglobulin administered via intravenous or subcutaneous routes." Immunol Allergy Clin North Am 28(4): 803-819, ix.

Bosch, D. and S. Schmid (2008). "Cholinergic mechanism underlying prepulse inhibition of the startle response in rats." Neuroscience **155**(1): 326-335.

Brackmann, M., C. Zhao, et al. (2004). "Cellular and subcellular localization of the inhibitory glycine receptor in hippocampal neurons." Biochem Biophys Res Commun **324**(3): 1137-1142.

Bradl, M., T. Misu, et al. (2009). "Neuromyelitis optica: pathogenicity of patient immunoglobulin in vivo." Ann Neurol **66**(5): 630-643.

Brown, P. and C. D. Marsden (1999). "The stiff man and stiff man plus syndromes." J Neurol **246**(8): 648-652.

Brown, P., J. C. Rothwell, et al. (1991). "The hyperekplexias and their relationship to the normal startle reflex." Brain **114 (Pt 4)**: 1903-1928.

Burns, T. M., L. H. Phillips, 2nd, et al. (2005). "Stiff person syndrome does not always occur with maternal passive transfer of GAD65 antibodies." Neurology **64**(2): 399-400; author reply 399-400.

Burton, A. R., Z. Baquet, et al. (2010). "Central nervous system destruction mediated by glutamic acid decarboxylase-specific CD4+ T cells." J Immunol **184**(9): 4863-4870.

Cabot, J. B., V. Alessi, et al. (1992). "Glycine-like immunoreactive input to sympathetic preganglionic neurons." Brain Res **571**(1): 1-18.

Celio, M.R. and Heizmann, C.W. (1981). "Calcium binding protein parvalbumin as a neuronal marker". Nature **293**(5830): 300-302.

Carvajal-Gonzalez, A., M. I. Leite, et al. (2014). "Glycine receptor antibodies in PERM and related syndromes: characteristics, clinical features and outcomes." Brain **137**(Pt 8): 2178-2192.

Cascio, M. (2004). "Structure and function of the glycine receptor and related nicotinicoid receptors." J Biol Chem **279**(19): 19383-19386.

Clardy, S. L., V. A. Lennon, et al. (2013). "Childhood onset of stiff-man syndrome." JAMA Neurol **70**(12): 1531-1536.

Clerinx, K., T. Breban, et al. (2011). "Progressive encephalomyelitis with rigidity and myoclonus: resolution after thymectomy." Neurology **76**(3): 303-304.

Costa, M., A. Saiz, et al. (2002). "T-cell reactivity to glutamic acid decarboxylase in stiff-man syndrome and cerebellar ataxia associated with polyendocrine autoimmunity." Clin Exp Immunol **129**(3): 471-478.

Coutinho, A., M. D. Kazatchkine, et al. (1995). "Natural autoantibodies." Curr Opin Immunol **7**(6): 812-818.

Craig, A. M., G. Banker, et al. (1996). "Clustering of gephyrin at GABAergic but not glutamatergic synapses in cultured rat hippocampal neurons." J Neurosci 16(10): 3166-3177.
Cubelos, B., C. Gimenez, et al. (2005). "Localization of the GLYT1 glycine transporter at glutamatergic synapses in the rat brain." Cereb Cortex **15**(4): 448-459.
Cutler, R. W., et al. (1970). "The origin and turnover rates of cerebrospinal fluid albumin and gamma-globulin in man." J Neurol Sci 10(3): 259-268.
Chang, T., H. Alexopoulos, et al. (2013). "Neuronal surface and glutamic acid decarboxylase autoantibodies in Nonparaneoplastic stiff person syndrome." JAMA Neurol **70**(9): 1140-1149.
Chang, T., H. Alexopoulos, et al. (2013). "Immunization against GAD induces antibody binding to GAD-independent antigens and brainstem GABAergic neuronal loss." PLoS One **8**(9): e72921.
Chattipakorn, S. C. and L. L. McMahon (2002). "Pharmacological characterization of glycine-gated chloride currents recorded in rat hippocampal slices." J Neurophysiol 87(3): 1515-1525.
Chaudhry, F. A., et al. (1998). "The vesicular GABA transporter, VGAT, localizes to synaptic vesicles in sets of glycinergic as well as GABAergic neurons." J Neurosci 18(23): 9733-9750.
Dalakas, M. C. (2009). "Stiff person syndrome: advances in pathogenesis and therapeutic interventions." Curr Treat Options Neurol **11**(2): 102-110.
Dalakas, M. C., M. Fujii, et al. (2001). "High-dose intravenous immune globulin for stiff-person syndrome." N Engl J Med **345**(26): 1870-1876.
Dalakas, M. C., M. Fujii, et al. (2000). "The clinical spectrum of anti-GAD antibody-positive patients with stiff-person syndrome." Neurology **55**(10): 1531-1535.
Dalakas, M. C., M. Li, et al. (2001). "Stiff person syndrome: quantification, specificity, and intrathecal synthesis of GAD65 antibodies." Neurology **57**(5): 780-784.
Dalmau, J., A. J. Gleichman, et al. (2008). "Anti-NMDA-receptor encephalitis: case series and analysis of the effects of antibodies." Lancet Neurol **7**(12): 1091-1098.
Damasio, J., M. I. Leite, et al. (2013). "Progressive encephalomyelitis with rigidity and myoclonus: the first pediatric case with glycine receptor antibodies." JAMA Neurol **70**(4): 498-501.
Danglot, L., P. Rostaing, et al. (2004). "Morphologically identified glycinergic synapses in the hippocampus." Mol Cell Neurosci **27**(4): 394-403.
Davidson, A. and B. Diamond (2001). "Autoimmune diseases." N Engl J Med **345**(5): 340-350.
Davis, M., T. Parisi, et al. (1982). "Habituation and sensitization of startle reflexes elicited electrically from the brainstem." Science **218**(4573): 688-690.
De Blauwe, S. N., P. Santens, et al. (2013). "Anti-glycine receptor antibody mediated progressive encephalomyelitis with rigidity and myoclonus associated with breast cancer." Case Rep Neurol Med **2013**: 589154.
de Petris, S. and M. C. Raff (1973). "Normal distribution, patching and capping of lymphocyte surface immunoglobulin studied by electron microscopy." Nat New Biol **241**(113): 257-259.
Deacon, R. M. (2013). "Measuring motor coordination in mice." J Vis Exp(75): e2609.
Deacon, R. M. (2013). "The successive alleys test of anxiety in mice and rats." J Vis Exp(76).

Deng, S. X., E. Hanson, et al. (2000). "In vivo cell penetration and intracellular transport of anti-Sm and anti-La autoantibodies." Int Immunol **12**(4): 415-423.
Dieudonne, S. (1995). "Glycinergic synaptic currents in Golgi cells of the rat cerebellum." Proc Natl Acad Sci U S A **92**(5): 1441-1445.
Dinkel, K., H. M. Meinck, et al. (1998). "Inhibition of gamma-aminobutyric acid synthesis by glutamic acid decarboxylase autoantibodies in stiff-man syndrome." Ann Neurol **44**(2): 194-201.
Drachman, D. B., C. W. Angus, et al. (1978). "Myasthenic antibodies cross-link acetylcholine receptors to accelerate degradation." N Engl J Med **298**(20): 1116-1122.
Dreissen, Y. E., M. J. Bakker, et al. (2012). "Exaggerated startle reactions." Clin Neurophysiol **123**(1): 34-44.
Duddy, M. E. and M. R. Baker (2009). "Stiff person syndrome." Front Neurol Neurosci **26**: 147-165.
Dumoulin, A., et al. (2000). "Formation of mixed glycine and GABAergic synapses in cultured spinal cord neurons." Eur J Neurosci 12(11): 3883-3892.
Dumoulin, A., et al. (1999). "Presence of the vesicular inhibitory amino acid transporter in GABAergic and glycinergic synaptic terminal boutons." J Cell Sci 112 (Pt 6): 811-823.
Dutertre, S., C. M. Becker, et al. (2012). "Inhibitory glycine receptors: an update." J Biol Chem **287**(48): 40216-40223.
Eichler, S. A., B. Forstera, et al. (2009). "Splice-specific roles of glycine receptor alpha3 in the hippocampus." Eur J Neurosci **30**(6): 1077-1091.
Ekizoglu, E., E. Tuzun, et al. (2014). "Investigation of neuronal autoantibodies in two different focal epilepsy syndromes." Epilepsia **55**(3): 414-422.
Espay, A. J. and R. Chen (2006). "Rigidity and spasms from autoimmune encephalomyelopathies: stiff-person syndrome." Muscle Nerve **34**(6): 677-690.
Ferragamo, M. J., N. L. Golding, et al. (1998). "Synaptic inputs to stellate cells in the ventral cochlear nucleus." J Neurophysiol **79**(1): 51-63.
Finke, C., et al. (2012). "Cognitive deficits following anti-NMDA receptor encephalitis." J Neurol Neurosurg Psychiatry **83**(2): 195-198.
Flint, A. C., X. Liu, et al. (1998). "Nonsynaptic glycine receptor activation during early neocortical development." Neuron **20**(1): 43-53.
Floeter, M. K., F. Andermann, et al. (1996). "Physiological studies of spinal inhibitory pathways in patients with hereditary hyperekplexia." Neurology **46**(3): 766-772.
Floeter, M. K., J. Valls-Sole, et al. (1998). "Physiologic studies of spinal inhibitory circuits in patients with stiff-person syndrome." Neurology **51**(1): 85-93.
Fort, P., P. H. Luppi, et al. (1993). "Glycine-immunoreactive neurones in the cat brain stem reticular formation." Neuroreport **4**(9): 1123-1126.
Frostholm, A. and A. Rotter (1985). "Glycine receptor distribution in mouse CNS: autoradiographic localization of [3H]strychnine binding sites." Brain Res Bull 15(5): 473-486.
Fulton, J. F. and D. Nachmansohn (1943). "Acetylcholine and the Physiology of the Nervous System." Science **97**(2530): 569-571.
Gamblin, T. C., K. Nachmanoff, et al, (1996). "Recombinant Microtubule-Associated Protein 2c Reduces the Dynamic Instability of Individual Microtubules". Biochemistry **35**(38): 12576-12586.
Garcia-Alcocer, G., C. Mejia, et al. (2008). "Developmental expression of glycine receptor subunits in rat cerebellum." Int J Dev Neurosci **26**(3-4): 319-322.

Geis, C., M. Beck, et al. (2009). "Stiff person syndrome associated anti-amphiphysin antibodies reduce GABA associated [Ca(2+)]i rise in embryonic motoneurons." Neurobiol Dis **36**(1): 191-199.

Geis, C., B. Grunewald, et al. (2012). "Human IgG directed against amphiphysin induces anxiety behavior in a rat model after intrathecal passive transfer." J Neural Transm **119**(8): 981-985.

Geis, C., A. Weishaupt, et al. (2010). "Stiff person syndrome-associated autoantibodies to amphiphysin mediate reduced GABAergic inhibition." Brain **133**(11): 3166-3180.

Geis, H. R. and S. Schmid (2011). "Glycine inhibits startle-mediating neurons in the caudal pontine reticular formation but is not involved in synaptic depression underlying short-term habituation of startle." Neurosci Res **71**(2): 114-123.

Goldrath, A. W. and M. J. Bevan (1999). "Selecting and maintaining a diverse T-cell repertoire." Nature **402**(6759): 255-262.

Graus, F., F. Keime-Guibert, et al. (2001). "Anti-Hu-associated paraneoplastic encephalomyelitis: analysis of 200 patients." Brain **124**(Pt 6): 1138-1148.

Grenningloh, G., I. Pribilla, et al. (1990). "Cloning and expression of the 58 kd beta subunit of the inhibitory glycine receptor." Neuron **4**(6): 963-970.

Grenningloh, G., A. Rienitz, et al. (1987). "The strychnine-binding subunit of the glycine receptor shows homology with nicotinic acetylcholine receptors." Nature **328**(6127): 215-220.

Grenningloh, G., V. Schmieden, et al. (1990). "Alpha subunit variants of the human glycine receptor: primary structures, functional expression and chromosomal localization of the corresponding genes." EMBO J **9**(3): 771-776.

Griffon, N., C. Buttner, et al. (1999). "Molecular determinants of glycine receptor subunit assembly." EMBO J **18**(17): 4711-4721.

Grunert, U. and H. Wassle (1993). "Immunocytochemical localization of glycine receptors in the mammalian retina." J Comp Neurol **335**(4): 523-537.

Gu, H., D. Tarlinton, et al. (1991). "Most peripheral B cells in mice are ligand selected." J Exp Med **173**(6): 1357-1371.

Hansen, N., B. Grunewald, et al. (2013). "Human Stiff person syndrome IgG-containing high-titer anti-GAD65 autoantibodies induce motor dysfunction in rats." Exp Neurol **239**: 202-209.

Harvey, R. J., U. B. Depner, et al. (2004). "GlyR alpha3: an essential target for spinal PGE2-mediated inflammatory pain sensitization." Science **304**(5672): 884-887.

Harvey, R. J. and J. M. Rigo (2010). "Glycinergic transmission: physiological, developmental and pathological implications." Front Mol Neurosci **3**.

Harvey, R. J., M. Topf, et al. (2008). "The genetics of hyperekplexia: more than startle!" Trends Genet **24**(9): 439-447.

Hausser, M. A., W. H. Yung, et al. (1992). "Taurine and glycine activate the same Cl-conductance in substantia nigra dopamine neurones." Brain Res **571**(1): 103-108.

Haverkamp, S., U. Muller, et al. (2003). "Diversity of glycine receptors in the mouse retina: localization of the alpha3 subunit." J Comp Neurol **465**(4): 524-539.

Haverkamp, S., U. Muller, et al. (2004). "Diversity of glycine receptors in the mouse retina: localization of the alpha2 subunit." J Comp Neurol **477**(4): 399-411.

Heinze, L., R. J. Harvey, et al. (2007). "Diversity of glycine receptors in the mouse retina: localization of the alpha4 subunit." J Comp Neurol **500**(4): 693-707.

Henningsen, P. and H. M. Meinck (2003). "Specific phobia is a frequent non-motor feature in stiff man syndrome." J Neurol Neurosurg Psychiatry **74**(4): 462-465.
Hickey, W. F. (2001). "Basic principles of immunological surveillance of the normal central nervous system." Glia **36**(2): 118-124.
Hiemstra, H. S., N. C. Schloot, et al. (2001). "Cytomegalovirus in autoimmunity: T cell crossreactivity to viral antigen and autoantigen glutamic acid decarboxylase." Proc Natl Acad Sci U S A **98**(7): 3988-3991.
Hinckley, C., B. Seebach, et al. (2005). "Distinct roles of glycinergic and GABAergic inhibition in coordinating locomotor-like rhythms in the neonatal mouse spinal cord." Neuroscience **131**(3): 745-758.
Hinson, S. R., S. J. Pittock, et al. (2007). "Pathogenic potential of IgG binding to water channel extracellular domain in neuromyelitis optica." Neurology **69**(24): 2221-2231.
Hinson, S. R., S. F. Roemer, et al. (2008). "Aquaporin-4-binding autoantibodies in patients with neuromyelitis optica impair glutamate transport by down-regulating EAAT2." J Exp Med **205**(11): 2473-2481.
Hirzel, K., U. Muller, et al. (2006). "Hyperekplexia phenotype of glycine receptor alpha1 subunit mutant mice identifies Zn(2+) as an essential endogenous modulator of glycinergic neurotransmission." Neuron **52**(4): 679-690.
Holmoy, T., G. Skorstad, et al. (2009). "Stiff person syndrome associated with lower motor neuron disease and infiltration of cytotoxic T cells in the spinal cord." Clin Neurol Neurosurg **111**(8): 708-712.
Honnorat, J., A. Saiz, et al. (2001). "Cerebellar ataxia with anti-glutamic acid decarboxylase antibodies: study of 14 patients." Arch Neurol **58**(2): 225-230.
Howell, D. A., A. J. Lees, et al. (1979). "Spinal internuncial neurones in progressive encephalomyelitis with rigidity." J Neurol Neurosurg Psychiatry **42**(9): 773-785.
Huang, R., S. He, et al. (2007). "Mechanisms of homomeric alpha1 glycine receptor endocytosis." Biochemistry 46(41): 11484-11493.
Huerta, P. T., et al. (2006). "Immunity and behavior: antibodies alter emotion." Proc Natl Acad Sci U S A 103(3): 678-683.
Hughes, E. G., X. Peng, et al. (2010). "Cellular and synaptic mechanisms of anti-NMDA receptor encephalitis." J Neurosci **30**(17): 5866-5875.
Hutchinson, M., P. Waters, et al. (2008). "Progressive encephalomyelitis, rigidity, and myoclonus: a novel glycine receptor antibody." Neurology **71**(16): 1291-1292.
Ichikawa, H. and K. Itoh (2011). "Blood-arachnoid barrier disruption in experimental rat meningitis detected using gadolinium-enhancement ratio imaging." Brain Res **1390**: 142-149.
Iizuka, T., M. I. Leite, et al. (2012). "Glycine receptor antibodies are detected in progressive encephalomyelitis with rigidity and myoclonus (PERM) but not in saccadic oscillations." J Neurol **259**(8): 1566-1573.
Irani, S. R., K. Bera, et al. (2010). "N-methyl-D-aspartate antibody encephalitis: temporal progression of clinical and paraclinical observations in a predominantly non-paraneoplastic disorder of both sexes." Brain **133**(Pt 6): 1655-1667.
Ishida, K., H. Mitoma, et al. (1999). "Selective suppression of cerebellar GABAergic transmission by an autoantibody to glutamic acid decarboxylase." Ann Neurol **46**(2): 263-267.
Jande, S., L. Maler et al. (1981). “Immunohistochemical mapping of vitamin D-dependent calcium-binding protein in brain”. Nature **294**(5843): 765-767.

Jonas, P., J. Bischofberger, et al. (1998). "Corelease of two fast neurotransmitters at a central synapse." Science **281**(5375): 419-424.

Jursky, F. and N. Nelson (1995). "Localization of glycine neurotransmitter transporter (GLYT2) reveals correlation with the distribution of glycine receptor." J Neurochem **64**(3): 1026-1033.

Jursky, F. and N. Nelson (1996). "Developmental expression of the glycine transporters GLYT1 and GLYT2 in mouse brain." J Neurochem **67**(1): 336-344.

Kandel, E., Schwartz, J.H. et al. (2012). "Principles of neural science". 5th Ed. McGraw Hill.

Kaneda, M., M. Farrant, et al. (1995). "Whole-cell and single-channel currents activated by GABA and glycine in granule cells of the rat cerebellum." J Physiol **485 (Pt 2)**: 419-435.

Kawa, K. (2003). "Glycine receptors and glycinergic synaptic transmission in the deep cerebellar nuclei of the rat: a patch-clamp study." J Neurophysiol **90**(5): 3490-3500.

Kehne, J. H., D. W. Gallager, et al. (1981). "Strychnine: brainstem and spinal mediation of excitatory effects on acoustic startle." Eur J Pharmacol **76**(2-3): 177-186.

Kemp, J. A. and P. D. Leeson (1993). "The glycine site of the NMDA receptor--five years on." Trends Pharmacol Sci **14**(1): 20-25.

Kent, S., R. M. Bluthe, et al. (1992). "Sickness behavior as a new target for drug development." Trends Pharmacol Sci **13**(1): 24-28.

Khasani, S., K. Becker, et al. (2004). "Hyperekplexia and stiff-man syndrome: abnormal brainstem reflexes suggest a physiological relationship." J Neurol Neurosurg Psychiatry **75**(9): 1265-1269.

Kinoshita, M., Y. Nakatsuji, et al. (2009). "Neuromyelitis optica: Passive transfer to rats by human immunoglobulin." Biochem Biophys Res Commun **386**(4): 623-627.

Kirsch, J. (2006). "Glycinergic transmission." Cell Tissue Res **326**(2): 535-540.

Knikou, M. (2008). "The H-reflex as a probe: pathways and pitfalls." J Neurosci Methods **171**(1): 1-12.

Koch, M. (1999). "The neurobiology of startle." Prog Neurobiol **59**(2): 107-128.

Koch, M. and E. Friauf (1995). "Glycine receptors in the caudal pontine reticular formation: are they important for the inhibition of the acoustic startle response?" Brain Res **671**(1): 63-72.

Koerner, C., B. Wieland, et al. (2004). "Stiff-person syndromes: motor cortex hyperexcitability correlates with anti-GAD autoimmunity." Neurology **62**(8): 1357-1362.

Kotak, V. C., S. Korada, et al. (1998). "A developmental shift from GABAergic to glycinergic transmission in the central auditory system." J Neurosci **18**(12): 4646-4655.

Kowal, C., et al. (2004). "Cognition and immunity; antibody impairs memory." Immunity 21(2): 179-188.

Kubota, H., H. Alle, et al. (2010). "Presynaptic glycine receptors on hippocampal mossy fibers." Biochem Biophys Res Commun **393**(4): 587-591.

Kunkel-Bagden, E., H. N. Dai, et al. (1993). "Methods to assess the development and recovery of locomotor function after spinal cord injury in rats." Exp Neurol **119**(2): 153-164.

Lacroix-Desmazes, S., S. V. Kaveri, et al. (1998). "Self-reactive antibodies (natural autoantibodies) in healthy individuals." J Immunol Methods **216**(1-2): 117-137.

Lancaster, E. and J. Dalmau (2012). "Neuronal autoantigens--pathogenesis, associated disorders and antibody testing." Nat Rev Neurol **8**(7): 380-390.

Lang, B., J. Newsom-Davis, et al. (1983). "Antibodies to motor nerve terminals: an electrophysiological study of a human myasthenic syndrome transferred to mouse." J Physiol **344**: 335-345.

Lang, B., J. Newsom-Davis, et al. (1981). "Autoimmune aetiology for myasthenic (Eaton-Lambert) syndrome." Lancet **2**(8240): 224-226.

Lang, B. and A. Vincent (2003). "Autoantibodies to ion channels at the neuromuscular junction." Autoimmun Rev **2**(2): 94-100.

Lee, Y., D. E. Lopez, et al. (1996). "A primary acoustic startle pathway: obligatory role of cochlear root neurons and the nucleus reticularis pontis caudalis." J Neurosci **16**(11): 3775-3789.

Legendre, P. (2001). "The glycinergic inhibitory synapse." Cell Mol Life Sci **58**(5-6): 760-793.

Lehmann, H. C., G. Meyer Zu Horste, et al. (2009). "Pathogenesis and treatment of immune-mediated neuropathies." Ther Adv Neurol Disord **2**(4): 261-281.

Leite, M. I., S. Jacob, et al. (2008). "IgG1 antibodies to acetylcholine receptors in 'seronegative' myasthenia gravis." Brain **131**(Pt 7): 1940-1952.

Lennon, V. A., et al. (2005). "IgG marker of optic-spinal multiple sclerosis binds to the aquaporin-4 water channel." J Exp Med 202(4): 473-477.

Levy, L. M., M. C. Dalakas, et al. (1999). "The stiff-person syndrome: an autoimmune disorder affecting neurotransmission of gamma-aminobutyric acid." Ann Intern Med **131**(7): 522-530.

Liedtke, W., W. Edelmann, et al. (1996). "GFAP is necessary for the integrity of CNS white matter architecture and long-term maintenance of myelination." Neuron 17(4): 607-615.

Lingenhohl, K. and E. Friauf (1994). "Giant neurons in the rat reticular formation: a sensorimotor interface in the elementary acoustic startle circuit?" J Neurosci **14**(3 Pt 1): 1176-1194.

Lohmann, T., M. Londei, et al. (2003). "Humoral and cellular autoimmune responses in stiff person syndrome." Ann N Y Acad Sci **998**: 215-222.

Lynch, J. W. (2004). "Molecular structure and function of the glycine receptor chloride channel." Physiol Rev **84**(4): 1051-1095.

Lynch, J. W. (2009). "Native glycine receptor subtypes and their physiological roles." Neuropharmacology **56**(1): 303-309.

Malosio, M. L., B. Marqueze-Pouey, et al. (1991). "Widespread expression of glycine receptor subunit mRNAs in the adult and developing rat brain." EMBO J **10**(9): 2401-2409.

Malter, M. P., C. Helmstaedter, et al. (2010). "Antibodies to glutamic acid decarboxylase define a form of limbic encephalitis." Ann Neurol **67**(4): 470-478.

Malter, M. P., et al. (2014). "Outcome of limbic encephalitis with VGKC-complex antibodies: relation to antigenic specificity." J Neurol 261(9): 1695-1705.

Manto, M., J. Dalmau, et al. (2010). "In vivo effects of antibodies from patients with anti-NMDA receptor encephalitis: further evidence of synaptic glutamatergic dysfunction." Orphanet J Rare Dis 5: 31.

Manto, M. U., C. S. Hampe, et al. (2011). "Respective implications of glutamate decarboxylase antibodies in stiff person syndrome and cerebellar ataxia." Orphanet J Rare Dis **6**: 3.

Marrack, P., J. Kappler, et al. (2001). "Autoimmune disease: why and where it occurs." Nat Med **7**(8): 899-905.
Martinez-Martinez, P., et al. (2013). "Autoantibodies to neurotransmitter receptors and ion channels: from neuromuscular to neuropsychiatric disorders." Front Genet 4: 181.
Mas, N., A. Saiz, et al. (2011). "Antiglycine-receptor encephalomyelitis with rigidity." J Neurol Neurosurg Psychiatry **82**(12): 1399-1401.
Matsumoto, J. Y., J. N. Caviness, et al. (1994). "The acoustic startle reflex in stiff-man syndrome." Neurology **44**(10): 1952-1955.
McCool, B. A. and A. Chappell (2007). "Strychnine and taurine modulation of amygdala-associated anxiety-like behavior is 'state' dependent." Behav Brain Res **178**(1): 70-81.
McKeon, A., E. Martinez-Hernandez, et al. (2013). "Glycine receptor autoimmune spectrum with stiff-man syndrome phenotype." JAMA Neurol **70**(1): 44-50.
McKeon, A., M. T. Robinson, et al. (2012). "Stiff-man syndrome and variants: clinical course, treatments, and outcomes." Arch Neurol **69**(2): 230-238.
Meinck, H. M. (2006). "Startle and its disorders." Neurophysiol Clin **36**(5-6): 357-364.
Meinck, H. M., L. Faber, et al. (2001). "Antibodies against glutamic acid decarboxylase: prevalence in neurological diseases." J Neurol Neurosurg Psychiatry **71**(1): 100-103.
Meinck, H. M. and P. D. Thompson (2002). "Stiff man syndrome and related conditions." Mov Disord **17**(5): 853-866.
Melzer, N., S. G. Meuth, et al. (2013). "Paraneoplastic and non-paraneoplastic autoimmunity to neurons in the central nervous system." J Neurol **260**(5): 1215-1233.
Metz, G. A. and I. Q. Whishaw (2009). "The ladder rung walking task: a scoring system and its practical application." J Vis Exp(28).
Mikasova, L., P. De Rossi, et al. (2012). "Disrupted surface cross-talk between NMDA and Ephrin-B2 receptors in anti-NMDA encephalitis." Brain 135(Pt 5): 1606-1621.
Mitoma, H., S. Y. Song, et al. (2000). "Presynaptic impairment of cerebellar inhibitory synapses by an autoantibody to glutamate decarboxylase." J Neurol Sci **175**(1): 40-44.
Mossman, S., A. Vincent, et al. (1986). "Myasthenia gravis without acetylcholine-receptor antibody: a distinct disease entity." Lancet **1**(8473): 116-119.
Mukherjee, A. and A. Chakravarty (2010). "Spasticity mechanisms - for the clinician." Front Neurol **1**: 149.
Murinson, B. B. (2004). "Stiff-person syndrome." Neurologist **10**(3): 131-137.
Naas, E., K. Zilles, et al. (1991). "Glycine receptor immunoreactivity in rat and human cerebral cortex." Brain Res **561**(1): 139-146.
Nibbeling, N., H. A. Daanen, et al. (2012). "Effects of anxiety on running with and without an aiming task." J Sports Sci **30**(1): 11-19.
Nikolic, Z., B. Laube, et al. (1998). "The human glycine receptor subunit alpha3. Glra3 gene structure, chromosomal localization, and functional characterization of alternative transcripts." J Biol Chem **273**(31): 19708-19714.
Noris, M. and G. Remuzzi (2013). "Overview of complement activation and regulation." Semin Nephrol **33**(6): 479-492.
O'Brien, J. A. and A. J. Berger (1999). "Cotransmission of GABA and glycine to brain stem motoneurons." J Neurophysiol **82**(3): 1638-1641.

Paton, J. F. and D. W. Richter (1995). "Role of fast inhibitory synaptic mechanisms in respiratory rhythm generation in the maturing mouse." J Physiol **484 (Pt 2)**: 505-521.

Peeters, E., P. Vanacker, et al. (2012). "Supranuclear gaze palsy in glycine receptor antibody-positive progressive encephalomyelitis with rigidity and myoclonus." Mov Disord **27**(14): 1830-1832.

Plappert, C. F. and P. K. Pilz (2001). "The acoustic startle response as an effective model for elucidating the effect of genes on the neural mechanism of behavior in mice." Behav Brain Res **125**(1-2): 183-188.

Poduslo, J. F., G. L. Curran, et al. (1994). "Macromolecular permeability across the blood-nerve and blood-brain barriers." Proc Natl Acad Sci U S A 91(12): 5705-5709.

Porter, R.S., Kaplan, J.L. et al (2011). "The merck manual". 19th Ed. Medical Library Association.

Racke, M. K. (2009). "Immunopathogenesis of multiple sclerosis." Ann Indian Acad Neurol **12**(4): 215-220.

Raju, R., J. Foote, et al. (2005). "Analysis of GAD65 autoantibodies in Stiff-Person syndrome patients." J Immunol **175**(11): 7755-7762.

Rakocevic, G. and M. K. Floeter (2012). "Autoimmune stiff person syndrome and related myelopathies: understanding of electrophysiological and immunological processes." Muscle Nerve **45**(5): 623-634.

Rampon, C., P. H. Luppi, et al. (1996). "Distribution of glycine-immunoreactive cell bodies and fibers in the rat brain." Neuroscience **75**(3): 737-755.

Ratelade, J., J. L. Bennett, et al. (2011). "Evidence against cellular internalization in vivo of NMO-IgG, aquaporin-4, and excitatory amino acid transporter 2 in neuromyelitis optica." J Biol Chem **286**(52): 45156-45164.

Rees, M. I., K. Harvey, et al. (2006). "Mutations in the gene encoding GlyT2 (SLC6A5) define a presynaptic component of human startle disease." Nat Genet **38**(7): 801-806.

Rogers, J., M. Khan, et al. (1990). "Calretinin and other CaBPs in the nervous system." Adv Exp Med Biol 269: 195-203.

Rose, N. R. and C. Bona (1993). "Defining criteria for autoimmune diseases (Witebsky's postulates revisited)." Immunol Today **14**(9): 426-430.

Russier, M., I. L. Kopysova, et al. (2002). "GABA and glycine co-release optimizes functional inhibition in rat brainstem motoneurons in vitro." J Physiol **541**(Pt 1): 123-137.

Saadoun, S., et al. (2010). "Intra-cerebral injection of neuromyelitis optica immunoglobulin G and human complement produces neuromyelitis optica lesions in mice." Brain 133(Pt 2): 349-361.

Saiz, A., Y. Blanco, et al. (2008). "Spectrum of neurological syndromes associated with glutamic acid decarboxylase antibodies: diagnostic clues for this association." Brain **131**(Pt 10): 2553-2563.

Sato, K., J. H. Zhang, et al. (1991). "Localization of glycine receptor alpha 1 subunit mRNA-containing neurons in the rat brain: an analysis using in situ hybridization histochemistry." Neuroscience **43**(2-3): 381-395.

Shriner, A. M., F. R. Drever, et al. (2009). "The development of skilled walking in the rat." Behav Brain Res **205**(2): 426-435.

Sillevis Smitt, P., A. Kinoshita, et al. (2000). "Paraneoplastic cerebellar ataxia due to autoantibodies against a glutamate receptor." N Engl J Med 342(1): 21-27.

Sipila, S. T., et al. (2014). "Glycine transporter-1 controls nonsynaptic inhibitory actions of glycine receptors in the neonatal rat hippocampus." J Neurosci 34(30): 10003-10009.

Skorstad, G., A. L. Hestvik, et al. (2009). "Cerebrospinal fluid T cell responses against glutamic acid decarboxylase 65 in patients with stiff person syndrome." J Autoimmun **32**(1): 24-32.

Smith, A. J., S. Owens, et al. (2000). "Characterisation of inhibitory and excitatory postsynaptic currents of the rat medial superior olive." J Physiol **529 Pt 3**: 681-698.

Sommer, C., A. Weishaupt, et al. (2005). "Paraneoplastic stiff-person syndrome: passive transfer to rats by means of IgG antibodies to amphiphysin." Lancet **365**(9468): 1406-1411.

Song, W., S. C. Chattipakorn, et al. (2006). "Glycine-gated chloride channels depress synaptic transmission in rat hippocampus." J Neurophysiol **95**(4): 2366-2379.

Stern, W. M., R. Howard, et al. (2013). "Glycine receptor antibody mediated Progressive Encephalomyelitis with Rigidity and Myoclonus (PERM): a rare but treatable neurological syndrome." Pract Neurol.

Tijssen, M. A., L. M. Voorkamp, et al. (1997). "Startle responses in hereditary hyperekplexia." Arch Neurol **54**(4): 388-393.

Todd, A. J., C. Watt, et al. (1996). "Colocalization of GABA, glycine, and their receptors at synapses in the rat spinal cord." J Neurosci **16**(3): 974-982.

Toyka, K. V., D. B. Brachman, et al. (1975). "Myasthenia gravis: passive transfer from man to mouse." Science **190**(4212): 397-399.

Turner, M. R., S. R. Irani, et al. (2011). "Progressive encephalomyelitis with rigidity and myoclonus: glycine and NMDA receptor antibodies." Neurology **77**(5): 439-443.

Tuzun, E., L. Zhou, et al. (2009). "Evidence for antibody-mediated pathogenesis in anti-NMDAR encephalitis associated with ovarian teratoma." Acta Neuropathol **118**(6): 737-743.

Vianello, M., G. Bisson, et al. (2008). "Increased spontaneous activity of a network of hippocampal neurons in culture caused by suppression of inhibitory potentials mediated by anti-gad antibodies." Autoimmunity **41**(1): 66-73.

Viegas, S., L. Jacobson, et al. (2012). "Passive and active immunization models of MuSK-Ab positive myasthenia: electrophysiological evidence for pre and postsynaptic defects." Exp Neurol **234**(2): 506-512.

Vincent, A. (2002). "Unravelling the pathogenesis of myasthenia gravis." Nat Rev Immunol **2**(10): 797-804.

Vincent, A. (2010). "Autoimmune channelopathies: well-established and emerging immunotherapy-responsive diseases of the peripheral and central nervous systems." J Clin Immunol **30 Suppl 1**: S97-102.

Vincent, A. (2010). "Successful 'passive transfer' of paraneoplastic stiff person syndrome with antibodies to an intracellular antigen." Brain **133**(11): 3164-3165.

Vincent, A. and J. Newsom-Davis (1982). "Acetylcholine receptor antibody characteristics in myasthenia gravis. I. Patients with generalized myasthenia or disease restricted to ocular muscles." Clin Exp Immunol **49**(2): 257-265.

von Wegerer, J., K. Becker, et al. (2003). "Spinal inhibitory synaptic transmission in the glycine receptor mouse mutant spastic." Neurosci Lett **345**(1): 45-48.

Waldvogel, H. J., K. Baer, et al. (2007). "Glycine receptors in the striatum, globus pallidus, and substantia nigra of the human brain: an immunohistochemical study." J Comp Neurol **502**(6): 1012-1029.
Waldvogel, H. J., K. Baer, et al. (2010). "Differential localization of gamma-aminobutyric acid type A and glycine receptor subunits and gephyrin in the human pons, medulla oblongata and uppermost cervical segment of the spinal cord: an immunohistochemical study." J Comp Neurol **518**(3): 305-328.
Walker, M. C. and A. Semyanov (2008). "Regulation of excitability by extrasynaptic GABA(A) receptors." Results Probl Cell Differ **44**: 29-48.
Wassle, H., L. Heinze, et al. (2009). "Glycinergic transmission in the Mammalian retina." Front Mol Neurosci **2**: 6.
Watanabe, K., T. Shimizu, et al. (1984). "[An autopsy case with unusual muscle rigidity resembling the stiff-man syndrome]." Rinsho Shinkeigaku **24**(8): 839-847.
Webb, T. I. and J. W. Lynch (2007). "Molecular pharmacology of the glycine receptor chloride channel." Curr Pharm Des **13**(23): 2350-2367.
Weltzien, F., C. Puller, et al. (2012). "Distribution of the glycine receptor beta-subunit in the mouse CNS as revealed by a novel monoclonal antibody." J Comp Neurol **520**(17): 3962-3981.
Wenthold, R. J., K. K. Skaggs, et al. (1984). "Retrograde axonal transport of antibodies to synaptic membrane components." Brain Res **304**(1): 162-165.
Whiteley, A. M., M. Swash, et al. (1976). "Progressive encephalomyelitis with rigidity." Brain **99**(1): 27-42.
Witebsky, E., N. R. Rose, et al. (1957). "Chronic thyroiditis and autoimmunization." J Am Med Assoc **164**(13): 1439-1447.
Wuerfel, E., C. G. Bien, et al. (2014). "Glycine receptor antibodies in a boy with focal epilepsy and episodic behavioral disorder." J Neurol Sci **343**(1-2): 180-182.
Xu, T. L. and N. Gong (2010). "Glycine and glycine receptor signaling in hippocampal neurons: diversity, function and regulation." Prog Neurobiol **91**(4): 349-361.
Yaddanapudi, K., M. Hornig, et al. (2010). "Passive transfer of streptococcus-induced antibodies reproduces behavioral disturbances in a mouse model of pediatric autoimmune neuropsychiatric disorders associated with streptococcal infection." Mol Psychiatry **15**(7): 712-726.
Yang, H. W., M. Y. Min, et al. (1997). "Glycine-immunoreactive terminals in the rat trigeminal motor nucleus: light- and electron-microscopic analysis of their relationships with motoneurones and with GABA-immunoreactive terminals." Brain Res **749**(2): 301-319.
Yeomans, J. S., D. Bosch, et al. (2010). "GABA receptors and prepulse inhibition of acoustic startle in mice and rats." Eur J Neurosci **31**(11): 2053-2061.
Yeomans, J. S., J. Lee, et al. (2006). "Midbrain pathways for prepulse inhibition and startle activation in rat." Neuroscience **142**(4): 921-929.
Yirmiya, R., H. Rosen, et al. (1994). "Behavioral effects of lipopolysaccharide in rats: involvement of endogenous opioids." Brain Res **648**(1): 80-86.
Zafra, F., J. Gomeza, et al. (1995). "Regional distribution and developmental variation of the glycine transporters GLYT1 and GLYT2 in the rat CNS." Eur J Neurosci **7**(6): 1342-1352.
Zarbin, M. A., J. K. Wamsley, et al. (1981). "Glycine receptor: light microscopic autoradiographic localization with [3H]strychnine." J Neurosci **1**(5): 532-547.
Zeilhofer, H. U., et al. (2012). "Fast synaptic inhibition in spinal sensory processing and pain control." Physiol Rev 92(1): 193-235.

Zuliani, L., F. Graus, et al. (2012). "Central nervous system neuronal surface antibody associated syndromes: review and guidelines for recognition." J Neurol Neurosurg Psychiatry **83**(6): 638-645.